

Nitrogen Containing Heterocyclic Moiety for Interlocked Structure and Heterometallic Complex

By
SIDHESWARI PRUSTY

CHEM11201104013

**National Institute of Science Education and Research
Bhubaneswar
Jatni, Khurda, Odisha – 752050**

*A thesis submitted to the
Board of Studies in Chemical Sciences
In partial fulfilment of requirements
For the degree of*

DOCTOR OF PHILOSOPHY

of

HOMI BHABHA NATIONAL INSTITUTE

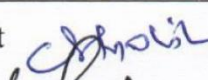
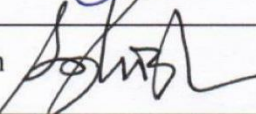
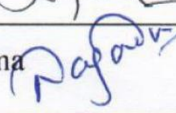
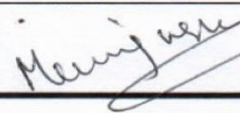


December, 2018

Homi Bhabha National Institute

Recommendations of the Viva Voce Committee

As members of the Viva Voce Committee, we certify that we have read the dissertation prepared by **SIDHESWARI PRUSTY** entitled “**Nitrogen Containing Heterocyclic Moiety for Interlocked Structure and Heterometallic Complex**” and recommend that it may be accepted as fulfilling the thesis requirement for the award of Degree of Doctor of Philosophy.

Chairman -	Prof. A.Srinivasan		Date: 6.6.19
Guide / Convener -	Dr. Chandra Shekhar Purohit		Date: 06/06/19
Examiner -	Prof. Sundargopal Ghosh		Date: 6/6/2019
Member 1-	Dr. Jogendra Nath Behera		Date: 6/6/19.
Member 2-	Dr. Nagendra Kumar Sharma		Date: Nag 06/06/19
Member 3-	Dr. Manjusha Dixit		Date: 06/06/19

Final approval and acceptance of this thesis is contingent upon the candidate's submission of the final copies of the thesis to HBNI.

I/We hereby certify that I/we have read this thesis prepared under my/our direction and recommend that it may be accepted as fulfilling the thesis requirement.

Date: 06.06.2019

Place: Bhubaneswar


(Dr. Chandra Shekhar Purohit)
Guide

STATEMENT BY AUTHOR

This dissertation has been submitted in partial fulfillment of requirements for an advanced degree at Homi Bhabha National Institute (HBNI) and is deposited in the Library to be made available to borrowers under rules of the HBNI.

Brief quotations from this dissertation are allowable without special permission, provided that accurate acknowledgement of source is made. Requests for permission for extended quotation from or reproduction of this manuscript in whole or in part may be granted by the Competent Authority of HBNI when in his or her judgment the proposed use of the material is in the interests of scholarship. In all other instances, however, permission must be obtained from the author.

Sidheswari prusty

SIDHESWARI PRUSTY

DECLARATION

I, hereby declare that the investigation presented in the thesis has been carried out by me. The work is original and has not been submitted earlier as a whole or in part for a degree / diploma at this or any other Institution / University.

Sidheswari prusty

SIDHESWARI PRUSTY

List of Publications arising from the thesis

Journals

Published

1. Heterometallic Coordination Polymers with Pyrazine 2, 6-dicarboxamide: Sequential Metallation of Co(III) and Ag(I), **Sidheswari Prusty**; Chandra Shekhar Purohit, *Chemistry Select*, **2018**, 3, 8051-8055.
2. A Molecular figure of eight: Synthesis and Characterization, **Sidheswari Prusty**, Mana Bhanjan Podh; Chandra Shekhar Purohit, *Chemistry select* **2018**, 3, 9690-9693

Conferences

- a. **Poster Presentation:** INTER IISER & NISER CHEMISTRY MEET (IINCM – 2017) at NISER Bhubaneswar, India during 22 – 24 December, 2017
- b. **Poster Presentation:** 19th Odisha Bigyan ‘O’ Paribesh Congress on Science & Technology for Environmental Security at KIIT University, Bhubaneswar, India

c. **Poster Presentation:** National Conference on New Prospective to Advanced Functional Materials at Ravenshaw University, Cuttack, Odisha.

Sidheswari prusty
SIDHESWARI PRUSTY

Dedicated to My Family

ACKNOWLEDGEMENTS

This work might not have been possible without the copious contributions from others. First, I would like to thank my research advisor, Dr. Chandra Shekhar Purohit for his valuable guidance, continuous support, helpful discussions and providing space for free thinking throughout the years. I am thankful to Prof. Sudhakar Panda (Director NISER). I am thankful to Prof. T. K. Chandrashekar, founder Director-NISER and Prof. V. Chandrashekar, former Director-NISER for the laboratory facilities and obviously DST-INSPIRE for financial support. I would like to recognize my thesis monitoring committee (TMC) members Prof. A.Srinivasan, Dr. J. N. Behera, Dr. N. K. Sharma and Dr. Manjusha Dixit and chairperson-SCS, Prof. A.Srinivasan, and all other faculty members in SCS for their support and useful suggestions. I would like to thank Prof. T. K. Chandrashekar, Doctors A. Ghosh, N. K. Sharma, P. Mal, J. N. Behera and Sudip Barman, for teaching me in my course work, which had uplifted my understanding of chemistry. I sincerely thank Dr. Arun Kumar for helping me by providing lab chemicals whenever I need. I sincerely thank Sanjaya for recording the NMR spectra of my samples and Anuradha for recording GC of my samples. I would also like to acknowledge Amit for recording mass spectra of my samples. I am thankful to Deepak for data collection of my single crystals. I thank all the non-academic staffs of School of Chemical Sciences and the Institute. I am extremely fortunate to have lab mates like Dr. Pardhasaradhi Satha, Dr. Giriteja Illa, Nayan, Krushna, Sohan, Arun, Mana, Sanjay, and Priyanka. Their cheerful accompany, traceless discussion, generous cooperation have provided a thought-provoking and

friendly environment which helps this journey smooth. I thank all of my NISER friends for the memorable moments.

Most importantly, I would like to thank my parents, husband, brother and family who were witness to every step of the way and provided me support and confidence whenever I needed it the most. Thank you all so much for your unconditional love and unwavering support.

Above all, Thank You GOD for everything.....

Sidheswari prusty

SIDHESWARI PRUSTY

CONTENTS

	Page No.
Summary	11 - 12
List of Schemes	13 - 15
List of Figures	16 - 25
List of Tables	26 - 26
List of Abbreviations	27 - 29
Chapter-1	31 - 101
Chapter-2	102 - 143
Chapter-3	144 - 180

SUMMARY

Coordination polymers have involved much attention due to their distinctive properties and wide applications. Sometimes these materials mimic the enzymes but have their multiple catalytic sites that has an equal chemical environment due to crystalline environment of the material. Heterometallic coordination complexes are utilized in absorption, sensing, catalysis etc. Pyrazine with an extra nitrogen atom than pyridine, may offer similar advantage but its poor coordination ability hinders its efficient use. Moreover, such systems are less explored and reported in the literature. Our objective was to synthesize a series of heterometallic coordination polymer with pyridine based pyrazine- 2, 6, dicarboxamide as ligand. For this purpose, we have exploited 2, 6-pyrazine dicarboxamide appended with pyridines as building blocks. We have discussed about the synthesis and supramolecular assembly of two heterometallic and a homometallic complex with Co(III) and Ag(I) by stepwise method which are confirmed by single X-ray crystallography, PXRD, IR and TGA analysis. The use of transition metal ions as template and structural elements were advance strategies in the development of effective method for the synthesis of mechanically interlocked architectures such as catenane, rotaxane and higher interlocked architectures. Figure of eight structure can be synthesized by different approaches. Figure of eight conformation is a key intermediate in biological genetic recombination of circular DNA. Our objective was to synthesize a molecular figure of eight complex by metal templated approach using derivative of pyridine 2, 6-dicarboxamide ligand followed by click chemistry. We reported the synthesis of molecular figure of

eight, with Co(III) template using click chemistry for ring closing. However, this reaction may yield both [2]-catenane and figure of eight complexes. In order to prove the conformation, we synthesized an analogous [2]-catenane Co(III) complex exclusively, using a different strategy. Both the compounds are successfully characterized by NMR spectroscopy and HPLC.

LIST OF SCHEMES

	Page no.
Scheme 1.1. Mononuclear metalloligand with Be(II)	34
Scheme 1.2. Synthesis of squaregrid network, 1D double chain and 2D chain	34
Scheme 1.3. Synthesis of Polynuclear metalloligand with Ag(I)	35
Scheme 1.4. Synthesis of L^1 -ZnCl ₂ complex	37
Scheme 1.5. Synthesis of M(II)-L ² -M(II) complex	38
Scheme 1.6. Beckmann rearrangement catalysed by Zn(II)-L ² -Zn(II)	38
Scheme 1.7. Strecker synthesis catalysed by Cd(II)-L ² -Cd(II) complex	39
Scheme 1.8. Ring opening of epoxide catalysed by 2 and 3	42
Scheme 1.9. Ring opening of epoxide catalysed by 2 and 3	43
Scheme 1.10. Synthesis of Homometallic complex Co(III)-Co(II) Hetero metallic complex Fe(III)-Co(II)	43
Scheme 1.11. Knoevenagel reaction catalysed by complex 6	45
Scheme 1.12. Cyanohydrin formation with catalyst 8-12	48
Scheme 1.13. Epoxide synthesis with catalyst 12	48

Scheme 1.14. Synthesis of thiazoline based metalloligand	53
Scheme 1.15. Ring opening reaction of oxirane and thairane with heterogeneous catalyst	55
Scheme 1.16. Cyanation reaction catalysed by heterogeneous catalyst	55
Scheme 1.17. Synthesis of heterometallic complex with Eu(III) and Tb(III)	56
Scheme 1.18. synthesis of heterometallic complex 33 and 34	58
Scheme 1.19. A3 coupling reaction catalysed by heterogeneous catalyst 33 and 34	61
Scheme 1.20. Henry reaction catalysed by 35	63
Scheme 1.21. Knoevenagel reaction catalysed by 35	63
Scheme 2.1. Synthesis of pyrazine based cobalt complex, 4a , 4b and 4c	112
Scheme 2.2. Synthesis of pyrazine based Ag(I)-Co(III) Heterometallic complex, 5a , 5b	113
Scheme 3.1. Synthesis of 5	154
Scheme 3.2. Synthesis of 10	154
Scheme 3.3. Synthesis of 9	155
Scheme 3.4. Molecular figure-of-eight complex, 11 by click chemistry	156

Scheme 3.5. Macrocyclic 12 by click chemistry approach	157
Scheme.3.6. Synthesis of 13	158
Scheme 3.7. [2]Catenane, 14 by click chemistry	159

LIST OF FIGURES

	Page no.
Figure 1.1. Cu(I) metalloligand with 1D ladder and 2D squaregrid	35
Figure 1.2. Synthesis of Zn(II) 2D sheet and Cu(I) 1D chain	36
Figure 1.3. Different types of Co(III) based metalloligand	37
Figure 1.4. 2D network from metalloligand L3 and Cd(II)/ Zn(II)	40
Figure 1.5. Hexagonal network from L ³ and Zn(II)	40
Figure 1.6. Heterometallic complex with Eu(III)/Tb(III)	41
Figure 1.7. Packing diagram showing weak interaction of 2	41
Figure 1.8. Packing diagram showing the waek interaction of 3	42
Figure 1.9. Coordination polymeric network of 6 along crystallographic b-axis	44
Figure 1.10. Optimized route for synthesis of complex 8-12	45
Figure 1.11. Single X-ray crystal structure of 8	46
Figure 1.12. Single X-ray crystal structure of 9	47
Figure 1.13. Single X-ray crystal structure of 12	47
Figure 1.14. Coordination of cobalt based metalloligand with zinc(II)	49
Figure 1.15. Coordination of cobalt based metalloligand with Cd(II)	49

Figure 1.16. Coordination of cobalt based metalloligand with Zinc(II)	49
Figure 1.17. Coordination of cobalt based metalloligand with Zinc(II)	50
Figure 1.18. Coordination of carboxylicacid based metalloligand metalloligand with zinc(II)	50
Figure 1.19. Space filling model Heterometallic complex 20	51
Figure 1.20. Coordination of carboxylicacid based metalloligand metalloligand with zinc(II)	51
Figure 1.21. Coordination of carboxylicacid based metalloligand metalloligand with zinc(II)	51
Figure 1.22. X-ray crystal structure of heterometallic complex 21	52
Figure 1.23. X-ray crystal structure of heterometallic complex 22	52
Figure 1.24. Hetero metallic complex 25 from 24	53
Figure 1.25. Hetero metallic complex 26 from 24	54
Figure 1.26. Hetero metallic complex 26 from 24	54
Figure 1.27. X-ray showing the 1D and 2D arrangement of heterometallic polymer of Eu(III)	56
Figure 1.28. X-ray showing the 1D arrangement of heterometallic polymer of Tb(III) with water molecules by hydrogen bonding	57
Figure 1.29. X-ray crystal structure showing 2D polymeric network	58

of 33	
Figure 1.30. X-ray crystal structure showing argentophilic interaction of 2D polymeric network of 33	59
Figure 1.31. Partial X-ray crystal structure of 34 showing coordination to Ag(I)	59
Figure 1.32. Packing diagram of complex 34 showing coordination to Ag(I)	60
Figure. 1.33. Partial X-ray crystal structure of 35 showing coordination to Zn(II)	61
Figure 1.34. Partial X-ray crystal structure of 36 showing coordination to Cd(II)	62
Figure 1.35. Partial X-ray crystal structure of 34 showing coordination to Sm(II)	62
Figure 1.36. Schematic representation of coordination driven selfassembly	66
Figure 1.37. Cyclization by Ni(II) ion	67
Figure 1.38. Synthesized molecular cage encapsulating fullerene guest	68
Figure 1.39. Synthesized Open box network with porphyrin cavity	68
Figure 1.40. Examples of different interlocked architecture	69
Figure 1.41. First [2]Catenane by Wasserman	70

Figure 1.42. [2]Catenane by Sauvage	70
Figure 1.43. Amide based [2]Catenane by Vogtle and Hunter	71
Figure 1.44. [2]Catenane by anion templated approach	72
Figure 1.45. Yoshima's [2]Catenane by using salt bridge	73
Figure 1.46. P ^H control molecular switch by Sauvage	73
Figure 1.47. [3]Catenane by Fujita	74
Figure 1.48. [3]Catenane by Mayer	75
Figure 1.49. Stoddart's Borromean ring	75
Figure 1.50. Interlocked molecular cage by Cooper	76
Figure 1.51. X-ray crystal structure of Cooper's interlocked molecular cage	77
Figure 1.52. Sander's trefoil knot	77
Figure 1.53. Schematic representation of trefoil knot	78
Figure 1.54. Trefoil knot by Active metal template approach	79
Figure 1.55. Trefoil knot by metal templated approach	80
Figure 1.56. X-ray crystal structure showing trefoil knot with Eu(III) and Lu(III)	81

Figure 1.57. X-ray crystal structure of molecular trefoil knot	81
Figure 1.58. Molecular trefoil knot by Leigh	82
Figure 1.59. Synthesis of molecular trefoil knot with Zn(II) template	83
Figure 1.60. Solid state structure of Zn(II) trefoil knot	84
Figure 1.61. Leigh's molecular pentafoil knot	85
Figure 1.62. 3D-Molecular cage by Stoddart	86
Figure 1.63. Solid state structure of 3D-molecular cage	86
Figure 1.64. Schematic representation of molecular composite knot	87
Figure 1.65. Synthesized molecular composite knot by Leigh	88
Figure 1.66. X-ray structure of Leigh's composite knot	89
Figure 1.67. Molecular granny knot by Leigh	90
Figure 1.68. Solid state nature of metal free 6^2_3 knot	91
Figure 1.69. Two station Catenane by Loeb	92
Figure 1.70. Clever's molecular container	92
Figure 1.71. Solid state structure of Clever's molecular container	93
Figure 1.72. Stoddart's Six Borromean ring	94
Figure 2.1. Ni(II) or Cu(II) coordination with $[L^5]-2$ resulting	105

[2 x 2] molecular grid

Figure 2.2. Coordination of Co(III) with [L ⁶]- 2 resulting [2 x 2] molecular grid	106
Figure 2.3. Synthesis of Ag ₂ (HL ⁷) ₂ and Co(L ⁷) ₂ from HL ⁷	106
Figure 2.4. Synthesis of Ag(I) dimer	107
Figure 2.5. Three different ligands 2a , 2b and 2c coordination to metal	107
Figure 2.6. Molecular structures of the 2a , 2b and 2c	108
Figure 2.7. X-ray crystal structure of complex 3 indicating the AgNO ₃ coordination and possible Hydrogen bonding.	109
Figure 2.8. A complete Packing representation of complex 3 along crystallographic a-axis displaying the three dimensional(3D) polymer.	110
Figure 2.9. Packing diagrammatic representation of 3 showing H-bond interaction between amide nitrogen and the water (H ₂ O) molecule	111
Figure 2.10. TGA analysis for complex 3	111
Figure 2.11. Ag(I) mode of Coordination in complex 5a	114
Figure 2.12. Packing diagrammatic representation of complex 5a along crystallographic b-axis	115
Figure 2.13. TGA analysis for 5a	116
Figure 2.14. Binding of Ag(I) in complex 5b	116

Figure 2.15. Packing diagrammatic representation of complex 5b along crystallographic b-axis	117
Figure 2.16. TGA analysis for 5b	118
Figure 2.17. ^1H NMR of precursor ligand 2a	127
Figure 2.18. ^{13}C NMR of precursor ligand 2a	127
Figure 2.19. ^1H NMR of precursor ligand 2b	128
Figure 2.20. ^{13}C NMR of precursor ligand 2b	128
Figure 2.21. ^1H NMR of precursor ligand 2c	129
Figure. 2.22. ^{13}C NMR of precursor ligand 2C	129
Figure. 2.23. ^1H NMR of metal complex 4a	130
Figure 2.24. ^{13}C NMR of metal complex 4a	130
Figure 2.25. ^1H NMR of metal complex 4b	131
Figure 2.26. ^{13}C NMR of metal complex 4b	131
Figure 2.27. ^1H NMR of metal complex 4c	132
Figure 2.28. ^{13}C NMR of metal complex 4c	132
Figure 2.29. ESI-MS spectrum of precursor ligand 2a	133
Figure 2.30. ESI-MS spectrum of precursor ligand 2b	133

Figure 2.31. ESI-MS spectrum of metal complex 4a	134
Figure 2.32. ESI-MS spectrum of metal complex 4b	134
Figure 2.33. IR spectra of complex 3	135
Figure 2.34. IR spectra of complex 5a	135
Figure 2.35. IR spectra of complex 5b	135
Figure 2.36. PXRD data for 3	136
Figure 2.37. PXRD data for 5a	136
Figure 2.38. PXRD data for 5b	136
Figure 3.1. Synthesis of porphyrin based figure of eight	147
Figure 3.2. Figure of eight structure with Fe ²⁺ /Cu ⁺	148
Figure 3.3. Synthesis of [2]Catenane, and a large macrocycle	150
Figure 3.4. Synthesis of dinuclear Ir(I) complex	150
Figure 3.5. Stoddert's figure of eight with Cis and Trans configuration	151
Figure 3.6. Synthesis of Cobalt(III) complex with figure of eight structure	152
Figure 3.7. Graphic design of Molecular Figure of eight and [2]Catenane complex	153
Figure 3.8. Comparative ¹ H NMR spectra of [2]catenane, 14 with that of figure of eight complex, 11	160

Figure 3.9. HPLC data of compound 11 and 14	161
Figure 3.10. ^1H NMR of 5	169
Figure 3.11. ^{13}C NMR of 5	169
Figure 3.12. ^1H NMR spectra of 9	170
Figure 3.13. ^{13}C NMR spectra of 9	170
Figure 3.14. ^1H NMR spectra of 10	171
Figure 3.15. ^{13}C NMR spectra of 10	171
Figure 3.16. ^1H NMR spectra of 11	172
Figure 3.17. ^{13}C NMR spectra of 11	172
Figure 3.18. ^1H NMR spectra of 12	173
Figure 3.19. ^{13}C NMR spectra of 12	173
Figure 3.20. ^1H NMR spectra of 14	174
Figure 3.21. ^{13}C NMR spectra of 14	174
Figure 3.22. ESI-MS Spectra of 5	175
Figure 3.23. ESI-MS Spectra of 9	175
Figure 3.24. ESI-MS Spectra of 10	176
Figure 3.25. ESI-MS Spectra of 11	176
Figure 3.26. ESI-MS Spectra of 12	177

Figure 3.27. ESI-MS Spectra of 13	177
Figure 3.28. ESI-MS Spectra of 14	178
Figure 3.29. HPLC graph of compound 14 and 11	179
Figure 3.30. ROESY spectra of compound 11	179

LIST OF TABLES

	Page no.
Table 2.1. Crystallographic structure refinement factors for complexes 3 , 5a and 5b	137
Table 2.2. Bond length and Bond angle of coordination complex 3	138
Table 2.3. Bond length and Bond angle of coordination complex 5a	139
Table 2.4. Bond length and Bond angle of coordination complex 5b	140
Table 2.5. Possible Hydrogen bonds for 3	143
Table 2.6. Possible Hydrogen bonds for 5b	143
Table 3.1. HPLC data for the compound 11 and 14	179

LIST OF ABBREVIATIONS

CH ₃ CN	Acetonitrile
BF ₃ .OEt ₂	Borontrifluoridediethyletherate
BBr ₃	Borontribromide
Br-	Bromide ion
BF ₄	Tetrafluoroborate ion
Cl-	Chloride ion
CCDC	Cambridge crystallographic data centre
CHCl ₃	Chloroform
CD ₃ OC ₂ D ₅	Deuteriated acetone
CD ₃ OD	Deuteriated methanol
CDCl ₃	Deuteriated chloroform
CD ₃ CN	Deuteriated acetonitrile
CTV	Cyclotrimeratrylene
CTC	Cyclotricatechylene
CTG	Cyclotriguaiacylene
DCM	Dichloromethane
DMF	Dimethylformamide
DMA	Dimethyl acetamide
DFT	Density functional theory
DMSO	Dimethylsulphoxide
FT-IR	Fourier transformation infra red

EtOAc	Ethyl acetate
ESI	Electron spray ionization
Equiv.	Equivalents
h	hours
K ₂ CO ₃	Potassium Carbonate
min	minutes
NMR	Nuclear magnetic resonance
Na ₂ SO ₄	Sodium Sulphate
H ₂ SO ₄	Sulfuric acid
HPLC	High performance liquid chromatography
TFA	Trifluoroacetic acid
THF	Tetrahydrofuran
UV	Ultraviolet
TLC	Thin layer chromatography
TMS	Tetramethylsilane
p-TSA	para-toluene sulphonic acid
PF ₆	Hexafluorophosphate ion
Phe	1,10-Phenanthroline
PXRD	Powder x-ray diffraction
ROESY	Rotating-frame Overhauser Spectroscopy
TBA	Tetrabutyl ammonium
TBACl	Tetrabutyl ammonium chloride
TBABr	Tetrabutyl ammonium bromide

TBAI	Tetrabutyl ammonium iodide
TGA	Thermogravimetric analysis

Chapter-1

INDEX

Introduction

Part-I

1.1. Coordination polymer

Part-II

1.2. Interlocked Architectures

1.3. References.

Introduction

Coordination polymer

Heterocyclic compounds are the cyclic compounds containing at least one heteroatom in one or more rings. These compounds are universal in nature and are vital for many biological functions. Heterocyclic containing DNA and RNA carry genetic information. Some amino acids contains heterocyclic residue which are essential for human body. Most of the drugs, pesticides, herbicides and dyes contain heterocyclic moiety.

Apart from biological and medicinal applications, Heterocyclic compounds play a major role in coordination and supramolecular chemistry which are the chemistry of noncovalent interactions. Utilizing the hydrogen bonding and metal coordinating ability of hetero atom of heterocyclic rings many supramolecular architectures were synthesized. Among heterocyclics pyridine moiety was well studied for the construction of variety of supramolecular assemblies such as metal-organic architectures, interlocked molecules etc.

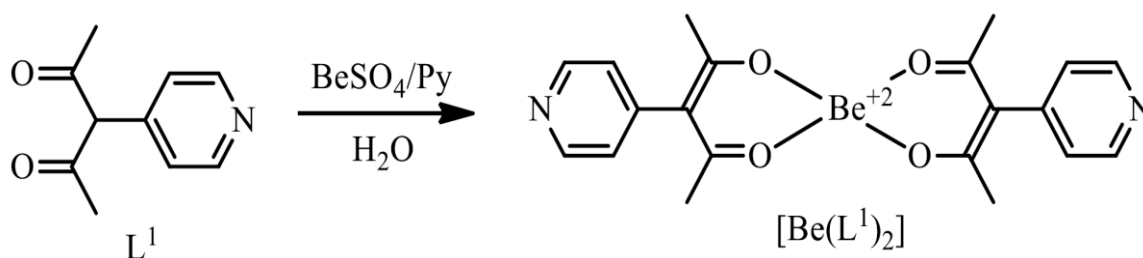
Our aim is to investigate the ability of pyridine moiety (a) for the formation of homometallic and heterometallic coordination polymer. (b) For the construction of interlocked molecule figure of eight.

The materials with useful properties has directed to improvement of inorganic organic hybrid compounds, because they offer vast advantages which emerge from both metal and ligand. Coordination polymers belong to this new class of materials with vast potential applications in several fields such as absorption, gas storage,¹ separation,² sensing,³ ion exchange and transport,⁴ luminescent materials and

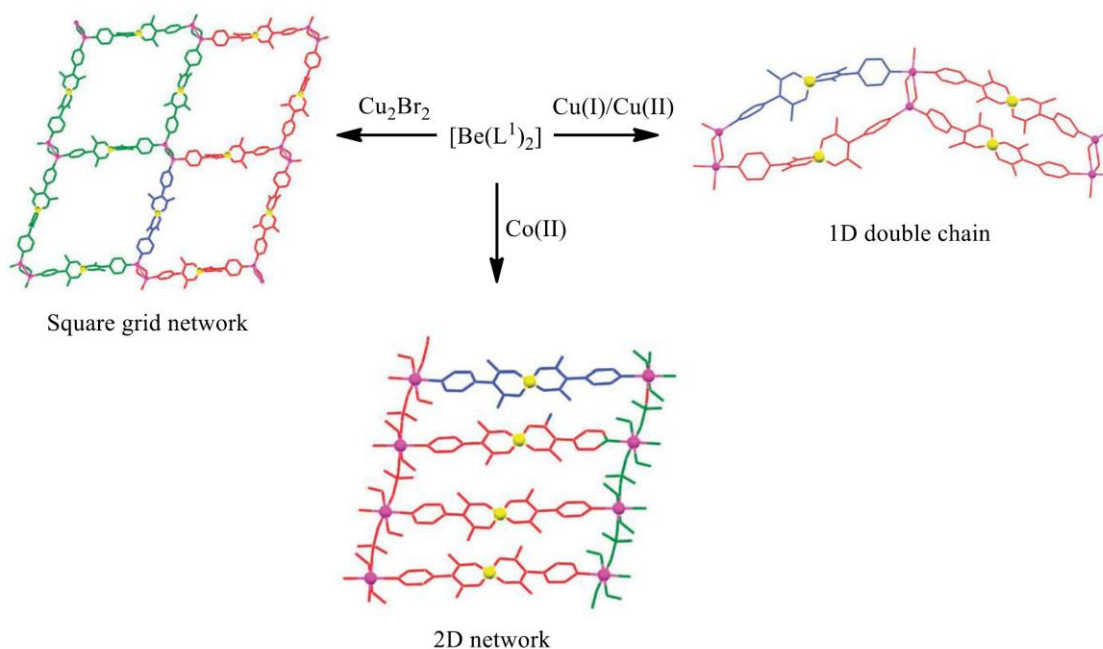
devices,⁵ magnetism⁶ and catalysis.⁷ Due to crystalline nature of material, the material has a single active site which has an identical chemical environment. The geometry of the coordinated metal ion and nature of ligands should provide the construction manual for any self-assembly process. So, the selection of appropriate metal ion(s) and ligand(s) is very important, as observed in various literature.⁸⁻¹⁰ Metal organic frameworks, coordination polymers, coordination networks were synthesized by mixing organic ligand with metal salt.¹¹⁻¹² The major disadvantage is the formation of mixture of different architectures if different metal salts were used. Due to this, stepwise method was adventitious. Here the metalloligand was first synthesized by coordination of metal ion with ligand having proper coordination sites. Thereafter the synthesized corresponding metalloligand can be converted to different heterometallic architecture by coordination with different metal ions. A metalloligand is defined as a discrete coordinate complex which consists of vacant coordinating sites for secondary metal ions. The metalloligands can be mono, di, polynuclear depending upon the choice of ligand.

Mononuclear metalloligand is defined as an organic ligand with proper vacant coordination sites can be coordinated to a single metal ion. Several mononuclear ligands are reported in literatures.¹³ These include derivatives of acetylacetonate, β -diketonate, dipyrromethane, porphyrin, salen, 2, 5-pyridine dicarboxylate etc. Domasevitch and coworkers synthesized a metalloligand $[\text{Be}(\text{L}^1)_2]$ by reacting the ligand 3-pyridylactetylacetonate (L^1) with BeSO_4 and pyridine in the aqueous conditions (scheme 1.1).¹⁴ The Be^{2+} coordinated metalloligand further coordinated to CoSO_4 resulted a 2D polymeric network in which SO_4^{2-} coordinated to two

cobalt metal atoms. Similarly this same metalloligand can coordinate with Cu^{2+} metal salts resulting different coordinated polymeric network (scheme 1.2).



Scheme 1.1. Mononuclear metalloligand with $\text{Be}(\text{II})$



Scheme 1.2. Synthesis of squaregrid network, 1D double chain and 2D chain

The same acetylacetonato ligand was also utilized by maverick and co-workers for the synthesis of Cu coordinated metalloligand.¹⁵ The metalloligand later reacted with $\text{Cd}(\text{NO}_3)_2$ results 1D ladder structure and with square planar CdCl_2 forms 2D square grid structure (figure 1.1). Due to highest degree of porosity these two

structures later can be used for host-guest interactions at Cu^{2+} sites, but these were not stable under solvent/ guest exchange circumstance.

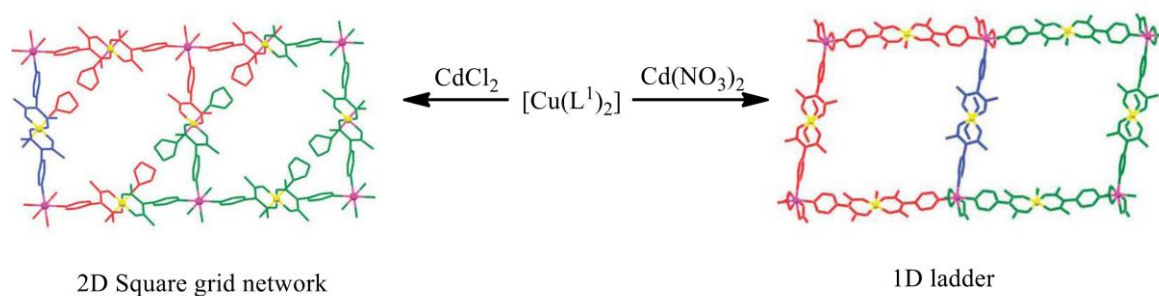
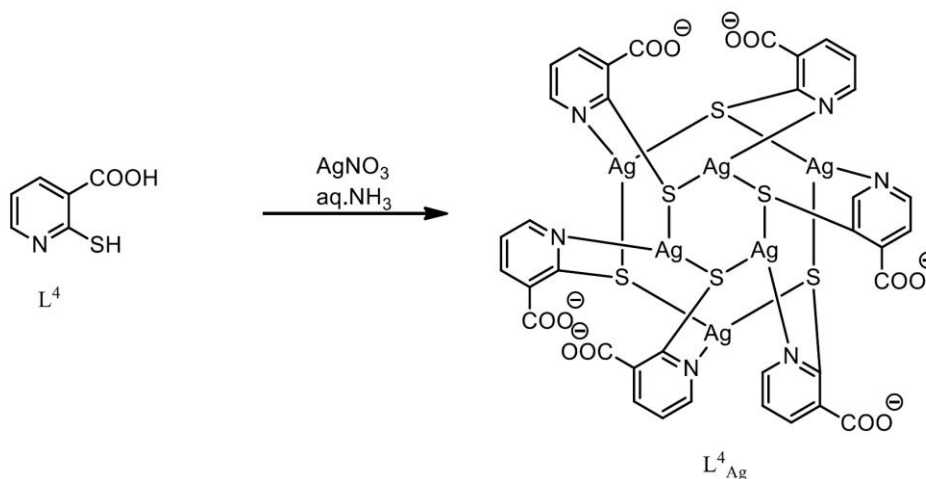


Figure 1.1. Cu(I) metalloligand with 1D ladder and 2D squaregrid

Dinuclear metalloligands having two metal ions are supported by organic ligands with vacant sites. Some ligands in this class are known such as ortho-Phenylene-bis(oxamate), pyrazolyl pyridine derivatives etc.¹⁶



Scheme 1.3. Synthesis of Polynuclear metalloligand with Ag(I)

The coordination complex having two or more metal ions coordinated to organic ligand is known as polynuclear metalloligands. For example 2-mercaptopyridine-5-carboxylic acid (L^4) reacted with AgNO_3 in water gives precipitate (scheme 1.3).¹⁷ The

precipitate was treated with aq.NH₃ to achieve silver coordinated hexanuclear anionic metalloligand. The silver coordinated metalloligand was treated with Cu(OAc)₂ and bipyridine ensuing a 1D heterometallic complex where as with Zn(OAc)₂ and ethylene diamine produces a 2D sheet structure (figure 1.2).

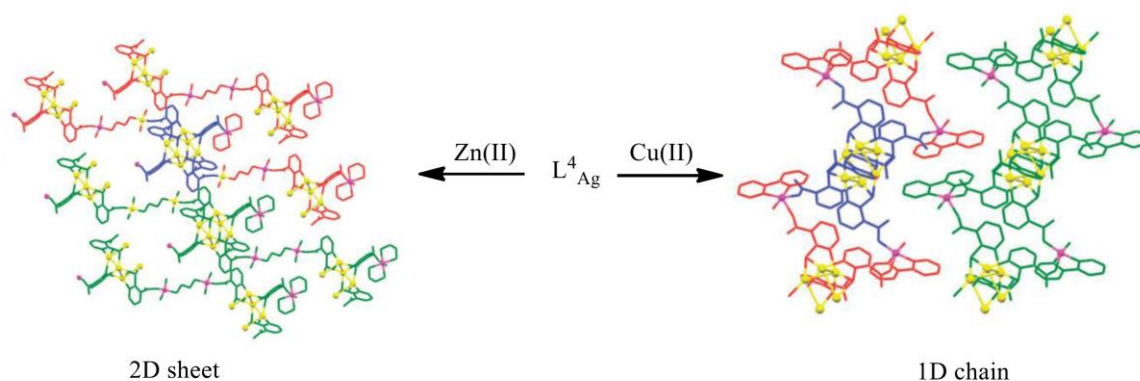


Figure 1.2. Synthesis of Zn(II) 2D sheet and Cu(I) 1D chain

Schmittl and co-workers exploited the heteroleptic phenanthroline and terpyridine¹⁸ for synthesizing a wide range of heteroleptic nanoracks,¹⁹ dumbbells,¹⁸ nanogrids,²⁰ supramolecular boxes,²¹ and nanotubular assemblies with void space,²² ladder, molecular prism²³ and molecular wheel²⁴ etc. Pyridine amide based ligands were magnificently involved in the synthesis of heterometallic complexes which are reported in the literature. Because in the presence of primary metal ion amide ligand forms structurally rigid scaffold subsequently places the appended functional groups in geometrically particular direction.

Pyridine based amide ligands have extensively used by Gupta *et al* for the construction of discreet and network based homometallic and heterometallic architectures.^{13a-25} A variety of pyridine based appended pyridine ligands were

synthesized by them in which the position of nitrogen atoms in appended pyridine ring changed i.e. 2-pyridyl, 3-pyridyl, 4-pyridyl groups (figure 1.3).^{26 27}

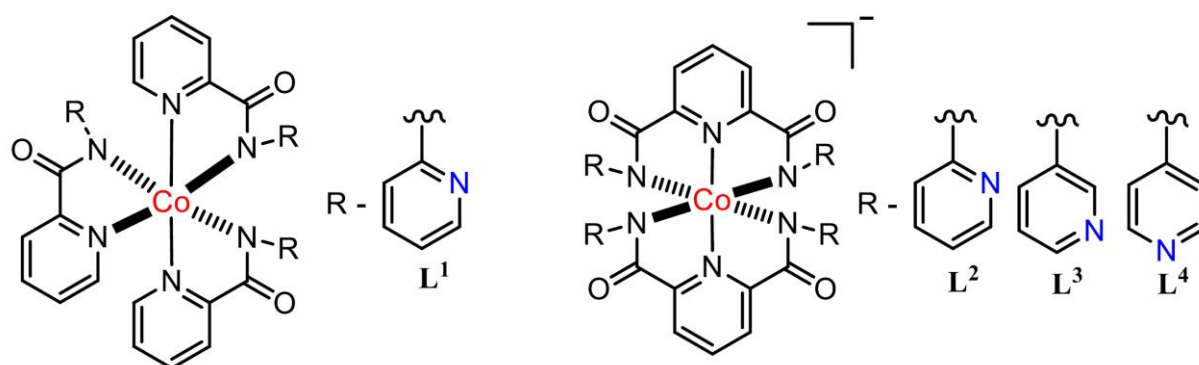
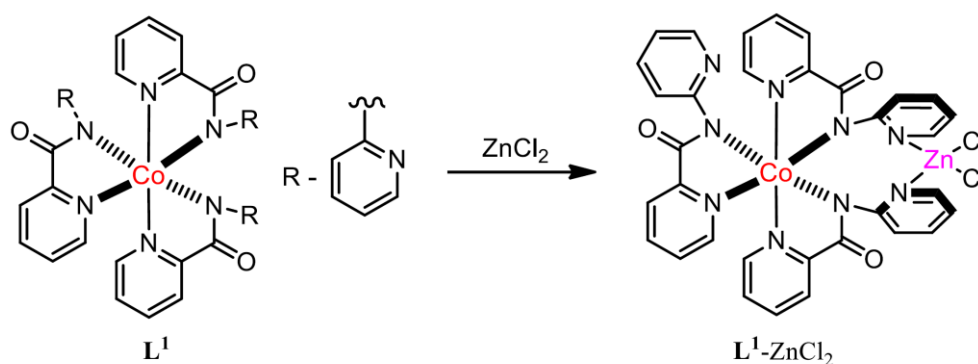
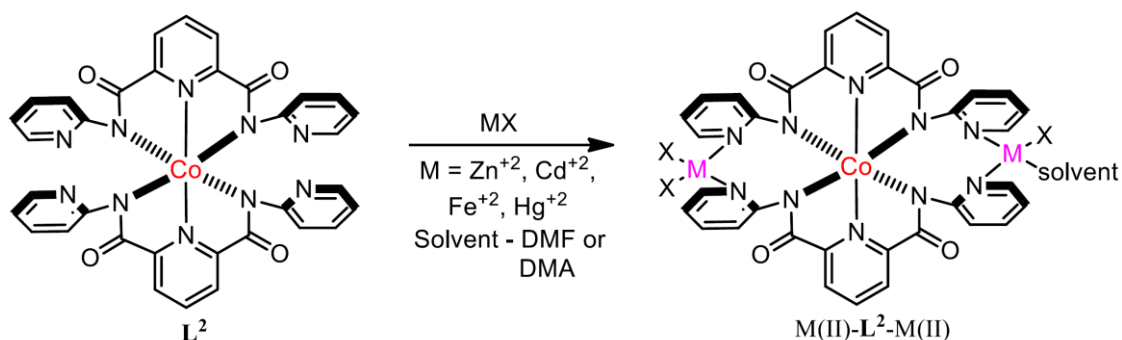


Figure 1.3. Different types of Co(III) based metalloligand

The ligands HL^1 , $H2L^{2-4}$ were deprotonated with NaOH followed by metalation with Co(II) under inert atmosphere obtained metalloligands L^1-L^4 which is converted to Co(III) ion by exposing to open air. The metalloligand having vacant coordination sites as pyridine nitrogen that can be coordinated with the different metal ions i.e. (M – Zn, Cd, Hg, Fe) resulted different heterometallic architectures. The metalloligand L^1 was coordinated with $ZnCl_2$ resulting L^1-ZnCl_2 complex (scheme 1.4-1.5).

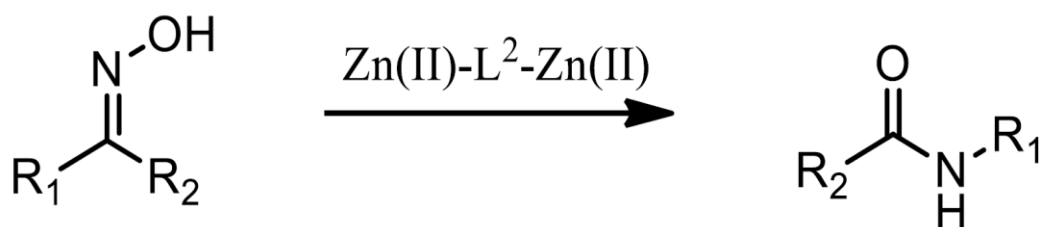


Scheme 1.4. Synthesis of L^1-ZnCl_2 complex



Scheme 1.5. Synthesis of M(II)-L²-M(II) complex

The Zn(II)-L²-Zn(II) heterometallic complex was very effective towards Beckmann rearrangement i.e. conversion of aldoxime or ketoxime to corresponding amides under acidic medium (scheme 1.6). Only ZnCl₂ was ineffective for this conversion to amide from corresponding aldoxime and ketoxime.

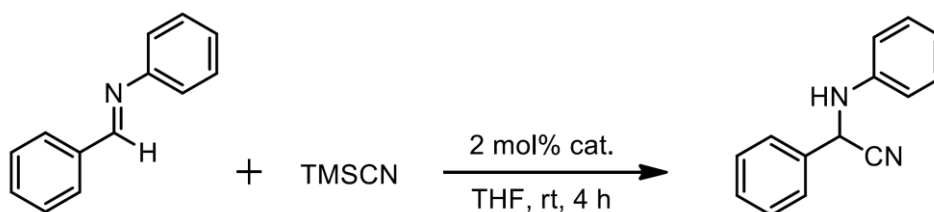


Scheme 1.6. Beckmann rearrangement catalyzed by Zn(II)-L²-Zn(II)

A range of aldoximes and ketoximes investigated were found to be successful. Aldoximes undergo conversion to only primary amides without traces of nitrile and aldehyde which are common by-products in this reaction shows the advantage of heterometallic complex. But the Cd(II)-L²-Cd(II) heterometallic complex was very ineffective for this conversion shows the uniqueness of Zn(II)-L²-Zn(II) complex.

Utmost significantly this complex can be recycled which is tested eight times without any conversion.

The catalytic activity of Cd(II)-L²-Cd(II) complex was extremely operative towards strecker synthesis which is the acid catalysed cyanation of imines to cyanohydrin. These are the significant precursors for the synthesis of α -amino acids and other heterocyclic compounds. Remarkably the Zn(II)-L²-Zn(II) heterometallic complex is virtually unsuccessful for the strecker synthesis. Generally strecker synthesis process are often use of expensive reagents, strong acidic and harsh conditions, high catalyst packing, longer reaction time resulting numerous by-products. But with Cd(II)-L²-Cd(II) heterometallic complex the reaction involves less amount of catalyst (2 mol%), lesser reaction time (4 h) under at room temperature (scheme 1.7). This displays the potential application of these type of heterometallic complexes in the catalysis.



Scheme 1.7. Strecker synthesis catalyzed by Cd(II)-L²-Cd(II) complex

The uncoordinated 3-pyridyl and 4-pyridyl groups in metalloligands L³, L⁴ reacted with different metals M(II) (M – Zn, Cd,) leads to different 2D-network instead of discrete network of heterocyclic compound as with L¹(figure 1.4 -1.5).²⁸

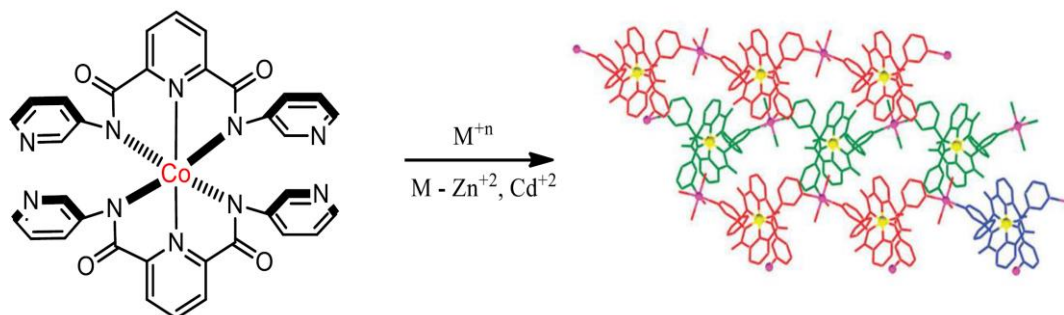


Figure 1.4. 2D network from metalloligand L^3 and Cd(II)/ Zn(II)

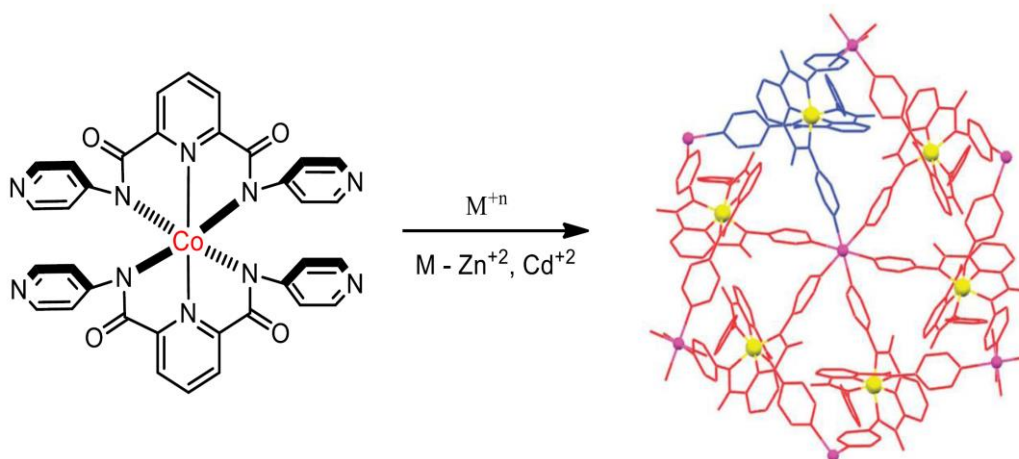


Figure 1.5. Hexagonal network from L^3 and Zn(II)

Gupta *et al* synthesized two heterodimetallic coordination polymers Co(III)-L-Eu(III) and Co(III)-L-Tb(III) using Co(III) metalloligand as a building block.²⁹ In this two heterometallic complexes lanthanide atoms are coordinated to cobalt complex by amide oxygen atoms which resulted a zigzag one dimensional polymeric network. Also individual chains coordinated together resulted several 2D polymeric network. They treated building block **1** with exact amount of $\text{Ln}(\text{OTf})_3$

in presence of methanolic solution and obtained heterometallic complex **2** and **3** (figure 1.6 -1.8).

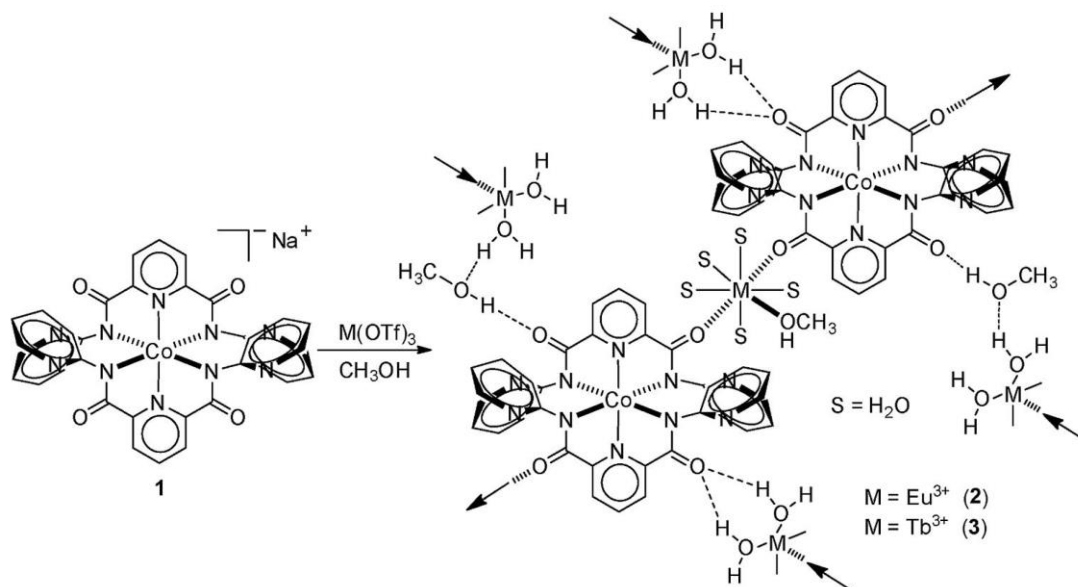


Figure 1.6. Heterometallic complex with Eu(III)/Tb(III)

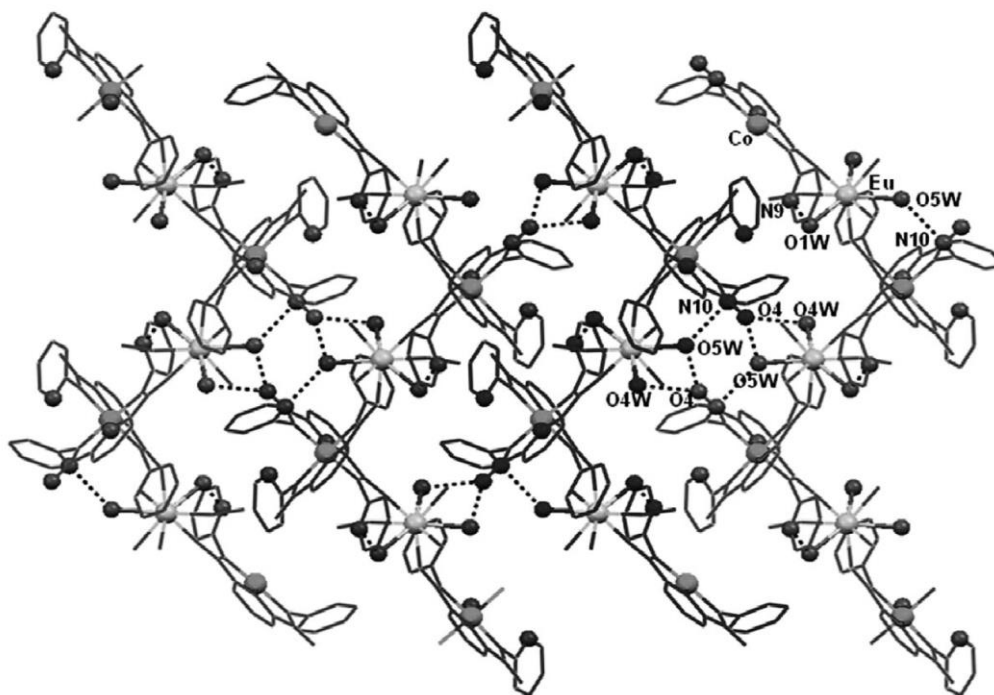


Figure 1.7. Packing diagram showing weak interaction of **2**

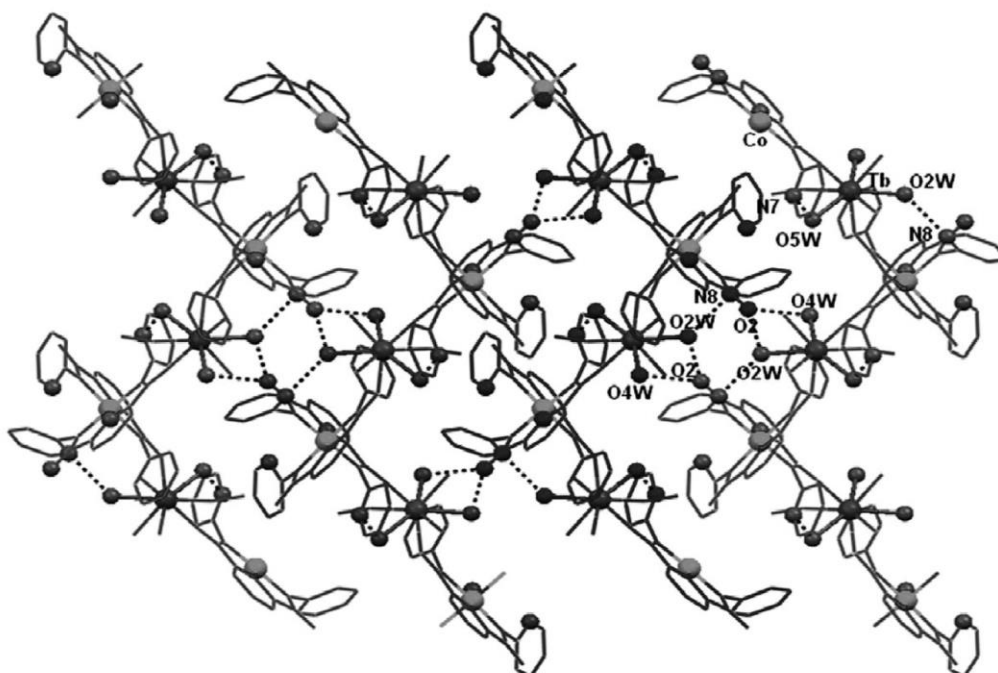
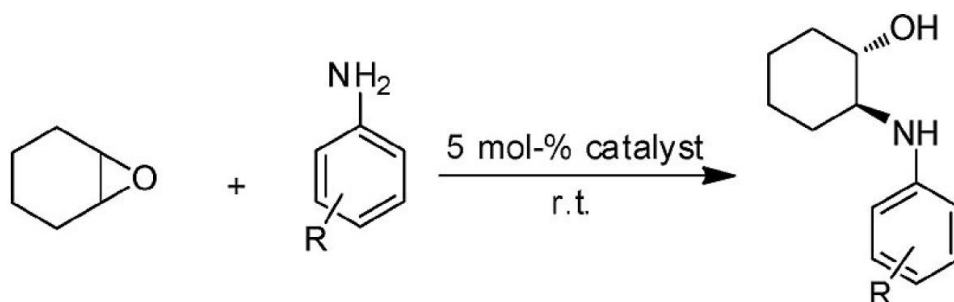
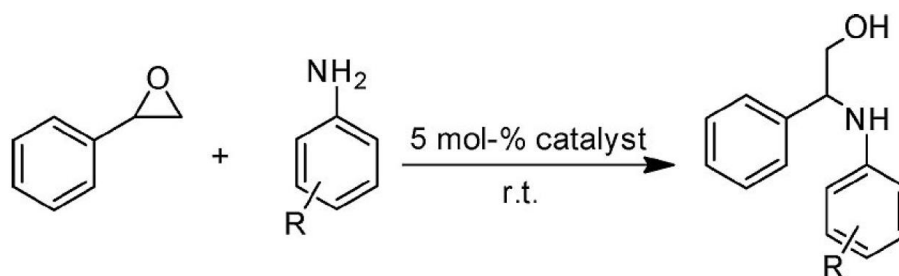


Figure 1.8. Packing diagram showing the weak interaction of **3**

These coordination polymers were used as a catalyst for several organic transformations. These are ring-opening reactions of epoxides with anilines and alcohols under solvent-free and heterogeneous conditions amination and alcoholysis ring-opening reaction of styrene oxide (scheme 1.8 -1.9).

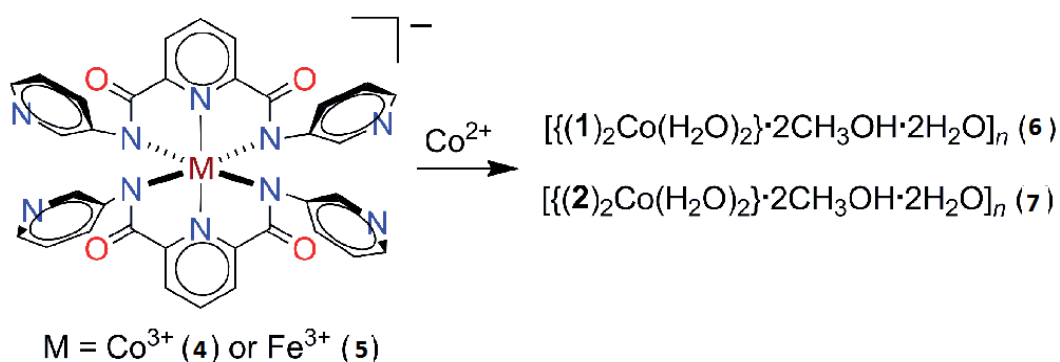


Scheme 1.8. Ring opening of epoxide catalyzed by **2** and **3**



Scheme 1.9. Ring opening of epoxide catalyzed by **2** and **3**

After that the same group synthesized Co(III)-L-Co(II) two-dimensional homodimetallic (figure 1.9) and Fe(III)-L-Co(II) heterodimetallic coordination polymer with Co(III) and Fe(III) based metalloligands.³⁰ Here the metalloligands are coordinated through Co(II) ions. In this system, the metalloligand **4** and **5** reacted with $\text{Co}(\text{NO}_3)_2 \cdot 6\text{H}_2\text{O}$ under methanolic solutions resulted homometallic Co(III)-Co(II) complex and heterometallic Fe(III)-Co(II) complexes (scheme 1.10 and figure 1.9).



Scheme 1.10. Synthesis of Homometallic complex Co(III)-Co(II) Hetero metallic complex Fe(III)-Co(II)

Due to lewis acidic behaviour as well as kinetic labile nature of Co(II) ions, these homometallic and heterometallic complex are used as a heterogeneous catalyst in different organic reactions i.e. knoevenagel condensation³¹ and cyanation of aldehydes.³²

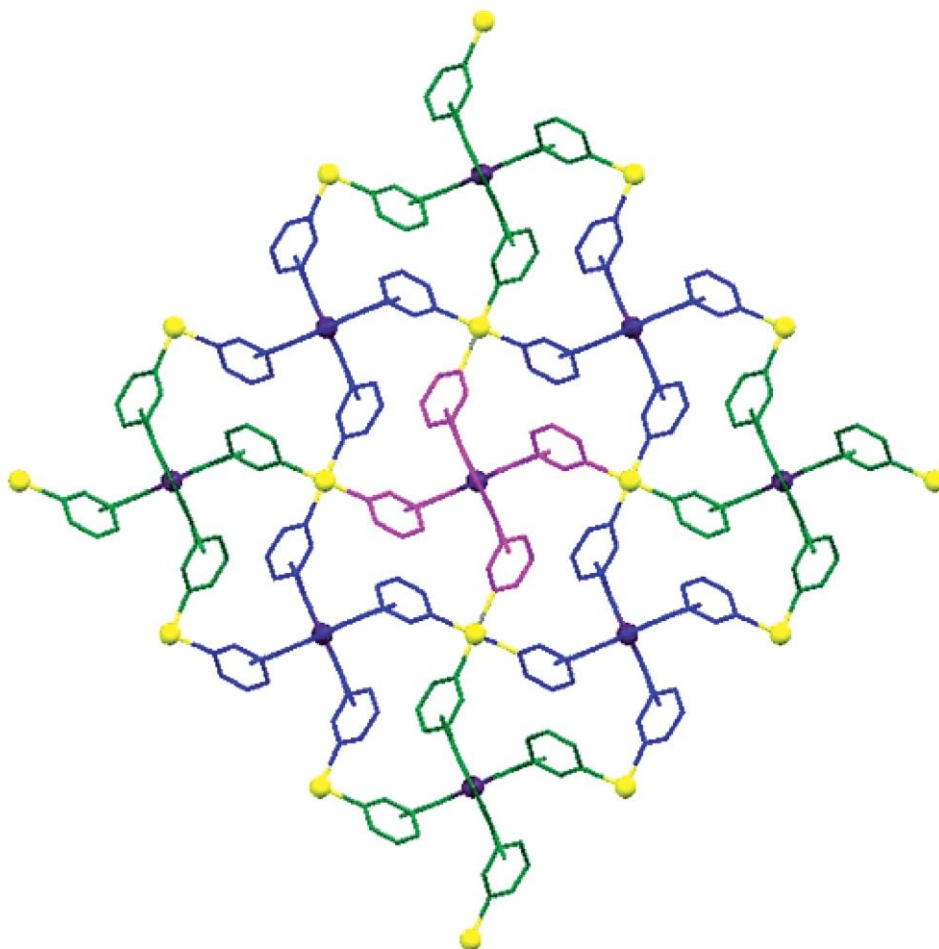
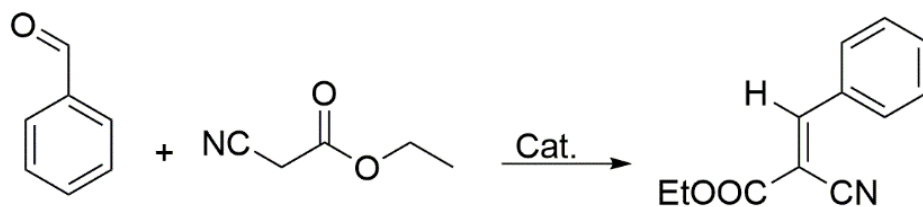


Figure 1.9. Coordination polymeric network of **6** along crystallographic b-axis

They described knoevenagel condensation as the oxygen based substrate utilized to displace the coordinated water molecules in presence of this heterogeneous catalyst **6**. This resulted carbon carbon double bond species. Here benzaldehyde treated with

ethyl cyanoacetate or malononitrile under xylene at 100 °C obtained ethyl-2-cyano-3-phenylacrylate and 2-benzylidenemalononitrile etc (scheme 1.11).



Scheme.1.11. Knoevenagel reaction catalyzed by complex 6

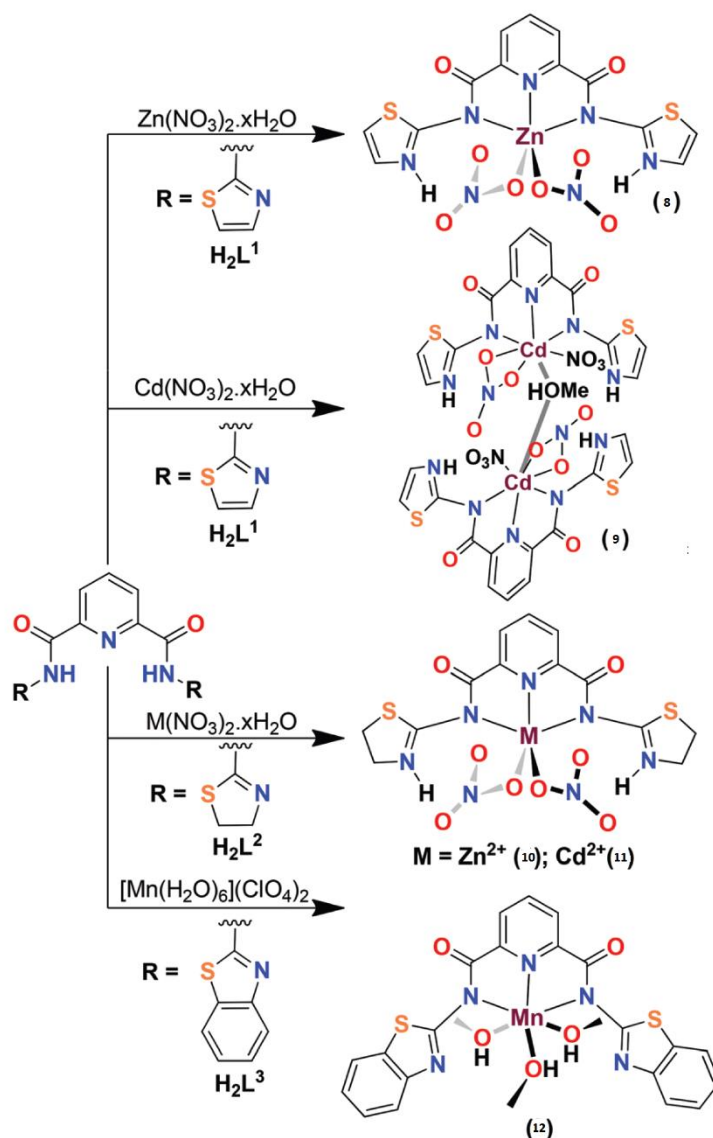


Figure 1.10. Optimized route for synthesis of complex 8 -12

Pyridine-2, 6-dicarboxamide ligands holding benzothiazole, thiazole, and thiazoline appended group were utilized for the synthesis of several mononuclear complexes with different metals.³³ The metal ions Zn(II), Cd(II) and Mn(II) were coordinated with amide ligands resulted Zn²⁺ (**8** and **10**), Cd²⁺ complexes (**9** and **11**), and a Mn²⁺ complex (**12**) (figure 1.10 -1.13). Here proton shift from amidic N-H to heterocyclic moiety resulted metal complexation. The deprotonated form of these ligands makes a pincer cavity through two amide group and attaching pyridine hold the metal ions. And the hanging functional groups are used for secondary metal coordination.³⁴ In all these complexes the ligand creates a meridional N3 site to coordinate metal and remaining sites are occupied by NO₃⁻ ions.

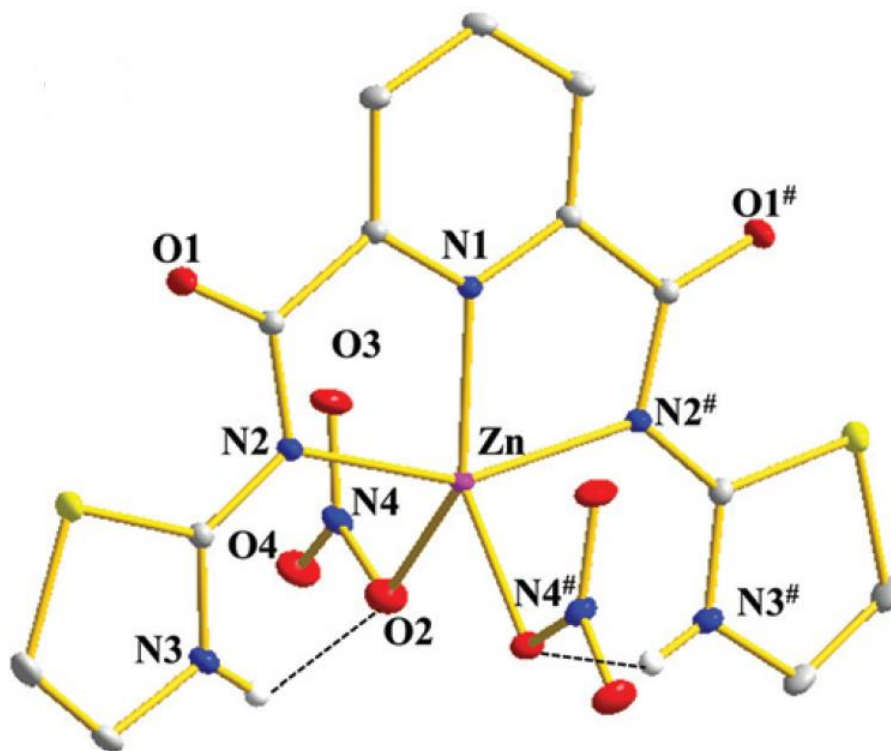


Figure 1.11. single X-ray crystal structure of **8**

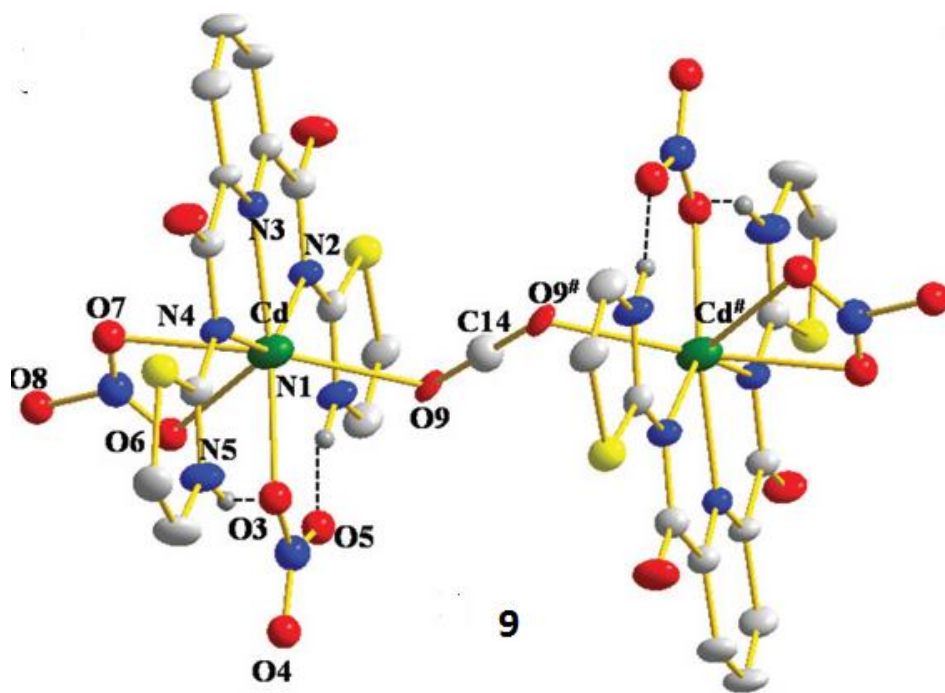


Figure 1.12. Single X-ray crystal structure of 9

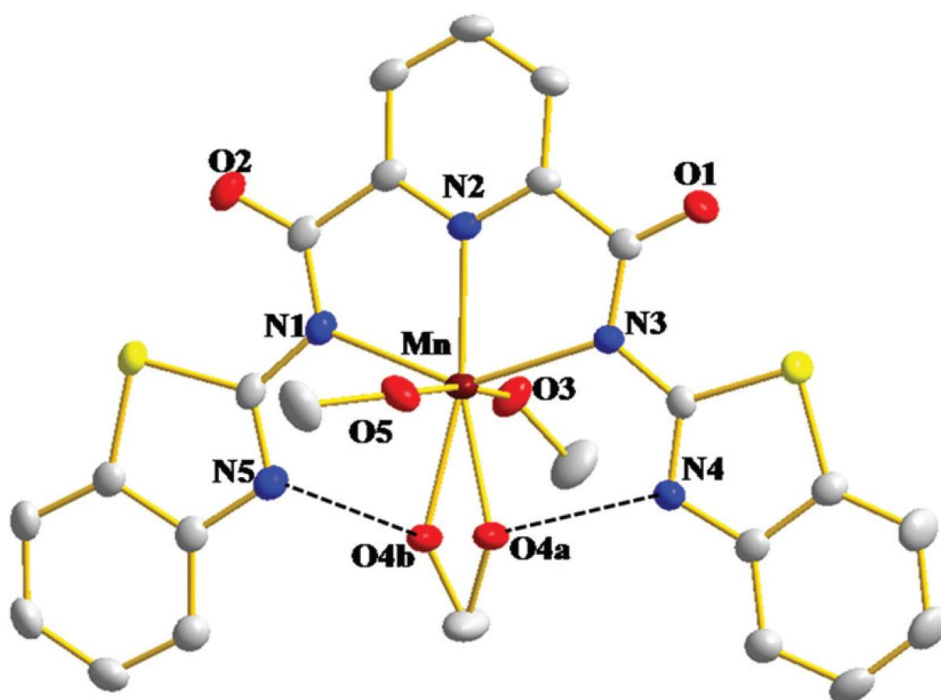
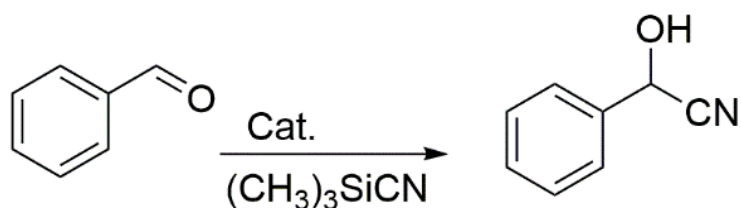
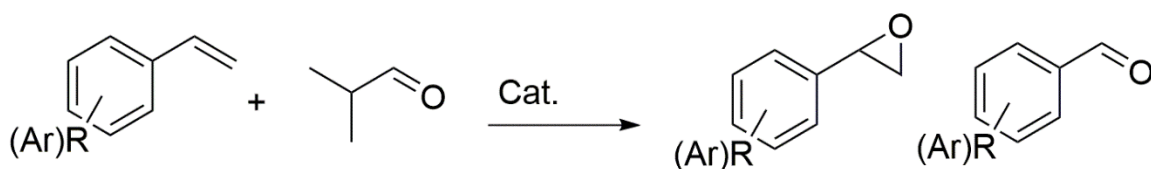


Figure 1.13. Single X-ray crystal structure of 12

Pyridine-2,6-dicarboxamide ligands appended with pyridine, pyrimidine or quinolone rings is utilized by Fiedler and co-workers to organise L-Cu(II) complexes.³⁵ Wright and co-workers have also recycled an analogous ligand to organise a Ru(II) complex where chloro ligand are coordinated through H-bond with protonated pyridine rings.³⁶ The Zn²⁺ (**8** and **10**), Cd²⁺ complexes (**9** and **11**) did not show any catalytic behaviour but Mn²⁺ (**12**) complex are further utilized as an excellent heterogeneous catalyst in various organic transformation i.e. cyanohydrin formation from aldehyde (scheme 1.12) and epoxidation of carbon carbon double bonds (scheme 1.13).



Scheme 1.12. Cyanohydrin formation with catalyst **8** -**12**



Scheme 1.13. Epoxide synthesis with catalyst **12**

Heterometallic coordination complex of Co(III)-Zn(II) and Co(III)- Cd(II) were synthesized by Gupta and co-worker by utilising Co(III) metalloligands contain the side chain as hanging aryl dicarboxylic acid group.³⁷ Such appended acid group were linked through secondary metal atoms resulting three dimensional

coordination network. $\text{Zn}(\text{OAc})_2 \cdot 2\text{H}_2\text{O}$ (figure 1.14 and 1.16) and $\text{Cd}(\text{OAc})_2 \cdot 2\text{H}_2\text{O}$ (figure 1.15 and 1.17) are used for this network formation.

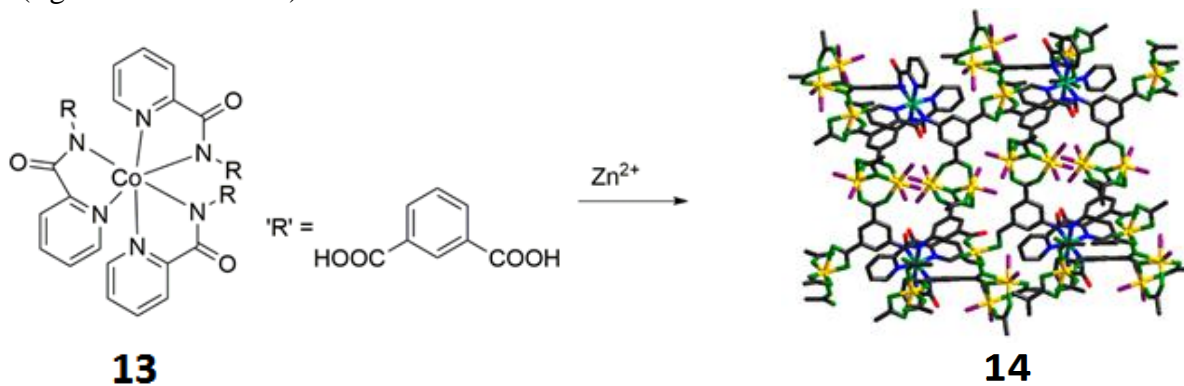


Figure 1.14. Coordination of cobalt based metalloligand with zinc(II)

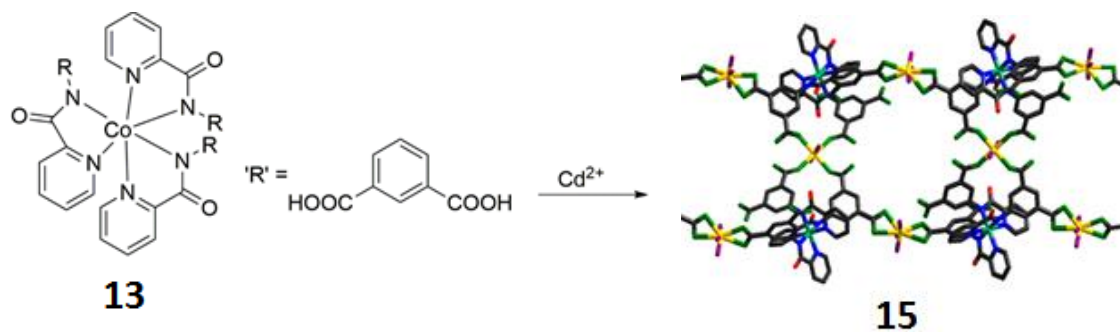


Figure 1.15. Coordination of cobalt based metalloligand with Cadmium(II)

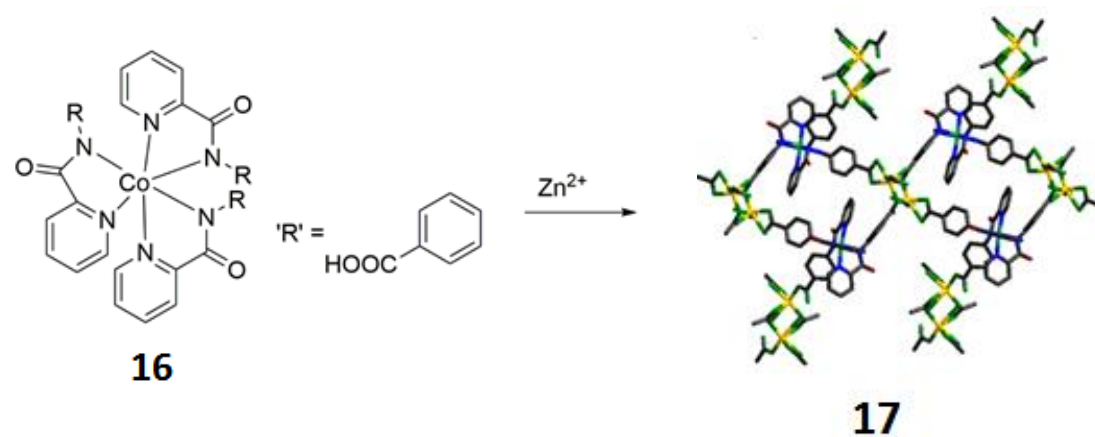


Figure 1.16. Coordination of cobalt based metalloligand with Zinc(II)

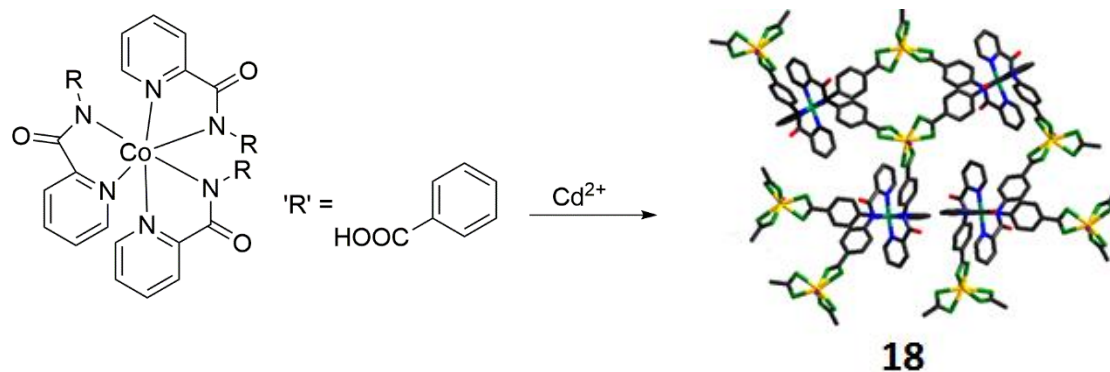


Figure 1.17. Coordination of cobalt based metalloligand with Zinc(II)

The coordination networks are used as heterogeneous catalyst in knoevenagal type condensation reaction.

Three different heterometallic coordination polymers are synthesized from the metallo ligand having appended four dicarboxylic acid groups. These heterometallic complexes are synthesized by varying different types of metal ions as Zn^{2+} , Cd^{2+} and Mn^{2+} .³⁸ From the topological studies it indicates that metalloligand behaves like a node which were linked to secondary building unit. The secondary building units are composed of different metals Zn^{2+} , Cd^{2+} and Mn^{2+} which are joined by carboxylate groups (figure 1.18 - 1.23). These three dimensional heterometallic polymers find potential applications in heterogeneous catalysis.

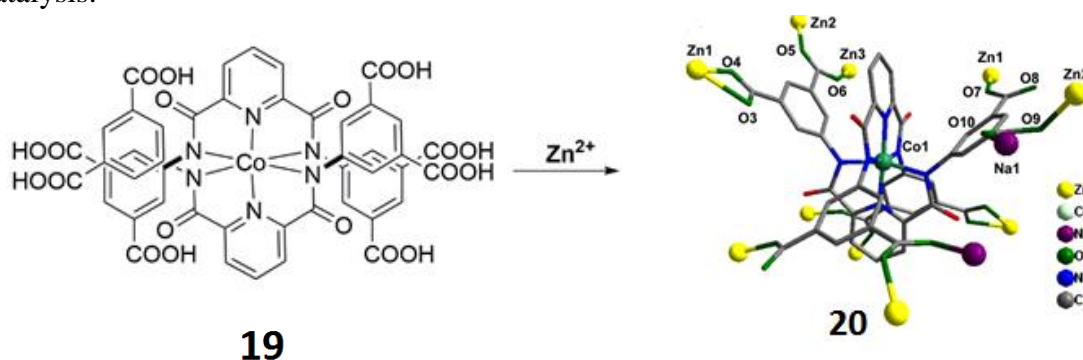


Figure 1.18. Coordination of carboxylic acid based metalloligand with zinc(II)

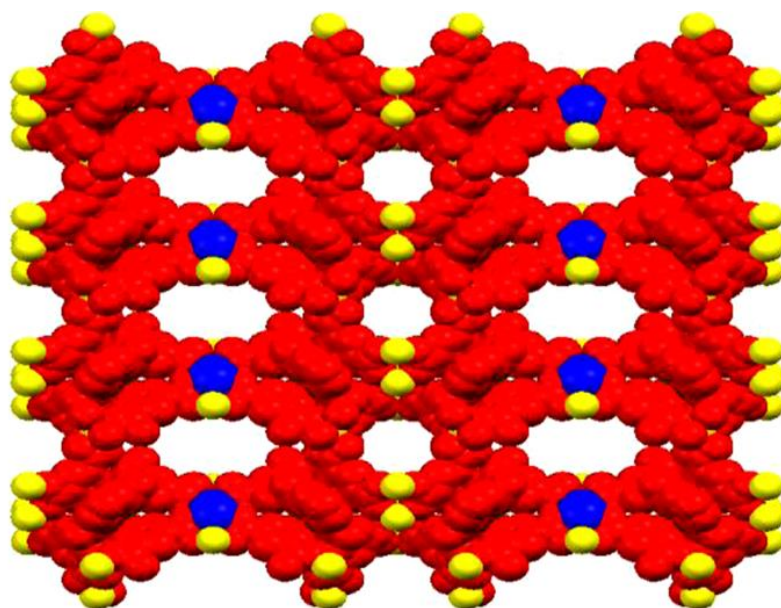


Figure 1.19. Space filling model Heterometallic complex **20**



Figure 1.20. Coordination of carboxylic acid based metalloligand with zinc(II)



Figure 1.21. Coordination of carboxylic acid based metalloligand with zinc(II)

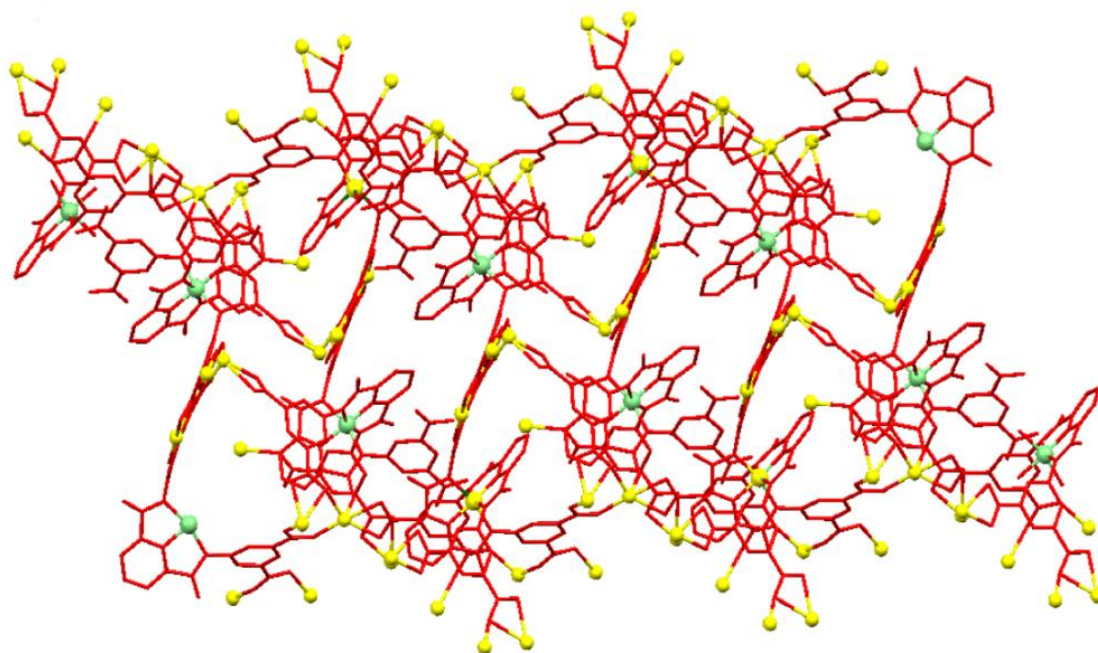


Figure 1.22. X-ray crystal structure of heterometallic complex **21**

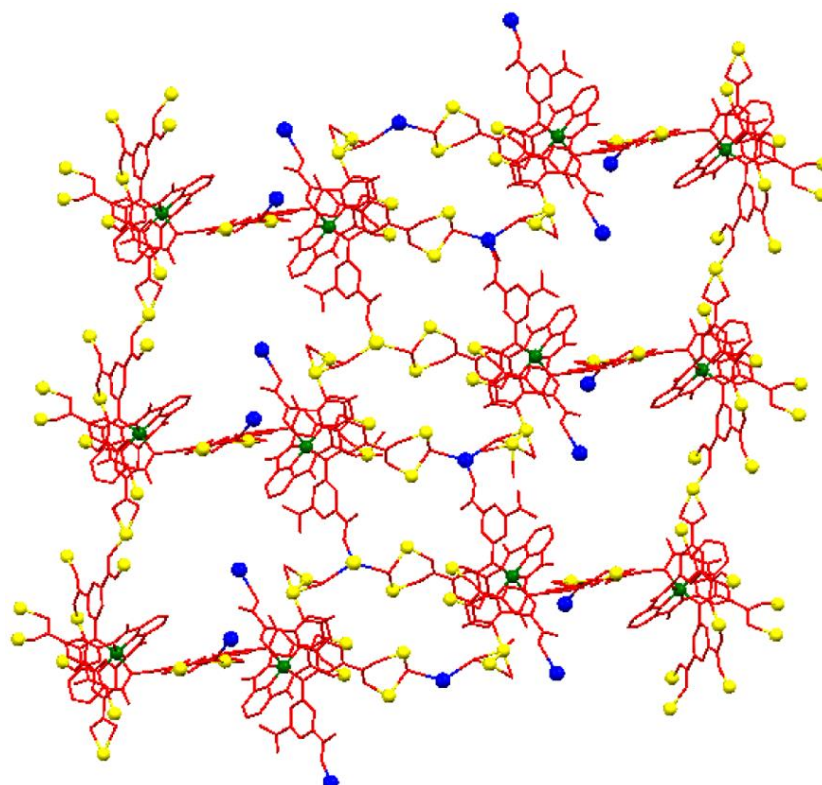
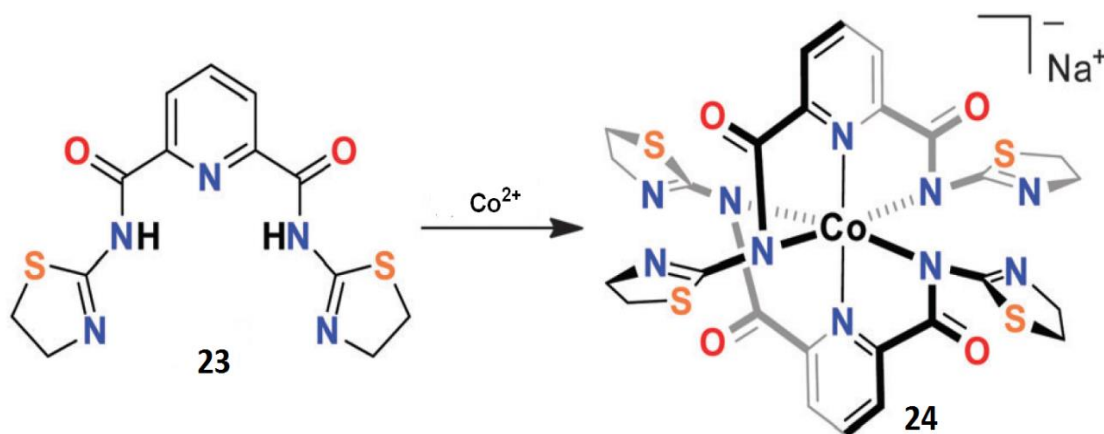


Figure 1.23. X-ray crystal structure of heterometallic complex **22**

Again the same group also reported three heterometallic coordination polymers with the metal Zn, Cd and Hg.³⁹ In these heterometallic complex, the metalloligand contains octahedral Co^{3+} core with the hanging thiazoline rings (scheme 1.14). These tridentated hanging thiazoline units are utilized for secondary coordination to metal ions (figure 1.24-1.26).



Scheme 1.14. Synthesis of thiazoline based metalloligand

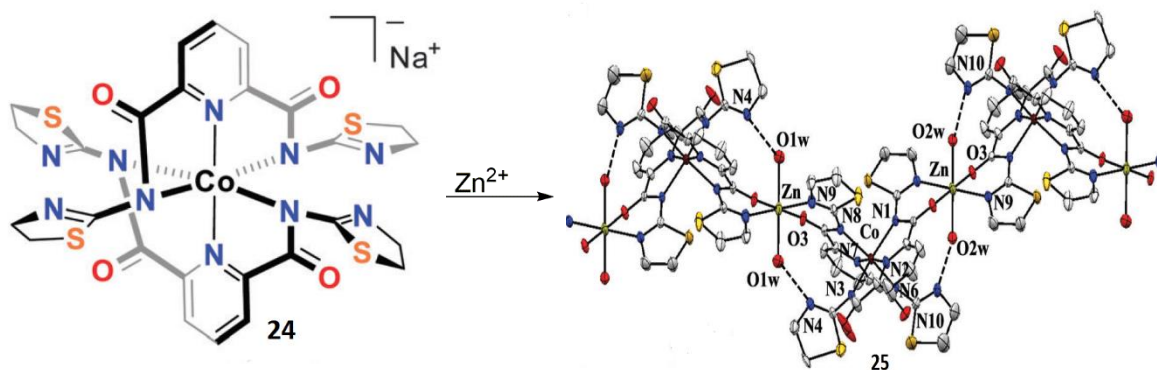


Figure 1.24. Hetero metallic complex 25 from 24

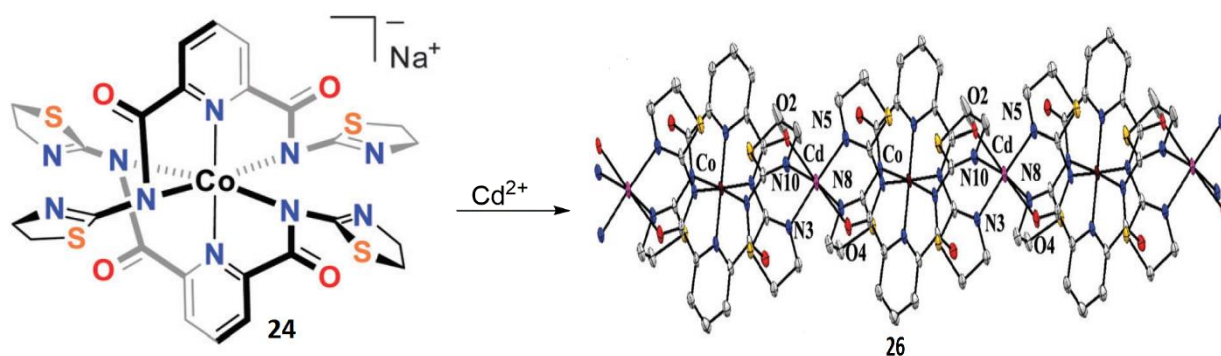


Figure 1.25. Hetero metallic complex 26 from 24

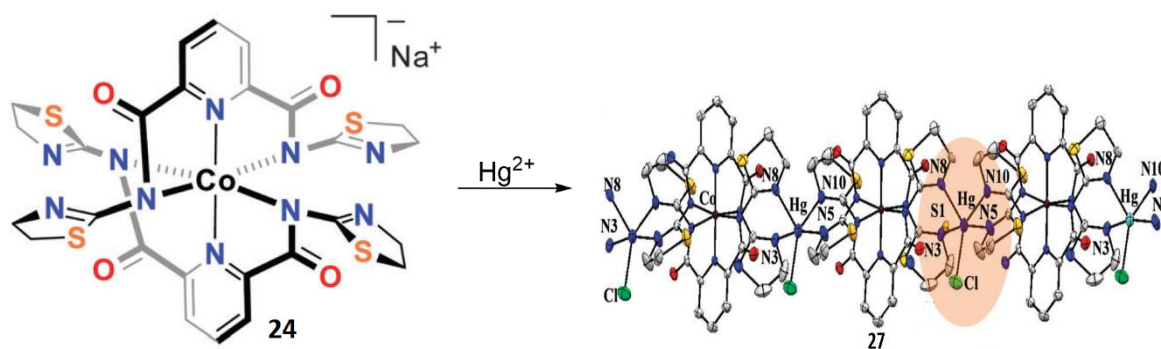
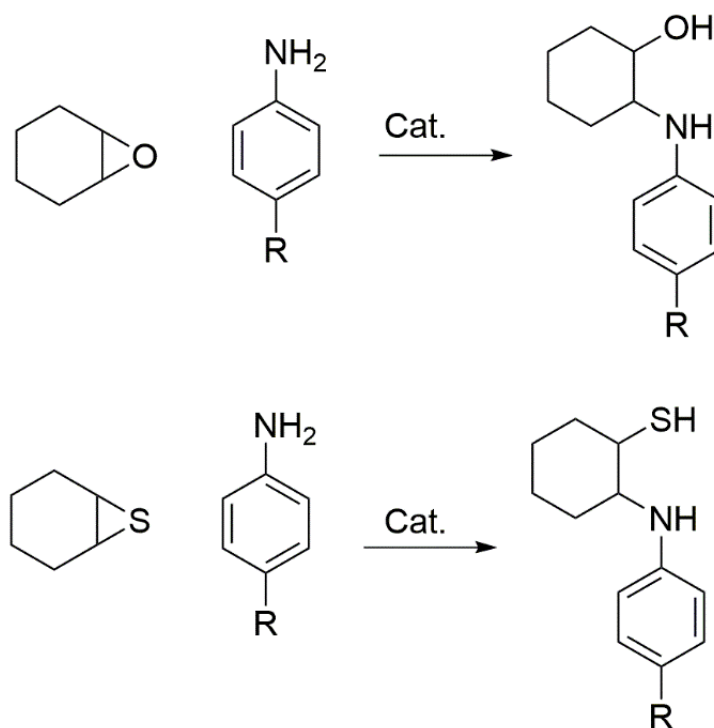
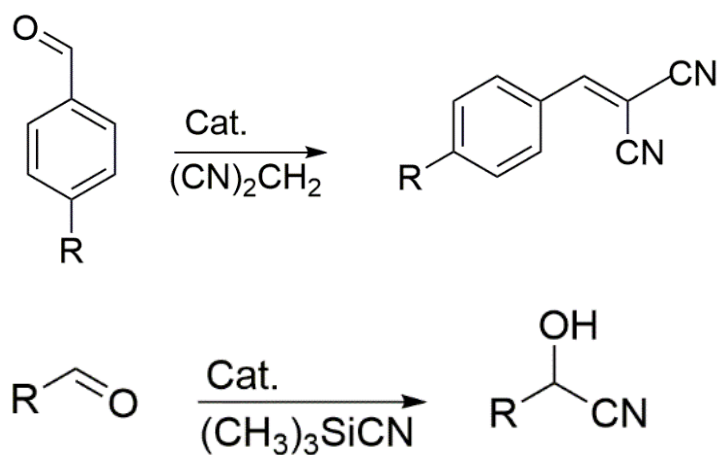


Figure 1.26. Hetero metallic complex 26 from 24

These heterometallic coordination polymeric networks play a significant role in heterogeneous catalysis for cyanohydrin formation from aldehydes and carbothialdehyde, knoevenagel condensation and oxiranes and thiaranes ring opening reactions. Ring opening of oxiranes and thiaranes with several nucleophiles are of vast interest because these products formed from them plays an important role in chemically and pharmaceutically research.⁴⁰ Oxirane and thiarane treated with p-substituted aniline in presence of heterogeneous catalyst (scheme 1.15). They formed substituted amide by ring opening reaction.

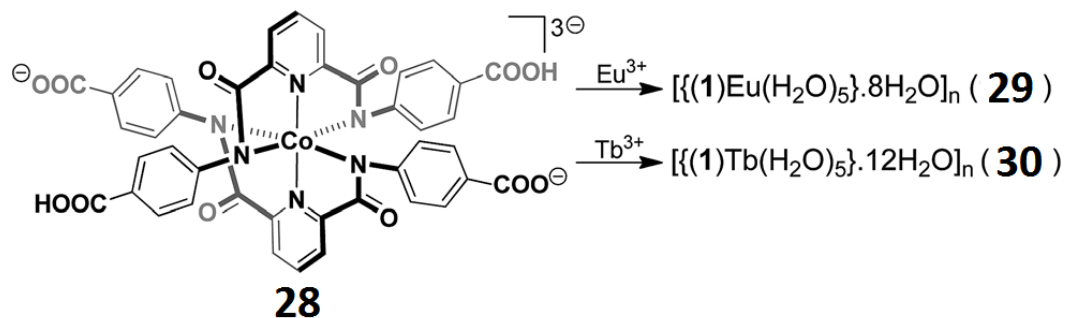


Scheme 1.15. Ring opening reaction of oxirane and thairane with heterogeneous catalyst



Scheme 1.16. Cyanation reaction catalyzed by heterogeneous catalyst

Substituted aldehyde and malanonitrile involved knoevenagel condensation in presence of heterogeneous catalyst resulted new carbon carbon bond formation (scheme 1.16).



Scheme 1.17. Synthesis of heterometallic complex with Eu(III) and Tb(III)

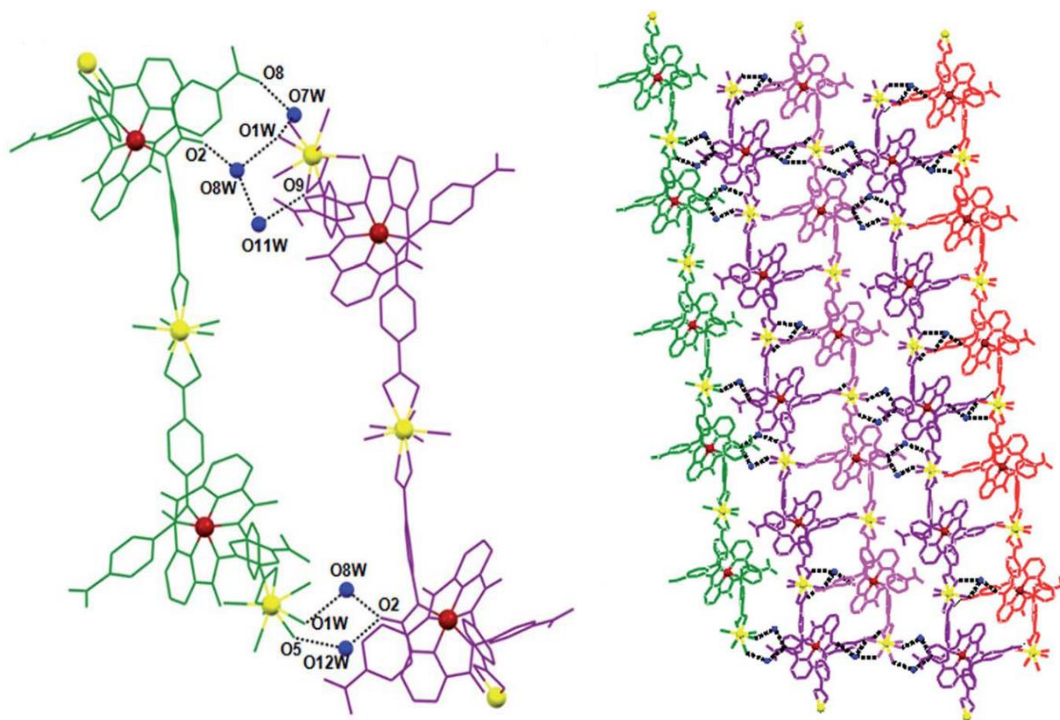


Figure 1.27. X-ray showing the 1D and 2D arrangement of heterometallic polymer of Eu(III)

A range of metalloligands reported by same group with high capacity of H-bond formation and can coordinate to profound functional group. Another report by same group based on the synthesis of coordination polymer with Eu(III) and Tb(III) (scheme 1.17).⁴¹ The coordination polymeric network was synthesized from the Co(III) based metalloligands with hanging tetra acid groups (figure 1.27 and 1.28). These two coordination polymers act as a recyclable heterogeneous catalysts in the ring-opening transformation exploiting various nucleophiles.

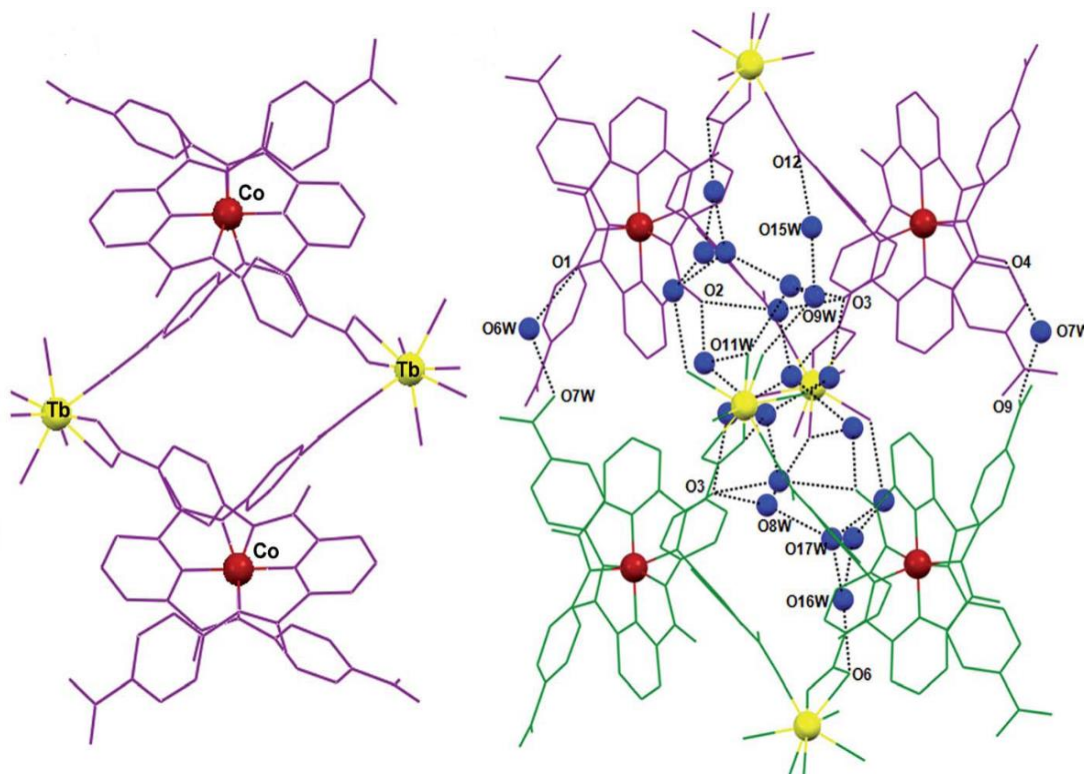
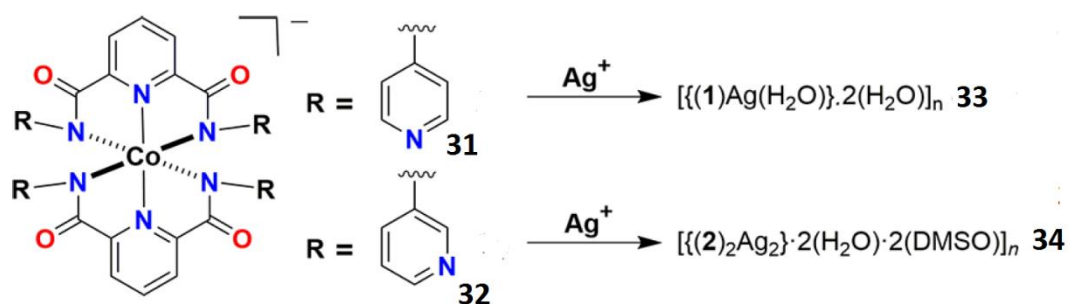


Figure 1.28. X-ray showing the 1D arrangement of heterometallic polymer of Tb(III) with water molecules by hydrogen bonding



Scheme 1.18. synthesis of heterometallic complex **33** and **34**

Gupta *et al* synthesized two Ag^+ based coordination polymeric network from the Co(III) based metalloligand (figure 1.29 -1.32).⁴² This metal ligand having hanging pyridyl groups which coordinated to secondary metal ion Ag^+ (scheme 1.18). In coordination polymer **33**, polymeric network shift from two to three dimensional polymeric network because of argentophilic exchanges. These two coordination polymer display interesting topology due to binding of silver(I) to metalloligands.

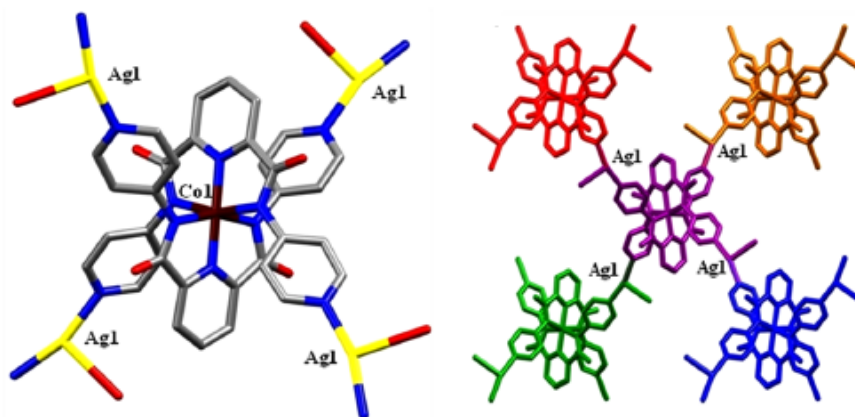


Figure 1.29. X-ray crystal structure showing 2D polymeric network of **33**

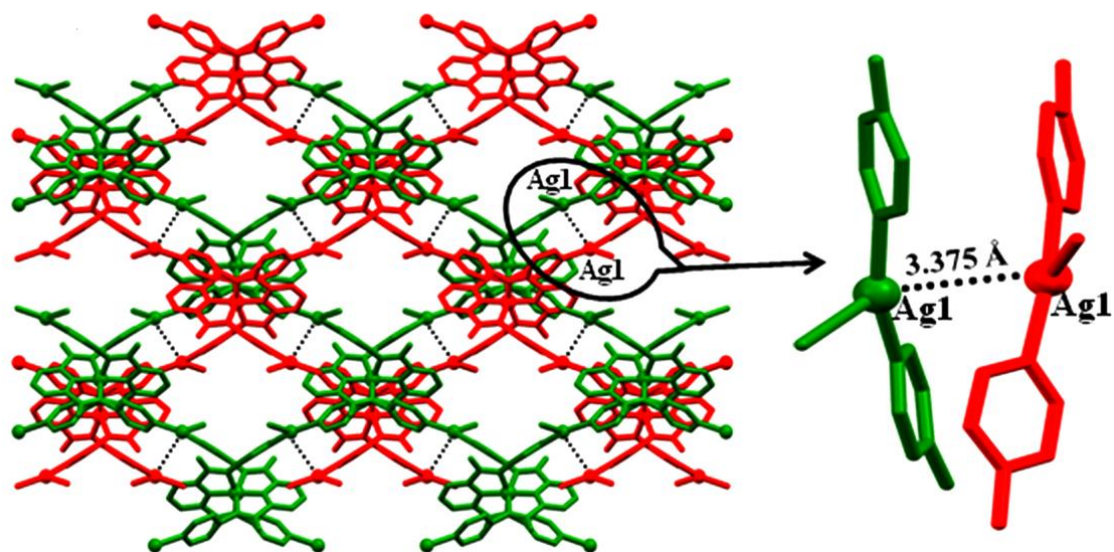


Figure 1.30. X-ray crystal structure showing argentophilic interaction of 2D polymeric network of **33**

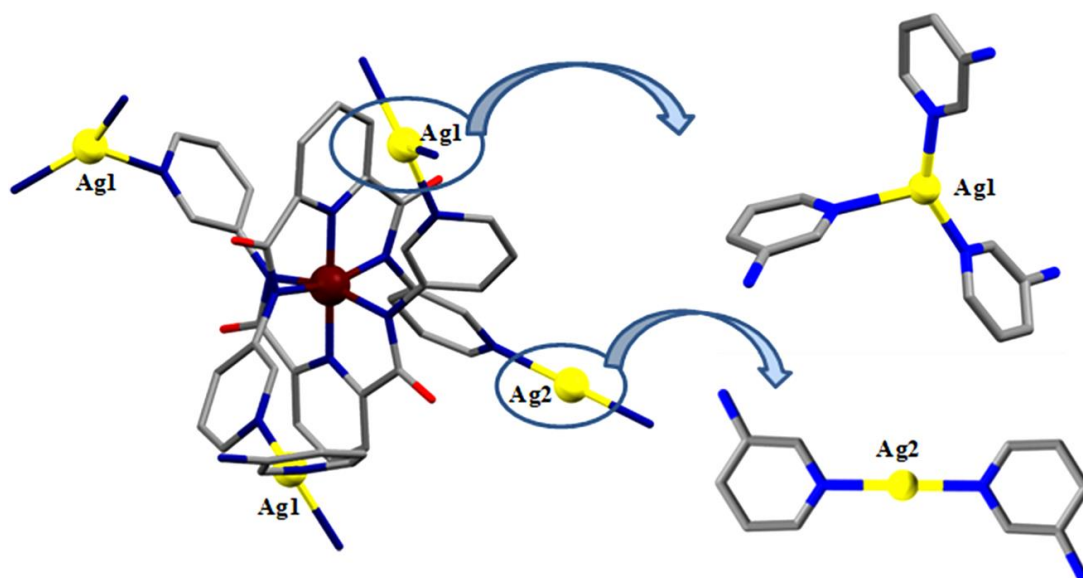


Figure 1.31. Partial X-ray crystal structure of **34** showing coordination to Ag(I)

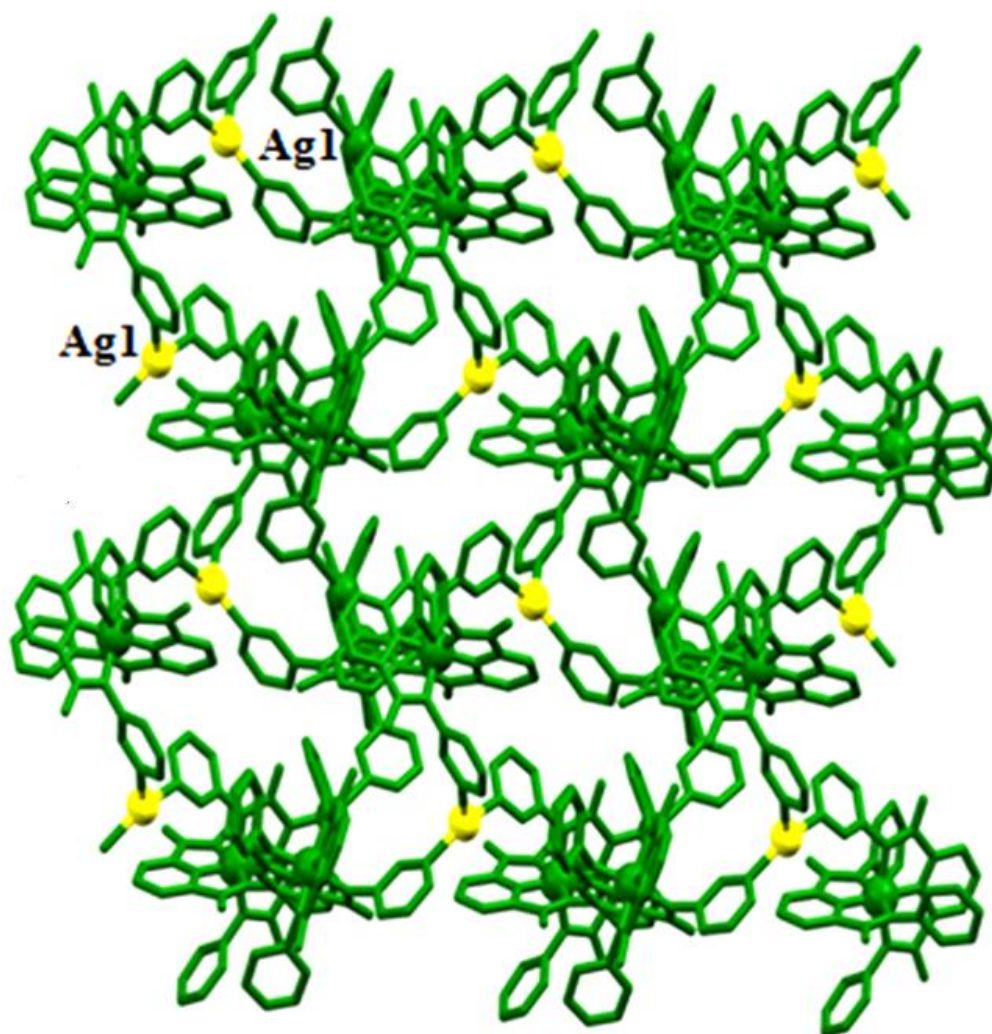
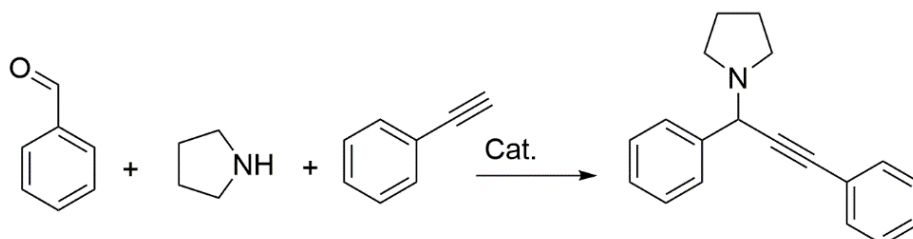


Figure 1.32. Packing diagram of complex **34** showing coordination to Ag(I)

The metalloligand in DMSO solution was layered on the aqueous solution of silver trifluoroacetate. To this medium again tertiary butanol was layered and kept under dark for crystallization. Light green coloured crystal of **1** was grown in 5-7 days.

These coordination polymer **33** and **34** are further utilized in A3 coupling of different compounds i.e. aldehyde, alkynes and 2° amine (scheme 1.19).



Scheme 1.19. A3 coupling reaction catalyzed by heterogeneous catalyst **33** and **34**

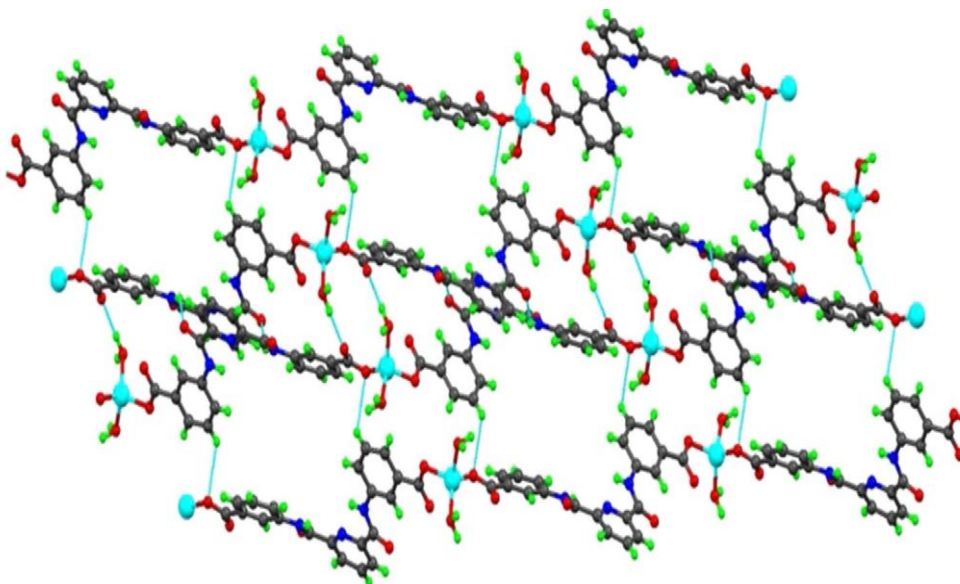


Figure 1.33. Partial X-ray crystal structure of **35** showing coordination to Zn(II)

Pombeiro and Coworkers synthesized coordination polymer as well as metallomacrocyclic with different metal salt as Zn^{2+} , Cd^{2+} and Sm^{2+} . here they have utilized 3,3'-[(pyridine-2,6-dicarbonyl)-bis(azanediyl)]-dibenzoic acid as the precursor ligand.⁴³ The corresponding ligand oriented in various conformations i.e. syn-syn for the compound **35** and anti – anti for the compound **36** and **37**. **35** and

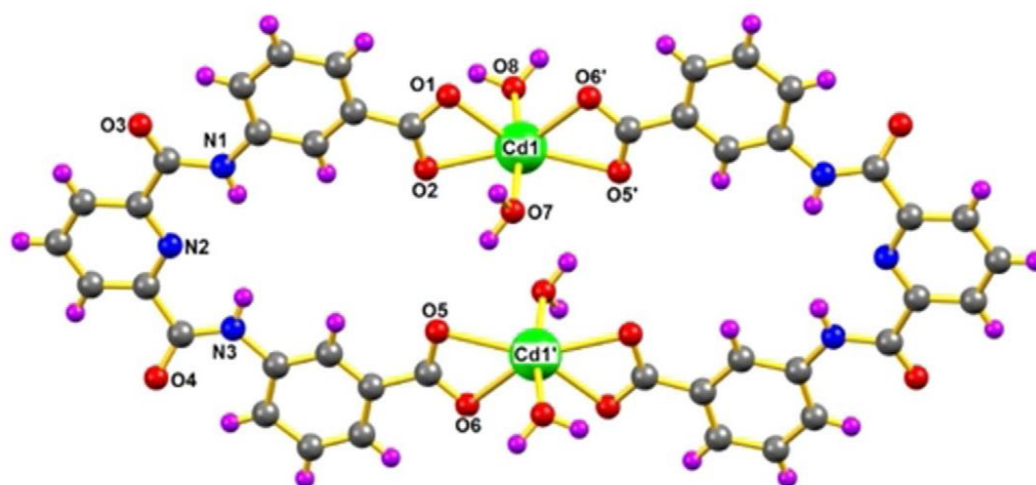


Figure 1.34. Partial X-ray crystal structure of **36** showing coordination to Cd(II)

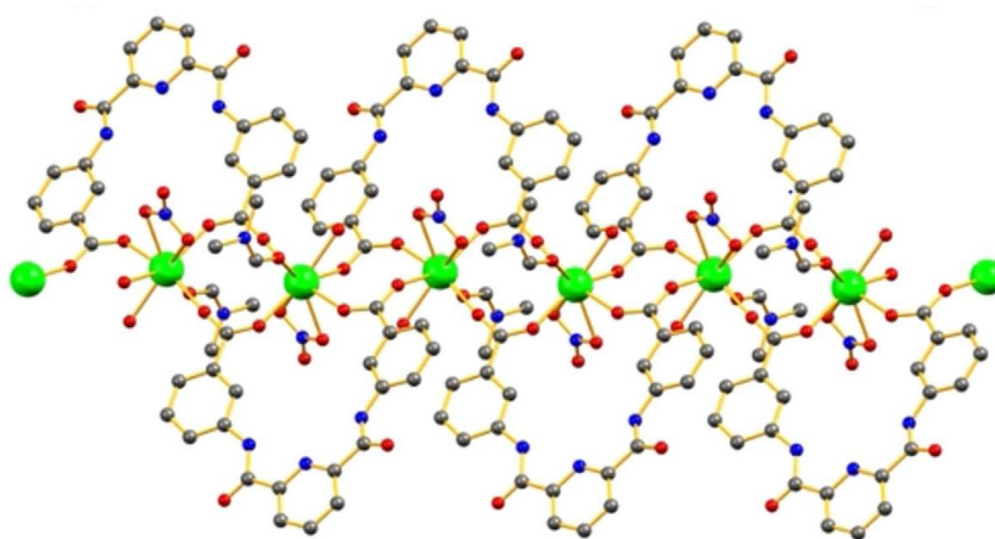
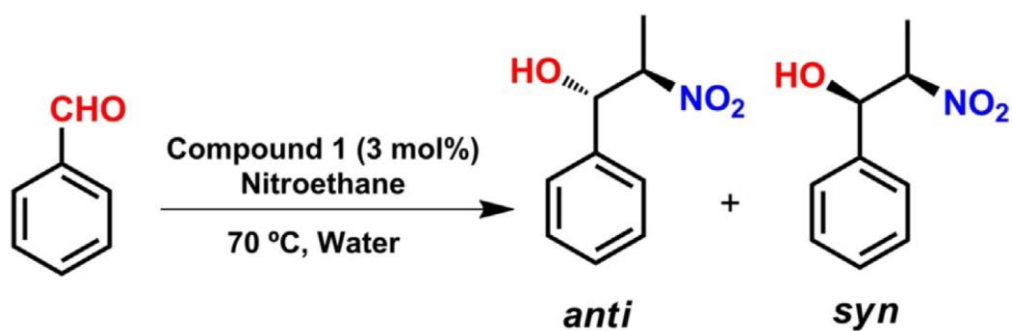
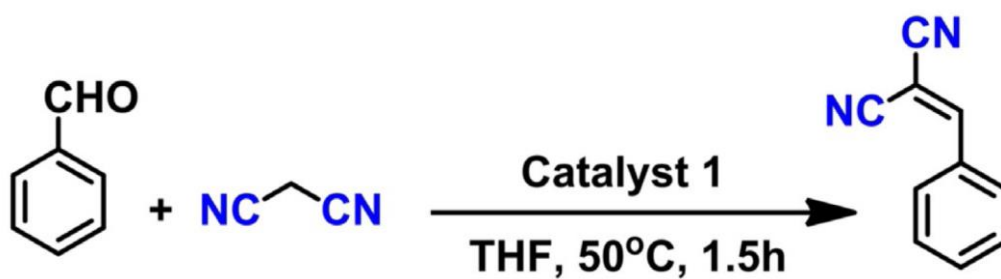


Figure 1.35. Partial X-ray crystal structure of **37** showing coordination to Sm(II)

37 forms one dimensional zigzag network and double chain arrangements, but **36** topographies a binuclear metallomacrocycle complex (figure 1.33 – 1.35).



Scheme 1.20. Henry reaction catalyzed by 35



Scheme 1.21. Knoevenagel reaction catalyzed by 35

These compounds are further used as heterogeneous catalysis in Knoevenagel and Henry reaction of various aldehydes.

Part II

1.2. Interlocked architectures

A vital feature of living organisms is the capacity to construct a highly complex structure from the comparatively simpler components. Although similar building units are arranged around large number of structure by thermodynamically control process. The biological arrangements with highest range of compartmentalization have developed from an impulsive self-assembly process. However covalent procedure was recycled to manufacture smaller molecules by kinetic controlled reaction. The formation of product depends highly on the reaction condition and proper choice of component to get targeted product.

The beginning of supramolecular chemistry lies in the introduction of *coordination theory* in 1893 by Alfred Werner and followed the *lock-and-key* concept in 1894 by Emil Fischer. The neglected non covalent interactions such as coordinative bond, ion-dipole, dipole-dipole, hydrogen bonding, π - π and van der Waals etc. are vastly used in the early 1960s by Lehn, Cram and Pederson to build definite supramolecular structures. From the *coordination theory* Werner proposes the coordination number (CN) had the oxidation number of the metal atom in a molecular system. Werner could suggest the correct geometry with structures of the coordination compounds by assigning the numbers and nature of the isomers obtained. However, very soon it was conceived as an independent research field of chemical research. Mostly, the coordination number varies with size of the metal ion and coordinating ligands. Also, in case of bonding between metal ion and ligands the *thermodynamic trans effect* and *kinetic trans effect* also play an

important role. With time, the coordination chemistry has become an integral part of supramolecular chemistry. However, applying the new techniques in supramolecular chemistry concerning the economic point of views are the most challenging for the researchers in recent years. One of the most recent developments in supramolecular chemistry has been sub component self-assembly, wherein the ligands of the metallo-supramolecular complexes are formed *in situ* from their subcomponents. The other way it is called as system chemistry. This emerging field allows to design complex networks, and might even give knowledge to understand the origin of life. In most cases, imine bonds were formed and the ligands as well as the corresponding complexes were achieved simultaneously.

The important aspect of supramolecular chemistry is to develop more functional and nanosized structure. Large supramolecules are obtained from the small building precursor by using the noncovalent interaction. Generally nature accumulate the simple precursors into very critical biomolecules by utilising the non-covalent interactions. But complex supramolecular architectures were constructed from simpler building precursor by utilising the self-assembly process with the formation of coordinate and covalent bonds. The research on molecular self-assembly thus branches out from the core discipline of synthetic chemistry into the areas of topology, materials science, and nanotechnology and will have a multidisciplinary impact that reaches beyond the chemical sciences.

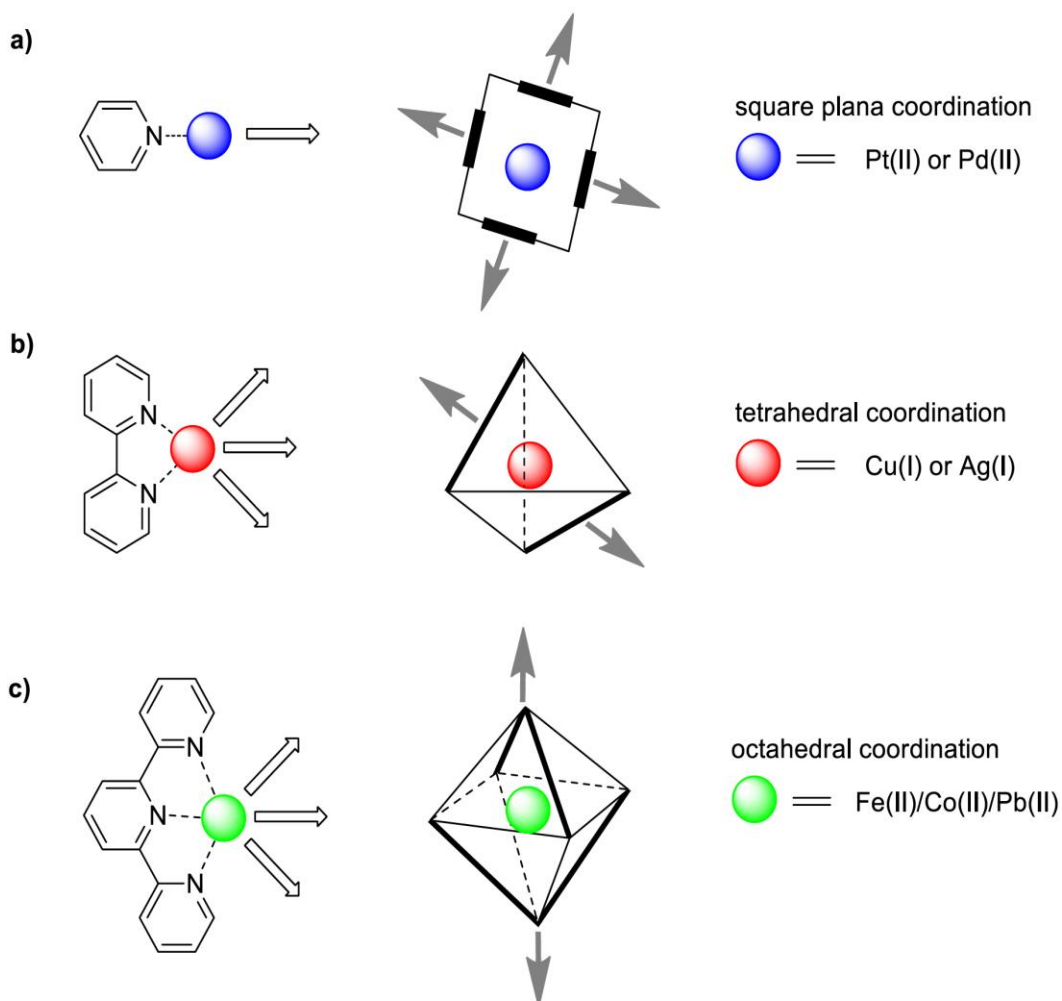


Figure 1.36. Schematic representation of coordination driven selfassembly

A synthesized self-assembled architecture generally depends on coordination number and geometry around the metal ions. Busch in 1960 first developed the concept of template effect. In template effect there should be proper choice of metal ions in order to get self-assembled architecture (figure 1.36).⁴⁴ A chemical template organizes an assembly of atoms or molecules with respect to one or more geometric loci, in order to achieve a particular linking of atoms. The ligand material geometry leads the building guide for self-assembled structure. Due to this, the suitable design of metal and ligand are more vital reported in literatures.⁴⁵

Herein, a generalized overview on nanoscale architectures built from monodentate (pyridine), bidentate (bipyridine, phenanthroline, catechol) and tridentate (terpyridines) ligands. As depicted in a simplified way in Fig. 1.36, most literature-known self-assemblies are constructed on Pd^{2+} or Pt^{2+} ions for square planar arrangement using monodentate ligands, at Cu^+ or Ag^+ ions for bidentate ligands, and at Co^{2+} , Cu^{2+} , Fe^{2+} , Zn^{2+} , Hg^{2+} etc., octahedral arrangement using terpyridine based chelating motifs.

Busch and co-workers synthesized first supramolecular structure by metal based templated approach. 1,2-diketones and 2-aminoethanethiol in presence of Ni^{2+} resulted tetrahedral arranged Ni(II) complex while in absence of metal it formed **38** (figure 1.37).

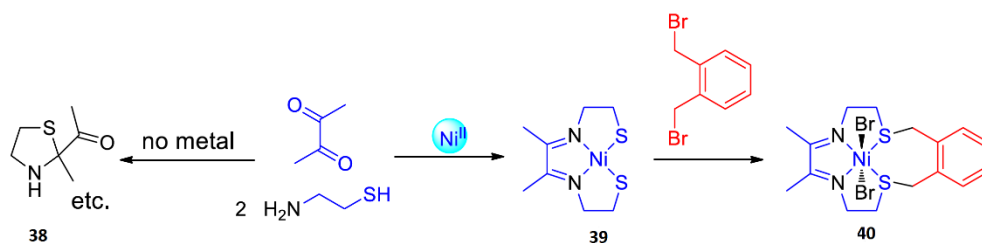


Figure 1.37. Cyclization by Ni(II) ion

A networked molecular cage was developed by Fujita *et al* which has crystalline cavity to bind fullerene and other organic guests.⁴⁶ It can also have the capacity to bind proteins and other guests' leads to metallosupramolecular cage (figure 1.38).⁴⁷

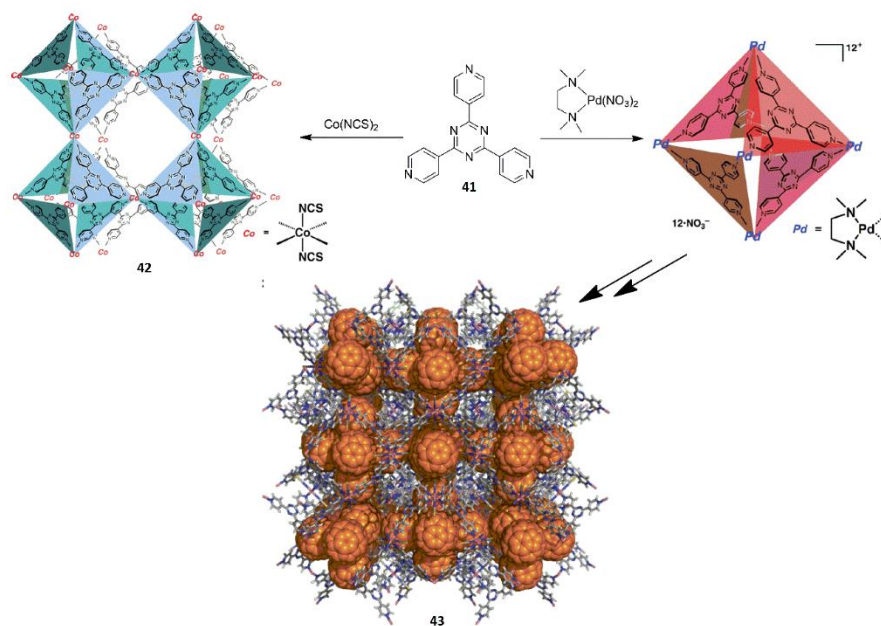


Figure 1.38. Synthesized molecular cage encapsulating fullerene guest

Mukherjee and co-workers constructed a nanoscopic architecture with Pd^{2+} and Pt^{2+} utilising the templated effect. They have developed a tetratopic unit with the right choice for designing an unprecedented hexagonal open box system (figure 1.39).⁴⁸ In a recent review, they have covered the literature on template-free multicomponent coordination driven Pd^{2+} and Pt^{2+} molecular cages and use of these systems in catalysis/host–guest Chemistry.⁴⁹

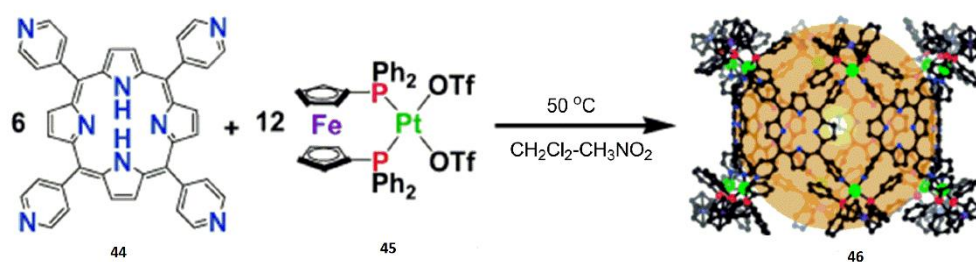
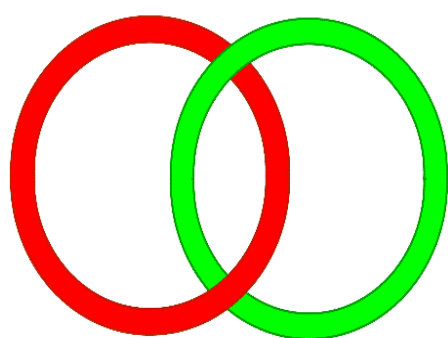
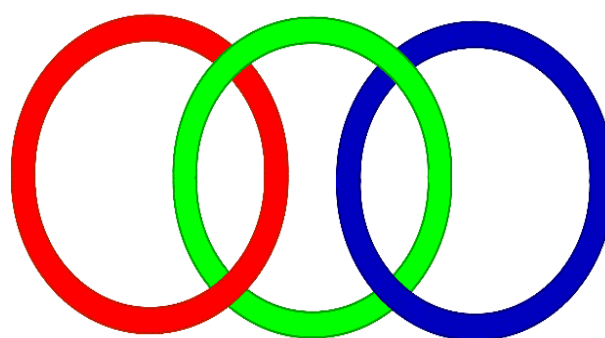


Figure 1.39. Synthesized Open box network with porphyrin cavity

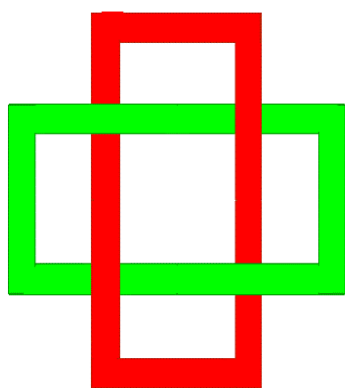
Interlocked architecture are defined as organic components are bind to each other by mechanical bond i.e that cannot be removed without breaking of any chemical bond. Some examples of interlocked structure are catenane, trefoil knot, Solomon link, pentafoil knot and boromen ring etc (figure 1.40). These molecules bears several potential applications that comprise molecular machines, molecular rotor, sensing and catalysis etc.⁵⁰



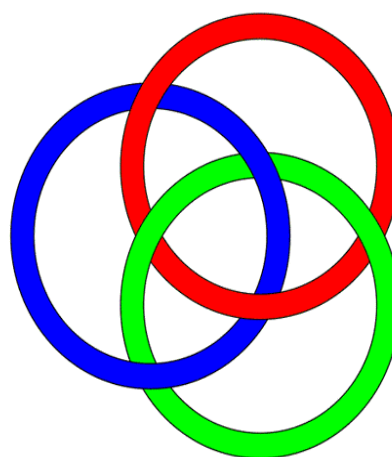
[2] Catenane



[3] Catenane



Solomon Link



Borromean Ring

Figure 1.40. Examples of different interlocked architecture

The first [2]Catenane was synthesized by Wasserman group utilising statistical methods (figure 1.41). They applied acyloin condensation in presence of a macrocycle resulted [2]Catenane.⁵¹

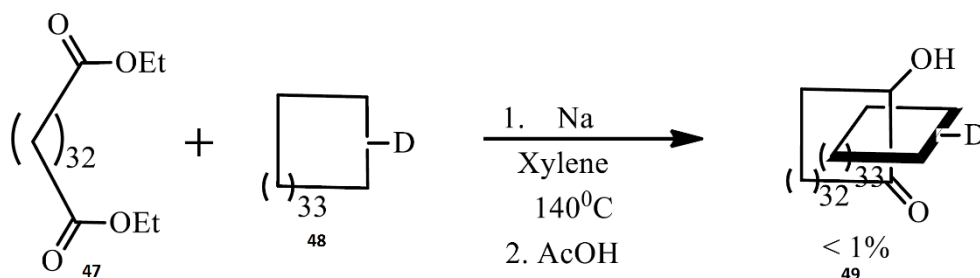


Figure 1.41. First [2]Catenane by Wasserman

After that templated approach was utilised to synthesize [2]catenane by Sauvage and co-workers.⁵² In this approach, metal ion acts as template that arranges ligand in a precise direction to create necessary crossing points. For that purpose they designed substituted hydroxy 2,9-diphenyl-1,10-phenanthroline ligand which coordinates to Cu(I) ion tetrahedrally (figure 1.42). Williamson ether cyclisation of hydroxyl groups of the resultant copper complex gives metalated [2]catenane. The Cu(I) ion was detached by KCN provides [2]catenane.

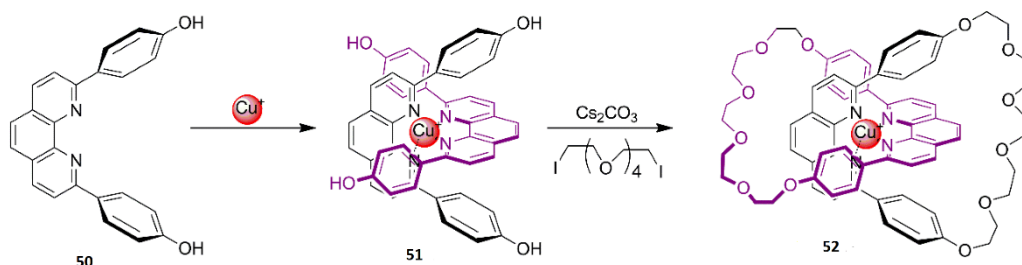


Figure 1.42. [2]Catenane by Sauvage

Motivated from this work, a wide range of metal templates i.e octahedral, squareplaner, trigonal bipyramidal were reported in literatures and also more fascinating templates which utilizes non-covalent interactions were developed that includes molecular interactions, hydrogen bonding, halogen bonding, anions, hydrophobic interaction, ion-pairing etc for the synthesis of mechanically interlocked molecules.

Vogle and Hunter synthesized amide based [2]Catenane using hydrogen bonding interaction of amide to $-C=O$ oxygen (figure 1.43).⁵³

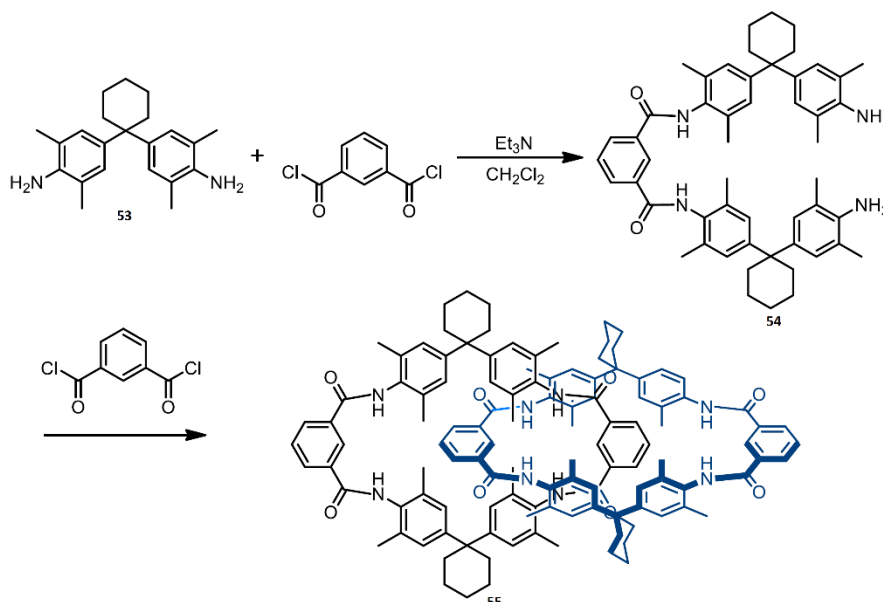


Figure 1.43. Amide based [2]Catenane by Vogtle and Hunter

After that [2]catenane was synthesized by Leigh and co-workers utilising hydrogen bond templated approach. Isophthaloyl dichloride reacted with paraxylene diamine to afford [2]Catenane. By utilising the chloride ion templating approach peer and co-workers synthesized [2]Catenane complex.⁵⁴ For that purpose, they used the ring closing metathesis of pyridinedichloride with isophthalamide macrocycle resulted

[2]Catenane in presence chloride ion (figure 1.44). But with bromide ion yield of targeted product decreased and no catenane formed with hexafluorophosphate.

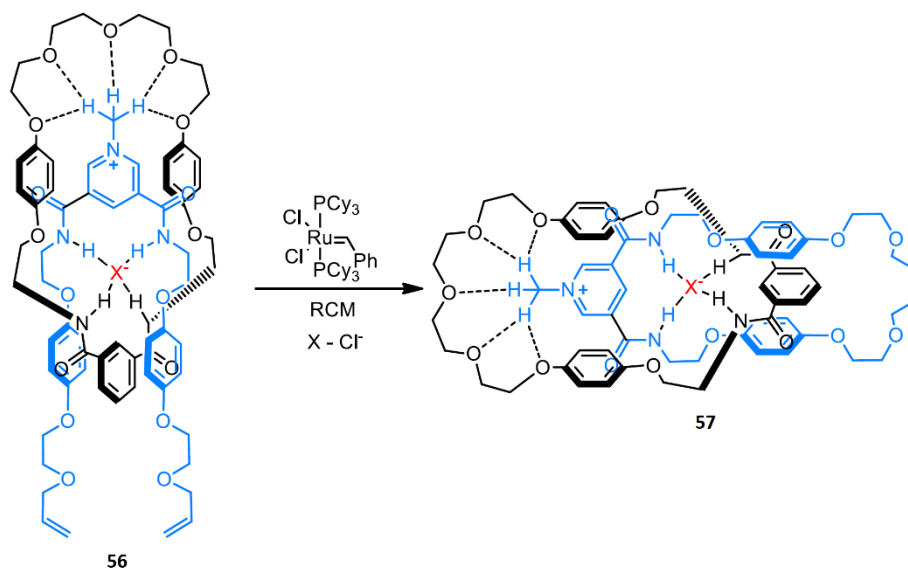


Figure 1.44. [2]Catenane by anion templated approach

Yoshima and co-workers described the synthesis of [2]Catenane by exploiting amide salt bridge monitored by ring closing metathesis (figure 1.45). Catenanes have a unique feature of independent motion (rotation and translation) of one ring with respect to the other ring made them attractive candidates for variety of applications such as molecular machines, molecular switches (figure 1.46) Apart from these Fujita's thermodynamically controlled [2]catenane,⁵⁵ several other approaches as crown ether dibenzylammonium catenane,⁵⁶ sodium templated approach, radical templated method,⁵⁷ Halogen bonding template⁵⁸ method etc. were also reported in the literature.

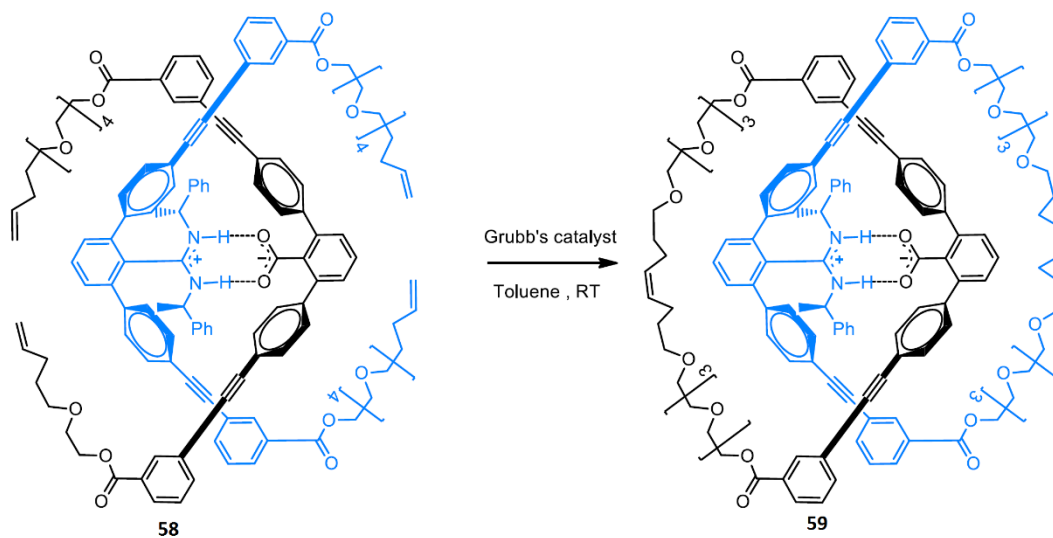


Figure 1.45. Yoshima's [2]Catenane by using salt bridge

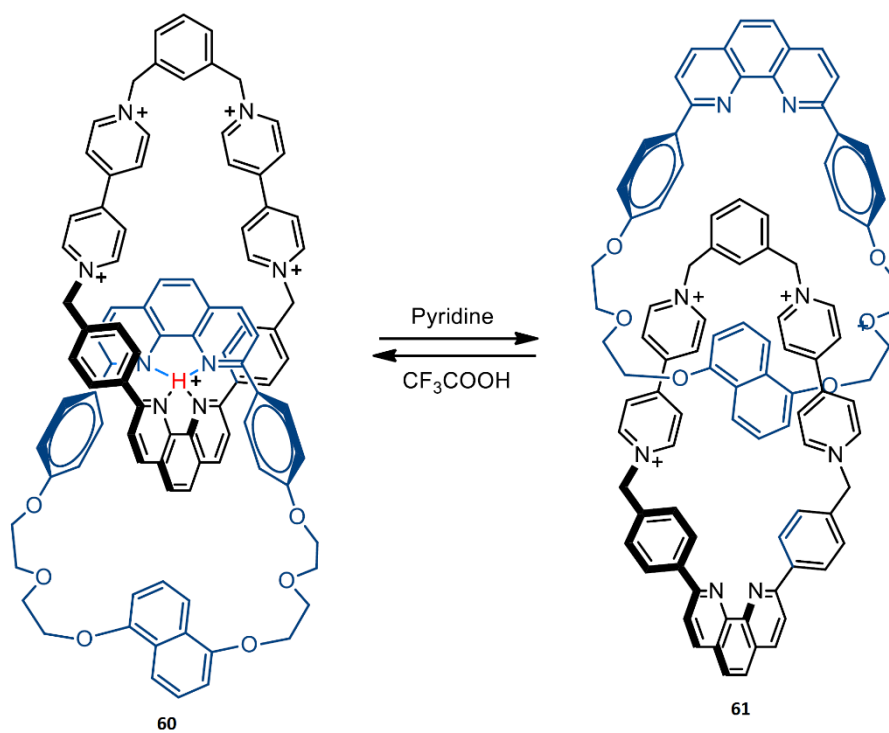


Figure 1.46. P^H control molecular switch by Sauvage

Apart from these, catenanes are anticipated to contribute remarkable properties when incorporated into polymeric material.⁵⁹ Polymeric catenanes are expected to have a low activation energies for viscous flow, large loss moduli and also effects on elasticity, friction, impact resistance etc. But unfortunately these properties were not properly studied experimentally because of difficulty in synthesis of [n]catenanes ($n > 2$).

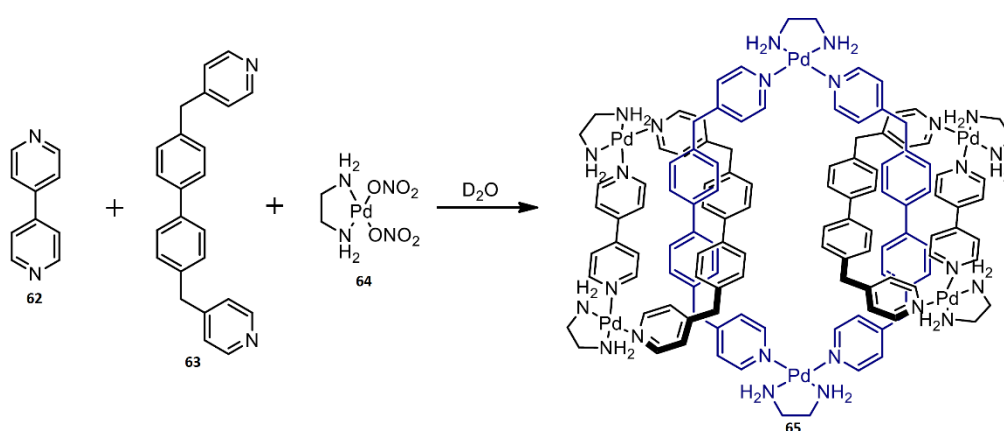


Figure 1.47. [3]Catenane by Fujita

Fujita *et al* demonstrated the self-assembly of [3]catenane from twelve components during the formation of thermodynamically stable product [2]catenane by DOSY-NMR (figure 1.47).⁶⁰ Mayer's group proposed and employed double ring closure strategy for the synthesis of [3]catenane (figure 1.48).⁶¹

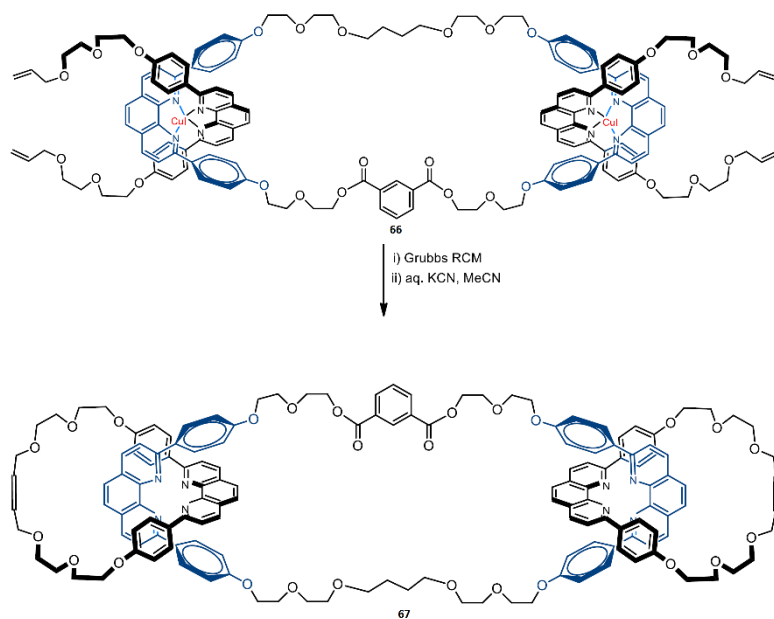


Figure 1.48. [3]Catenane by Mayer

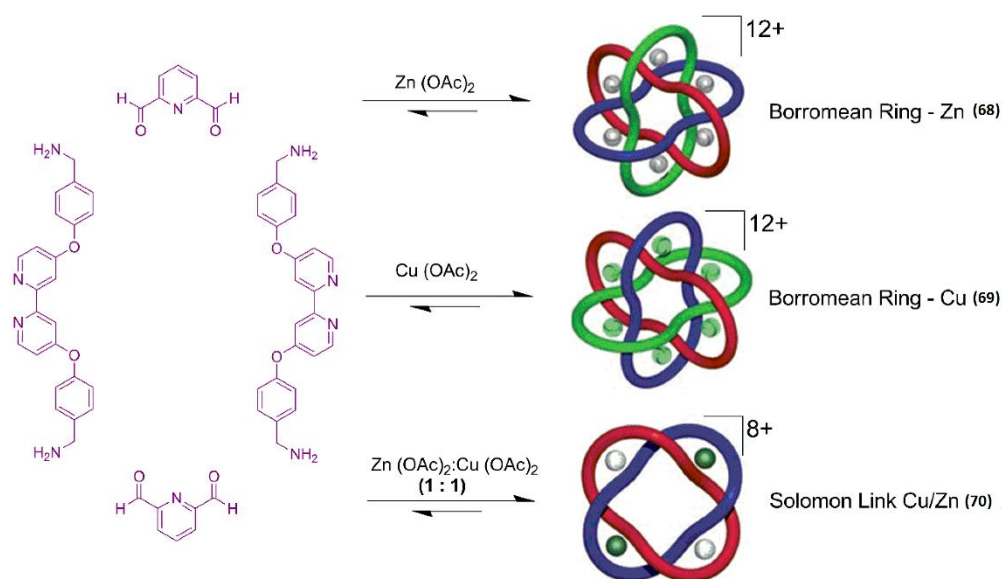


Figure 1.49. Stoddart's Borromean ring

Stoddart and co-workers synthesized solomon link and borromean ring using Zn(II) and Cu(II) metal ions (figure 1.49).⁶² Pyridine 2,6-dicarboxaldehyde and

substituted bipyridine amine reacted in presence of $\text{Zn}(\text{OAc})_2$ and $\text{Cu}(\text{OAc})_2$ afforded the highly interlocked boromen ring and in presence of 1:1 mixture of metal salts resulted a solomon knot. Cooper and co-workers designed a triply interconnected organic molecular cage in a single pot without the use of any template (figure 1.50 and 1.51).⁶³ This triply interlocked cage contains two tetrahedrally arranged cages. Each tetrahedral cage synthesized from four rigid nodes and six rigid linkers. Here triformyl benzene treated with propane-1, 2-diamine in acetonitrile and trifluoroacetic acid undergo cyclic amination resulted the triply interconnected cage. But monomeric non-interconnected organic cage was obtained without the use of trifluoroacetic acid.

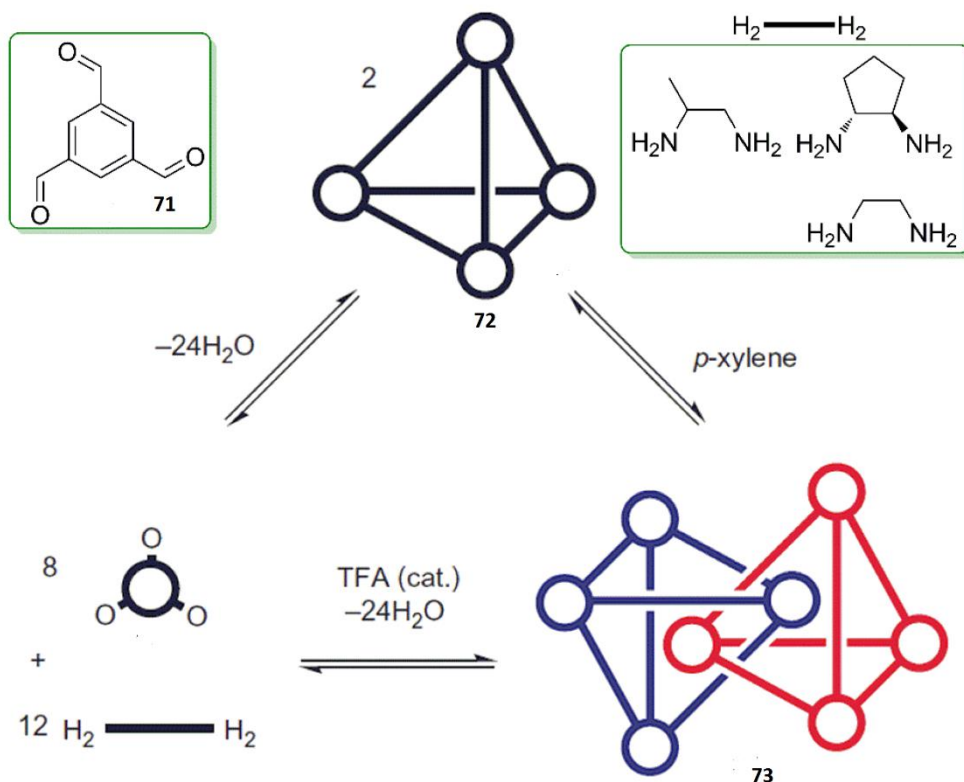


Figure 1.50. Interlocked molecular cage by Cooper

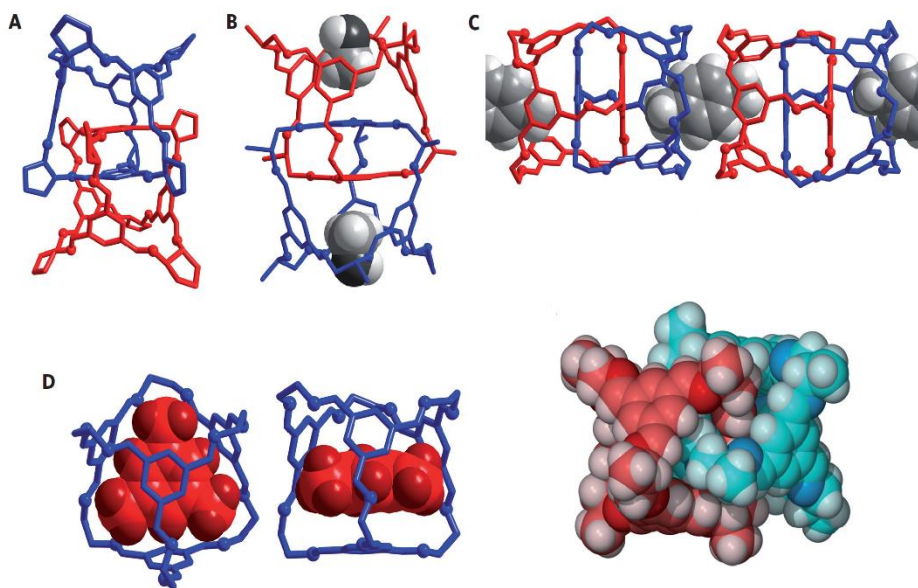


Figure 1.51. X-ray crystal structure of Cooper's interlocked molecular cage

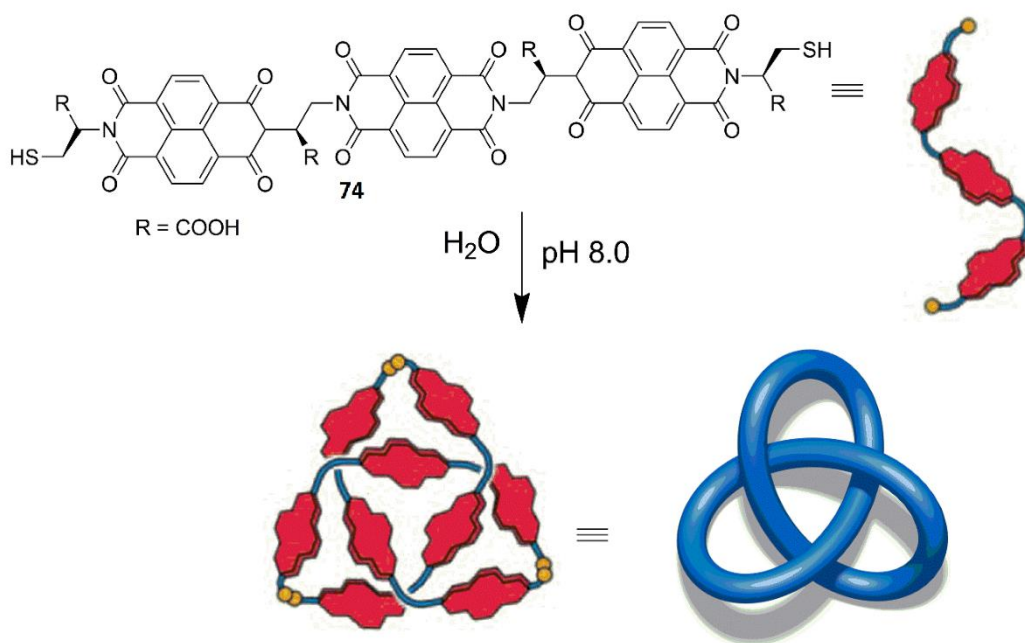


Figure 1.52. Sander's trefoil knot

Sander and co-workers reported highly ordered trefoil knot utilising the hydrophobic interaction (figure 1.52).⁶⁴ The ligands with side chain as disulphide functionality allowed the formation of trefoil knot. The building unit is consisted of three hydrophobic electron deficient 1, 4, 5, 8- naphthalene diimide joined with supple hydrophilic amino acid L-cysteine, which undergo di sulfide exchange and added $-\text{COO}^-$ for solubilisation of water. As a result strategy of building unit offer a suitable approach to highly knotted architecture in presence of water.

Leigh and co-workers reported a trifoil knot by exploiting the active metal template approach (figure 1.53-1.54).⁶⁵ Ligand has reactive end with alkyne and azide functionalities. Ligand was reacted with $[(\text{CH}_3\text{CN})_4\text{Cu}]\text{PF}_6$ in nitromethane under click condition resulted

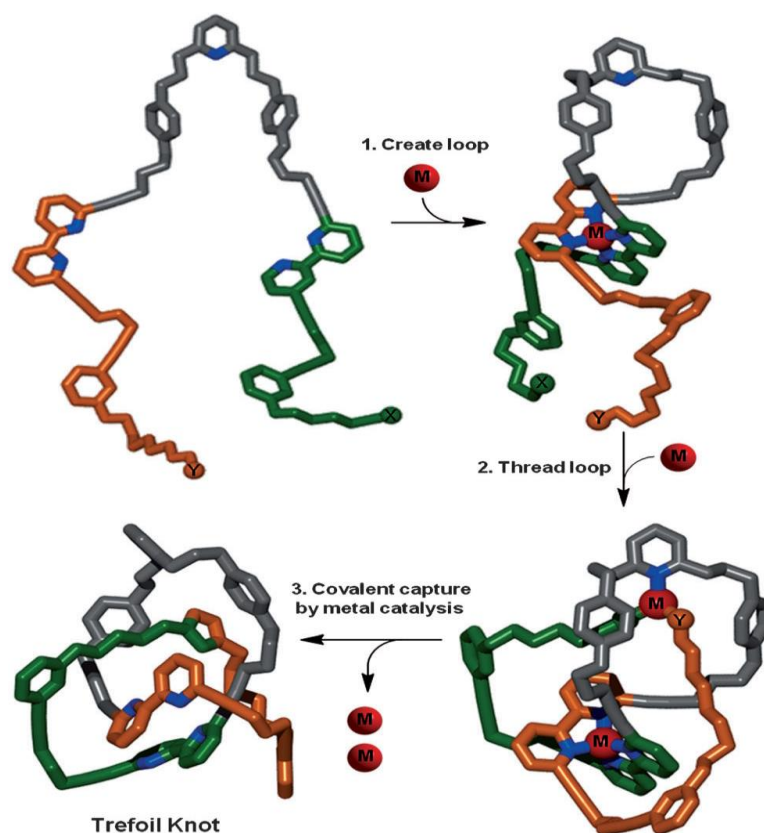


Figure 1.53. Schematic representation of trefoil knot

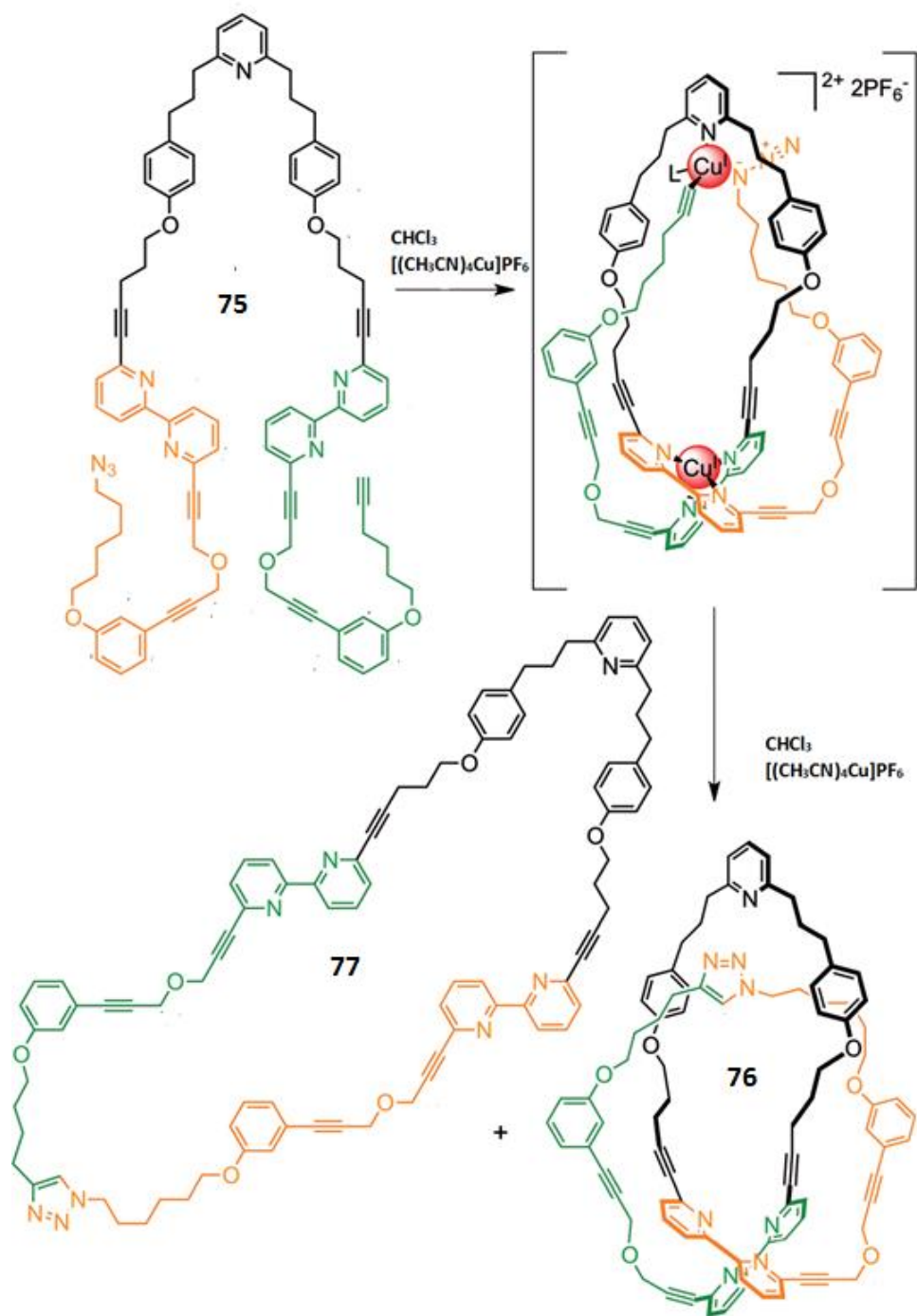


Figure 1.54. Trefoil knot by Active metal template approach

a trimeric interlocked structure. One of metal develops a ring whereas other copper metal was catalysing the covalent bond making reaction. Later the Cu(I) metal was

DE protected by Na-EDTA mixture. Leigh and co-workers synthesized a trefoil knot structure with Ln(III) based templated approach (figure 1.55 and 1.56).⁶⁶ A chiral 2, 6- pyridine dicarboxamide ligand having R-R and S-S conformation. The R-R conformation coordinated around Ln(III) resulted trefoil knot structure with one handedness while S-S conformation coordinated with Ln(III) resulted a trefoil knot assembly with whole stereochemistry. Though synthesis of knot is wholly stereo selective, a racemic tri-dentate ligands does not selfsort during the formation of complex. This chiral tridentate ligand also reacted with Lu(III) and Eu(III) resulted chiral trefoil knotted structure.

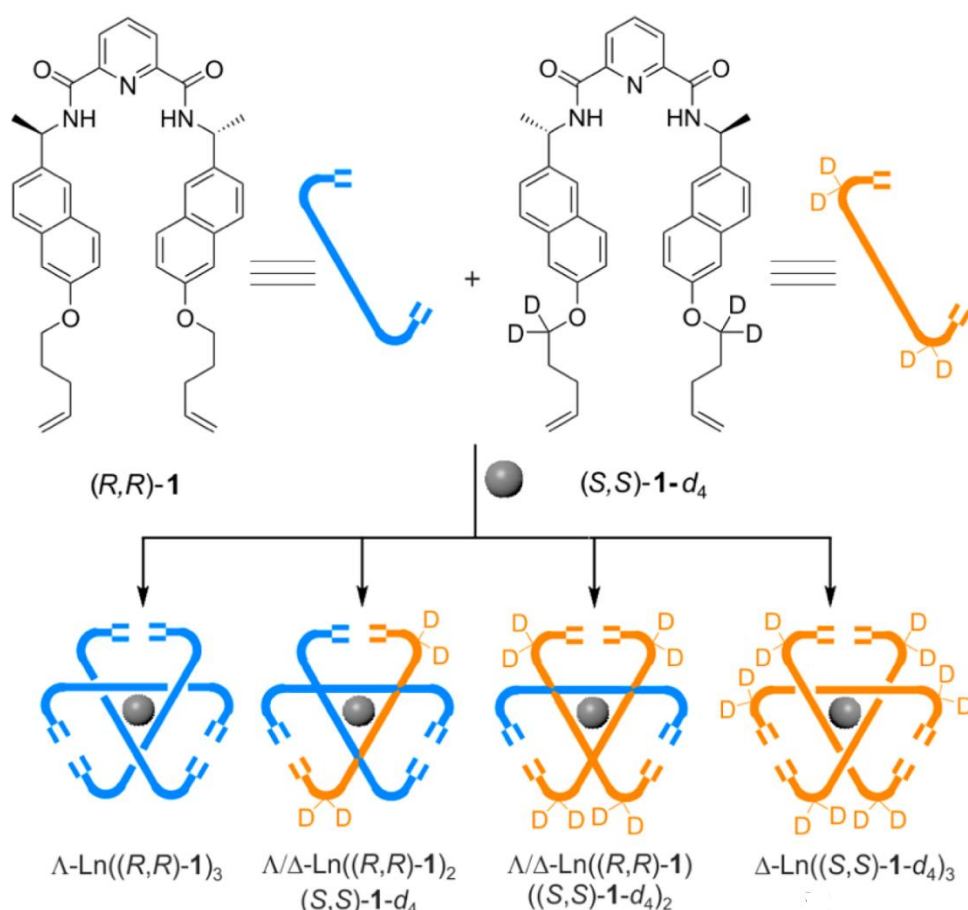


Figure 1.55. Trefoil knot by metal templated approach

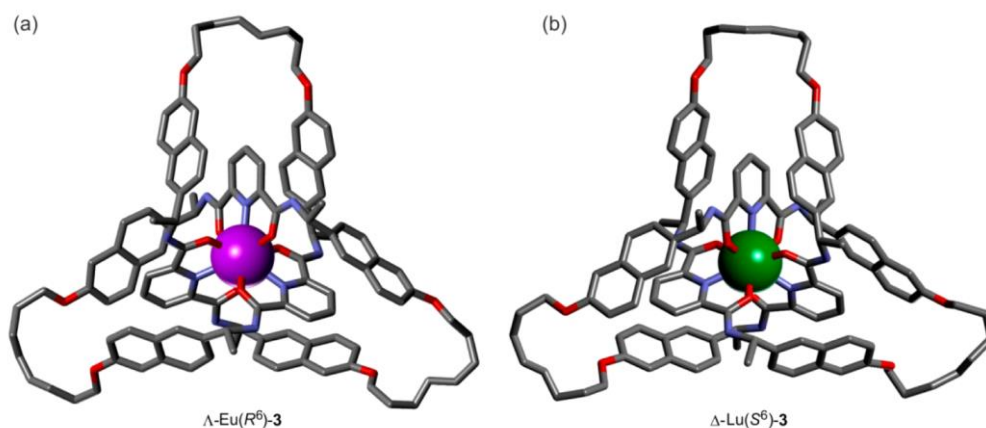


Figure 1.56. X-ray crystal structure showing trefoil knot with Eu(III) and Lu(III)

The same group also synthesized a trefoil knot using metal template approach.⁶⁷ They designed ligand as 2, 6- pyridine tricarboxamide having six asymmetric centres utilising Ln^{3+} as metal template (figure 1.57 and 1.58). The ligand coordinated to metal Ln^{3+} resulted an overhand knotted structure and after that the end groups are linked to each other by RCM to afford one enantiomer of trimeric knot. The trimeric knot are used as a catalyst in Mukaiyama Aldol type reaction.

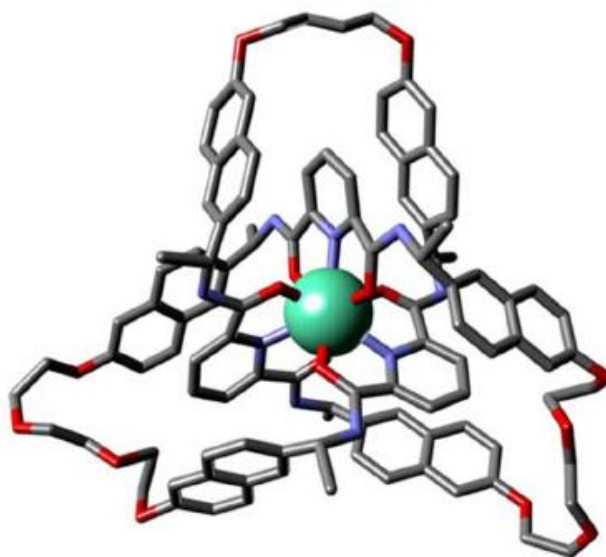


Figure 1.57. X-ray crystal structure of molecular trefoil knot

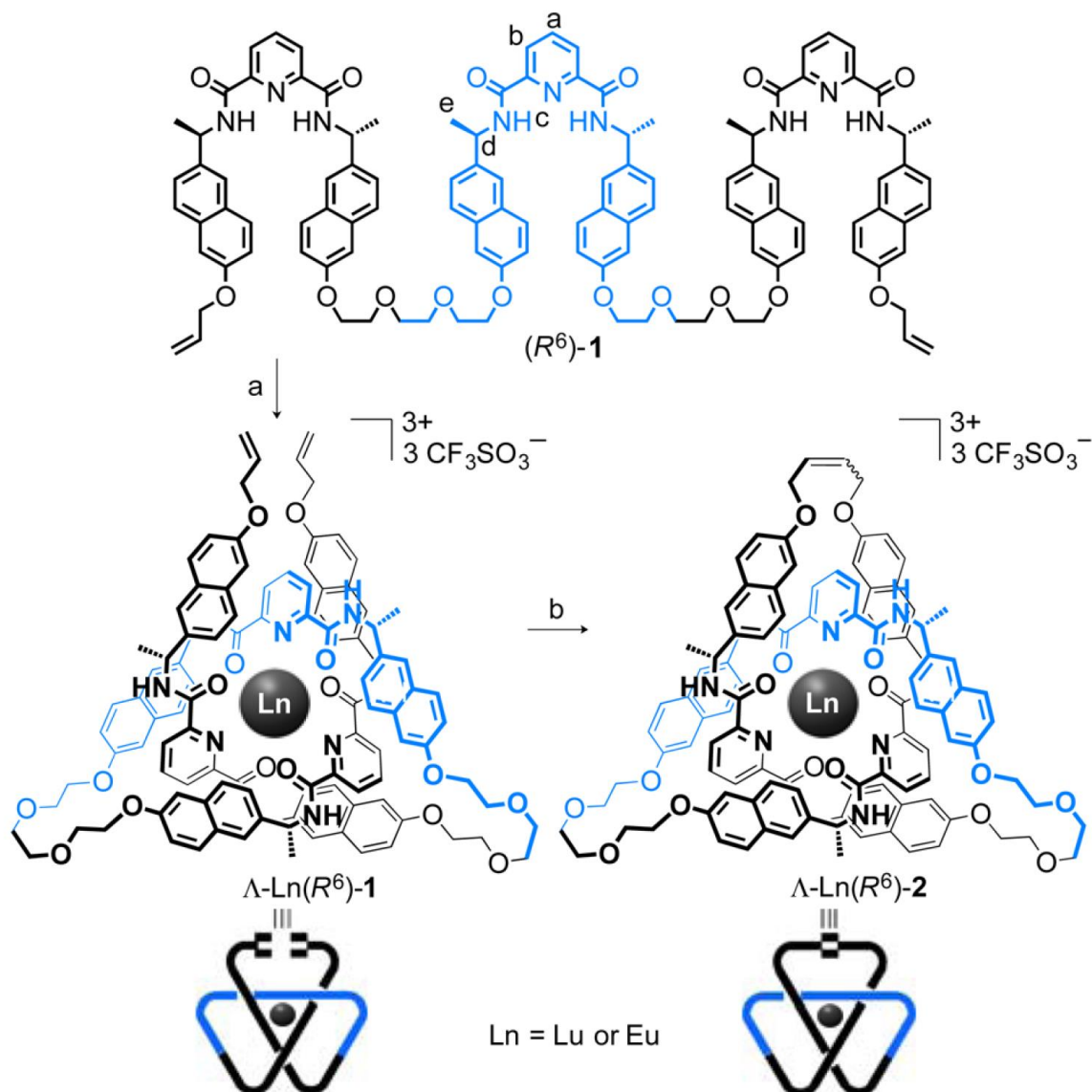


Figure 1.58. Molecular trefoil knot by Leigh

Molecular trefoil knot was prepared by Leigh *et al* using zinc template (figure 1.59 and 1.60).⁶⁸ Firstly a trimeric helical structure was synthesized from pyrazine dicarboxaldehyde and corresponding designed substituted amine in acetonitrile and $\text{Zn}(\text{BF}_4)_2 \cdot \text{H}_2\text{O}$. Subsequently the free end groups with alkene functionalities of the trimeric helicate are joined together by RCM to afford a trefoil knot assembly. Here,

these three zinc ions positioned the ligand in such a way that to cross over each other to evocative of the entwining in abridged demonstration of a trefoil knotted structure.

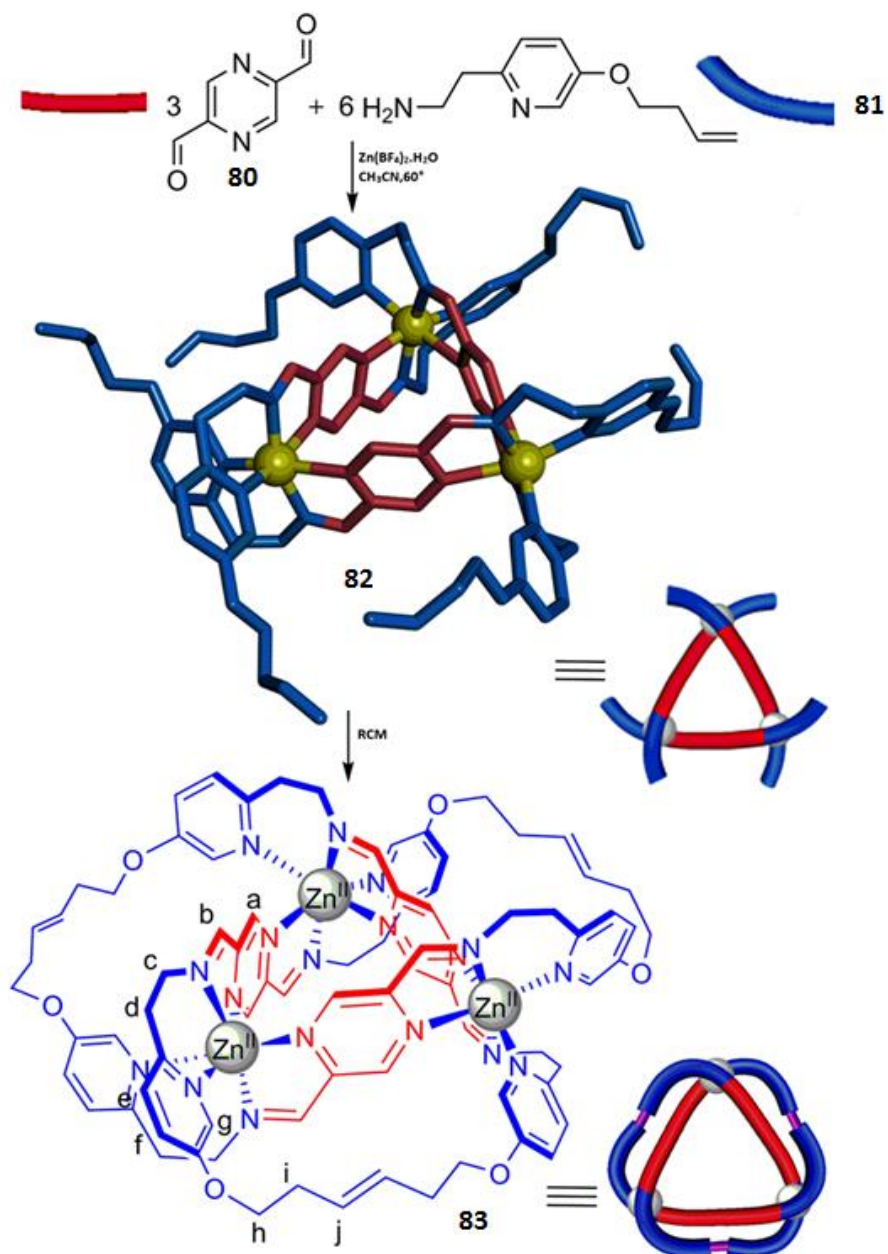


Figure 1.59. Synthesis of molecular trefoil knot with Zn(II) template

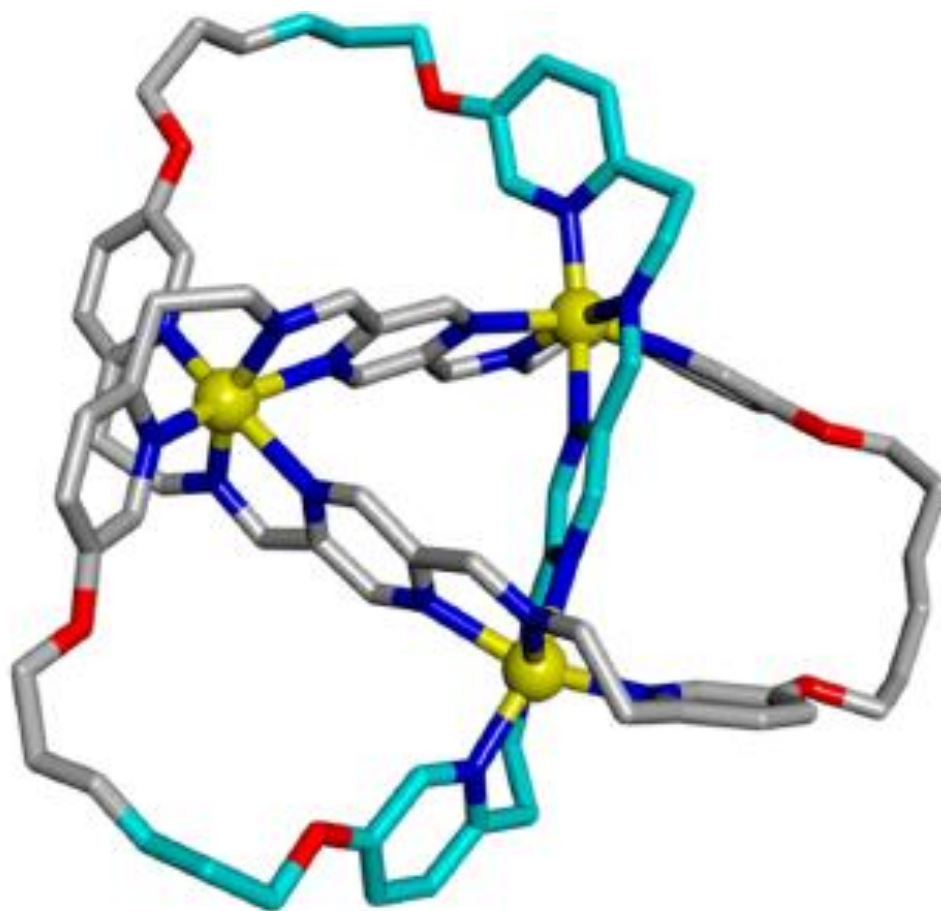


Figure 1.60. Solid state structure of Zn(II) trefoil knot

Leigh and co-workers reported a highly interlocked knot utilising reversible metal to imine bond under thermodynamically controlled manner (figure 1.61).⁶⁹ They designed precursor as bis di-aldehyde and hexane-1-amine. Reacting the bis di-aldehyde and corresponding amine in Iron(III) chloride in deuterated DMSO and a chloride ion resulted a molecular Penta foil knot in a single pot. The chloride ion was positioned with double helicates with hydrogen bonding interaction. Macro cyclization to produce the covalent strength of Molecular Penta foil knot using

stereo electronic effects to linking species and ligand to ligand connections to stimulate mechanical bond synthesis instead of polymer synthesis.

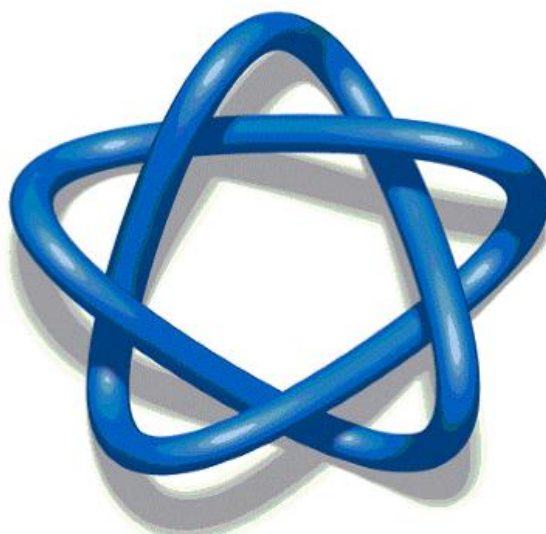
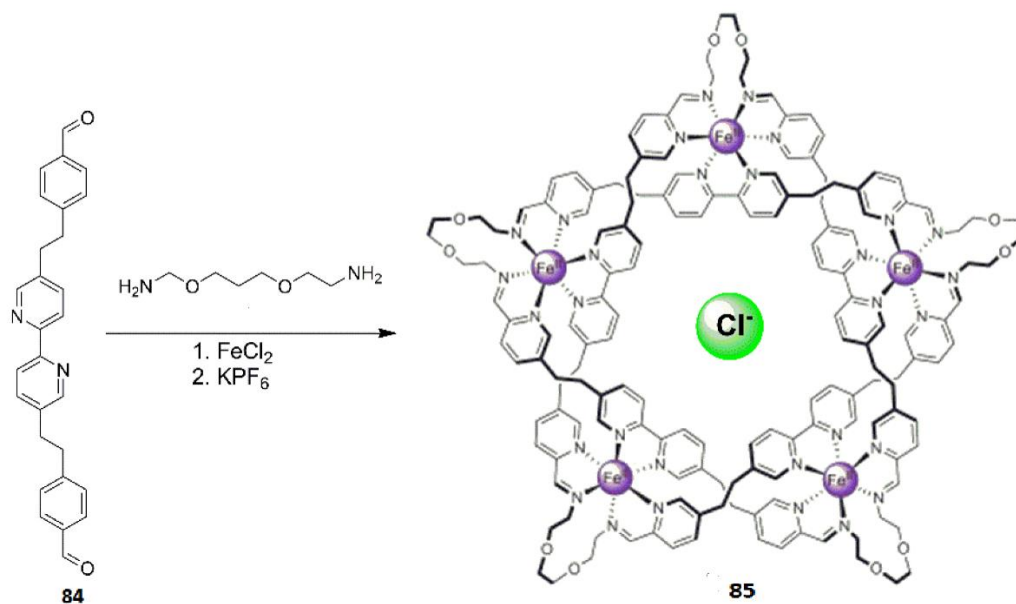


Figure 1.61. Leigh's molecular Pentafoil knot

A covalent bonded 3D organic cage was reported by Stoddart and co-workers using metal free approach (figure 1.62 and 1.63).⁷⁰ They designed the precursor for

molecular cage as a cyclophane consisted of two tetra phenyl porphyrin linked face to face by 4 viologen moiety in rhombohedral prismatic arrangement. Both the porphyrin and viologen moieties undergo ring closing reaction in presence of catalyst tetra-butylammoniumiodide. Due to the bulky cavity of the molecular cage and donor acceptor interaction among the porphyrin units, encapsulates the guests like fullerene C₆₀, C₇₀.

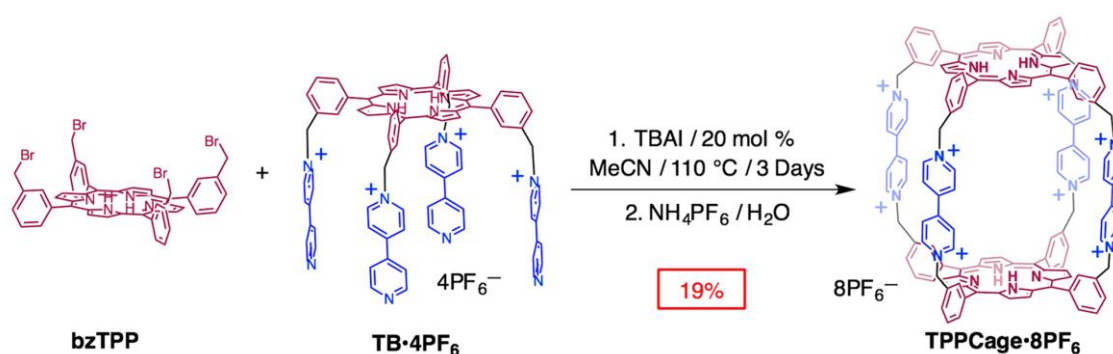


Figure 1.62. 3D-Molecular cage by Stoddart

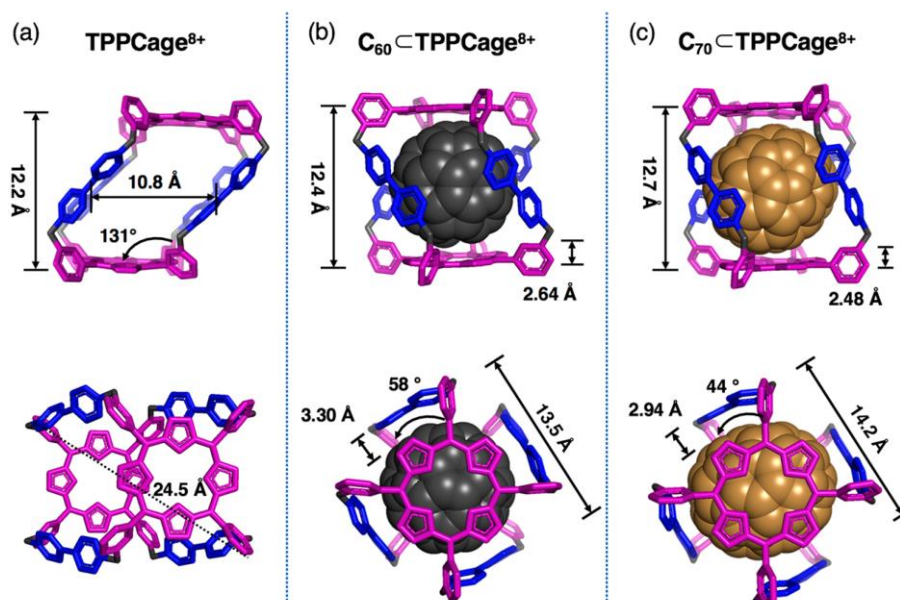


Figure 1.63. Solid state structure of 3D-molecular cage

Leigh groups reported a 324 membered molecular composite-knot with nine crossing points (figure 1.64, 1.65 and 1.66).⁷¹ The substituted bipyridine based alkenes reacted with Fe(II) salt in octahedral manner to form M-L helicate which entwining the six ligands and smaller linkers in order to favour double helical assemblies to triple helical assembly. Due to restricted rotation, only strand end react with terminal end of ligand coordinated to metal.

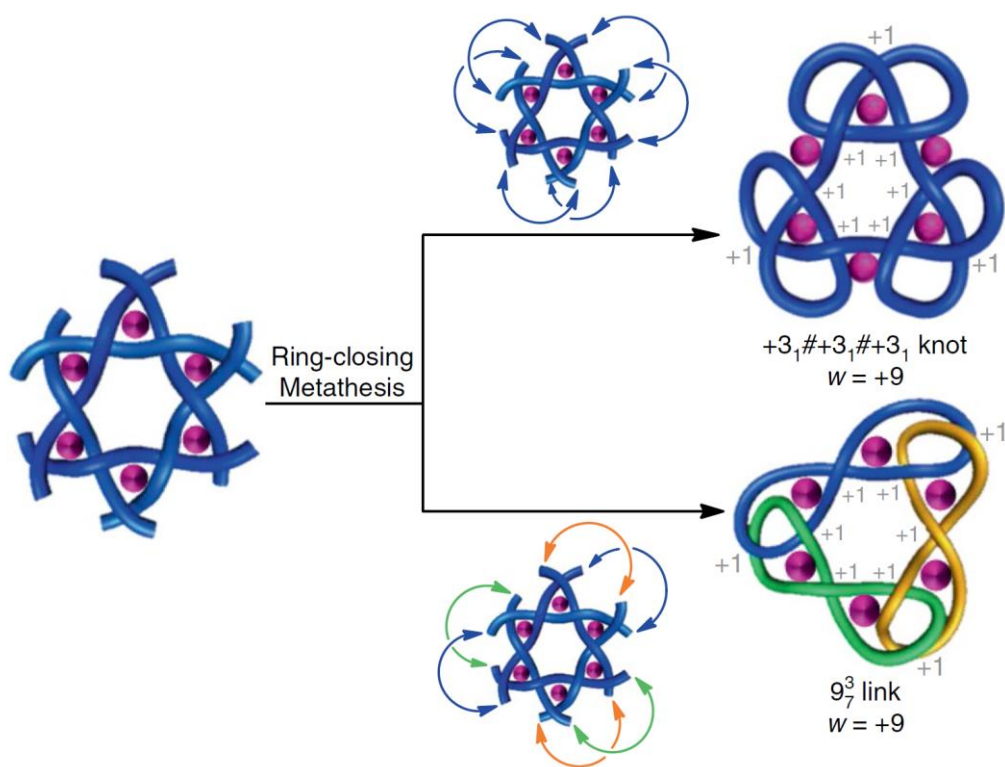


Figure 1.64. Schematic representation of molecular composite knot

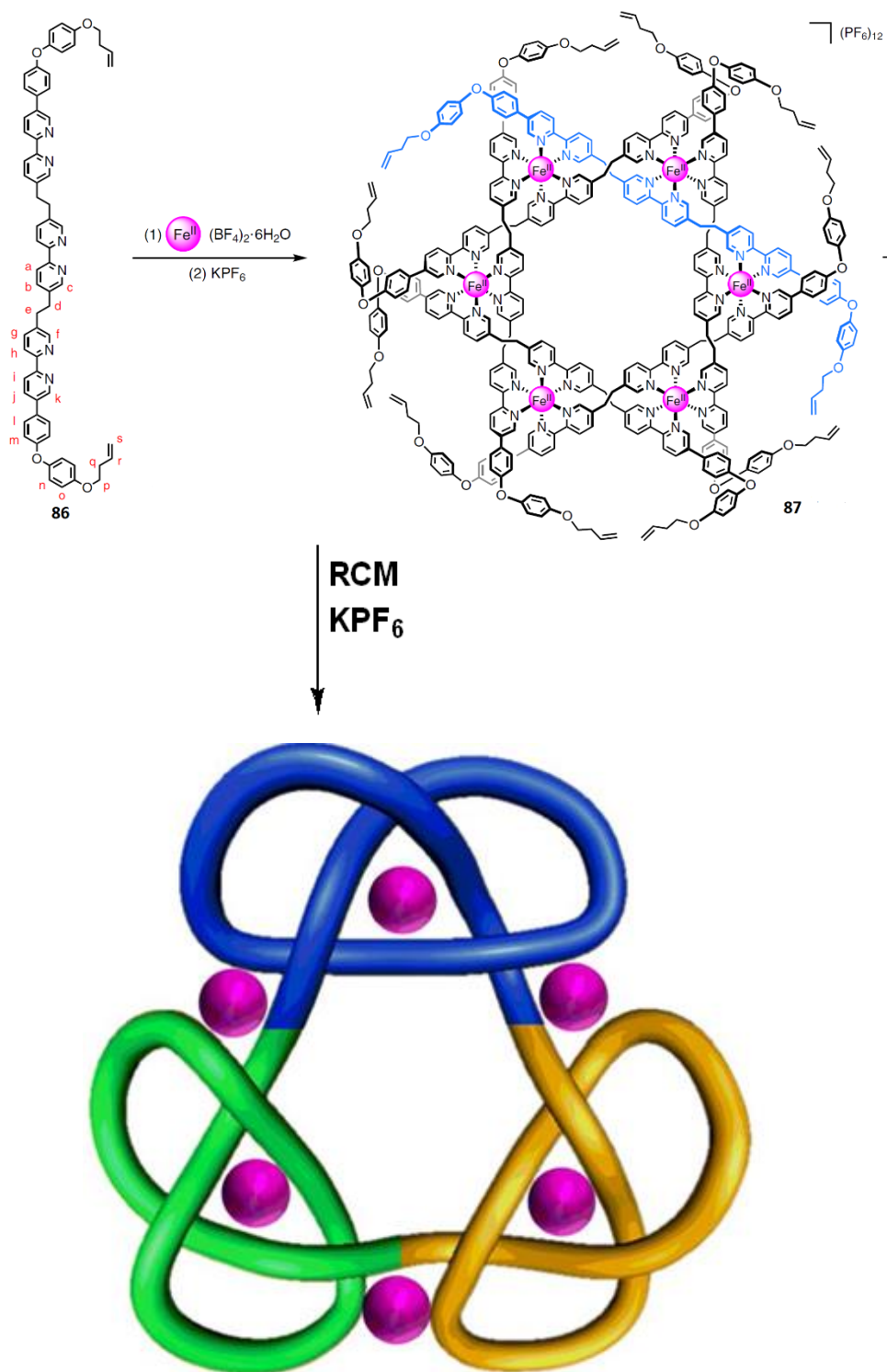


Figure 1.65. Synthesized molecular composite knot by Leigh

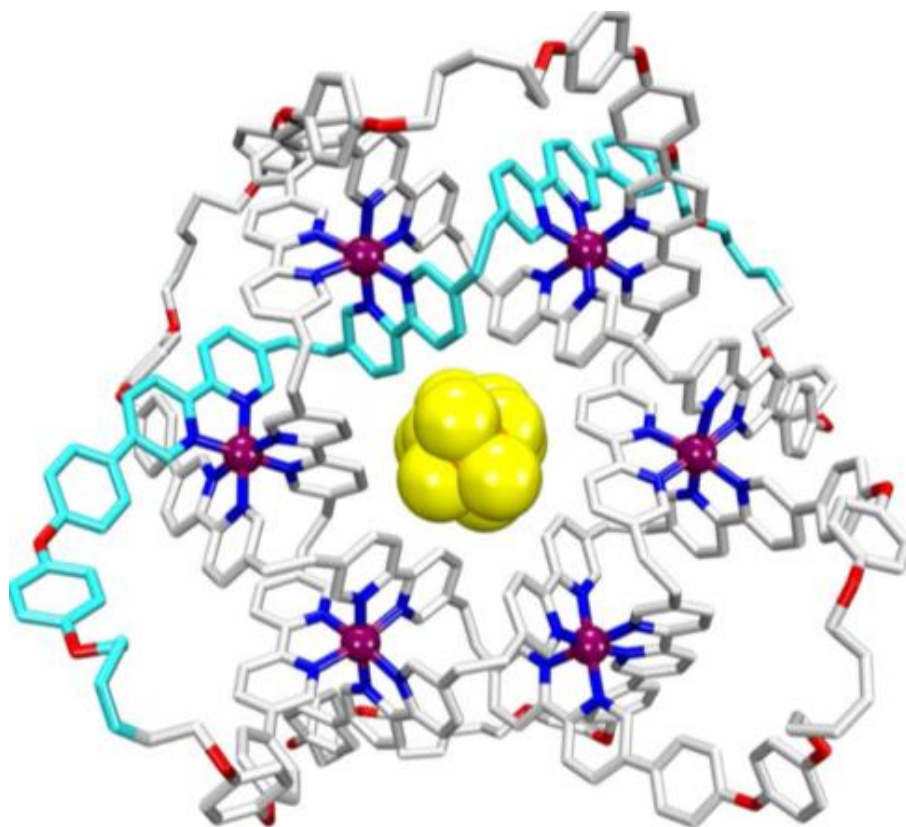


Figure 1.66. X-ray structure of Leigh's composite knot

A molecular link of six crossing points, interlocked, [2]Catenane with warped circles and a granny knot were built by Leigh et al using RCM of an Fe(II) linked 2×2 intertwined grid (figure 1.67 and 1.68).⁷² The hanging phenyl groups directed the connections in between designed ligand ends residing on same side of the intertwined grid. Here two bulky macrocycles coordinated with the ligand by complexation with exact amount of Fe(II)/ Zn(II) tetrafluoro borate salts in presence of CH₂Cl₂ and CH₃CN to obtain the intertwined grid structure which in presence of Grubb's catalyst resulted the corresponding granny knot.

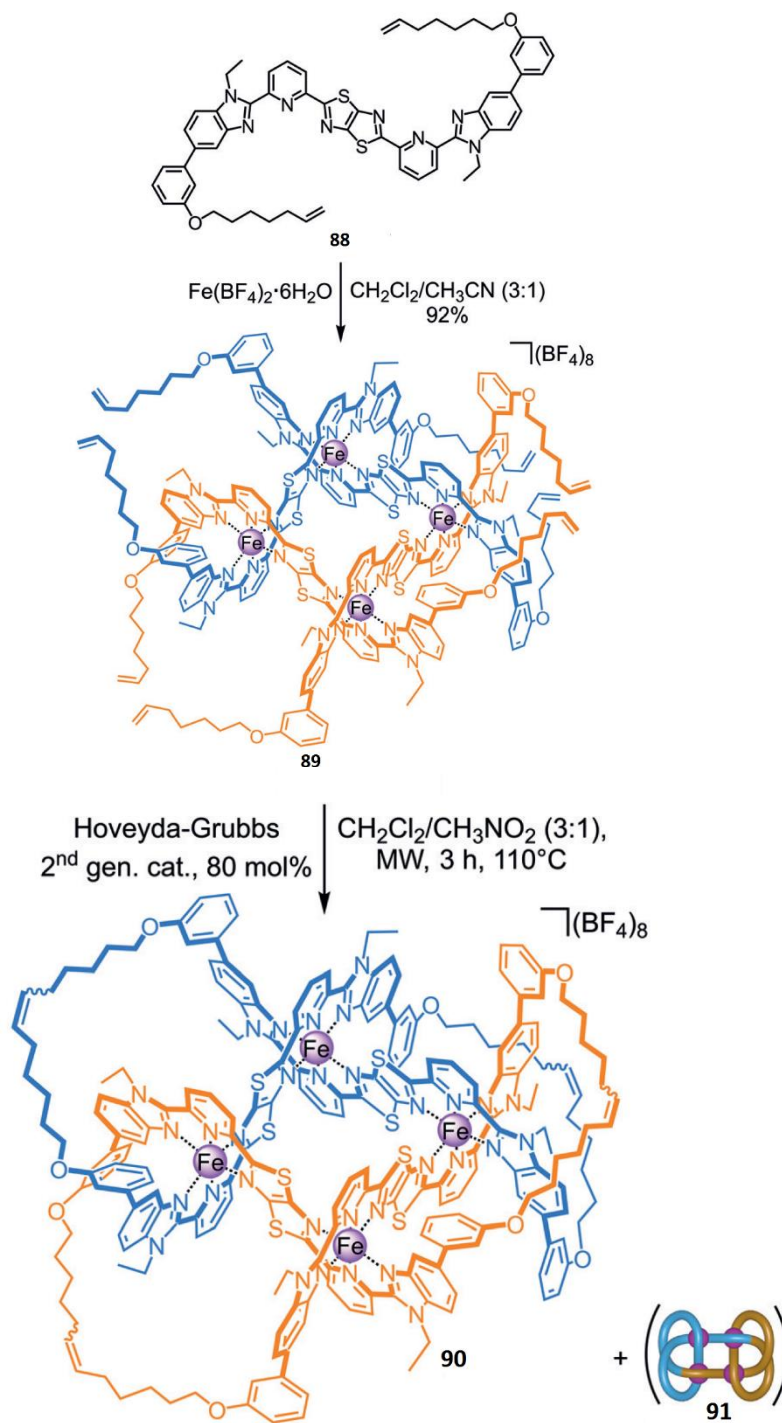


Figure 1.67. Molecular granny knot by Leigh

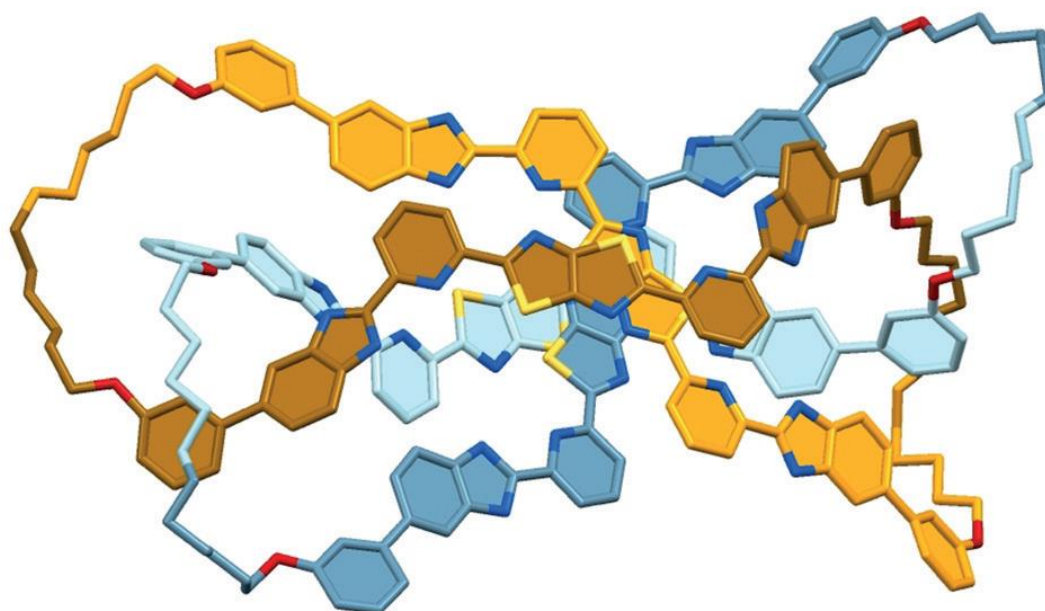


Figure 1.68. Solid state nature of metal free 6^2_3 knot

Loeb and co-workers reported a 2-station [2]catenane comprising a bulky macrocycle with two separate recognition units, i.e bis(pyridinium) ethane and otherone benzyl aniline, along with a smallest (DB24C8) ring. DB24C8 ring can incorporate in between 2 recognition units, depends on the protonated nature of large macrocycle (figure 1.69).⁷³ Then DB24C8 incorporates in between 2(two) charged recognition units which favours bis-(pyridinium)-ethane unit. Whereas un-protonated [2]catenane bears a profound yellow-orange color when DB24C8 ring exist in the bis-(pyridinium)-ethane site and consequently changed to colorless when the crown ether is circumrotating in between the two recognition units.

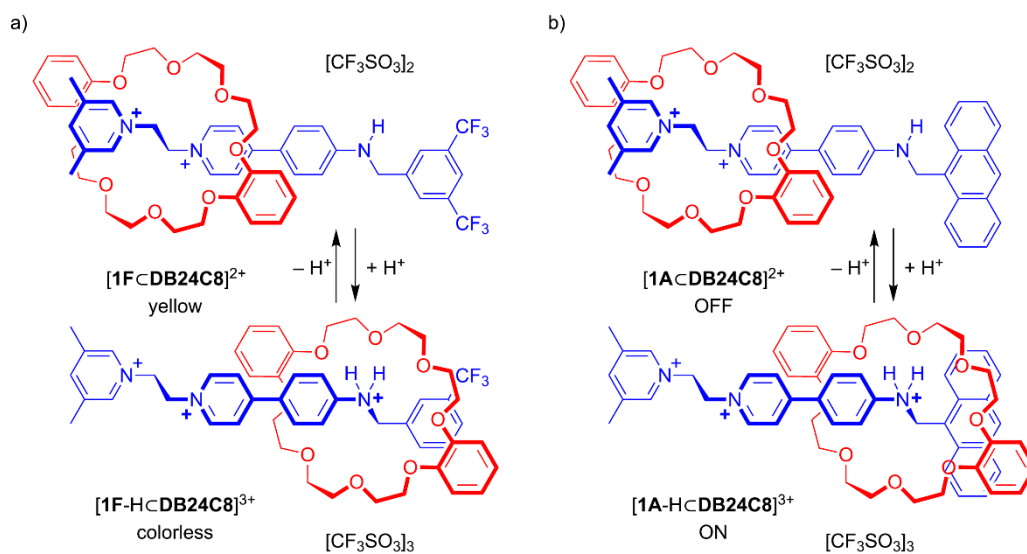


Figure 1.69. Two station Catenane by Loeb

Clever and co-workers reported highly interlocked M_8L_{16} utilising Pd^{2+} metal template. Sixteen molecules of phenanthrene derivative bridging ligands coordinated to palladium(II) resulted a new M_8L_{16} metallo-supramolecular container (figure 1.70 and 1.71).⁷⁴

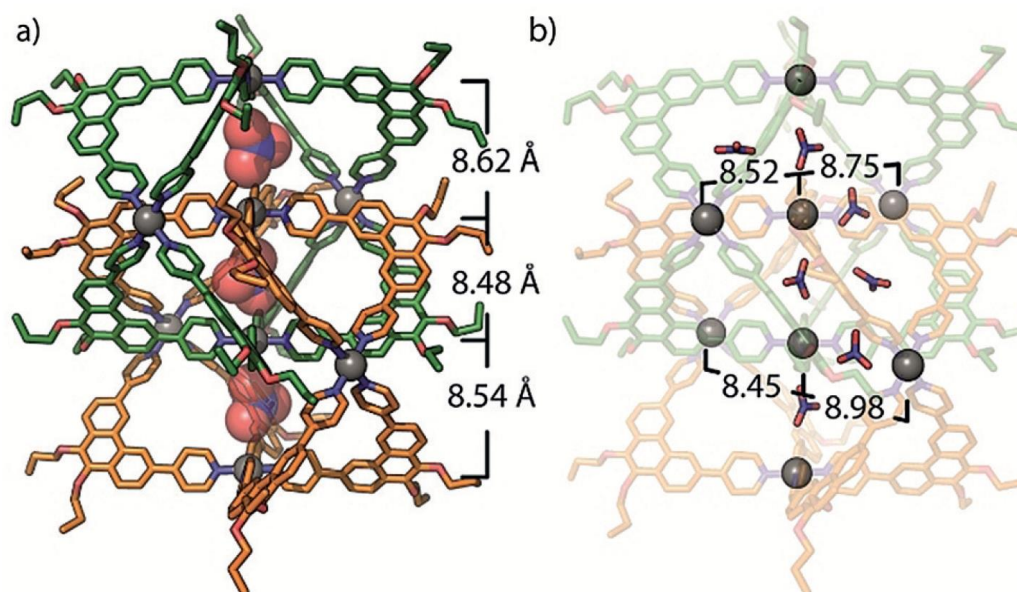


Figure 1.70. Clever's molecular container

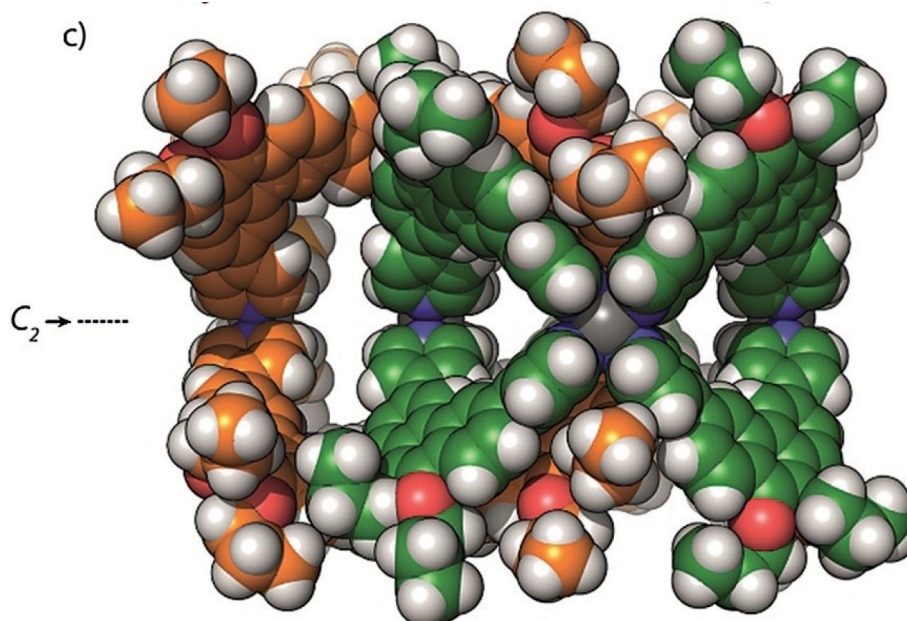


Figure 1.71. Space filling model of Clever's molecular container

Stoddart and co-workers synthesized the effective way of a sequence of Borromean rings (BRs), through which they attained template free Borromean ring synthesis with greatest yields in a highly controllable way (figure 1.72).⁷⁵ The ligand 2,5-dihydroxy- 1,4-benzoquinone (L1) and its other three dihalogenated-derivatives (L2–L4) treated with pentamethyl-cyclopentadienyl-Rh resulted half sandwiched Rh^{2+} complex. The half sandwiched complex then treated with 4,4'-bipyridylacetylene in acetonitrile-water mixture resulted metalla-rectangle reacted with dibromo benzene/ diiodobenzene to afford different Borromean rings, no Borromean ring formed with dichlorobenzene. This metalla-rectangle also reacted in presence of diethylether/tetrahydro furan resulted Borromean ring.

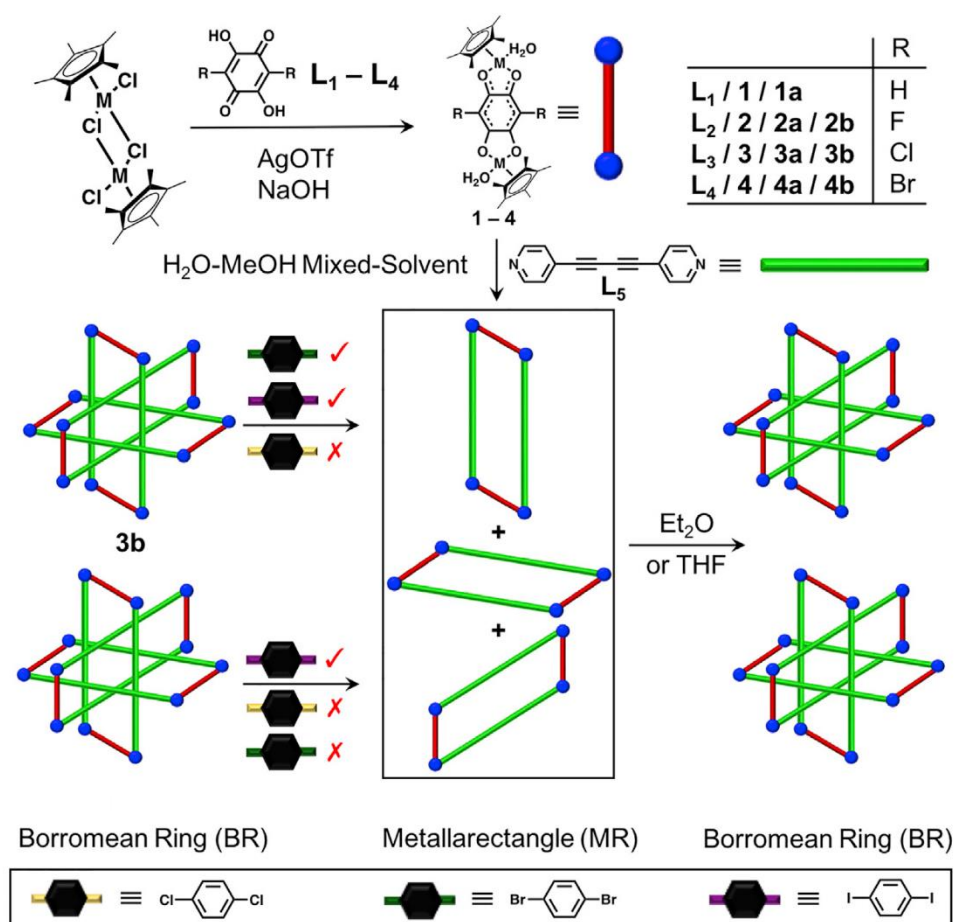


Figure 1.72. Stoddart's Six Borromean ring

Objective of the Thesis

The main objective of the thesis is (a) Heterometallic and homometallic complexes based on pyrazine are well documented. (b) Interlocked [2]Catenane and figure of eight structure are synthesized and studied.

1.3. REFERENCES

1. Cowan, M. G.; Miller, R. G.; Southon, P. D.; Price, J. R.; Yazaydin, O.; Lane, J. R.; Kepert, C. J.; Brooker, S., *Inorg. Chem.* **2014**, *53* (22), 12076-12083.
2. O’Keeffe, M.; Yaghi, O. M., *Chem. Rev.* **2012**, *112* (2), 675-702.
3. Hu, Z.; Deibert, B. J.; Li, J., *Chem. Soc. Rev.* **2014**, *43* (16), 5815-5840.
4. Brozek, C. K.; Dincă, M., *Chem. Soc. Rev.* **2014**, *43* (16), 5456-5467.
5. Wang, C.; Zhang, T.; Lin, W., *Chem. Rev.* **2012**, *112* (2), 1084-1104.
6. Wang, X.-Y.; Wang, Z.-M.; Gao, S., *Chem. Commun.* **2008**, (3), 281-294.
7. Ma, L.; Abney, C.; Lin, W., *Chem. Soc. Rev.* **2009**, *38* (5), 1248-1256.
8. (a) Lal Saha, M.; Schmittel, M., *Org. Biomol. Chem.* **2012**, *10* (24), 4651-4684; (b) Han, M.; Engelhard, D. M.; Clever, G. H., *Chem. Soc. Rev.* **2014**, *43* (6), 1848-1860.
9. Saha, M. L.; Mittal, N.; Bats, J. W.; Schmittel, M., *Chem. Commun.* **2014**, *50* (81), 12189-12192.
10. Wilson, A.; Gasparini, G.; Matile, S., *Chem. Soc. Rev.* **2014**, *43* (6), 1948-1962.
11. Cook, T. R.; Stang, P. J., *Chem. Rev.* **2015**, *115* (15), 7001-7045.
12. Kurmoo, M., *Chem. Soc. Rev.* **2009**, *38* (5), 1353-1379.
13. (a) Kumar, G.; Gupta, R., *Chem. Soc. Rev.* **2013**, *42* (24), 9403-9453; (b) Srivastava, S.; Gupta, R., *CrystEngComm* **2016**, *18* (48), 9185-9208.
14. Vreshch, V. D.; Chernega, A. N.; Howard, J. A. K.; Sieler, J.; Domasevitch, K. V., *Dalton Trans.* **2003**, (9), 1707-1711.

15. Chen, B.; Fronczek, F. R.; Maverick, A. W., *Inorg Chem* **2004**, *43* (26), 8209-8211.
16. Fenton, H.; Tidmarsh, I. S.; Ward, M. D., *Dalton Trans.* **2010**, *39* (16), 3805-3815.
17. Sun, D.; Wang, D.-F.; Han, X.-G.; Zhang, N.; Huang, R.-B.; Zheng, L.-S., *Chem. Commun.* **2011**, *47* (2), 746-748.
18. Schmittel, M.; Kalsani, V.; Mal, P.; Bats, J. W., *Inorg Chem* **2006**, *45* (16), 6370-6377.
19. Kalsani, V.; Bodenstedt, H.; Fenske, D.; Schmittel, M., *Euro. J. Inorg. Chem.* **2005**, *2005* (10), 1841-1849.
20. Schmittel, M.; Kalsani, V.; Fenske, D.; Wiegrefe, A., *Chem. Commun.* **2004**, (5), 490-491.
21. Kalsani, V.; Ammon, H.; Jäckel, F.; Rabe, J. P.; Schmittel, M., *Chem. Eur. J.* **2004**, *10* (21), 5481-5492.
22. Schmittel, M.; Kalsani, V.; Michel, C.; Mal, P.; Ammon, H.; Jäckel, F.; Rabe, J. P., *Chem. Eur. J.* **2007**, *13* (21), 6223-6237.
23. Schmittel, M.; He, B.; Mal, P., *Org. Lett.* **2008**, *10* (12), 2513-2516.
24. Schmittel, M.; Mal, P., *Chem. Commun.* **2008**, (8), 960-962.
25. Kumar, P.; Gupta, R., *Dalton Trans.* **2016**, *45* (47), 18769-18783.
26. (a) Mishra, A.; Ali, A.; Upreti, S.; Gupta, R., *Inorg. Chem.* **2008**, *47* (1), 154-161; (b) Srivastava, S.; Dagur, M. S.; Gupta, R., *Eur. J. Inorg. Chem.* **2014**, *2014* (29), 4966-4974.

27. Mishra, A.; Ali, A.; Upreti, S.; Whittingham, M. S.; Gupta, R., *Inorg. Chem.* **2009**, *48* (12), 5234-5243.
28. (a) Singh, A. P.; Ali, A.; Gupta, R., *Dalton Trans.* **2010**, *39* (35), 8135-8138; (b) Singh, A. P.; Kumar, G.; Gupta, R., *Dalton Trans.* **2011**, *40* (46), 12454-12461.
29. Kumar, G.; Singh, A. P.; Gupta, R., **2010**, *2010* (32), 5103-5112.
30. Srivastava, S.; Dagur, M. S.; Gupta, R., *Euro. J. Inorg. Chem.* **2014**, *2014* (29), 4966-4974.
31. Freeman, F., *Chem. Rev.* **1980**, *80* (4), 329-350.
32. Gregory, R. J. H., *Chem. Rev.* **1999**, *99* (12), 3649-3682.
33. Bansal, D.; Kumar, G.; Hundal, G.; Gupta, R., *Dalton Trans.* **2014**, *43* (39), 14865-14875.
34. Borovik, A. S., *Acc. Chem. Res.* **2005**, *38* (1), 54-61.
35. Wang, D.; Lindeman, S. V.; Fiedler, A. T., *Euro. J. Inorg. Chem.* **2013**, *2013* (25), 4473-4484.
36. Redmore, S. M.; Rickard, C. E. F.; Webb, S. J.; Wright, L. J., *Inorg Chem* **1997**, *36* (21), 4743-4748.
37. Srivastava, S.; Aggarwal, H.; Gupta, R., *T Crystal Growth & Design* **2015**, *15* (8), 4110-4122.
38. Srivastava, S.; Kumar, V.; Gupta, R., *Crystal Growth & Design* **2016**, *16* (5), 2874-2886.
39. Bansal, D.; Pandey, S.; Hundal, G.; Gupta, R., *New. J. Chem.* **2015**, *39* (12), 9772-9781.

40. Morten, C. J.; Byers, J. A.; Van Dyke, A. R.; Vilotijevic, I.; Jamison, T. F., *Chem. Soc. Rev.* **2009**, *38* (11), 3175-3192.
41. Kumar, G.; Kumar, G.; Gupta, R., *RSC Adv.* **2016**, *6* (26), 21352-21361.
42. Kumar, G.; Pandey, S.; Gupta, R., *Crystal Growth & Design* **2018**, *18* (9), 5501-5511.
43. Karmakar, A.; Rúbio, G. M. D. M.; Guedes da Silva, M. F. C.; Pombeiro, A. J. L., *ChemistryOpen.* **2018**, *7* (11), 865-877.
44. (a) Thompson, M. C.; Busch, D. H., *J. Am. Chem. Soc.* **1962**, *84* (9), 1762-1763; (b) Thompson, M. C.; Busch, D. H., *J. Am. Chem. Soc.* **1964**, *86* (18), 3651-3656.
45. Zhang, G.; Mastalerz, M., *Chem. Soc. Rev.* **2014**, *43* (6), 1934-1947.
46. Inokuma, Y.; Arai, T.; Fujita, M., *Nature Chemistry* **2010**, *2*, 780.
47. Schmidt, B. M.; Osuga, T.; Sawada, T.; Hoshino, M.; Fujita, M., *Angew. Chem. Inter. Ed.* **2016**, *55* (4), 1561-1564.
48. Bar, A. K.; Chakrabarty, R.; Mostafa, G.; Mukherjee, P. S., *Angew. Chem. Inter. Edition* **2008**, *47* (44), 8455-8459.
49. Mallet, A. M.; Liu, Y.; Bonizzoni, M., *Chem. Commun.* **2014**, *50* (39), 5003-5006.
50. Gil-Ramírez, G.; Leigh, D. A.; Stephens, A. J., *Angew. Chem. Inter. Ed.* **2015**, *54* (21), 6110-6150.
51. Wasserman, E., *J. Am. Chem. Soc.* **1960**, *82* (16), 4433-4434.
52. Dietrich-Buchecker, C.; Sauvage, J.-P., *Tetrahedron* **1990**, *46* (2), 503-512.

53. (a) Hunter, C. A., *J. Amer. Chem. Soc.* **1992**, *114* (13), 5303-5311; (b) Vögtle, F.; Meier, S.; Hoss, R., *Angew. Chem. Inter. Ed. Eng.* **1992**, *31* (12), 1619-1622.
54. Sambrook, M. R.; Beer, P. D.; Wisner, J. A.; Paul, R. L.; Cowley, A. R., *J. Am. Chem. Soc.* **2004**, *126* (47), 15364-15365.
55. Fujita, M.; Ibukuro, F.; Hagihara, H.; Ogura, K., *Nature* **1994**, *367*, 720.
56. Guidry, E. N.; Cantrill, S. J.; Stoddart, J. F.; Grubbs, R. H., *Org. Lett.* **2005**, *7* (11), 2129-2132.
57. Tung, S.-T.; Lai, C.-C.; Liu, Y.-H.; Peng, S.-M.; Chiu, S.-H., *Angew. Chem. Inter. Ed.* **2013**, *52* (50), 13269-13272.
58. Barnes, J. C.; Fahrenbach, A. C.; Cao, D.; Dyar, S. M.; Frasconi, M.; Giesener, M. A.; Benítez, D.; Tkatchouk, E.; Chernyashevskyy, O.; Shin, W. H.; Li, H.; Sampath, S.; Stern, C. L.; Sarjeant, A. A.; Hartlieb, K. J.; Liu, Z.; Carmieli, R.; Botros, Y. Y.; Choi, J. W.; Slawin, A. M. Z.; Ketterson, J. B.; Wasielewski, M. R.; Goddard, W. A.; Stoddart, J. F., *Science* **2013**, *339* (6118), 429-433.
59. Livoreil, A.; Dietrich-Buchecker, C. O.; Sauvage, J.-P., *J. Am. Chem. Soc.* **1994**, *116* (20), 9399-9400.
60. Hori, A.; Kumazawa, K.; Kusukawa, T.; Chand, D. K.; Fujita, M.; Sakamoto, S.; Yamaguchi, K., DOSY Study on Dynamic Catenation: *Chem. Eur. J.* **2001**, *7* (19), 4142-4149.
61. Gupta, M.; Kang, S.; Mayer, M. F., *Tetrahedron Letters* **2008**, *49* (18), 2946-2950.

62. Chichak, K. S.; Cantrill, S. J.; Pease, A. R.; Chiu, S.-H.; Cave, G. W. V.; Atwood, J. L.; Stoddart, J. F., *Science* **2004**, *304* (5675), 1308-1312.
63. (a) Hasell, T.; Wu, X.; Jones, J. T. A.; Bacsá, J.; Steiner, A.; Mitra, T.; Trewin, A.; Adams, D. J.; Cooper, A. I., *Nature Chemistry* **2010**, *2*, 750; (b) Holst, J. R.; Trewin, A.; Cooper, A. I., *Nature Chemistry* **2010**, *2*, 915.
64. Ponnuswamy, N.; Cougnon, F. B. L.; Clough, J. M.; Pantoş, G. D.; Sanders, J. K. M., *Science* **2012**, *338* (6108), 783-785.
65. Barran, P. E.; Cole, H. L.; Goldup, S. M.; Leigh, D. A.; McGonigal, P. R.; Symes, M. D.; Wu, J.; Zengerle, M., *Angew. Chem. Inter. Ed.* **2011**, *50* (51), 12280-12284.
66. Zhang, G.; Gil-Ramírez, G.; Markevicius, A.; Browne, C.; Vitorica-Yrezabal, I. J.; Leigh, D. A., *J. Am. Chem. Soc.* **2015**, *137* (32), 10437-10442.
67. Gil-Ramírez, G.; Hoekman, S.; Kitching, M. O.; Leigh, D. A.; Vitorica-Yrezabal, I. J.; Zhang, G., *J. Am. Chem. Soc.* **2016**, *138* (40), 13159-13162.
68. Zhang, L.; August, D. P.; Zhong, J.; Whitehead, G. F. S.; Vitorica-Yrezabal, I. J.; Leigh, D. A., *J. Am. Chem. Soc.* **2018**, *140* (15), 4982-4985.
69. Ayme, J.-F.; Beves, J. E.; Leigh, D. A.; McBurney, R. T.; Rissanen, K.; Schultz, D., *Nature Chemistry* **2011**, *4*, 15.
70. Shi, Y.; Cai, K.; Xiao, H.; Liu, Z.; Zhou, J.; Shen, D.; Qiu, Y.; Guo, Q.-H.; Stern, C.; Wasielewski, M. R.; Diederich, F.; Goddard, W. A.; Stoddart, J. F., *J. Am. Chem. Soc.* **2018**, *140* (42), 13835-13842.
71. Zhang, L.; Stephens, A.; L. Nussbaumer, A.; Lemonnier, J.-F.; Jurček, P.; Vitorica, I.; Leigh, D., 2018; Vol. 10.

72. Danon, J. J.; Leigh, D. A.; Pisano, S.; Valero, A.; Vitorica-Yrezabal, I. J., *Angew. Chem. Inter. Ed.* **2018**, *57* (42), 13833-13837.
73. Vella, S. J.; Loeb, S. J., *Beilstein J. Org. Chem.* **2018**, *14*, 1908-1916.
74. Bloch, W. M.; Holstein, J. J.; Dittrich, B.; Hiller, W.; Clever, G. H., *Angew. Chem. Inter. Ed.* **2018**, *57* (19), 5534-5538.
75. Wang, Y.; Stoddart, J. F., *Chem* **2017**, *3* (1), 17-18.

Chapter-2

Heterometallic Coordination Polymers with Pyrazine 2, 6-dicarboxamide:

Sequential Metallation of Co(III) and Ag(I)

2.1. Abstract

2.2. Introduction

2.3. Results and Discussion

2.4. Conclusion

2.5. Experimental Section

2.6. References

2.7. Spectral Data

2.8. Crystal Data

2.1. Abstract

A sequence of hetero-metallic complexes of Co(III) and Ag(I) were reported by stepwise manner utilising 2, 6-pyrazinedicarboxamide appended with pyridines as building unit. 2, 6-pyrazinedicarboxamide plays as active site for coordination of octahedral Cobalt(III) ion, whereas the pyridine unit are used for the silver(I) coordination. In 4-pyridine attached ligand, both pyridine and pyrazine units coordinated to Ag(I). Among the three complexes, two complexes were studied in solid state. They are, one i. e. **(5a)** $[\text{Co}(\text{L1})_2]\text{Ag}_3$ is coordinated to three of Ag(I) and other i. e. **(5b)** $[\text{Co}(\text{L2})_2]\text{Ag} \cdot 2\text{H}_2\text{O}$ exhibit an unexpected five coordinated Ag(I). One of these ligand is measured for Ag(I) coordination in solid state i.e. **(3)** $\text{Ag}(\text{H}_2\text{L1}) \cdot \text{NO}_3 \cdot 2(\text{H}_2\text{O})$.

2.2. Introduction

The study of coordination polymers have gained significant importance due to their unique structural properties and widespread application.^{1 2} Sometimes, these materials have multiple catalytic site that has an identical chemical environment due to crystalline nature of the material.³ The properties Heterometallic coordination polymers are the collection of two/more metals along with polymers. They are utilized in different areas such as ion exchange and transport, absorption,² separation,^{4 5} luminescent material ,sensing⁶ optics, and catalysis^{1 7} etc. The construction of heterometallic complexes can be performed by both single pot and stepwise manner. The major disadvantage in stepwise synthesis there would be the chances of formation of both homometallic and heterometallic complex. But the stepwise synthesis is more superior because of proper choice of metalions and ligands effects better result. Pyridine derivative deals an ingenious linking atmosphere for these kinds of purposes. The pyridine nitrogen atom can coordinate to several metals and if appropriately designed substituents are present it can be used for synthesis of heterometallic coordination polymer.⁸ One such kind of systems is 2, 6-pyridine dicarboxamide system where amide group behaves as a neutral ligand over carbonyl oxygens and as an anionic ligand by deprotonation of nitrogen atoms. One of advantages of pyridine based ligands is its structural flexibility.⁹ Due to this, it can provide a geometric requirement for the construction of different supramolecular architecture by coordinating to different functional groups. Pyridine dicarboxamide ligands are well deliberated in the synthesis of homometallic complex, ion recognition and catalytic activities etc.¹⁰ One of the system is bis pyridyl amide which discovers their valuable application in asymmetric-catalysis due to its tendency for stabilizing the different metal ions in their different oxidation state.¹¹ Supramolecular structural designs such as [2 × 2] molecular grid has reported earlier from pyridine derivatives diamide ligands and using as molecular storage devices.¹² Lehn and co-

workers had synthesized the first primary triply switchable scheme, the $[2 \times 2]$ grid $\text{Fe}_4(\text{II})$ 1, where spin crossover can be activated by action of light, temperature, and pressure. $[\text{Fe}_4\text{L}_4](\text{ClO}_4)_8$ complex was synthesized by extemporaneous assemblage of ligand 4, 6-bis (2', 2'')- bipyrid- 6'-yl) - 2- phenyl-pyrimidine with metal salt $\text{Fe}(\text{ClO}_4)_2 \cdot 6\text{H}_2\text{O}$ under acetonitrile solution at (RT)room temperature and precipitated with DEE(diethyl ether).¹² In pyrazine, there is more than one nitrogen atoms than pyridine ring may deal analogous advantages but its weak binding ability weaken its effective uses.¹³ This types of systems are less reported in the literature, however the binding nature of pyrazine 2, 6-dicarboxamide are less discovered. Sally Brooker and his co-workers synthesized $[2 \times 2]$ molecular grid with Cu^{2+} and Ni^{2+} metal salts in basic environment by utilising ligand as N,N-bis[2-(2-pyridyl)ethyl]pyrazine-2,3-dicarboxamide (figure 2.1).¹⁴With pyrazine 2, 5-diamide, it also forms a supramolecular square $[2 \times 2]$ grid in presence of $\text{Co}(\text{II})$ metal salts(figure 2.2).¹⁵

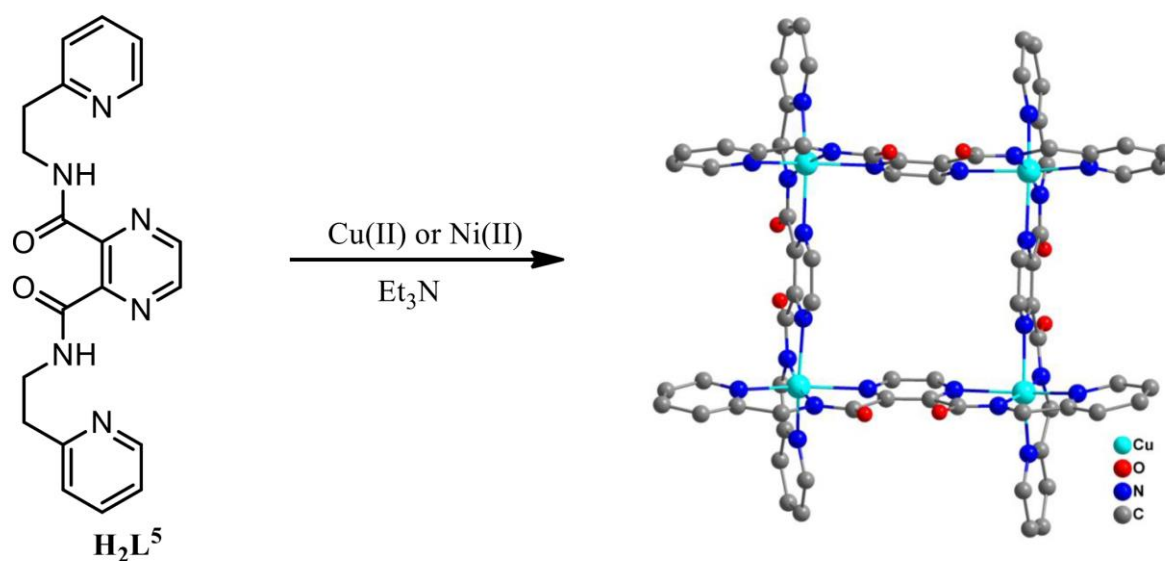


Figure 2.1. Ni(II) or Cu(II) coordination with $[\text{L}^5]\text{-2}$ resulting $[2 \times 2]$ molecular grid

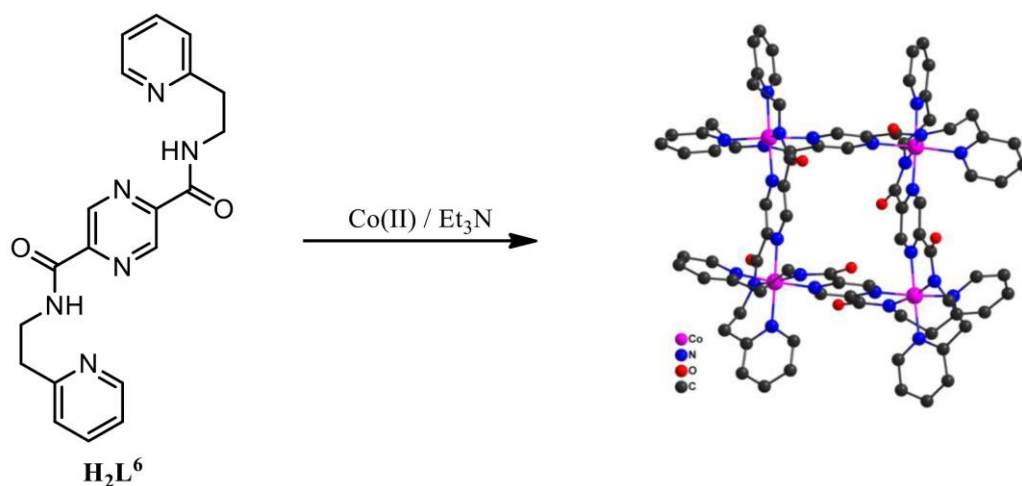


Figure 2.2. Coordination of Co(III) with $[\text{L}^6]\text{-2}$ resulting $[2 \times 2]$ molecular grid.

The synthesis and coordination mode of pyridine appended pyrazine-2-carboxamide ligand had revealed that in presence of Ag(I) ion it forms a metallomacrocyclic while in presence of base it forms Co(III) complex (figure 2.3).¹⁶

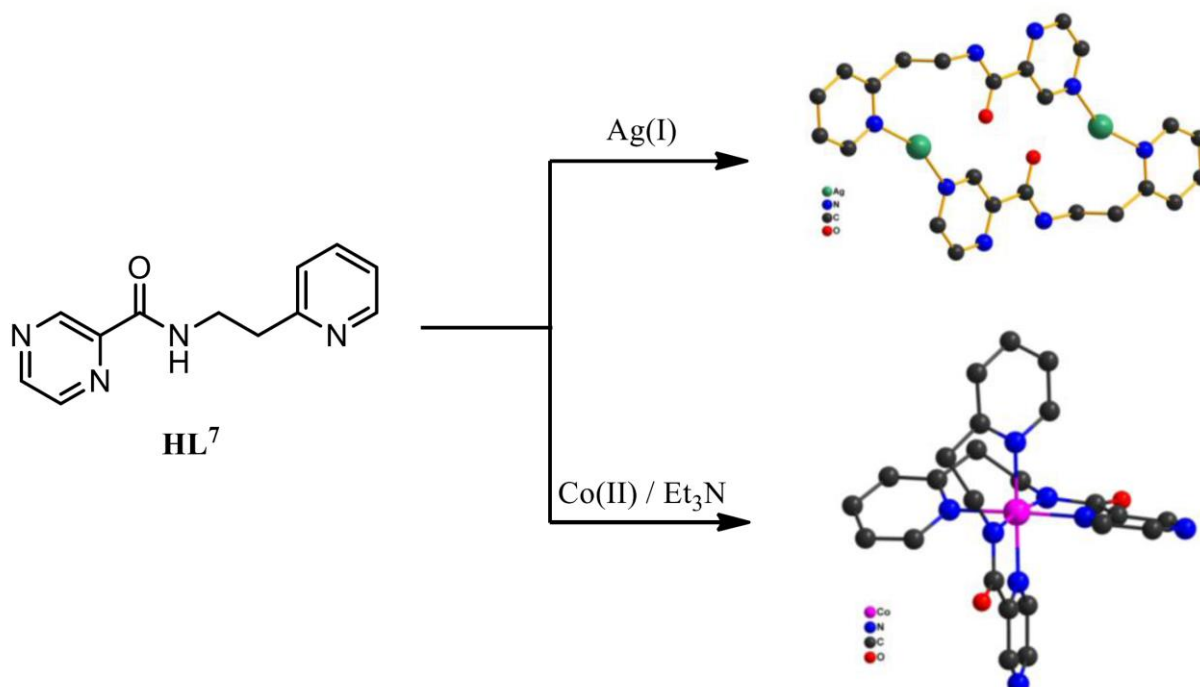


Figure 2.3. Synthesis of $\text{Ag}_2(\text{HL}^7)_2$ and $\text{Co}(\text{L}^7)_2$ from HL^7

By changing metal to ligand coordination, three kinds of various heterometallic complexes were produced. Constructed these ideas, herewith we have synthesized three of the newly pyrazine-2,6-dicarboxamide based pyridine frameworks having three different coordination positions (Figure 2.5).

Among these three different coordination positions, position 1 can be arranged in octahedral way with different metals like Co^{3+} , Fe^{3+} and position 2 can be coordinated to different soft metals as Ag^+ or Hg^{2+} . Position 3, which is a pyridine unit, can direct to several metal ions such as Pt^{2+} , Pd^{2+} , Ag^+ (Figure. 2.5). By sequentially coordination of ligands with metal ions Cobalt(III) and silver(I), three separate kinds of coordination polymers(CP) were manufactured.

2.3. Results and Discussion

The objective compound was produced succeeding literature methods by removing the benzyl amine with 4-methylaminopyridine. The synthesis was performed with readily accessible 2, 6-dimethylpyrazine. The 2, 6-dimethylpyrazine was oxidized with SeO_2 first and then following esterification procedure to obtain substituted derivatives of pyrazine diester **1**. **1** was reacted with different kinds of amines such as 4-methylaminopyridine, 3-methylaminopyridine and 2-methylaminopyridine afforded three different types of substituted amides derivatives, as **2a**, **2b** and **2c** etc. (Figure 2.6) and were analysed by ^1H NMR as well as ESI-MS spectroscopic technique. The anionic part of these molecules have two of the open pyrazine and two pyridine N-atoms as considered.

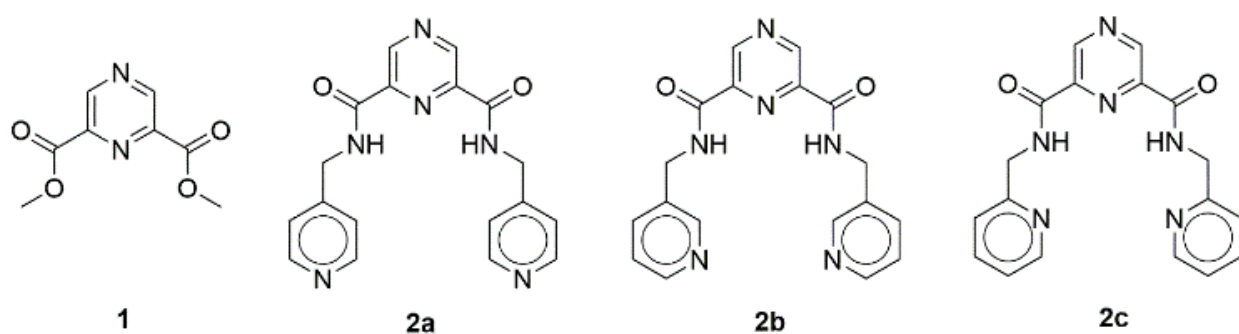


Figure 2.6. Molecular structures **2a**, **2b** and **2c**

Before continuing to prepare the heterometallic complexes, we planned for checking coordination of the ligands nature. We have chosen, **2a**, in which the molecule has a 4-pyridine unit can coordinate with metal Ag^+ . We have selected the silver(Ag) metal, because of the binding positions are of reduced nucleophilicity as a result of the strongest electron withdrawing capacity of the amide groups. As a result, it may organise with few softer metal ions such as Hg^{2+} and Ag^+ . Additionally, the Ag(I) complexes have several kinds of uses as antimicrobial-agents as antibiotics,¹⁹ biologically applicable coordination compounds,²⁰ and photo active materials²¹ and can produce various coordination complexes with coordination number(CN) 2, 3, 4, 5, 6, 7 in a appropriate ligand environment.²²

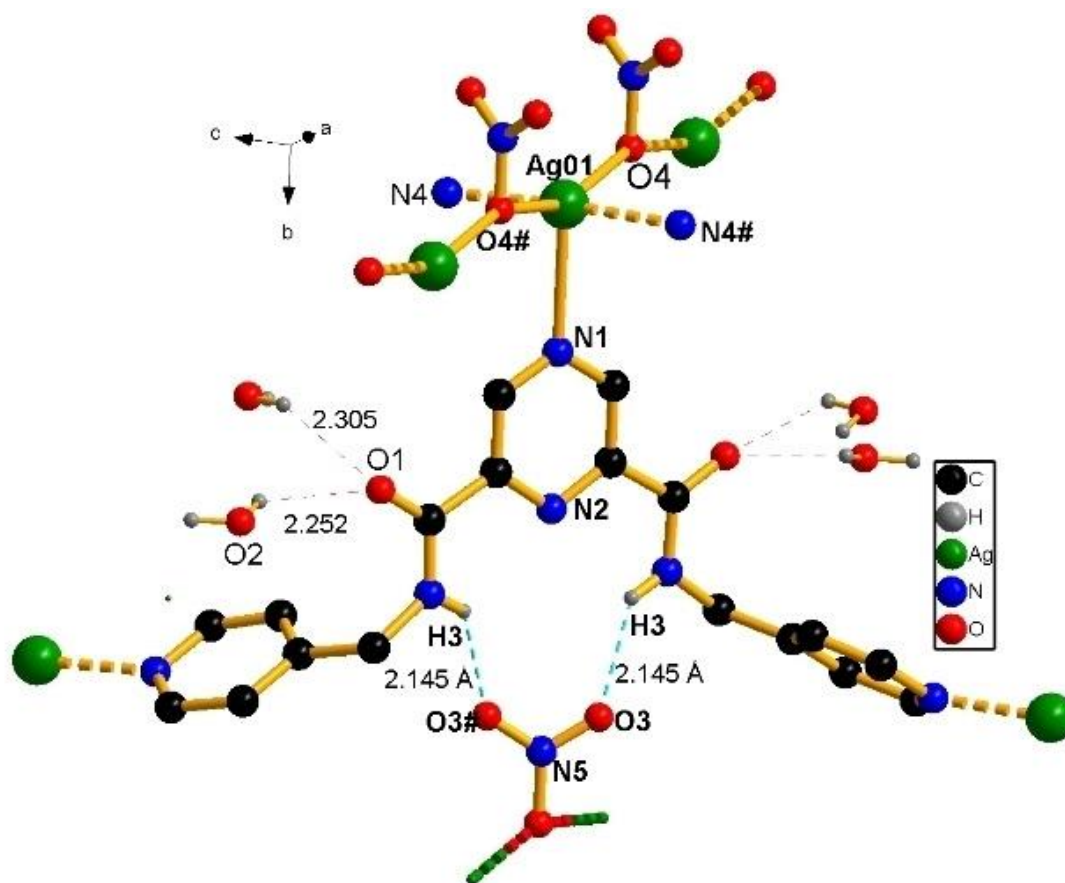


Figure 2.7. X-ray crystal structure of complex **3** indicating the AgNO_3 coordination and possible Hydrogen bonding.

For the coordination of metal, **2a** was solubilised in methanol and AgNO_3 (one equivalent) was added and continued stirring at room temperature. After thirty minutes a white precipitate was observed. Block shaped crystals were grown within fifteen days by dissolving this precipitate in 50% acetonitrile-chloroform mixture for solid state analysis. The molecule crystallized in Pbcn space group in orthorhombic crystal system. The asymmetric unit comprises partial ligand structure, half of pyrazine ring and NO_3^- anion and one pyridine ring, one H_2O molecule alongside with one Ag^+ ion. The molecular assembly indicates, the molecule is linked with three Ag^+ ions: two pyridine nitrogen ($\text{Ag1-N4}=2.20(7) \text{ \AA}$) and one pyrazine N-atoms ($\text{Ag1-N1}=2.61(7) \text{ \AA}$) alongside with an O-atom from a NO_3^- ion ($\text{Ag1-O4}=2.87(3) \text{ \AA}$). The Ag^+ ion exhibit a heavily loaded distorted tetrahedral coordination geometry with $\text{N4-Ag-N4}\#=175.8(9)^\circ$ and $\text{O4-Ag-O4}\#=161.8(9)^\circ$ (Figure 2.7) whereas the NO_3^- ion is creating a bridge between two Ag^+ ions over one of its O-atoms ($\text{Ag-O}=2.87(3) \text{ \AA}$) (Figure 2.7). The amide O-atoms are holding the water (H_2O) molecule by hydrogen bonding(H-bond) with $\text{O2-H2A}\dots\text{O1}$ $2.23(8) \text{ \AA}$, $154.0(9)^\circ$ and $\text{O2-H2B}\dots\text{O1}$ $2.10(9) \text{ \AA}$, $154.4(8)^\circ$ and with NO_3^- ion $\text{N3-H3}\dots\text{O3}$ ($2.14(8) \text{ \AA}$, $137.9(7)^\circ$).

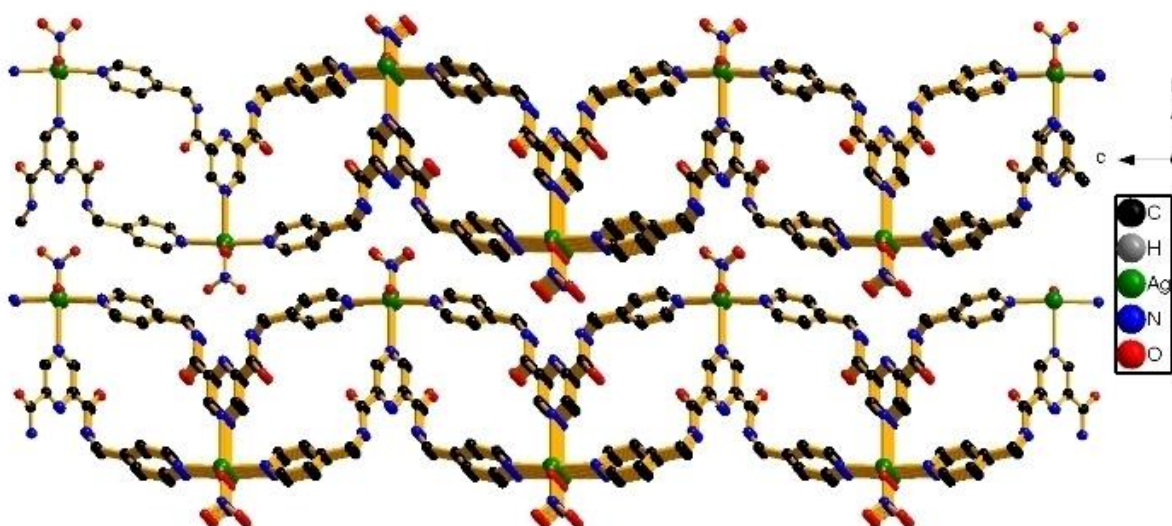


Figure 2.8. A complete Packing representation of complex **3** along crystallographic a-axis displaying the three dimensional (3D) polymer.

137.9(7)8). A simplified packing diagrammatic representation of complex **3** was revealed in (Figure 2.8 and 2.9). We also tried for the coordination behaviour of **2b** and **2c** with Ag(I) under the similar crystal conditions. Conversely, we were unable to achieve the single crystal after six months.

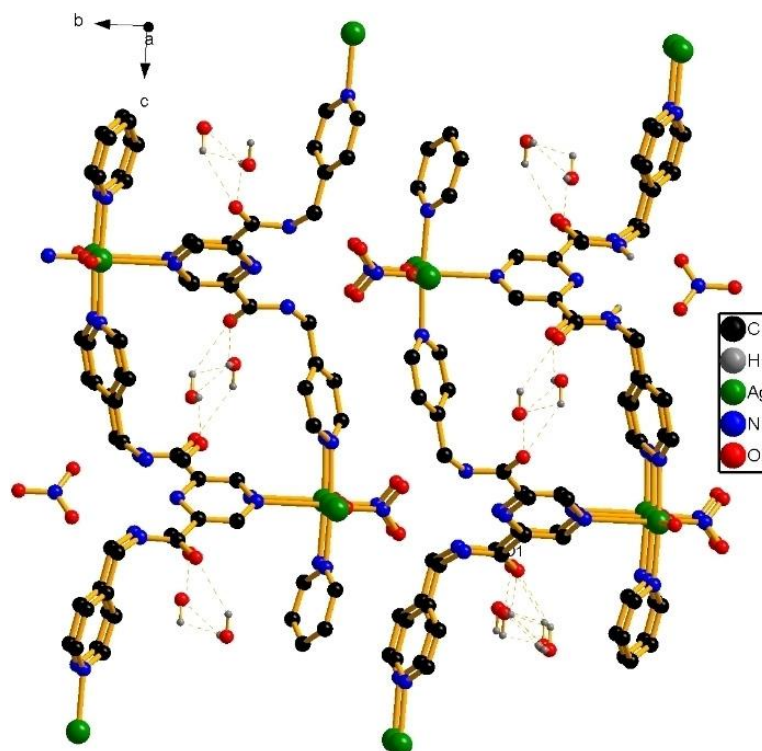


Figure 2.9. Packing diagrammatic representation of **3** showing H-bond interaction between amide nitrogen and the water (H₂O) molecule

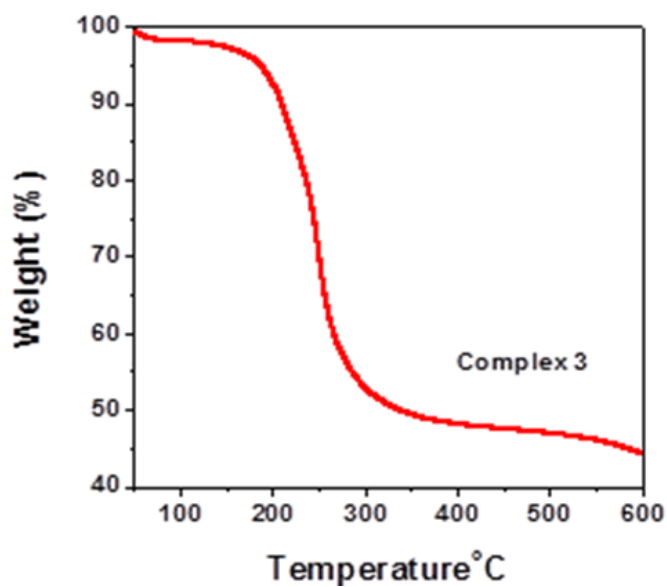
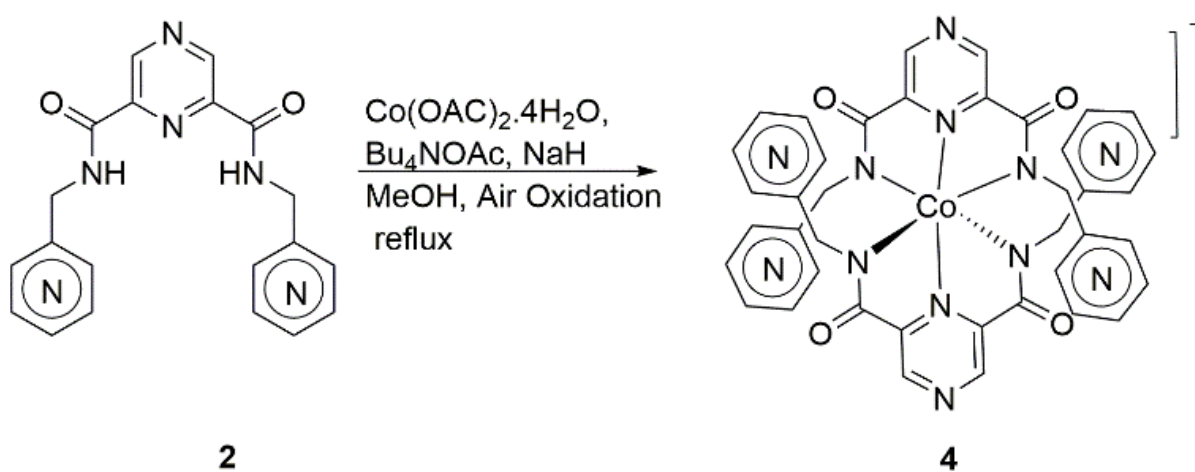


Figure 2.10. TGA analysis for complex **3**

The coordination complex **3** was further analysed by powder x-ray diffraction (PXRD), infrared spectroscopy (IR) and thermo gravimetric analysis (TGA) techniques. From the Powder x-ray diffraction analysis of coordination complex **3**, it is revealed that the phase purity of the complex was good in agreement with the simulated patterns (Figure.2.36). Infrared spectroscopic analysis of complex **3** indicated corresponding peak appears at 1680 cm^{-1} due to amide carbonyl stretching and a broad peak appears at $3500\text{--}3700\text{ cm}^{-1}$ due to presence of amide N-H stretching and present H_2O molecules (Figure.2.33). Thermogravimetric analysis explained that the thermal stability of coordination complex **3** was $210\text{ }^\circ\text{C}$ (Figure.2.10).

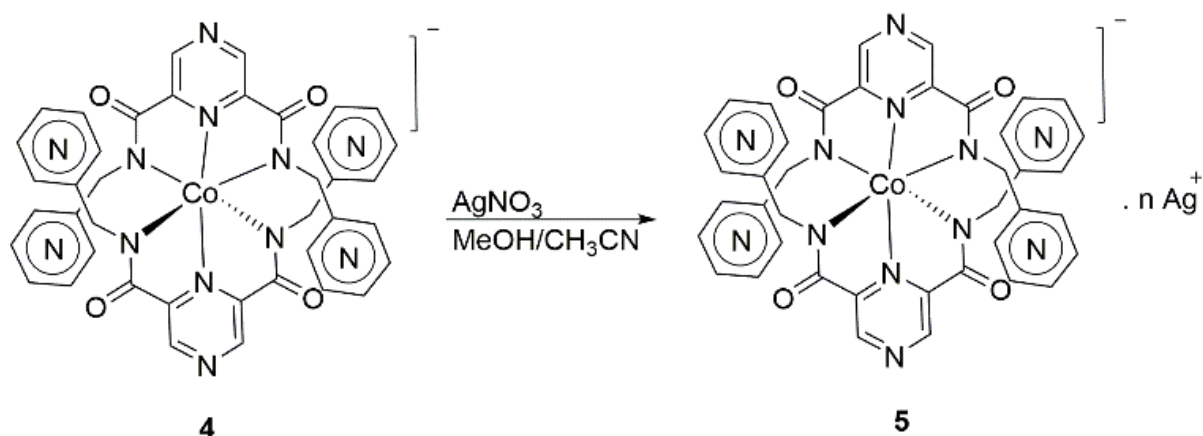
In order to successfully synthesizing the heterometallic complex from ligand **2**, we prepared the cobalt complexes of this ligand by following adopted literature procedure.²³ For synthesizing the cobalt complexes, N-H protons in respective dicarboxamide ligand were deprotonated with sodium hydride (NaH) followed by succeeding metalation with Co(II) was performed in a one pot under a continuous environment of nitrogen (scheme 2.1). When this reaction pot was unlocked to atmosphere, Co^{2+} was oxidized to Co^{3+} which may be observed by the color change of the reaction solution to deep green. Therefore, complexes **4a**, **4b**, and **4c** were produced and analysed by $^1\text{H-NMR}$ and ESI-MS spectroscopic technique.



Scheme 2.1. Synthesis of pyrazine based cobalt complex, **4a**, **4b** and **4c**

The ^1H NMR spectra clearly specifies that the vanishing of amide proton peak, as well as the appearance of a tart-butyl ammonium ion peak in ^1H -NMR spectra, specifies the presence of Co(III) complexes (Figure 2.23-2.28).

For the preparation of the heterometallic coordination polymers (HCP), **4a**, **4b** and **4c**, were solubilized in MeOH and treated with exact amount of AgNO_3 to obtain heterometallic complexes **5a** and **5b** respectively (scheme 2.2).



Scheme 2.2. Synthesis of pyrazine based Ag(I)-Co(III) Heterometallic complex, **5a**, **5b**

In order to prove the silver(Ag) mode of coordination behaviour, we have recorded ESI-MS under various solution conditions, still we didnot get any authentic peak in ESI-MS spectroscopic technique. It is obvious that the complex was not enough stable under mass-spectroscopic situation. Proving of solid state behaviour, we have also tried for finding the single crystal of **5a**, **5b** and **5c**. Crystals appropriate for X-ray diffraction for complex **5a** (Figure 2.11) were grown by dissolving the precipitate formed by (addition of silver nitrate (AgNO_3) to cobalt(III) complex, **4a**) in 50 % acetonitrile and methanol mixture. The crystals were grown in two months. It crystalized in I-42d space group in monoclinic crystal system. The asymmetric unit comprises one(1) molecule of **4a** along with two(2) of the silver(Ag) atoms. Ag1 was in 4-fold axis of symmetry and Ag2 was in 2-fold axis of symmetry however Co(III) was in 4-fold axis of symmetry generates +1.5 charge that is balanced by N1(2-fold axis of

symmetry) and N3. The molecular structure displays the complex was linked with six(6) silver ions: four(4) pyridine nitrogen ($\text{Ag2-N4} = 2.18(3) \text{ \AA}$) and two(2) pyrazine nitrogen atoms ($\text{Ag1-N2} = 2.19(3) \text{ \AA}$) (Figure 2.11). The Ag^+ ion has a linear coordination geometry with N2-Ag-N2\# bond angle is 180° . The bond distance between Ag1-Ag2 is of $6.10(6) \text{ \AA}$. As a result of coordination of silver(Ag) and the Ag-N bond the crystal lattice is making a three dimensional(3D) polymer assembly (Figure 2.12). Wholly all the six(6) accessible coordination sites are engaged by Ag^+ . It is significant that all twelve(12) nitrogen coordination sites are engaged.

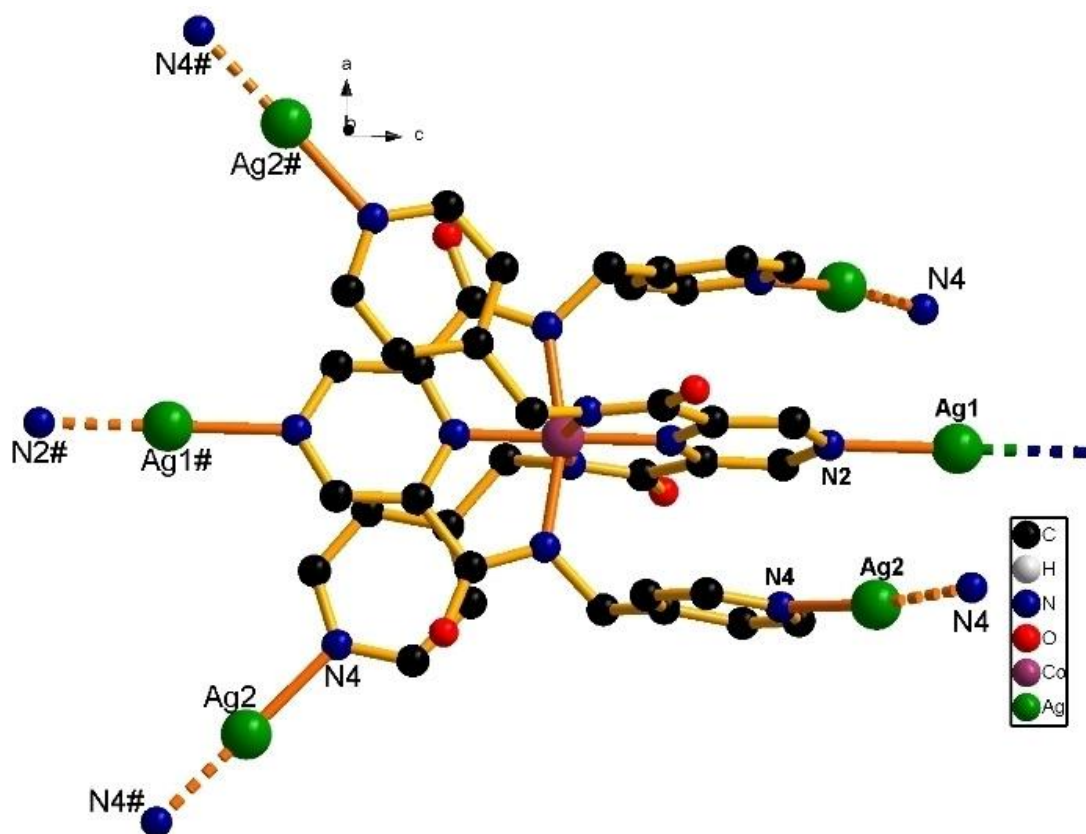


Figure 2.11. Ag(I) mode of Coordination in complex **5a**.

The complex **5a** was further analysed by powder x-ray diffraction (PXRD), infrared (IR) and thermogravimetric analysis (TGA) experiments. Powder x-ray diffraction (PXRD) analysis of heterometallic complex **5a**, discloses the phase purity of the complex which is similar with that of the simulated patterns (Figure.2.37). Infrared (IR) spectra for complex **5a** showing significant peak appears at $1530\text{--}1640\text{ cm}^{-1}$ due to amide carbonyl stretching frequency and a broad peak appears at $3500\text{--}3700\text{ cm}^{-1}$ due to presence of amide N-H stretching and present H_2O molecules (Figure 2.34). Thermogravimetric analysis (TGA) of heterometallic complex **5a** directed rate of decomposition in temperature range of $150\text{--}450\text{ }^\circ\text{C}$ (Figure.2.13). Decomposition of first step at a temperature of $150\text{ }^\circ\text{C}$ with loss of weight of 3% due to elimination of coordinated solvent molecules. In second step decomposition, **5a** decomposed at a temperature of $240\text{ }^\circ\text{C}$ and completely decomposed at a temperature of $450\text{ }^\circ\text{C}$.

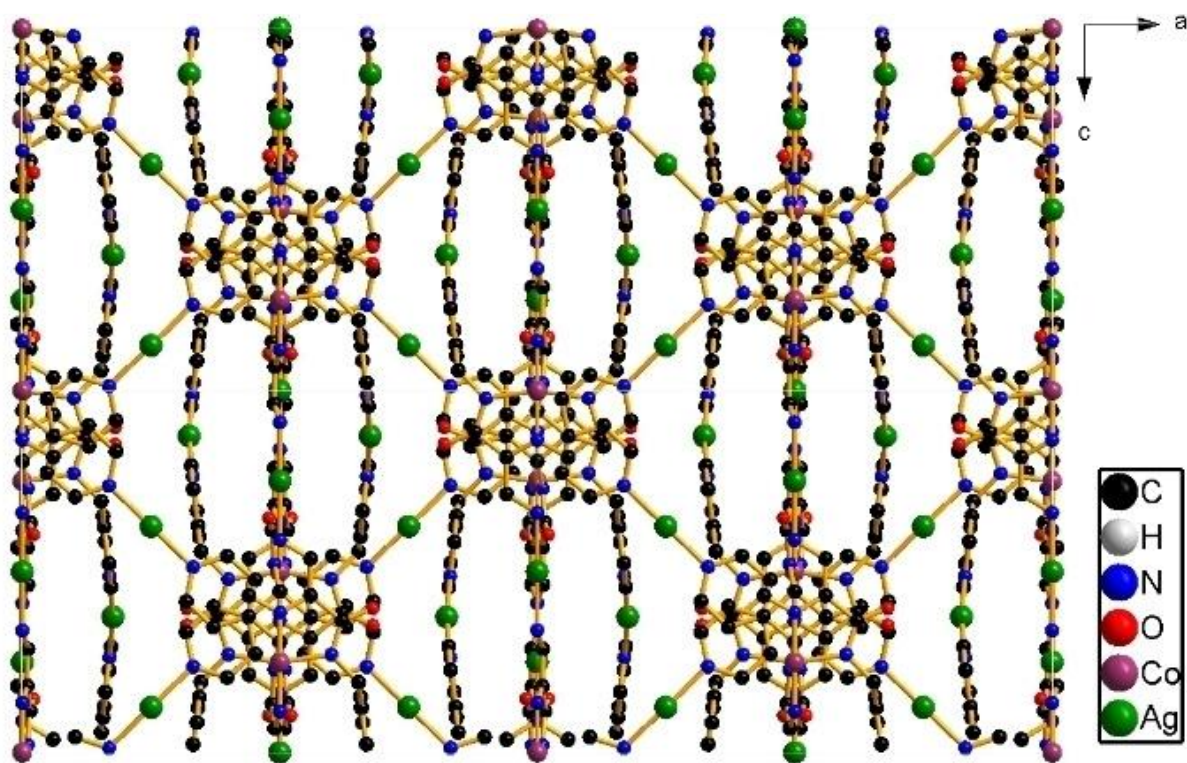


Figure 2.12. Packing diagrammatic representation of complex **5a** along crystallographic b-axis

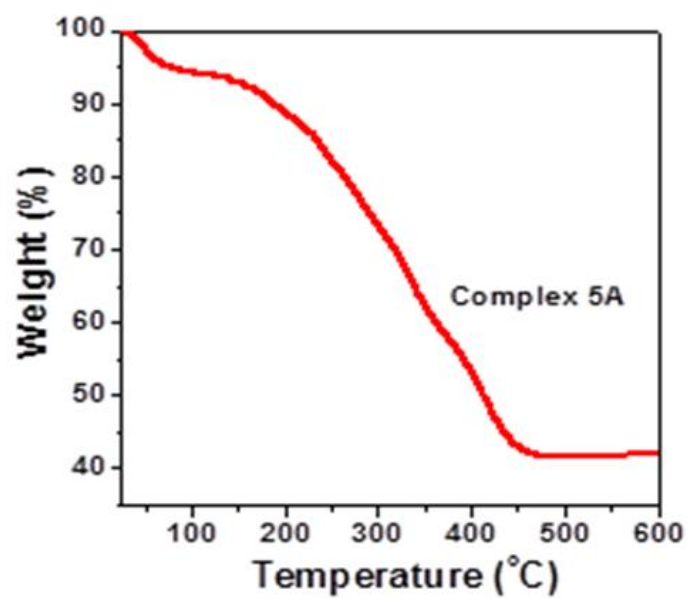


Figure 2.13. TGA analysis for 5a

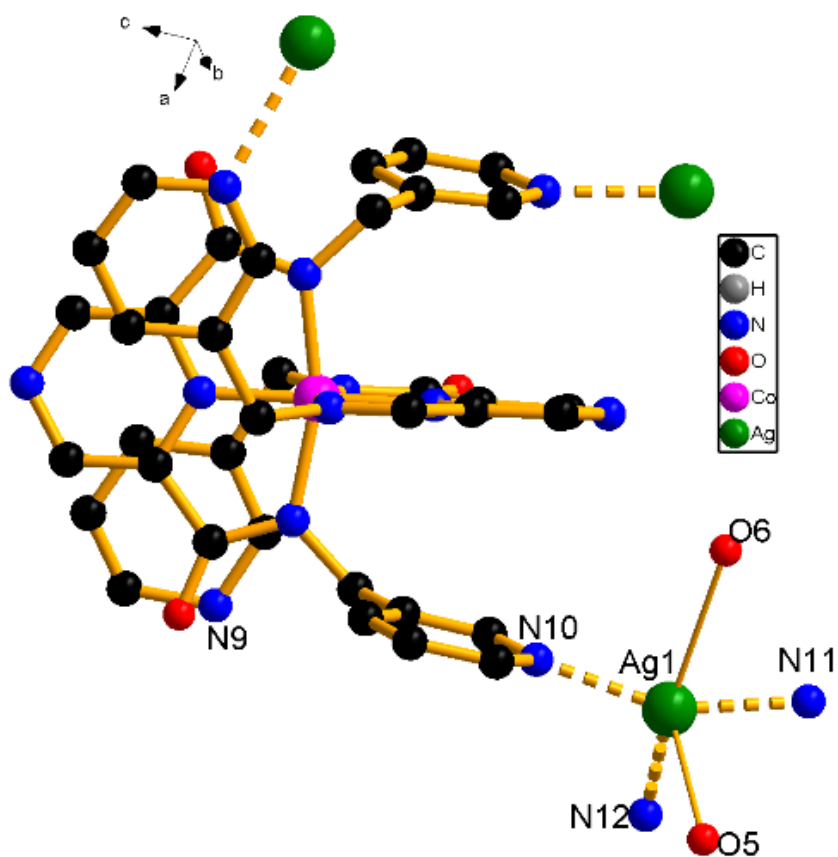


Figure. 2.14. Binding of Ag(I) in complex 5b.

Similarly, the suitable crystal for solid state analysis was grown for heterometallic complex **5b**. It crystallized in P212121 in orthorhombic crystal system. The asymmetric unit comprises one molecule of **5b** along with one silver(Ag) and two coordinated water(H₂O) molecules. This represents that the Ag⁺ ion was adjusting the charge of the anionic cobalt complex. Ag(I) is linked to the three(3) of the pyridine N-atoms from three(3) separate molecules with bond distance (N11-Ag1, N10-Ag1 and N12-Ag1 are 2.26(8), 2.23(7) and 2.65(8) Å respectively) and two of water(H₂O) molecules having bond distance of 2.60(8) Å and 2.86(5) Å (Figure 2.14). Hence, Ag(I) have five coordinated distorted square planer geometry. The bond angle between N10-Ag-N11, N6-Ag-O12 and N12-Ag-O5 are 155.1(8)°, 154.0(9)° and 86.0(2)° respectively. Due to collective outcome of reducing the nucleophilicity (as it is in ortho position w.r.t amide group) of amide N-atoms and steric crowding, N9 atom of pyridine ring was not involved in binding to Ag(I) in **5b**.

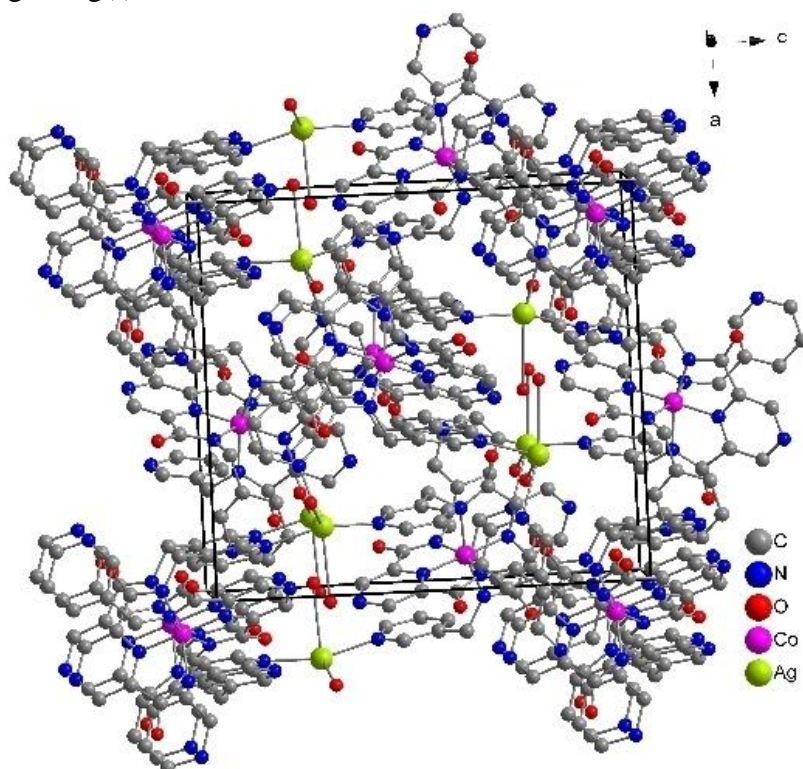


Figure 2.15. Packing diagrammatic representation of complex **5b** along crystallographic b-axis.

Hydrogen bond are developed between water(H₂O) molecules with amide O-atoms with lengths of O5-H5B...O3 1.95(8) Å and O(6)- H(6B)...O(4) 2.27(8) Å ; bond angle of 149.2(8)° and 124.8(8)° etc. A abridged packing diagrammatic representation of complex **5b** was revealed in Figure 2.15. As a result of binding of Ag-N bond and contact of water(H₂O) molecule to Ag(I), it caused a three dimensional (3D) polymer network. Powder x-ray diffraction analysis of complex **5b**, exposes the phase purity of the complex which matched with simulated patterns (Figure 2.38). Infrared spectroscopic data for complex **5b** shown significant peak appears at 1540–1650 cm⁻¹ due to amide carbonyl stretching frequency and a broad peak appears at 3500–3700 cm⁻¹ due to presence of amide N-H stretching and present water(H₂O) molecule in this complex (Figure.2.33). At first the heterometallic complex **5b** decomposed at a temperature of 260 °C with loss 4% weight because of exclusion of coordinated water(H₂O) molecules, secondly decomposed at a temperature of 320 °C and finally decomposed at 470 °C leaving the remaining metal oxides (Figure.2.16). We also tried the coordination nature of **4c** with Ag(I), but did not get single crystal of complex **5c** after several months.

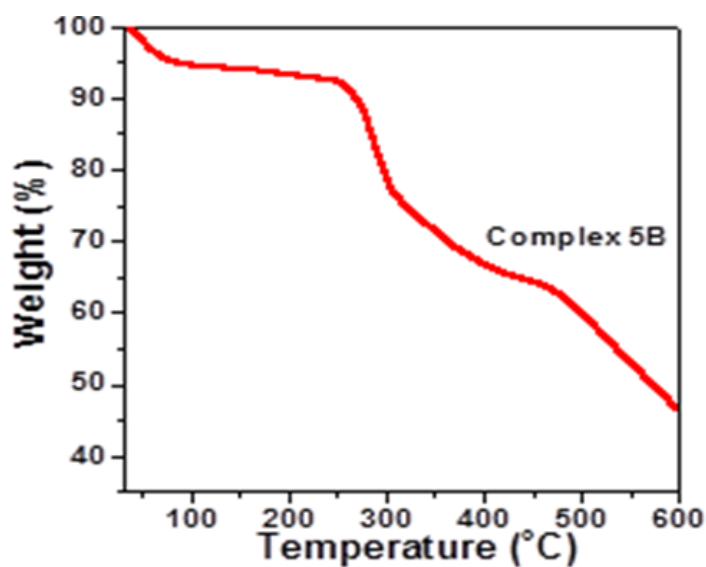


Figure 2.16. TGA analysis for **5b**

2.4. Conclusion

Three cobalt complexes were successfully prepared, those are further coordinated with silver(Ag^+) obtained to two(2) heterometallic and one(1) homometallic complexes. Among the two, one of the heterometallic complex **5a** $[\text{Co}(\text{L1})_2]\text{Ag}_3$, all the twelve(12) N-atoms are coordinated. In overall twelve (12) coordination, six (6) are coordinated to Co(III) and other six(6) are coordinated to Ag(I). The binding to Ag(I) afforded a three dimensional (3D) polymeric structure. In the other complex **5b** $[\text{Co}(\text{L2})_2]\text{Ag} \cdot 2\text{H}_2\text{O}$, three(3) of N-atoms were not involved in binding and other three N-atoms linked to Ag(I). The residual six(6) N-atoms linked to Cobalt(III). In this case an exceptional five coordinated Ag(I) mode of coordination was noticed with three(3) of ligands and two of water(H_2O) molecules linked to it. This affords Ag(I) bears a distorted square planer geometry. Whereas, the coordination complex **3** $\text{Ag}(\text{H}_2\text{L1}) \cdot \text{NO}_3 \cdot 2(\text{H}_2\text{O})$, Ag(I) was distorted tetrahedral geometry.

2.5. Experimental procedures

2.5.1. Material and Physical Measurements

The required chemicals were collected from sigma Aldrich and utilized as received. All the solvents were bought from Merck- India Limited. All the Solvents were purified by using the standardised methods. Nuclear magnetic resonance(NMR) were performed with a Bruker 400 MHz and 700 MHz instrument by using CD_3OD (methanol d_4) as a solvent. ESI-MS were done in a Bruker microTOF-Q II spectrometer utilising methanol(CH_3OH). Single crystals X-ray diffraction analysis were performed in a Bruker 4-circle Kappa APEX-II diffractometer prepared with a CCD detector, the X-ray source is Mo $\text{K}\alpha$ (wavelength 0.71073 Å) at room temperature(complex **5a** and **5b**) and Rigaku Oxford diffractometer with model no. XTALAB supernova prepared with PILATUS 200 K detector, the X-ray source is Cu $\text{K}\alpha$ (the wave-length 1.54178 Å) (complex **3**). Data collection was performed with Apex II software, and processing

was carried out with SADABS integrated with Apex II. The structure solution was formed with SHELXT and expanded by using Fourier technique. For **5a**, solvent could not be modelled, therefore squeeze technique was used to remove electron density of this molecule from the crystal data. TGA were carried out at a ramp rate of 10 °C min⁻¹ under a continuous flow of N₂ gas at a temperature range of 30– 600 °C using a Discovery TGA by TA Instruments-Waters Lab. Powder X-ray diffraction data were performed on a Bruker D8 Advance with DA VINCI design fitted with an HTK 16 temperature chamber X-ray powder diffractometer utilising CuK α radiation ($\lambda = 1.5418 \text{ \AA}$). Infrared spectra were performed on a Perkin-Elmer IR spectrometer prepared with a reduced total reflectance accessory.

Synthesis of compound **1**

1.00 g (9.25 mmol) of 2, 6-dimethyl pyrazine was solubilized in 20 mL of 10 % pyridine-water mixture. To that solution 5.132 g (46.25 mmol) of SeO₂ was added and refluxed at temperature of 80 °C for a period of twelve hour(12 h). After a thirty minutes, the mixture transforms to brown-red, and selenium subsequently precipitated as a greenish solid. The reaction solution was then cooled at room temperature and filtered. The precipitate was washed with NH₄OH (ammonium hydroxide) (10 mL). The filtrates were removed and dried under vacuum to result a targeted crude product as brownish solid of corresponding salt. The brownish ammonium salt was taken in MeOH (methanol) and 3.38 mL (46.25 mmol) of SOCl₂ was added and refluxed for 3 h at temperature 60 °C. Completion of this time, the reaction mixture was cooled to room temperature (RT), neutralized with saturated aqueous Na₂CO₃ solution and then extracted with CH₂Cl₂ (dichloromethane). This was then dried by using anhydrous Na₂SO₄, evaporated and the mixture was separated using column chromatographic technique followed by evaporation of solvent to get the targeted compound **1** as a white solid (1.25 g, 69 %). ¹H-NMR (400 MHz, CDCl₃) $\delta = 9.47$ (s), 4.06 (s). ¹³C-NMR (100 MHz, CDCl₃) $\delta = 163.9, 148.8, 148.7, 142.9, 53.5$. ESI-HRMS: m/z : 197.0585 [M + H]⁺ (calc. 197.0557).

Synthesis of (H2L1), **2a**

1 (0.100 g, 0.129 mmol) was suspended in 10 mL of methanol. To this 4-methylaminopyridine (0.129 mL, 1.207 mmol) was added and refluxed for a period of 12 h and the progress of the reaction was noticed by TLC (thin layer chromatography). The solvent was removed under vacuum and the crude reaction mixture was purified using column chromatographic technique to result the target compound **2a** as white solid (0.130 g, 74.4 %). ¹H-NMR (700 MHz, CD₃OD) δ = 9.50 (s), 8.51 (d, J = 7 Hz), 7.46 (d, J = 7 Hz), 4.75 (s). ¹³C-NMR (175 MHz, CD₃OD) δ = 165.23, 150.66, 150.52, 147.74, 144.32, 124.29 and 43.37. ESI-HRMS: m/z 349.1422 [M + H]⁺ (calc. 349.1408).

Synthesis of (H2L2) **2b**

1 (0.100 g, 0.129 mmol) was suspended in 10 mL of (MeOH) methanol. To this 3-methylaminopyridine (0.129 mL, 1.207 mmol) was added and refluxed for a period of twelve hour (12 h) and the progress of the reaction was checked by TLC (thin layer chromatography). The solvent was removed under vacuum and the crude reaction mixture was purified using column chromatographic technique to get the targeted compound **2b** as semisolid (0.120 g, 70 %). ¹H-NMR (700 MHz, CD₃OD) δ = 9.08 (s), 8.59 (s), 8.46 (t, J = 7 Hz), 7.88 (d, J = 14 Hz), 7.43 (t, J = 7 Hz), 4.71 (s), 1.30 (s). ¹³C-NMR (175 MHz, CD₃OD) δ = 165.01, 149.82, 1149.33, 147.61, 144.33, 138.06, 136.57, 125.61, and 41.94. ESI-HRMS: m/z 349.1427 [M + H]⁺ (calc. 349.1408).

Synthesis of (H2L3) **2c**

1 (0.100 g, 0.129 mmol) was suspended in 10 mL of methanol. To this 2-methylaminopyridine (0.129 mL, 1.207 mmol) was added and refluxed for a period of twelve hour (12 h) and the progress of the reaction was checked by TLC. The solvent was removed under vacuum and the crude reaction mixture was purified using column chromatographic method to get the target compound **2c** as white solid (0.135 g, 74 %). ¹H-NMR (700 MHz, CD₃OD) δ = 9.47 (s), 8.50

(d, $J = 7$ Hz), 7.81 (s), 7.49 (d, $J = 21$ Hz), 7.35 (s), 4.80 (s). ^{13}C -NMR (175 MHz, CD_3OD) $\delta = 165.12, 159.33, 150.19, 149.96, 144.47, 139.26, 124.28, 123.28$ and 43.74. ESI-HRMS: m/z 349.1427.

Synthesis of $\text{Ag}(\text{H}_2\text{L1})\cdot\text{NO}_3 \cdot 2(\text{H}_2\text{O})$ coordination polymer, **3**

The compound **2a** (0.050 g, 0.143 mmol) was suspended in 5 mL methanol. To this (0.024 g, 0.143 mmol) of silver nitrate (AgNO_3) in 3 mL methanol was added and stirred at room temperature for a period of 30 min, afforded a white coloured precipitate. Block shaped colorless crystals of **3** suitable for X-ray diffraction were grown by slow evaporation of precipitate in 50 % acetonitrile-chloroform mixture within two weeks.

Synthesis of $[\text{Co}(\text{L1})_2]\text{Bu}_4\text{N}$ complex, **4a**

A suspension of **2a** (0.100 g, 0.286 mmol), tetrabutylammonium acetate ($\text{Bu}_4\text{N}(\text{OAc})$) (0.043 g, 0.143 mmol) and $\text{Co}(\text{OAc})_2(\text{H}_2\text{O})_4$ (0.035 g, 0.143 mmol) in MeOH (10 mL), was refluxed under N_2 environment to give a clear, light pink, coloured solution. A solution of sodium methoxide (in situ generation of sodium hydride (NaH) (0.025 g of 60 % dispersion in oil, 0.630 mmol with MeOH)) was added noticing a colour change to deep purple. Upon contact with air, the colour of the solution changed to greenish over about 5 min after which it was refluxed for an extra 2 h. The solvent was evaporated under reduced pressure, the crude residue was purified using column chromatographic method and dried under vacuum to afford **4a** as a greenish solid (0.150 g, 69 %). ^1H -NMR (400 MHz, CD_3OD) $\delta = 9.04$ (s), 8.23 (s), 6.59(s), 3.42(s). ^{13}C -NMR (100 MHz, CD_3OD) $\delta = 168.94, 152.07, 150.00, 146.26, 126.61, 47.34$. ESI-HRMS (-ve mode) m/z $M^- = 751.1699$ (calc. 751.1683).

Synthesis of $[\text{Co}(\text{L2})_2]\text{Bu}_4\text{N}$ complex, **4b**

A suspension of **2b** (0.100 g, 0.286 mmol), tetrabutyl ammonium acetate ($\text{Bu}_4\text{N}(\text{OAc})$) (0.043 g, 0.143 mmol) and $\text{Co}(\text{OAc})_2(\text{H}_2\text{O})_4$ (0.035 g, 0.143 mmol) in MeOH (10 mL), was refluxed under N_2 environment to afford a clear, light pink, coloured solution. A solution of sodium

methoxide (in situ generation of sodium hydride (0.025 g of 60 % dispersion in oil, 0.630 mmol with MeOH)) was added observing a colour changed to deep purple. Upon contact to air, the colour of the solution changed to greenish over about 5 min after that it was again refluxed for an another 2 h. The solvent was evaporated under reduced pressure, the crude residue was purified using column chromatographic method and dried under vacuum to get **4b** as a greenish solid (0.160 g, 74 %). ¹H-NMR (400 MHz, CD₃OD) δ = 9.08 (s), 8.30 (d, J = 7 Hz), 7.35 (s), 7.17 (t, J = 7 Hz), 7.00 (d, J = 7 Hz), 3.41 (s), 3.26 (t, J = 7 Hz), 1.67 (q), 1.43 (q), 1.05 (t, J = 7 Hz). ¹³C-NMR (100 MHz, CD₃OD) δ = 168.84, 152.43, 149.09, 148.78, 148.24, 146.33, 137.30, 125.35, 45.28, 24.73, 21.02, 14.30. ESI-HRMS (-ve mode) *m/z* M⁻ = 751.1686 (calc. 751.1683)

Synthesis of [Co(L3)₂]Bu₄N complex, 4c

A suspension of **2c** (0.100 g, 0.286 mmol), tetrabutyl ammonium acetate (Bu₄N(OAc)) (0.043 g, 0.143 mmol) and Co(OAc)₂(H₂O)₄ (0.035 g, 0.143 mmol) in MeOH (10 mL), was refluxed under nitrogen to give a clear, light pink, coloured solution. A solution of sodium methoxide (in situ generation of sodium hydride (0.025 g of 60 % dispersion in oil, 0.630 mmol with MeOH)) was added observed a colour change to deep purple. Upon contact to air, the colour of the reaction solution changed to greenish after 5 min after that it was again refluxed for an another 2 h. The solvent was removed under reduced pressure, the crude residue was purified using column chromatographic method and dried under vacuum to afford **4c** as a greenish solid (0.165 g, 74 %). ¹H-NMR (400 MHz, CD₃OD) δ = 9.47 (s), 8.98 (s), 8.03 (s), 7.53 (s), 7.13 (s), 6.82 (s). ¹³C-NMR (100 MHz, CD₃OD) δ = 169.29, 159.86, 149.35, 145.64, 138.19, 124.20, 121.73. ESI-HRMS (-ve mode) *m/z* M⁻ = 751.1686

Synthesis of Co-Ag Heterometallic coordination polymer, [Co(L1)₂]Ag₃, 5a

The complex **4a** (0.050 g, 0.066 mmol) was suspended in 5 mL methanol. To this (0.011 g, 0.066 mmol) of silver nitrate (AgNO₃) in 3 mL methanol was added, and after 30 minutes an

off-greenish precipitate was obtained. The star shaped brown crystal (**5a**) suitable for X- ray diffraction was grown by slow evaporation of precipitate in 50 % acetonitrile-methanol mixture.

Synthesis of Co-Ag heterometallic coordination polymer [Co(L2)₂]Ag. 2H₂O, 5b

The complex **4b** (0.050 g, 0.066 mmol) was suspended in 5 mL methanol. To this (0.011 g, 0.066 mmol) of silver nitrate (AgNO₃) in 5 mL methanol was added, and after 30 minutes an off-greenish precipitate was afforded. The star shaped brown coloured crystal (**5b**) suitable for X- ray diffraction was grown by slow evaporation of complex in 50 % acetonitrile-methanol mixture.

2.6. REFERENCES

1. Ma, L.; Abney, C.; Lin, W., *Chem. Soc. Rev.* **2009**, *38* (5), 1248-1256.
2. Li, J.-R.; Kuppler, R. J.; Zhou, H.-C., *Chem. Soc. Rev.* **2009**, *38* (5), 1477-1504.
3. Kumar, G.; Singh, A. P.; Gupta, R., *Eur. J. Inorg. Chem.* **2010**, *2010* (32), 5103-5112.
4. Tranchemontagne, D. J.; Mendoza-Cortes, J. L.; O'Keeffe, M.; Yaghi, O. M., *Chem. Soc. Rev.* **2009**, *38* (5), 1257-1283.
5. O'Keeffe, M.; Yaghi, O. M., *Chem. Rev.* **2012**, *112* (2), 675-702.
6. (a) Hu, Z.; Deibert, B. J.; Li, J., *Chem. Soc. Rev.* **2014**, *43* (16), 5815-5840; (b) Potyrailo, R. A.; Surman, C.; Nagraj, N.; Burns, A., *Chem. Rev.* **2011**, *111* (11), 7315-7354; (c) Kreno, L. E.; Leong, K.; Farha, O. K.; Allendorf, M.; Van Duyne, R. P.; Hupp, J. T., *Chem. Rev.* **2012**, *112* (2), 1105-1125.
7. Liu, J.; Chen, L.; Cui, H.; Zhang, J.; Zhang, L.; Su, C.-Y., *Chem. Soc. Rev.* **2014**, *43* (16), 6011-6061.
8. (a) Cahill, C. L.; de Lill, D. T.; Frisch, M., *CrystEngComm* **2007**, *9* (1), 15-26; (b) Kumar Singh, A.; Mukherjee, R., *Dalton Trans.* **2005**, (17), 2886-2891.

9. Mishra, A.; Gupta, R., *Dalton Trans.* **2014**, 43 (21), 7668-7682.
10. (a) Rajput, A.; Mukherjee, R., *Coord. Chem. Rev.* **2013**, 257 (2), 350-368; (b) Matsumoto, K.; Suzuki, K.; Tsukuda, T.; Tsubomura, T., *Inorg Chem* **2010**, 49 (11), 4717-4719.
11. Hechavarría Fonseca, M.; König, B., *Adv. Synth. Catal.* **2003**, 345 (11), 1173-1185.
12. Breuning, E.; Ruben, M.; Lehn, J.-M.; Renz, F.; Garcia, Y.; Ksenofontov, V.; Gütlich, P.; Wegelius, E.; Rissanen, K., *Angew. Chem. Int. Ed.* **2000**, 39 (14), 2504-2507.
13. Ellsworth, J. M.; zur Loye, H.-C., *Dalton Trans.* **2008**, (43), 5823-5835.
14. Klingele, J.; Boas, J. F.; Pilbrow, J. R.; Moubaraki, B.; Murray, K. S.; Berry, K. J.; Hunter, K. A.; Jameson, G. B.; Boyd, P. D. W.; Brooker, S., *Dalton Trans.* **2007**, (6), 633-645.
15. Hausmann, J.; Brooker, S., *ChemComm* **2004**, (13), 1530-1531.
16. Hellyer, R. M.; Larsen, D. S.; Brooker, S., *Eur. J. Inorg. Chem.* **2009**, 2009 (9), 1162-1171.
17. Cowan, M. G.; Miller, R. G.; Southon, P. D.; Price, J. R.; Yazaydin, O.; Lane, J. R.; Kepert, C. J.; Brooker, S., *Inorg. Chem.* **2014**, 53 (22), 12076-12083.
18. Cati, D. S.; Stoeckli-Evans, H., *Acta Crystallographica Section E* **2017**, 73 (4), 535-538.
19. Kascatan-Nebioglu, A.; Panzner, M. J.; Tessier, C. A.; Cannon, C. L.; Youngs, W. J., *Coord. Chem. Rev.* **2007**, 251 (5), 884-895.
20. Purohit, C. S.; Verma, S., *J. Am. Chem. Soc.* **2006**, 128 (2), 400-401.
21. Xu, F.-B.; Weng, L.-H.; Sun, L.-J.; Zhang, Z.-Z.; Zhou, Z.-F., *Organometallics* **2000**, 19 (14), 2658-2660.
22. (a) Purohit, C. S.; Verma, S., *J. Am. Chem. Soc.* **2007**, 129 (12), 3488-3489; (b) Carvajal, M. A.; Novoa, J. J.; Alvarez, S., *J. Am. Chem. Soc.* **2004**, 126 (5), 1465-1477.

23. Leigh, D. A.; Lusby, P. J.; McBurney, R. T.; Morelli, A.; Slawin, A. M. Z.; Thomson, A. R.; Walker, D. B., *J. Am. Chem. Soc.* **2009**, *131* (10), 3762-3771.

2.7. Spectral Data

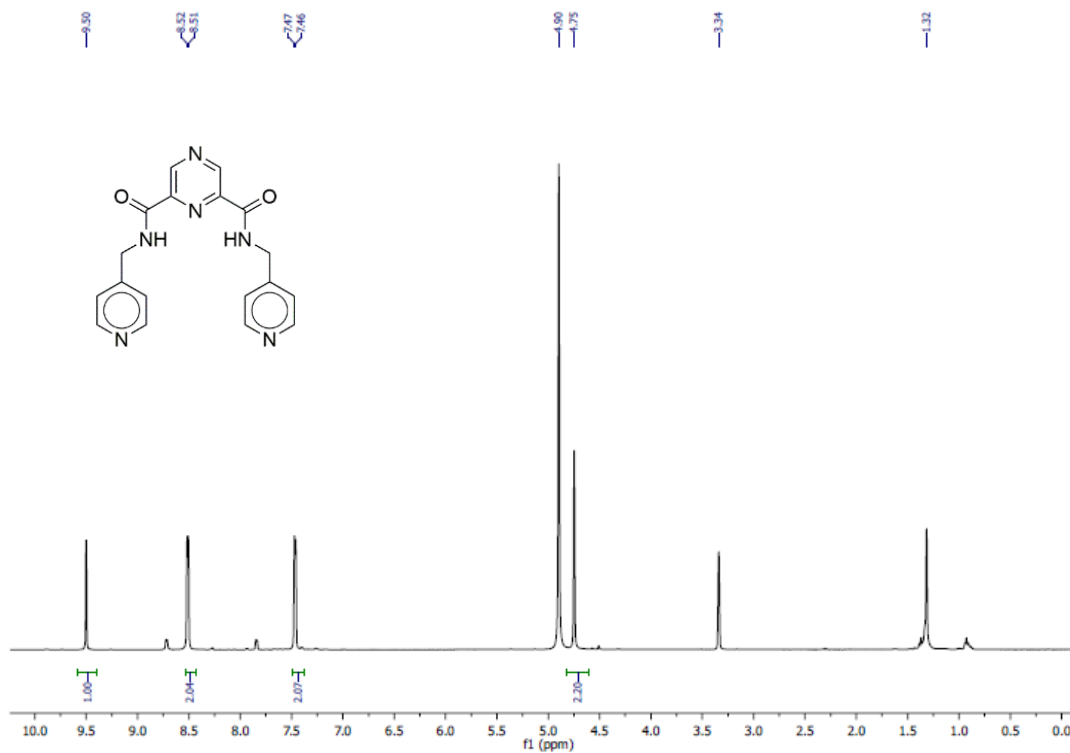


Figure 2.17. ¹H NMR of precursor ligand 2a

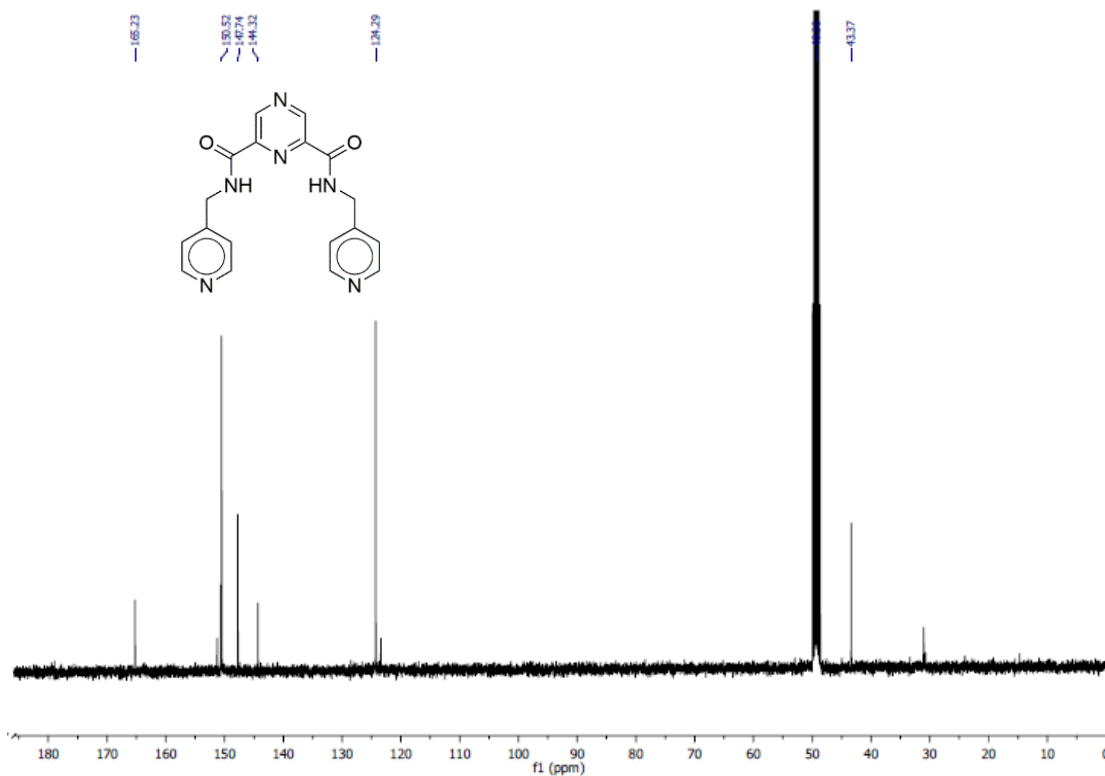


Figure 2.18. ¹³C NMR of precursor ligand 2a

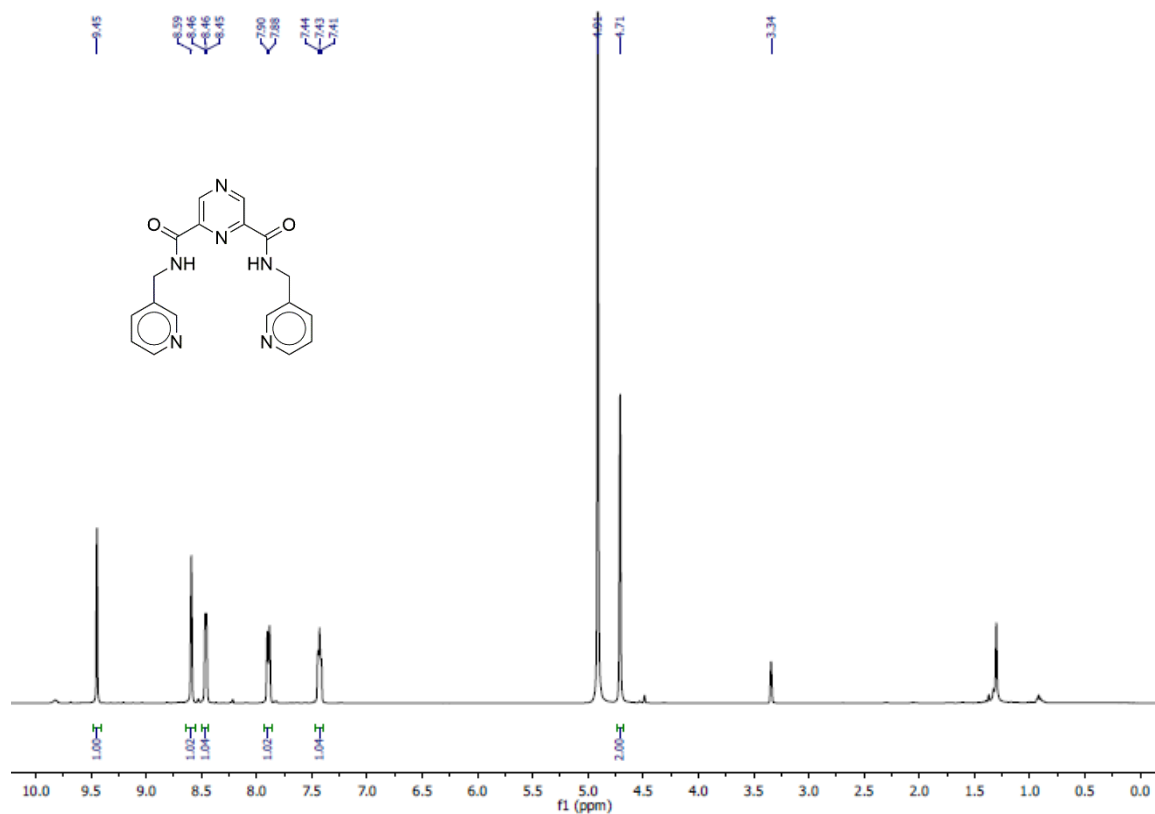


Figure 2.19. ^1H NMR of precursor ligand **2b**

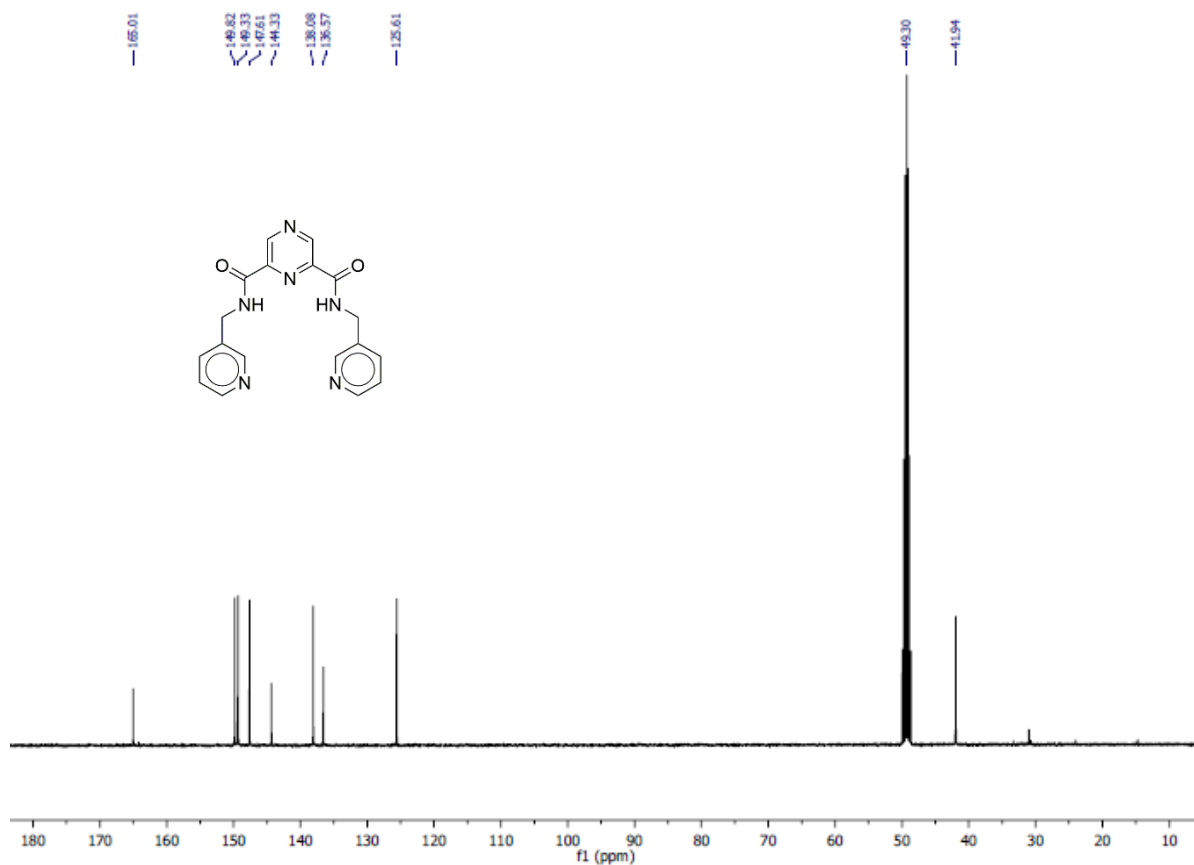


Figure 2.20. ^{13}C NMR of precursor ligand **2b**

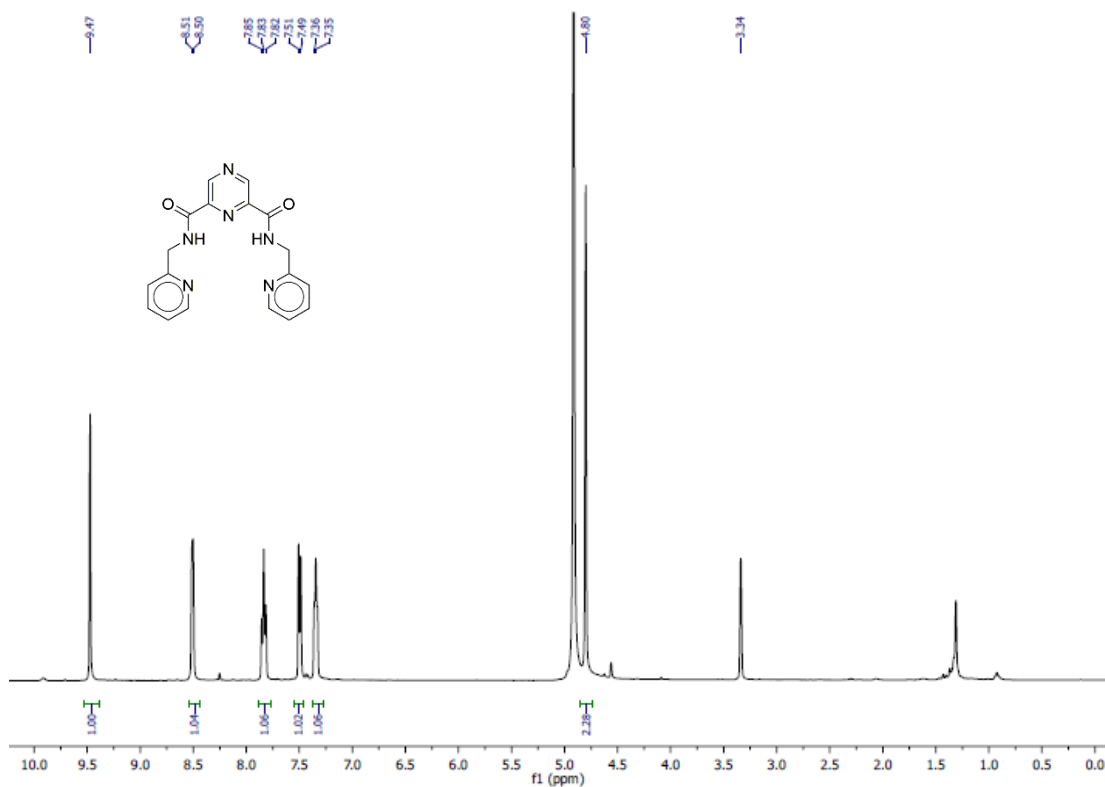


Figure 2.21. ¹H NMR of precursor ligand **2c**

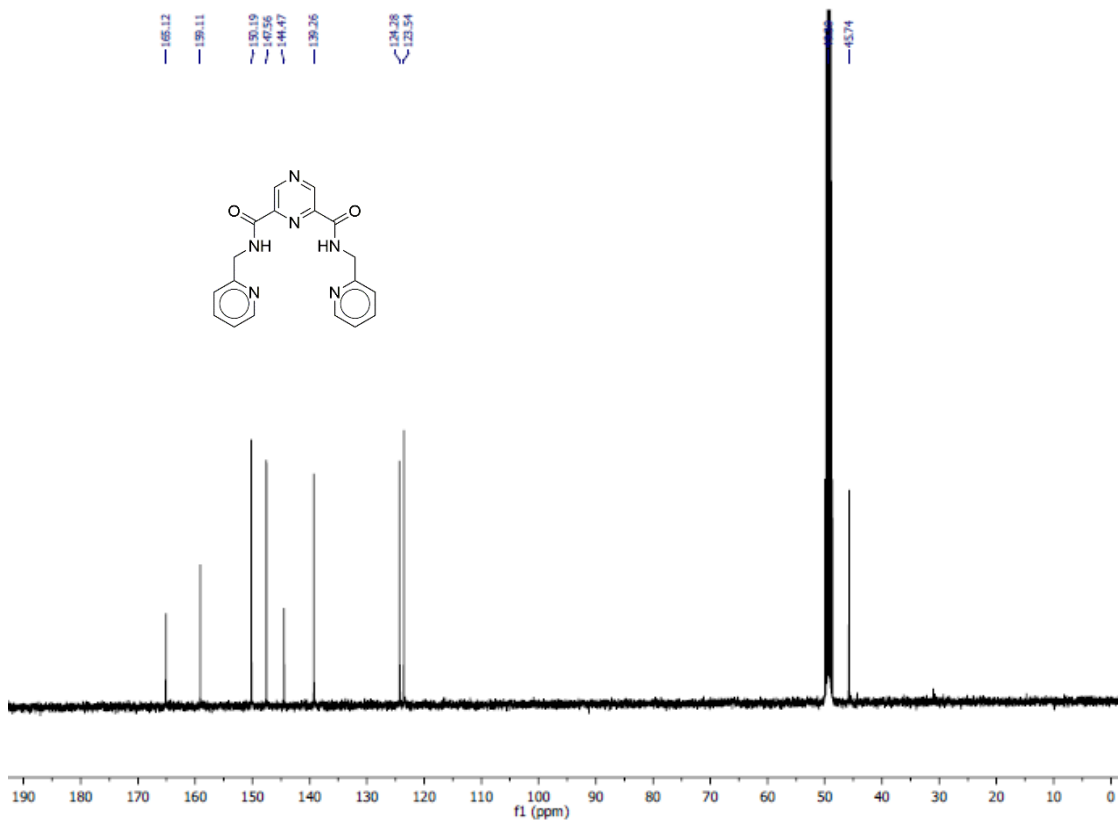


Figure 2.22. ¹³C NMR of precursor ligand **2c**

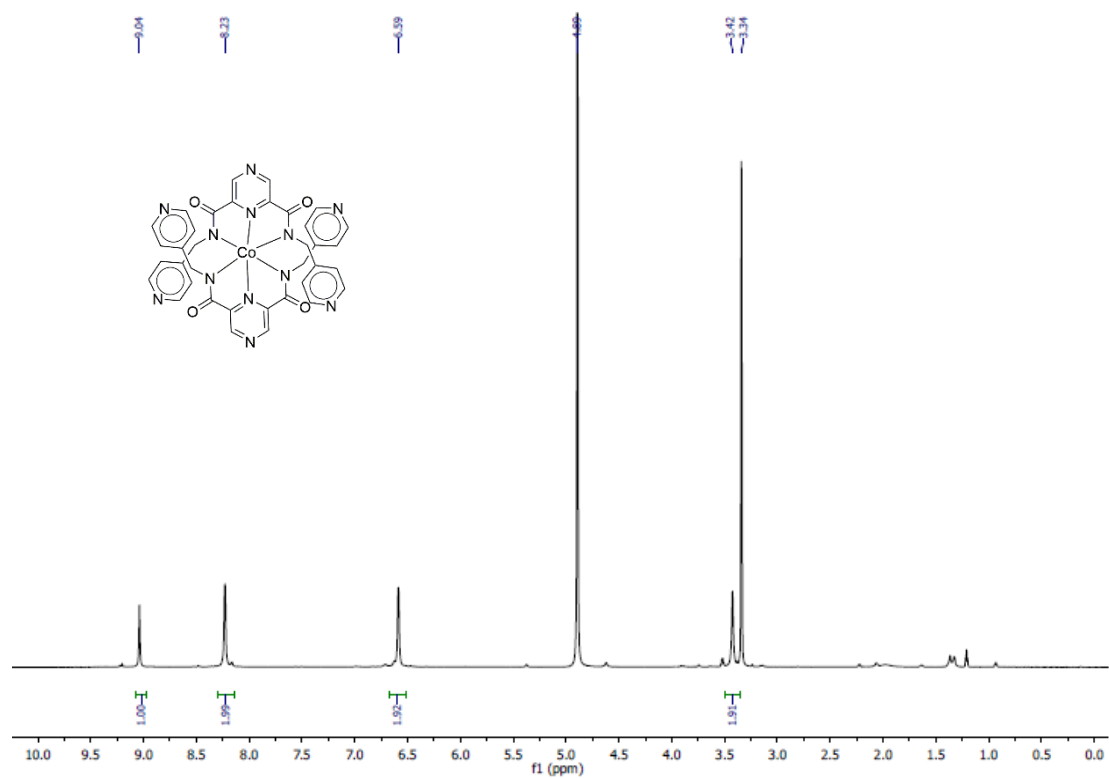


Figure 2.23. ^1H NMR of metal complex 4a

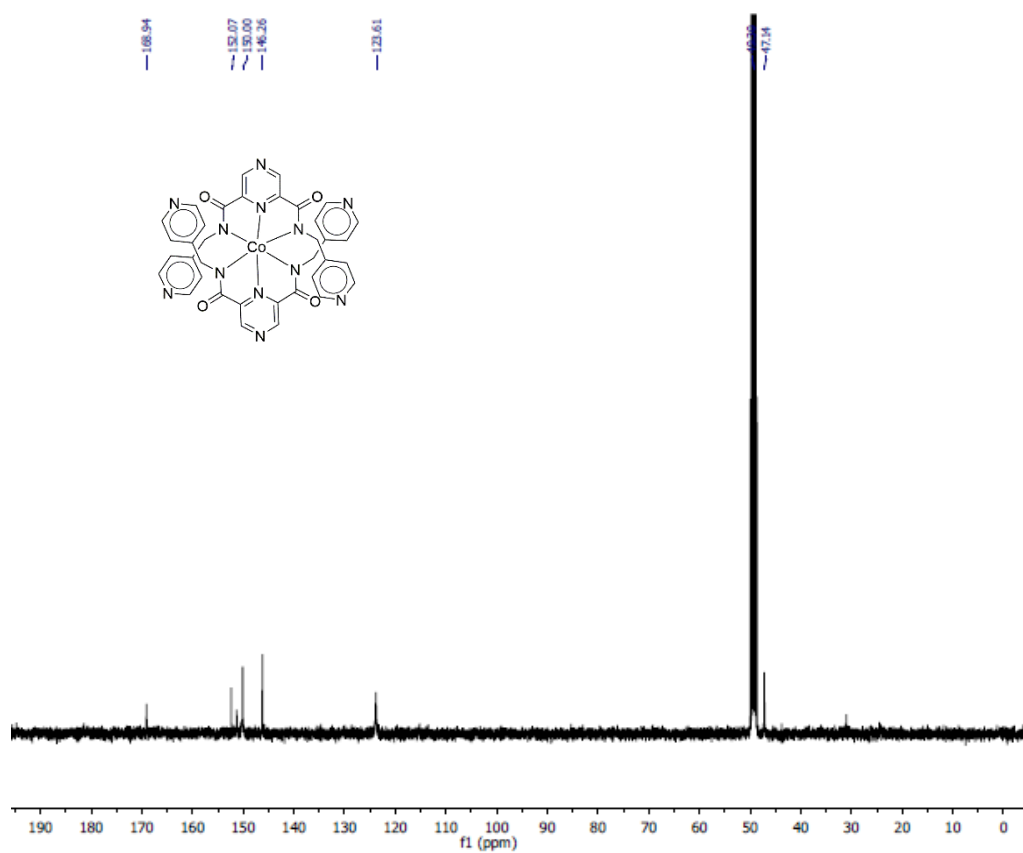


Figure 2.24. ^{13}C NMR of metal complex 4a

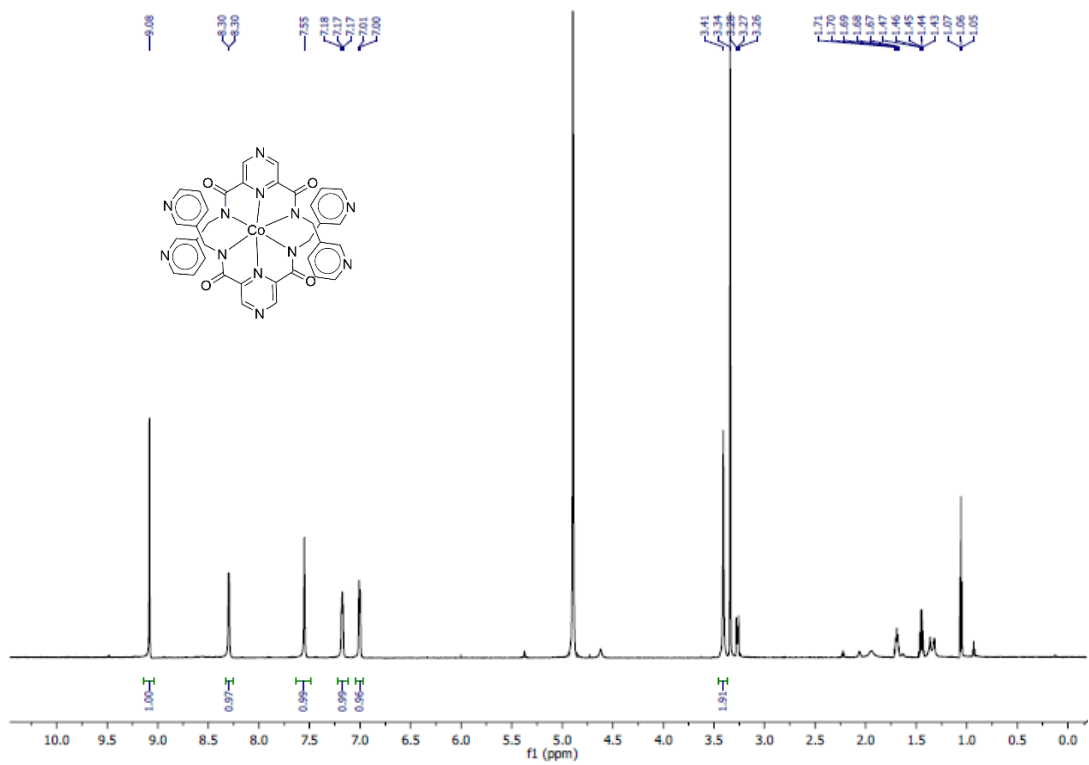


Figure 2.25. $^1\text{H NMR}$ of metal complex 4b

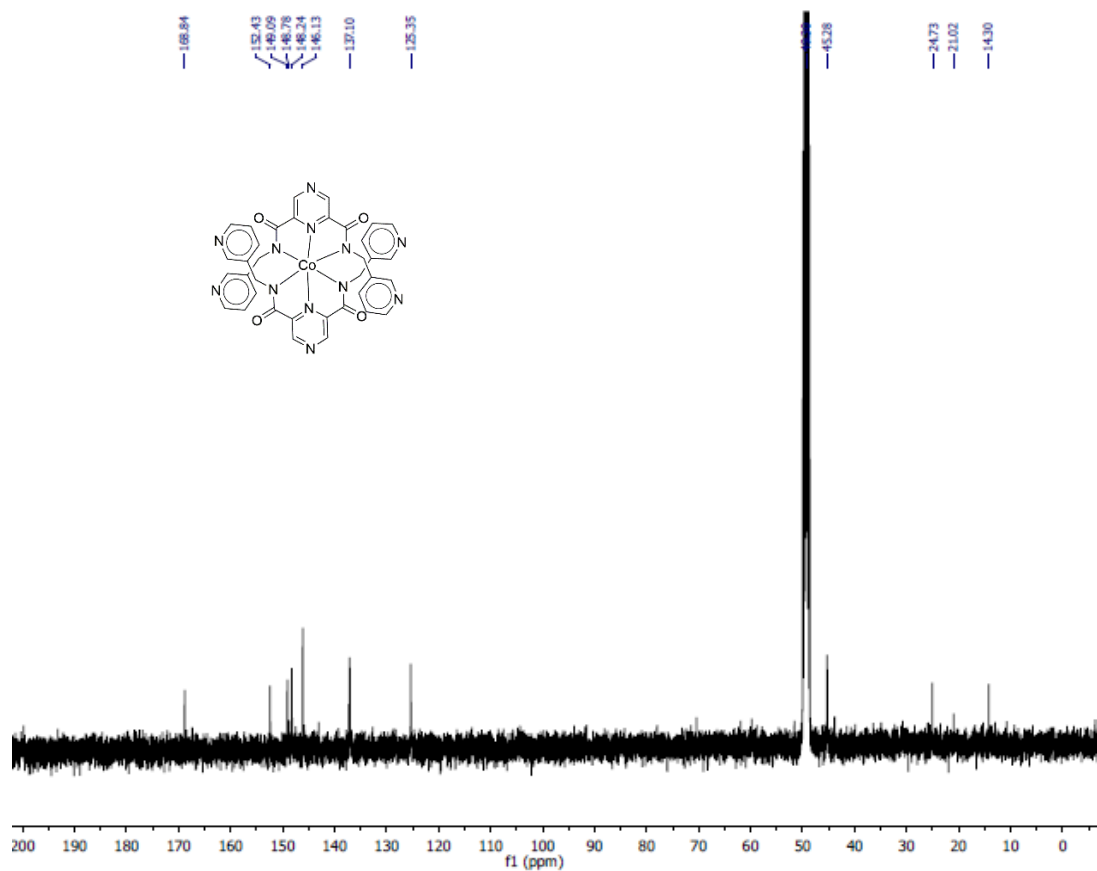


Figure 2.26. $^{13}\text{C NMR}$ of metal complex 4b

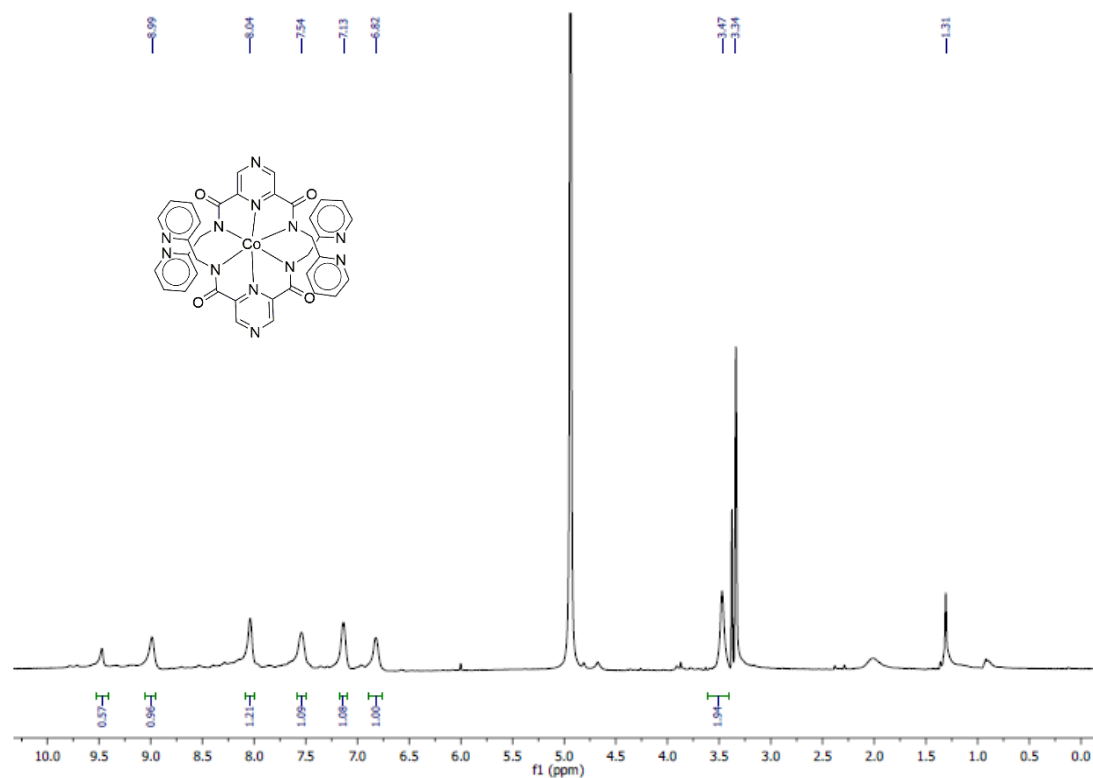


Figure 2.27. ^1H NMR of metal complex 4c

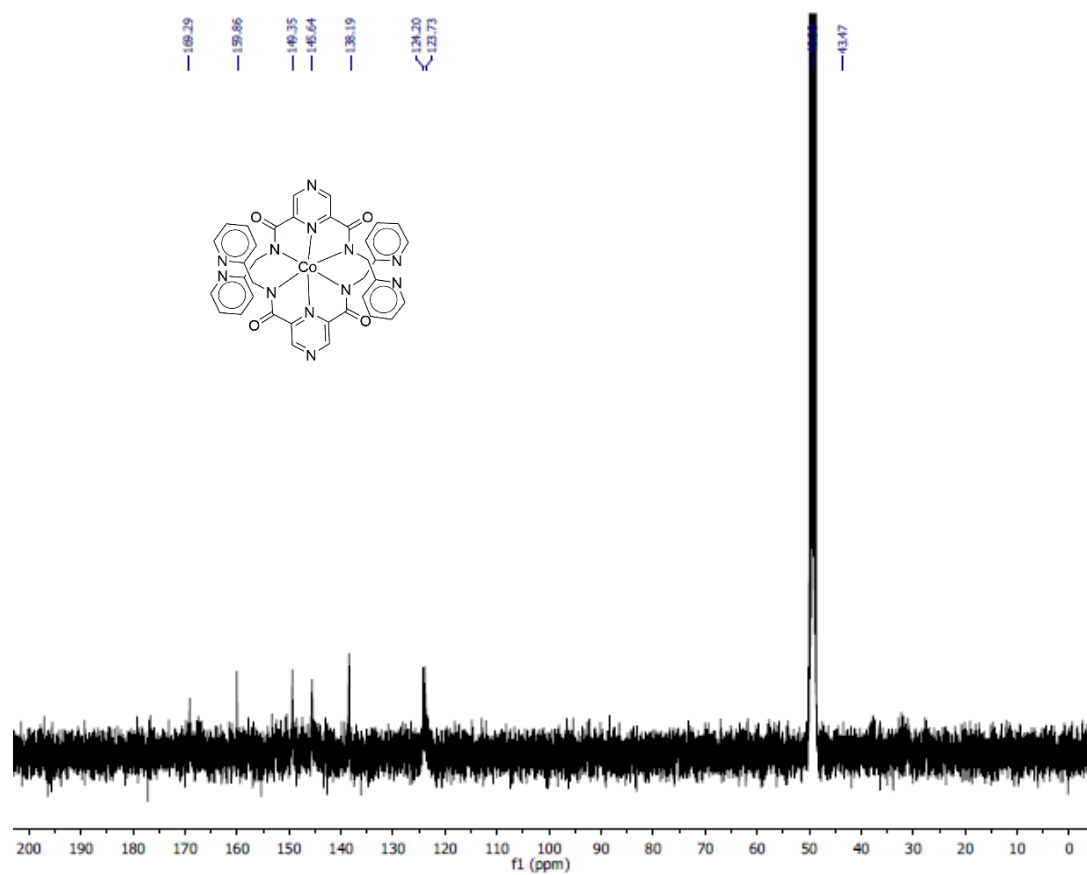


Figure 2.28. ^{13}C NMR of metal complex 4c

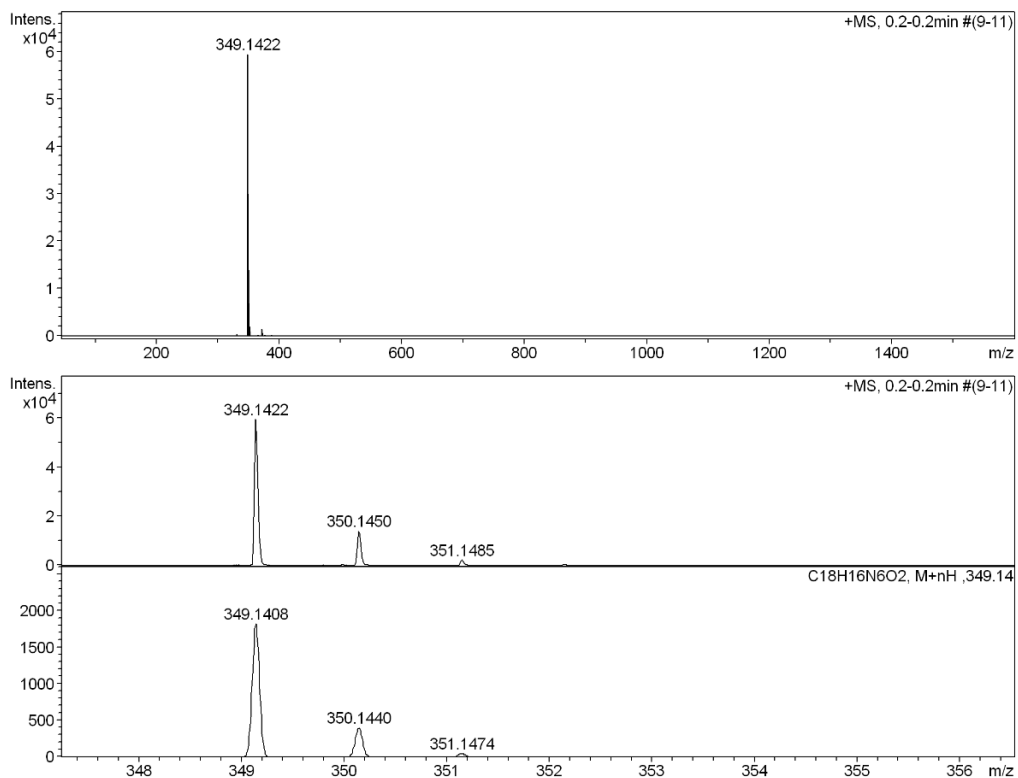


Figure 2.29. ESI-MS spectrum of precursor ligand 2a

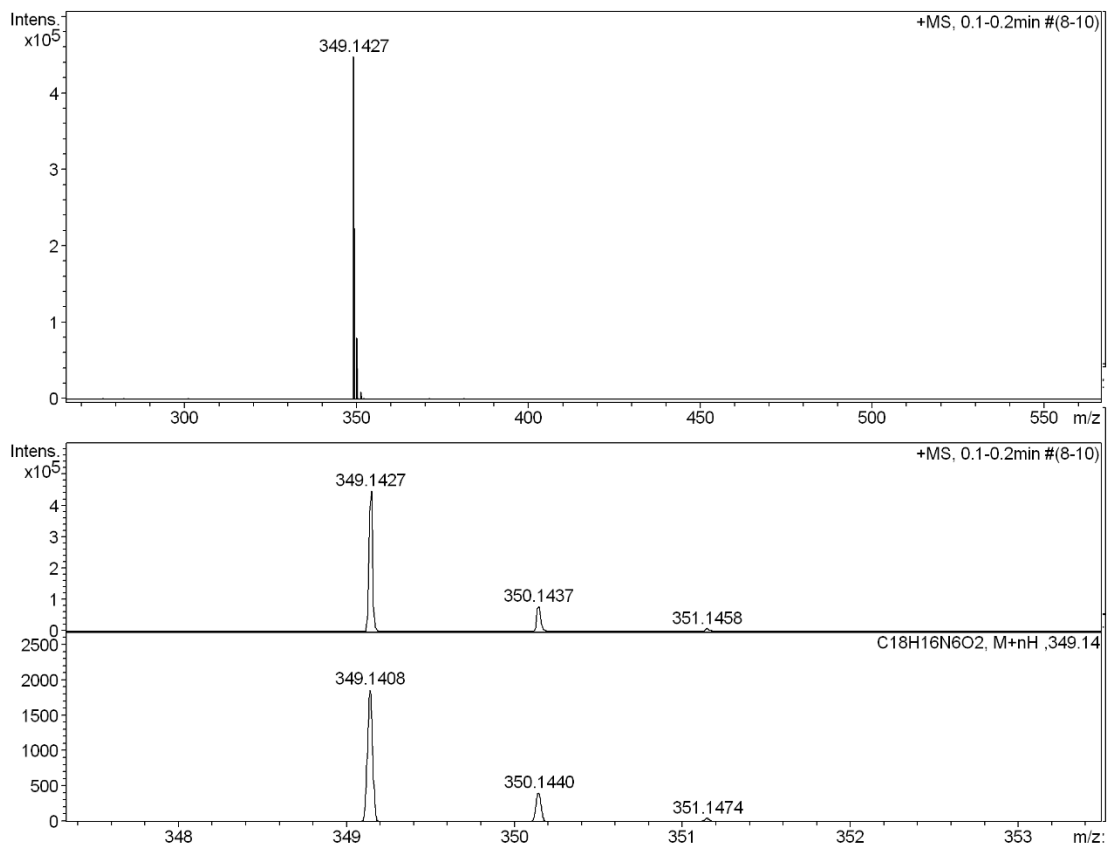


Figure 2.30. ESI-MS spectrum of precursor ligand 2b

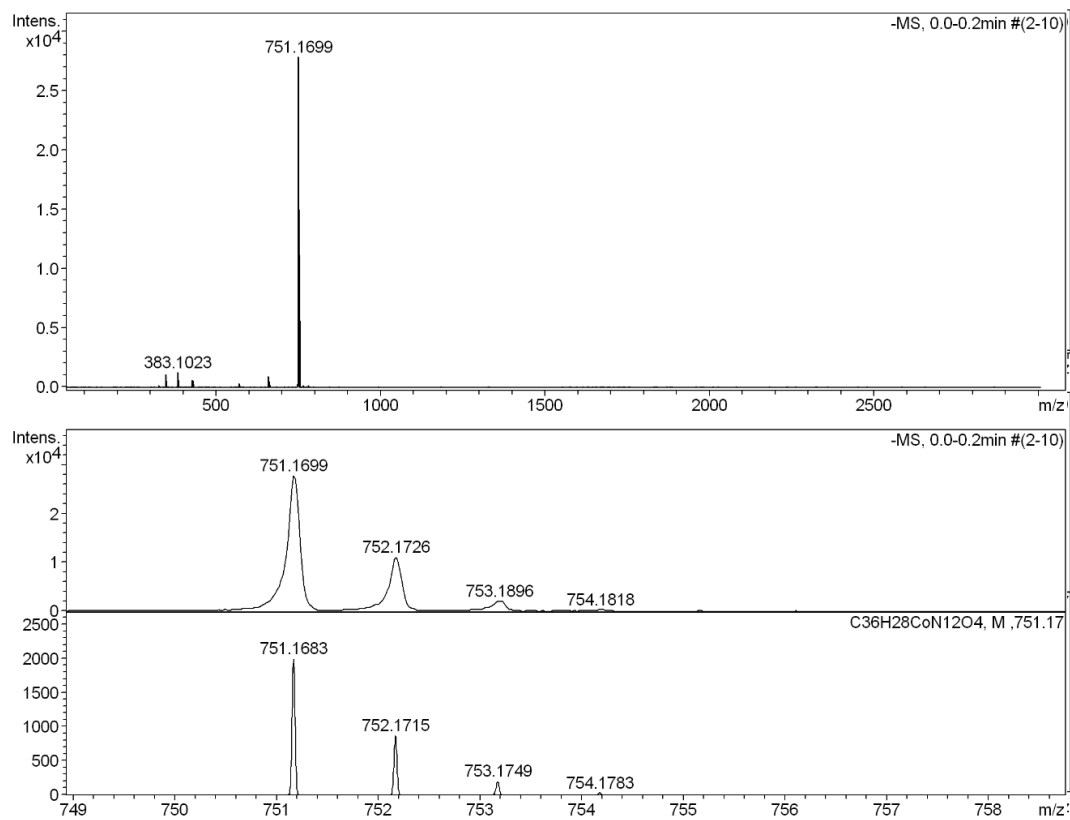


Figure 2.31. ESI-MS spectrum of metal complex **4a**

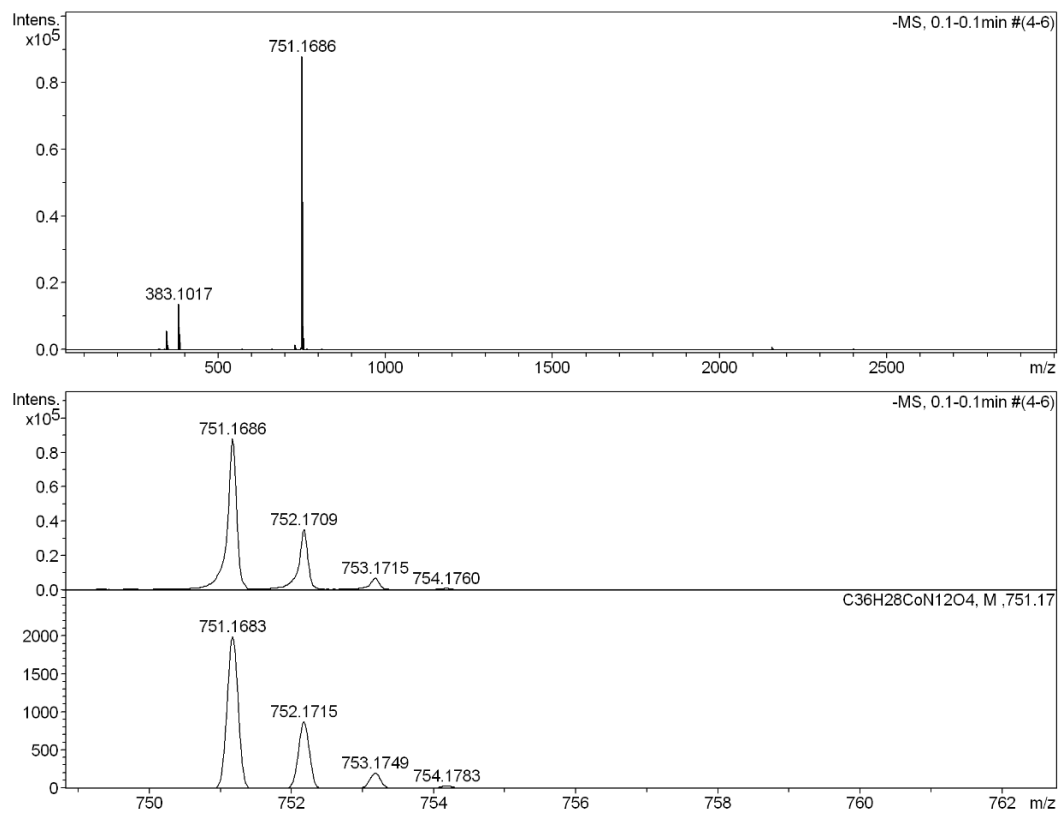


Figure 2.32. ESI-MS spectrum of metal complex **4b**

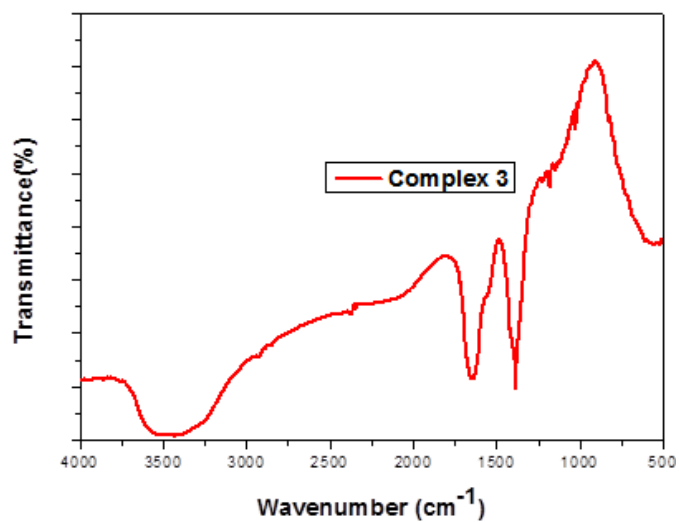


Figure 2.33. IR spectra of complex 3

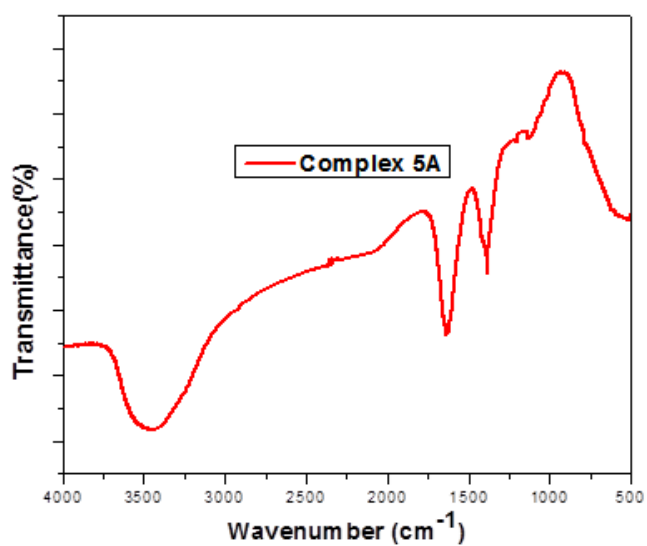


Figure 2.34. IR spectra of complex 5a

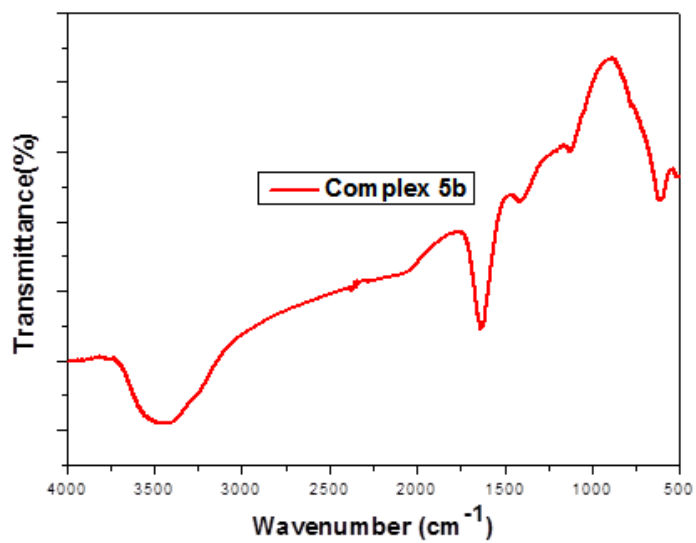


Figure 2.35. IR spectra of complex 5b

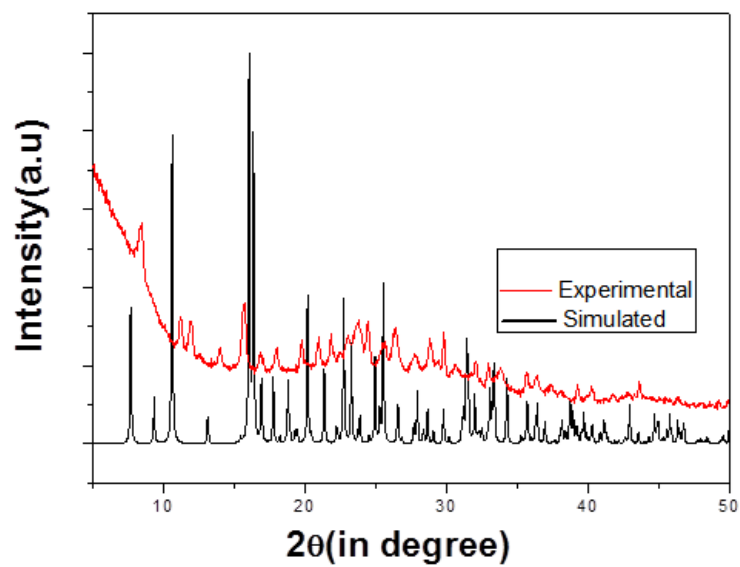


Figure 2.36. PXRD pattern for **3**

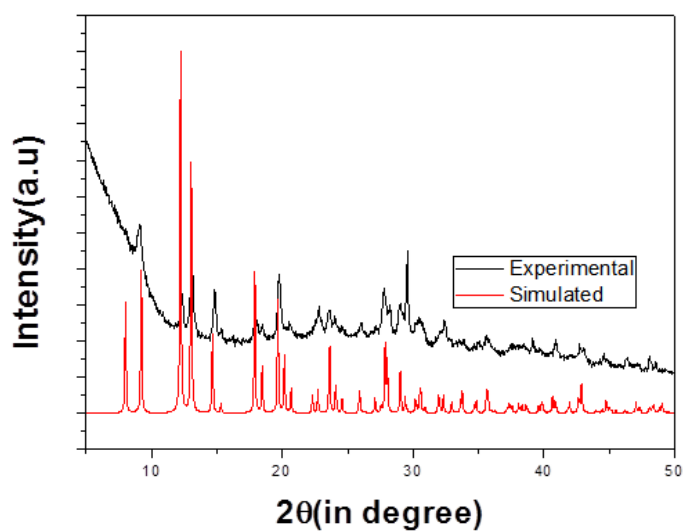


Figure 2.37. PXRD pattern for **5a**

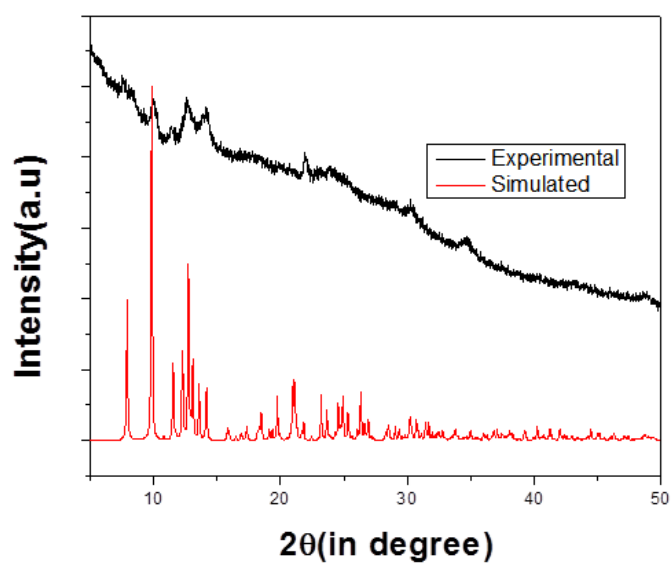


Figure 2.38. PXRD pattern for **5b**

2.8. Crystal Data

Table 2. 1. Crystallographic structure refinement factors for complexes **3**, **5a** and **5b**

	3	5a	5b
Empirical formula	C ₁₈ H ₂₀ AgN ₇ O ₇	C ₃₆ H ₂₈ Ag ₃ CoN ₁₂ O ₄	C ₃₆ H ₃₃ N ₁₂ O ₆ CoAg ₁
Formula weight	554.28	1075.24	896.54
Space group	<i>Pbcn</i>	<i>I-42d</i>	<i>P 2₁2₁2₁</i> [19]
Temperature	293 K	293 K	293 K
Wavelength	1.5418(4)	0.7107(3)	0.7107(3)
Crystal system	Orthorhombic	Tetragonal	Orthorhombic
a (Å)	5.67(4)	19.19(8)	15.063(8)
b(Å)	22.89(2)	19.19(8)	15.3339(2)
c (Å)	16.607(1)	13.484(2)	16.333(2)
α (deg)	90	90	90
β (deg)	90	90	90
γ (deg)	90	90	90
Volume (Å ³)	2157.1	4968.8	3785.86
Z	8	4	4
D _{calc.} (mg.mm ⁻³)	1.707	1.437	1.573
Absorption coefficient (mm ⁻¹)	8.005	1.536	1.018
F(000)	1120	2112.0	1820.0
Θ _{max}	66.996	28.724	26.060
Reflection collected	7356	71479	26321
Independent reflection	1904	3081	7469
Goodness of Fit	1.093	1.145	1.023
Final R indices [I > 2σ(I)]	R1=0.0899 WR2=0.2412	R1=0.0959 WR2=0.2404	R1= 0.0610 WR2= 0.1636
R indices (all data)	R1=0.1003 WR2=0.2483	R1=0.1256 WR2= 0.2645	R1=0.0886 WR2=0.2645
CCDC number	1826443	1826444	1826445

Table 2.2. Bond length and bond angle of coordination complex **3**

Bond length		Bond angle	
C(1)-N(1)	1.310(14)	N(1)-C(1)-C(2)	122.1(11)
C(1)-C(2)	1.365(13)	N(1)-C(1)-H(1)	119.0
C(1)-H(1)	0.9300	C(2)-C(1)-H(1)	119.0
C(2)-N(2)	1.358(11)	N(2)-C(2)-C(1)	122.2(9)
C(2)-C(3)	1.506(12)	N(2)-C(2)-C(3)	117.7(8)
C(3)-O(1)	1.221(11)	C(1)-C(2)-C(3)	120.1(9)
C(3)-N(3)	1.321(11)	O(1)-C(3)-N(3)	123.4(8)
C(4)-N(3)	1.449(11)	O(1)-C(3)-C(2)	119.7(9)
C(4)-C(5)	1.479(14)	N(3)-C(3)-C(2)	116.8(8)
C(4)-H(4A)	0.9700	N(3)-C(4)-C(5)	116.0(7)
C(4)-H(4B)	0.9700	N(3)-C(4)-H(4A)	108.3
C(5)-C(9)	1.377(11)	C(5)-C(4)-H(4A)	108.3
C(5)-C(6)	1.392(13)	N(3)-C(4)-H(4B)	108.3
C(6)-C(7)	1.372(13)	C(5)-C(4)-H(4B)	108.3
C(6)-H(6)	0.9300	H(4A)-C(4)-H(4B)	107.4
C(7)-N(4)	1.337(12)	C(9)-C(5)-C(6)	116.8(8)
C(7)-H(7)	0.9300	C(9)-C(5)-C(4)	118.9(8)
C(8)-N(4)	1.316(12)	C(6)-C(5)-C(4)	124.3(8)
C(8)-C(9)	1.397(13)	C(7)-C(6)-C(5)	120.2(9)
C(8)-H(8)	0.9300	C(7)-C(6)-H(6)	119.9
C(9)-H(9)	0.9300	C(5)-C(6)-H(6)	119.9
Ag(01)-N(4)	2.203(9)	N(4)-C(7)-C(6)	123.3(9)
Ag(01)-N(4)#1	2.203(9)	N(4)-C(7)-H(7)	118.3
Ag(01)-N(1)#2	2.621(14)	C(6)-C(7)-H(7)	118.3
N(1)-C(1)#3	1.310(14)	N(4)-C(8)-C(9)	124.4(9)
N(1)-Ag(01)#4	2.621(14)	N(4)-C(8)-H(8)	117.8
N(2)-C(2)#3	1.358(11)	C(9)-C(8)-H(8)	117.8
N(3)-H(3)	0.8600	C(5)-C(9)-C(8)	118.9(9)
N(5)-O(3)#3	1.151(14)	C(5)-C(9)-H(9)	120.6
N(5)-O(3)	1.151(14)	C(8)-C(9)-H(9)	120.6
N(5)-O(4)	1.279(17)	N(4)-Ag(01)-N(4)#1	176.0(4)
O(2)-H(2A)	0.8501	N(4)-Ag(01)-N(1)#2	88.02(19)
O(2)-H(2B)	0.8502	N(4)#1-Ag(01)-N(1)#2	88.02(19)
		C(1)-N(1)-C(1)#3	117.3(14)
		C(1)-N(1)-Ag(01)#4	121.3(7)
		C(1)#3-N(1)-Ag(01)#4	121.3(7)
		C(2)#3-N(2)-C(2)	113.9(11)
		C(3)-N(3)-C(4)	121.8(8)
		C(3)-N(3)-H(3)	119.1
		C(4)-N(3)-H(3)	119.1
		C(8)-N(4)-C(7)	116.5(9)
		C(8)-N(4)-Ag(01)	124.2(6)
		C(7)-N(4)-Ag(01)	117.6(6)
		O(3)#3-N(5)-O(3)	115.3(16)
		O(3)#3-N(5)-O(4)	122.4(8)
		O(3)-N(5)-O(4)	122.4(8)
		H(2A)-O(2)-H(2B)	109.5

Symmetry transformations utilized to create similar atoms:

#1 -x+1, y,-z+1/2 #2 -x+1/2,-y+1/2, z-1/2

#3 -x, y,-z+3/2 #4 -x+1/2,-y+1/2, z+1/2

Table 2.3. Bond length and Bond angle of coordination complex **5a**

Bond length		Bond angle	
C(1)-N(2)	1.353(13)	N(2)-C(1)-C(2)	120.9(11)
C(1)-C(2)	1.383(12)	N(1)-C(2)-C(1)	118.3(10)
C(2)-N(1)	1.323(11)	N(1)-C(2)-C(3)	113.3(8)
C(2)-C(3)	1.495(14)	C(1)-C(2)-C(3)	128.4(9)
C(3)-O(1)	1.237(12)	O(1)-C(3)-N(3)	128.9(10)
C(3)-N(3)	1.332(12)	O(1)-C(3)-C(2)	120.5(9)
C(4)-N(3)	1.461(12)	N(3)-C(3)-C(2)	110.5(8)
C(4)-C(5)	1.502(13)	N(3)-C(4)-C(5)	113.4(8)
C(5)-C(6)	1.377(16)	C(6)-C(5)-C(9)	117.2(9)
C(5)-C(9)	1.394(15)	C(6)-C(5)-C(4)	123.0(10)
C(6)-C(7)	1.397(17)	C(9)-C(5)-C(4)	119.7(10)
C(7)-N(4)	1.32(2)	C(5)-C(6)-C(7)	119.4(11)
C(8)-N(4)	1.33(2)	N(4)-C(7)-C(6)	122.3(13)
C(8)-C(9)	1.376(16)	N(4)-C(8)-C(9)	121.9(11)
N(1)-C(2)#1	1.323(11)	C(8)-C(9)-C(5)	120.0(11)
N(1)-Co(1)	1.844(10)	C(2)-N(1)-C(2)#1	123.2(11)
N(2)-C(1)#1	1.353(13)	C(2)-N(1)-Co(1)	118.4(5)
N(2)-Ag(1)	2.192(12)	C(2)#1-N(1)-Co(1)	118.4(5)
N(3)-Co(1)	1.951(7)	C(1)#1-N(2)-C(1)	118.3(12)
N(4)-Ag(2)	2.182(10)	C(1)#1-N(2)-Ag(1)	120.8(6)
Co(1)-N(1)#2	1.844(10)	C(1)-N(2)-Ag(1)	120.8(6)
Co(1)-N(3)#3	1.951(7)	C(3)-N(3)-C(4)	118.0(7)
Co(1)-N(3)#2	1.951(7)	C(3)-N(3)-Co(1)	116.0(6)
Co(1)-N(3)#1	1.951(7)	C(4)-N(3)-Co(1)	125.0(6)
Ag(1)-N(2)#4	2.192(12)	C(7)-N(4)-C(8)	119.1(10)
Ag(2)-N(4)#5	2.182(10)	C(7)-N(4)-Ag(2)	123.0(10)
		C(8)-N(4)-Ag(2)	117.9(10)
		N(1)-Co(1)-N(1)#2	180.0
		N(1)-Co(1)-N(3)	81.7(2)
		N(1)#2-Co(1)-N(3)	98.3(2)
		N(1)-Co(1)-N(3)#3	98.3(2)
		N(1)#2-Co(1)-N(3)#3	81.7(2)
		N(3)-Co(1)-N(3)#3	91.18(6)
		N(1)-Co(1)-N(3)#2	98.3(2)
		N(1)#2-Co(1)-N(3)#2	81.7(2)
		N(3)-Co(1)-N(3)#2	91.19(6)
		N(3)#3-Co(1)-N(3)#2	163.5(4)
		N(1)-Co(1)-N(3)#1	81.7(2)
		N(1)#2-Co(1)-N(3)#1	98.3(2)
		N(3)-Co(1)-N(3)#1	163.5(4)
		N(3)#3-Co(1)-N(3)#1	91.18(6)
		N(3)#2-Co(1)-N(3)#1	91.18(6)
		N(2)#4-Ag(1)-N(2)	180.0
		N(4)#5-Ag(2)-N(4)	173.3(6)

Symmetry transformations utilised to create identical atoms:

#1 -x+1,-y, z #2 -y+1/2, x-1/2,-z-1/2

#3 y+1/2,-x+1/2,-z-1/2 #4 -y+1/2, x-1/2,-z-3/2

#5 x,-y+1/2,-z+1/4

Table 2.4. Bond length and Bond angle of coordination complex **5b**

Bond length		Bond angle	
C(1)-N(1)	1.336(11)	N(1)-C(1)-C(2)	117.0(9)
C(1)-C(2)	1.407(13)	N(1)-C(1)-C(13)	113.7(7)
C(1)-C(13)	1.487(13)	C(2)-C(1)-C(13)	129.3(8)
C(2)-N(2)	1.334(14)	N(2)-C(2)-C(1)	122.5(9)
C(2)-H(2)	0.9300	N(2)-C(2)-H(2)	118.8
C(3)-N(2)	1.334(15)	C(1)-C(2)-H(2)	118.8
C(3)-C(4)	1.404(12)	N(2)-C(3)-C(4)	121.7(9)
C(3)-H(3)	0.9300	N(2)-C(3)-H(3)	119.2
C(4)-N(1)	1.325(11)	C(4)-C(3)-H(3)	119.2
C(4)-C(9)	1.493(12)	N(1)-C(4)-C(3)	118.2(8)
C(5)-N(3)	1.356(11)	N(1)-C(4)-C(9)	113.1(7)
C(5)-C(6)	1.394(13)	C(3)-C(4)-C(9)	128.6(8)
C(5)-C(12)	1.478(13)	N(3)-C(5)-C(6)	117.0(8)
C(6)-N(4)	1.318(13)	N(3)-C(5)-C(12)	112.8(7)
C(6)-H(6)	0.9300	C(6)-C(5)-C(12)	130.3(8)
C(7)-N(4)	1.346(13)	N(4)-C(6)-C(5)	122.6(9)
C(7)-C(8)	1.378(13)	N(4)-C(6)-H(6)	118.7
C(7)-H(7)	0.9300	C(5)-C(6)-H(6)	118.7
C(8)-N(3)	1.331(11)	N(4)-C(7)-C(8)	121.7(10)
C(8)-C(11)	1.489(12)	N(4)-C(7)-H(7)	119.1
C(9)-O(1)	1.233(10)	C(8)-C(7)-H(7)	119.1
C(9)-N(5)	1.318(11)	N(3)-C(8)-C(7)	118.5(8)
C(10)-N(5)	1.476(11)	N(3)-C(8)-C(11)	112.6(7)
C(10)-C(20)	1.497(14)	C(7)-C(8)-C(11)	128.8(9)
C(10)-H(10A)	0.9700	O(1)-C(9)-N(5)	128.7(8)
C(10)-H(10B)	0.9700	O(1)-C(9)-C(4)	120.9(8)
C(11)-O(4)	1.233(11)	N(5)-C(9)-C(4)	110.4(7)
C(11)-N(7)	1.335(12)	N(5)-C(10)-C(20)	112.1(8)
C(12)-O(3)	1.247(11)	N(5)-C(10)-H(10A)	109.2
C(12)-N(8)	1.347(11)	C(20)-C(10)-H(10A)	109.2
C(13)-O(2)	1.229(11)	N(5)-C(10)-H(10B)	109.2
C(13)-N(6)	1.346(12)	C(20)-C(10)-H(10B)	109.2
C(14)-N(6)	1.471(11)	H(10A)-C(10)-H(10B)	107.9
C(14)-C(15)	1.493(14)	O(4)-C(11)-N(7)	128.5(8)
C(14)-H(14A)	0.9700	O(4)-C(11)-C(8)	121.1(8)
C(14)-H(14B)	0.9700	N(7)-C(11)-C(8)	110.4(8)
C(15)-C(19)	1.365(15)	O(3)-C(12)-N(8)	127.7(8)
C(15)-C(16)	1.392(16)	O(3)-C(12)-C(5)	121.9(8)
C(16)-C(17)	1.377(16)	N(8)-C(12)-C(5)	110.4(7)
C(16)-H(16)	0.9300	O(2)-C(13)-N(6)	129.0(9)
C(17)-C(18)	1.354(18)	O(2)-C(13)-C(1)	122.2(8)
C(17)-H(17)	0.9300	N(6)-C(13)-C(1)	108.8(7)
C(18)-N(12)	1.322(16)	N(6)-C(14)-C(15)	112.5(8)
C(18)-H(18)	0.9300	N(6)-C(14)-H(14A)	109.1
C(19)-N(12)	1.291(15)	C(15)-C(14)-H(14A)	109.1
C(19)-H(19)	0.9300	N(6)-C(14)-H(14B)	109.1
C(20)-C(21)	1.367(17)	C(15)-C(14)-H(14B)	109.1
C(20)-C(24)	1.410(16)	H(14A)-C(14)-H(14B)	107.8
C(21)-N(9)	1.410(18)	C(19)-C(15)-C(16)	115.0(10)
C(21)-H(21)	0.9300	C(19)-C(15)-C(14)	123.9(10)
C(22)-C(23)	1.27(3)	C(16)-C(15)-C(14)	121.0(9)
C(22)-N(9)	1.45(3)	C(17)-C(16)-C(15)	120.2(11)
C(22)-H(22)	0.9300	C(17)-C(16)-H(16)	119.9

C(23)-C(24)	1.36(2)	C(15)-C(16)-H(16)	119.9
C(23)-H(23)	0.9300	C(18)-C(17)-C(16)	118.4(11)
C(24)-H(24)	0.9300	C(18)-C(17)-H(17)	120.8
C(25)-N(7)	1.474(11)	C(16)-C(17)-H(17)	120.8
C(25)-C(26)	1.484(13)	N(12)-C(18)-C(17)	122.0(11)
C(25)-H(25A)	0.9700	N(12)-C(18)-H(18)	119.0
C(25)-H(25B)	0.9700	C(17)-C(18)-H(18)	119.0
C(26)-C(30)	1.376(13)	N(12)-C(19)-C(15)	125.5(11)
C(26)-C(27)	1.394(15)	N(12)-C(19)-H(19)	117.2
C(27)-C(29)	1.312(15)	C(15)-C(19)-H(19)	117.2
C(27)-H(27)	0.9300	C(21)-C(20)-C(24)	119.7(12)
C(28)-N(10)	1.349(16)	C(21)-C(20)-C(10)	121.1(10)
C(28)-C(29)	1.350(17)	C(24)-C(20)-C(10)	119.2(11)
C(28)-H(28)	0.9300	C(20)-C(21)-N(9)	120.9(14)
C(29)-H(29)	0.9300	C(20)-C(21)-H(21)	119.6
C(30)-N(10)	1.323(14)	N(9)-C(21)-H(21)	119.6
C(30)-H(30)	0.9300	C(23)-C(22)-N(9)	124.5(15)
C(31)-N(8)	1.473(11)	C(23)-C(22)-H(22)	117.7
C(31)-C(32)	1.508(14)	N(9)-C(22)-H(22)	117.7
C(31)-H(31A)	0.9700	C(22)-C(23)-C(24)	120.4(15)
C(31)-H(31B)	0.9700	C(22)-C(23)-H(23)	119.8
C(32)-C(36)	1.399(15)	C(24)-C(23)-H(23)	119.8
C(32)-C(33)	1.399(16)	C(23)-C(24)-C(20)	120.0(16)
C(33)-C(34)	1.42(2)	C(23)-C(24)-H(24)	120.0
C(33)-H(33)	0.9300	C(20)-C(24)-H(24)	120.0
C(34)-C(35)	1.40(2)	N(7)-C(25)-C(26)	114.8(8)
C(34)-H(34)	0.9300	N(7)-C(25)-H(25A)	108.6
C(35)-N(11)	1.330(18)	C(26)-C(25)-H(25A)	108.6
C(35)-H(35)	0.9300	N(7)-C(25)-H(25B)	108.6
C(36)-N(11)	1.328(14)	C(26)-C(25)-H(25B)	108.6
C(36)-H(36)	0.9300	H(25A)-C(25)-H(25B)	107.6
N(1)-Co(1)	1.840(7)	C(30)-C(26)-C(27)	114.5(10)
N(3)-Co(1)	1.837(7)	C(30)-C(26)-C(25)	121.7(9)
N(5)-Co(1)	1.960(7)	C(27)-C(26)-C(25)	123.8(9)
N(6)-Co(1)	1.937(7)	C(29)-C(27)-C(26)	120.8(10)
N(7)-Co(1)	1.949(7)	C(29)-C(27)-H(27)	119.6
N(8)-Co(1)	1.955(7)	C(26)-C(27)-H(27)	119.6
N(9)-H(9)	0.8600	N(10)-C(28)-C(29)	121.8(11)
N(10)-Ag(1)#1	2.243(9)	N(10)-C(28)-H(28)	119.1
N(11)-Ag(1)	2.262(10)	C(29)-C(28)-H(28)	119.1
N(12)-Ag(1)#2	2.610(11)	C(27)-C(29)-C(28)	121.0(12)
O(5)-Ag(1)	2.501(12)	C(27)-C(29)-H(29)	119.5
O(5)-H(5A)	0.8868	C(28)-C(29)-H(29)	119.5
O(5)-H(5B)	0.8850	N(10)-C(30)-C(26)	125.9(11)
Ag(1)-N(10)#3	2.243(9)	N(10)-C(30)-H(30)	117.1
Ag(1)-N(12)#4	2.610(11)	C(26)-C(30)-H(30)	117.1
O(6)-H(6A)	0.8500	N(8)-C(31)-C(32)	110.5(7)
O(6)-H(6B)	0.8505	N(8)-C(31)-H(31A)	109.5
		C(32)-C(31)-H(31A)	109.5
		N(8)-C(31)-H(31B)	109.5
		C(32)-C(31)-H(31B)	109.5
		H(31A)-C(31)-H(31B)	108.1
		C(36)-C(32)-C(33)	118.0(10)
		C(36)-C(32)-C(31)	122.6(9)
		C(33)-C(32)-C(31)	119.4(10)
		C(32)-C(33)-C(34)	117.7(12)
		C(32)-C(33)-H(33)	121.1
		C(34)-C(33)-H(33)	121.1
		C(35)-C(34)-C(33)	118.7(13)

	C(35)-C(34)-H(34)	120.6
	C(33)-C(34)-H(34)	120.6
	N(11)-C(35)-C(34)	122.8(12)
	N(11)-C(35)-H(35)	118.6
	C(34)-C(35)-H(35)	118.6
	N(11)-C(36)-C(32)	124.2(10)
	N(11)-C(36)-H(36)	117.9
	C(32)-C(36)-H(36)	117.9
	C(4)-N(1)-C(1)	122.7(7)
	C(4)-N(1)-Co(1)	118.8(6)
	C(1)-N(1)-Co(1)	118.6(6)
	C(3)-N(2)-C(2)	117.9(8)
	C(8)-N(3)-C(5)	122.0(7)
	C(8)-N(3)-Co(1)	119.2(6)
	C(5)-N(3)-Co(1)	118.8(6)
	C(6)-N(4)-C(7)	118.3(8)
	C(9)-N(5)-C(10)	117.6(7)
	C(9)-N(5)-Co(1)	116.5(6)
	C(10)-N(5)-Co(1)	125.7(6)
	C(13)-N(6)-C(14)	117.0(7)
	C(13)-N(6)-Co(1)	117.6(6)
	C(14)-N(6)-Co(1)	125.2(6)
	C(11)-N(7)-C(25)	117.1(7)
	C(11)-N(7)-Co(1)	116.4(6)
	C(25)-N(7)-Co(1)	126.4(6)
	C(12)-N(8)-C(31)	117.0(7)
	C(12)-N(8)-Co(1)	116.6(6)
	C(31)-N(8)-Co(1)	126.4(6)
	C(21)-N(9)-C(22)	114.3(16)
	C(21)-N(9)-H(9)	112.2
	C(22)-N(9)-H(9)	112.3
	C(30)-N(10)-C(28)	115.9(10)
	C(30)-N(10)-Ag(1)#1	122.0(8)
	C(28)-N(10)-Ag(1)#1	121.9(7)
	C(36)-N(11)-C(35)	118.3(11)
	C(36)-N(11)-Ag(1)	128.8(8)
	C(35)-N(11)-Ag(1)	112.7(8)
	C(19)-N(12)-C(18)	118.8(11)
	C(19)-N(12)-Ag(1)#2	123.1(8)
	C(18)-N(12)-Ag(1)#2	116.1(8)
	Ag(1)-O(5)-H(5A)	110.8
	Ag(1)-O(5)-H(5B)	110.3
	H(5A)-O(5)-H(5B)	107.7
	N(3)-Co(1)-N(1)	179.4(3)
	N(3)-Co(1)-N(6)	98.4(3)
	N(1)-Co(1)-N(6)	81.2(3)
	N(3)-Co(1)-N(7)	81.3(3)
	N(1)-Co(1)-N(7)	98.3(3)
	N(6)-Co(1)-N(7)	91.1(3)
	N(3)-Co(1)-N(8)	81.3(3)
	N(1)-Co(1)-N(8)	99.1(3)
	N(6)-Co(1)-N(8)	92.0(3)
	N(7)-Co(1)-N(8)	162.6(3)
	N(3)-Co(1)-N(5)	99.2(3)
	N(1)-Co(1)-N(5)	81.1(3)
	N(6)-Co(1)-N(5)	162.3(3)
	N(7)-Co(1)-N(5)	91.6(3)
	N(8)-Co(1)-N(5)	90.6(3)
	N(10)#3-Ag(1)-N(11)	155.2(4)

	N(10)#3-Ag(1)-O(5)	115.0(5)
	N(11)-Ag(1)-O(5)	88.9(4)
	N(10)#3-Ag(1)-N(12)#4	99.6(3)
	N(11)-Ag(1)-N(12)#4	88.0(3)
	O(5)-Ag(1)-N(12)#4	86.0(4)
	H(6A)-O(6)-H(6B)	109.4

Symmetry transformations utilized to create similar atoms:

#1 -x+1, y+1/2, -z+3/2 #2 -x+3/2, -y, z-1/2

#3 -x+1, y-1/2, -z+3/2 #4 -x+3/2, -y, z+1/2

Table 2.5. Possible Hydrogen bonds for **3**.

	Bond distance	Bond angle
O(2)-H(2A)...O(1)	2.24	154.1
O(2)-H(2B)...O(1)#	2.11	154.5
N(3)-H(3)...O(3)	2.148	137.97

Table 2.6. Possible Hydrogen bonds for **5b**.

	Bond distance	Bond angle
O(5)-H(5B)...O(3)#4	1.96	149.4
O(6)-H(6B)...O(4)#9	2.28	124.9

Chapter-3

A Molecular Figure of Eight: Synthesis and Characterization

3.1. Abstract

3.2. Introduction

3.3. Results and Discussion

3.4. Conclusion

3.5. Experimental Section

3.6. References

3.7. Spectral Data

3.1. Abstract

Topologically similar elements with various structure are impossible to prove without their molecular arrangement. Herewith we reported the preparation of molecular figure of eight structure, with Co^{3+} through metal-templated method followed the closing of ring by Cu(I) catalysed click chemistry. Still, this reaction can produce both molecular [2]Catenane and molecular figure of eight structures. For conforming the preparation of figure of eight structure, we planned and synthesized an equivalent [2]Catenane structure solely, using an completely different approach. These two structures are analysed by both NMR spectroscopic method and high performance liquid chromatography (HPLC).

3.2. Introduction

In molecular interaction and reaction dynamics, molecular conformation plays a significant role. In biological system, conformation of molecules are very crucial for functional properties of the molecule. The best example, DNA (Deoxy-ribose nucleic acid) double helical structure is vital for its functional properties. Chemical topology is the part of chemistry to investigate flexible molecules that can make various knotted architectures established from last two decade.¹ Several supramolecular knotted architecture those were still chemically challenging were reported from this period.² A molecular figure of eight structure is a significant structural theme in assembly of different types of knots. In order to genetic recombine of circular DNA (Deoxy-ribose nucleic acid), molecular figure of eight structure acts a target intermediate in biological system. Among the smallest molecules, complex analogue of porphyrin assumes figure of eight structure. Vogel and coworker synthesized a molecular figure of eight structure from the condensation of a dialdehyde and diacid followed by catalytic hydrogenation with Pd/C (figure 3.1).³ The linear porphyrin tetrameric structure was oxidatively coupled in the occurrence of the hexa-pyridyl template to afford Figure of eight structure by Vernier tempting approach.⁴

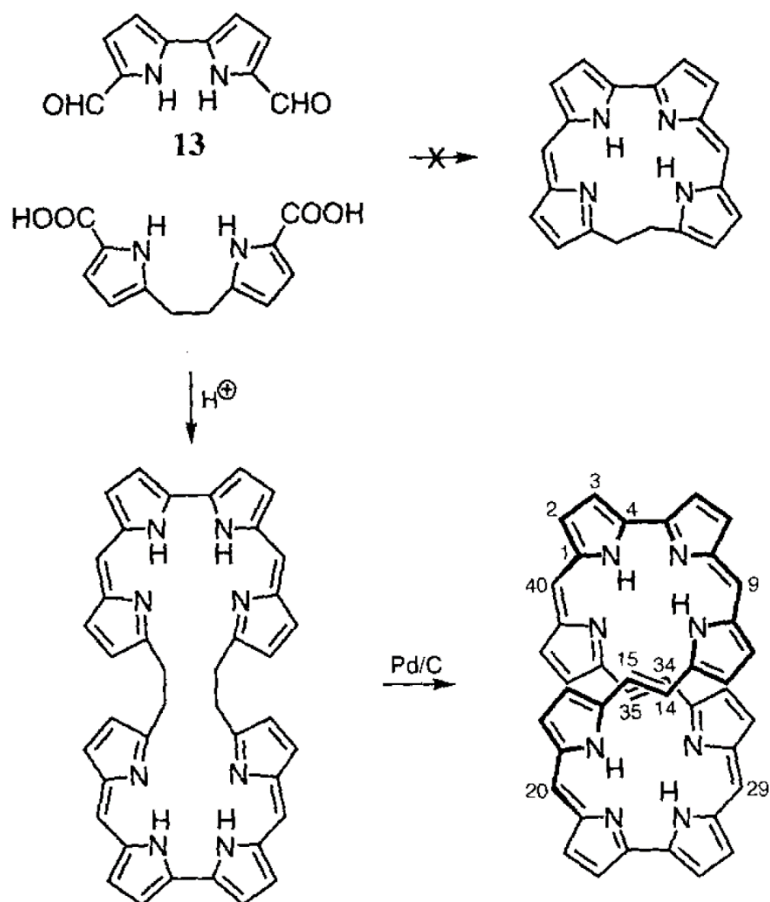


Figure 3.1. Synthesis of porphyrin based figure of eight

Sauvage and co-workers synthesized a figure of eight conformation that has been utilized like artificial muscle in a larger cyclic molecule.⁵ Here, a large metallomacrocyclic of 78-membered ring, with two different types of binding fragments, coordinated with different kinds of transition metals in a bimodal way (figure 3.2). The way of ring coordination depends on the nature of the transition metal used or its oxidation state. Additionally, each metal complexed formed

depends on the shape of a figure-of eight, with required crossing point in between the two loops of the cycle.

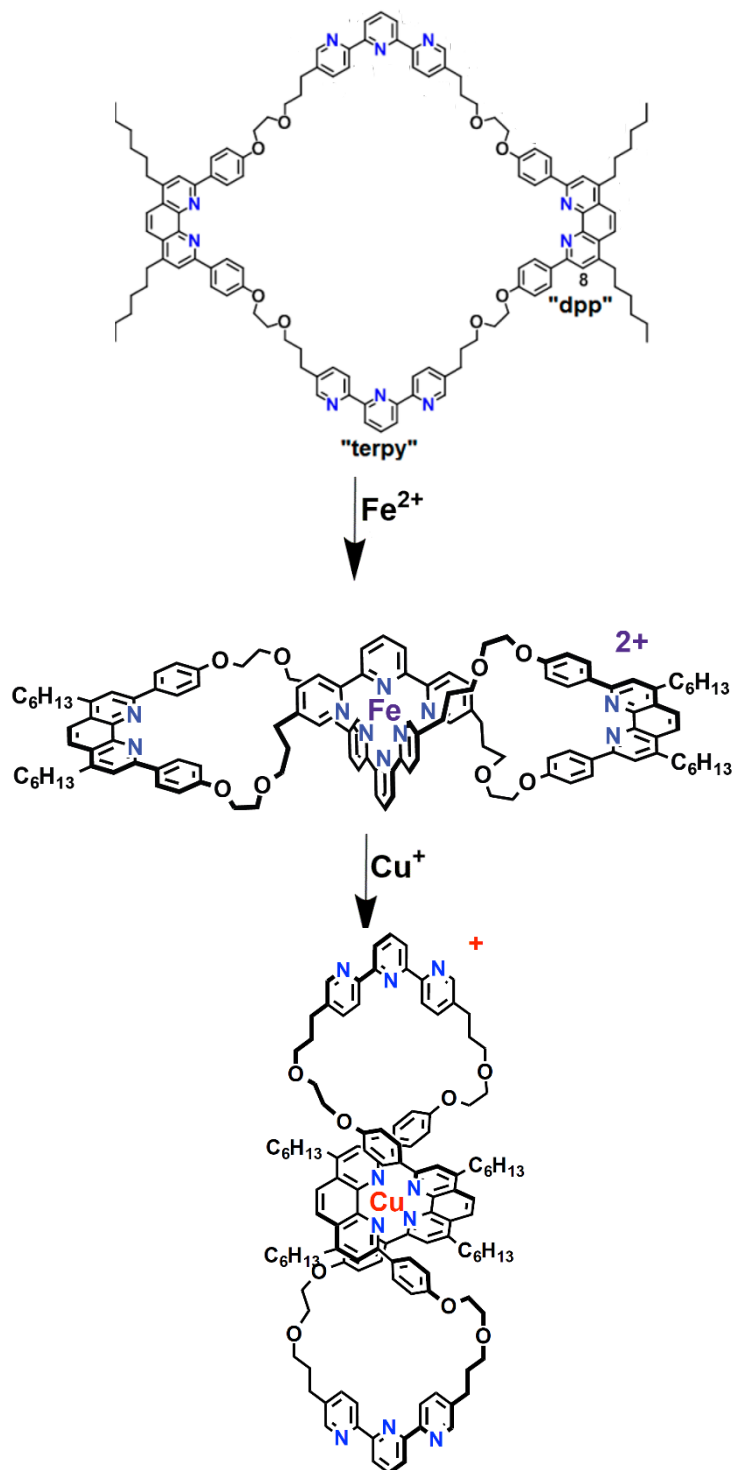
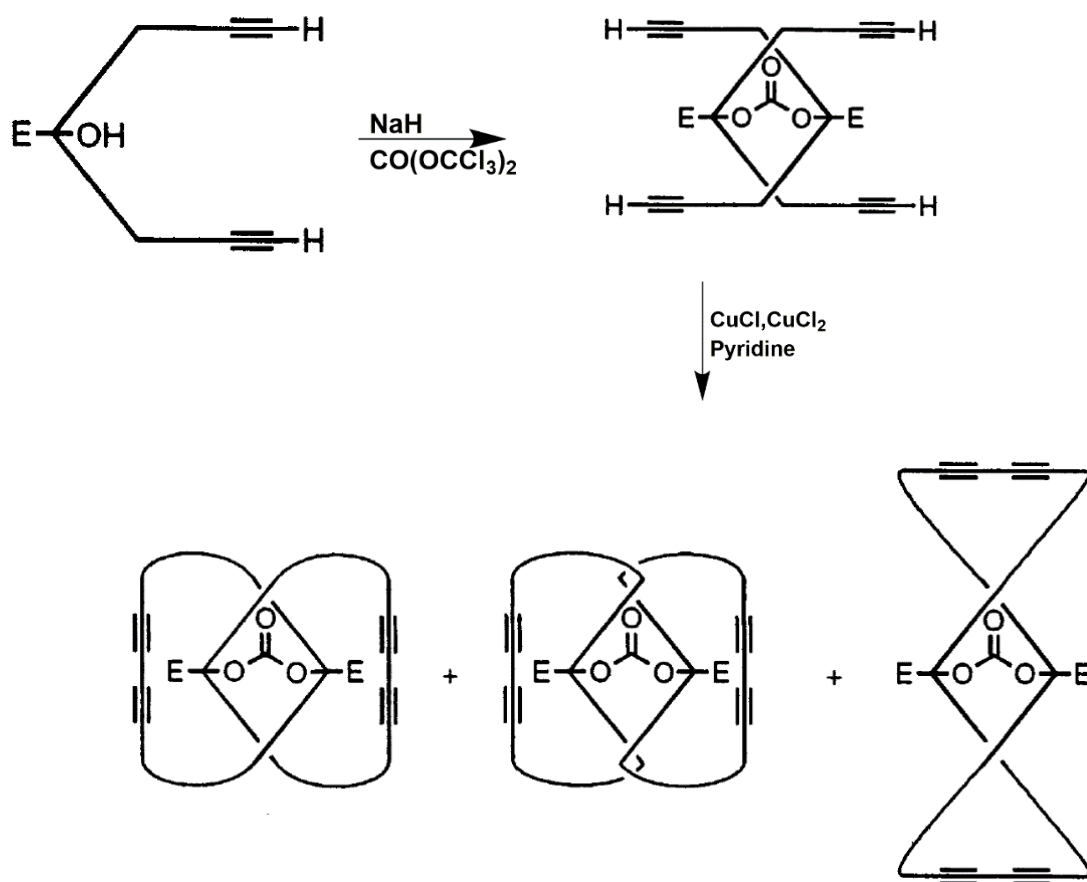
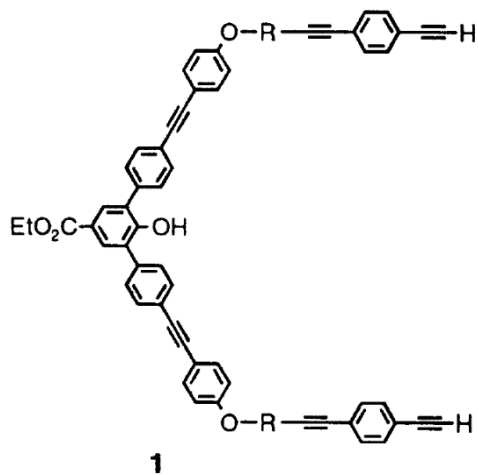


Figure 3.2. Figure of eight structure with $\text{Fe}^{2+}/\text{Cu}^+$

Adelheid Godt and co-workers synthesized large macrocycle from a figure of eight complex by using covalent template approach (figure 3.3).⁶



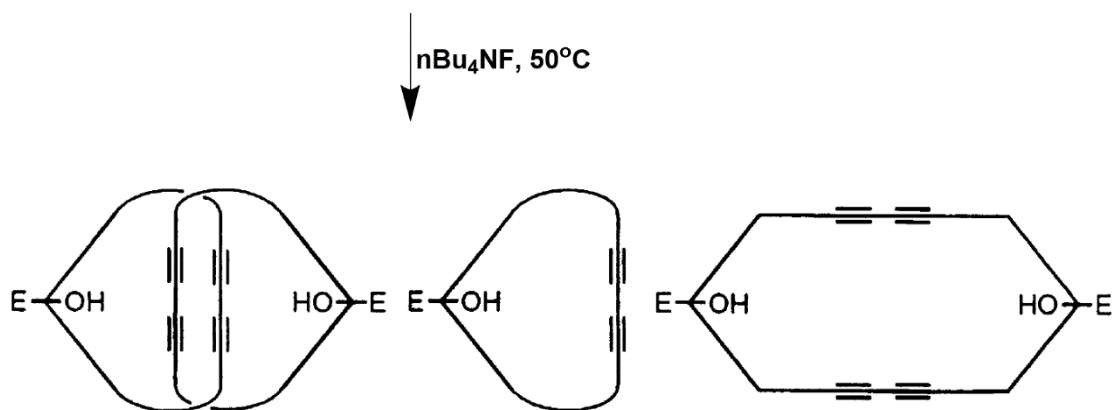


Figure 3.3. Synthesis of [2]Catenane, and a large macrocycle

Molecular Figure of eight is achieved as an unexpected product throughout the chemical synthesis of [2]Catenane.⁷ Pierre Braunstein and co-workers reported a dinuclear, cationic Ir(I) NHC(N-heterocyclic carbene) complex with a figure-of-eight structure. The bis-imidazolium precursor [1,1'-((4,6-dimethyl-1,3-phenylene)bis(methylene))bis(3-methyl-1H-imidazol-3-ium)dihexafluorophosphate ($\text{H}_2\text{L}\cdot 2\text{PF}_6$) (figure 3.4) was treated with $[\text{Ir}(\text{m-Cl})(\text{cod})]_2$ in the presence of the base Cs_2CO_3 to give the dinuclear iridium(I) complex, which is confirmed by single X-ray crystal diffraction.⁸

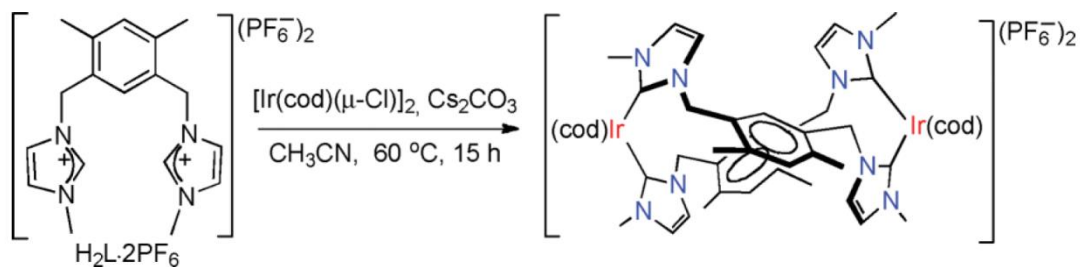


Figure 3.4. Synthesis of dinuclear Ir(I) complex

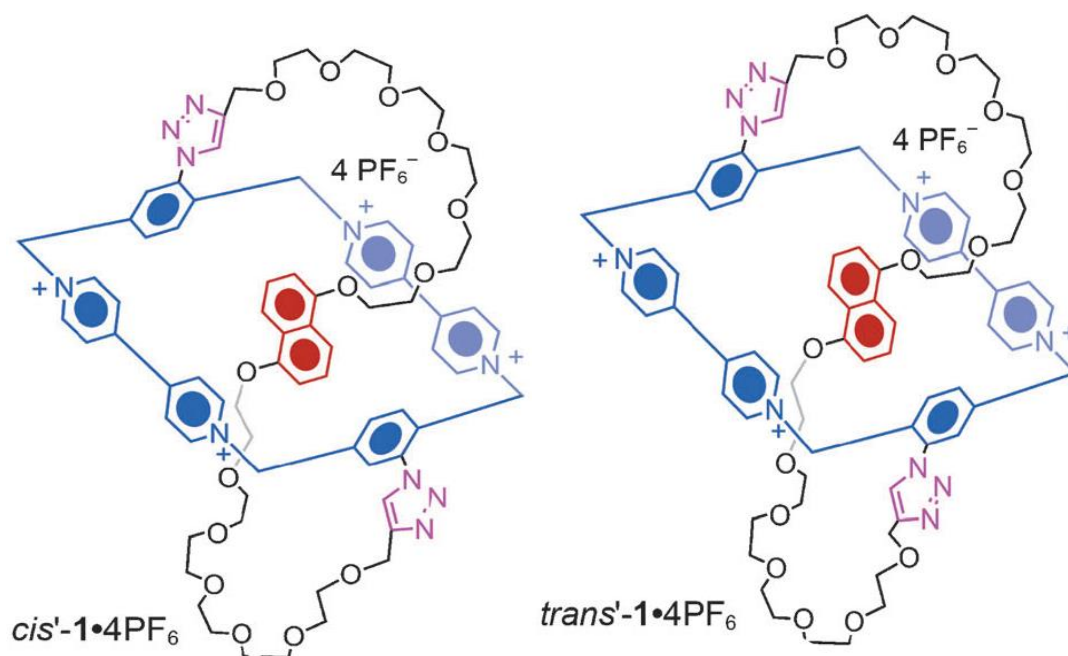


Figure 3.5. Stoddart's figure of eight with Cis and Trans configuration

Stoddart and coworkers utilized Copper(I)-catalyzed click chemistry approach to synthesize figure of eight isomer.⁹ In this case, an electron-withdrawing cyclo-bis(paraquat-p-phenylene) derivative holding trans-disposed azide derivatives between its two phenylene rings reacted with a bispropargyl derivative of a polyether chain under click reaction (figure 3.5). It resulted both cis and trans form of molecular figure of eight structural isomer in solution.

Molecular system are capable of naturally forming figure of eight conformation and can also produce the same because of aurophilic interaction in inorganic coordination.¹⁰ Transition metal plays an important role for synthesizing different supramolecular architectures with different ligands in an appropriate geometrical

fashion. Leigh and co-workers described the three dimensional (3D) template approach to build numerous supra-molecular designs. One of these method used the tridentate dianionic pyridine-2, 6-dicarboxamido ligands holding the Co(III) ion in an octahedral manner to create the essential crossing-points (figure 3.6).¹¹

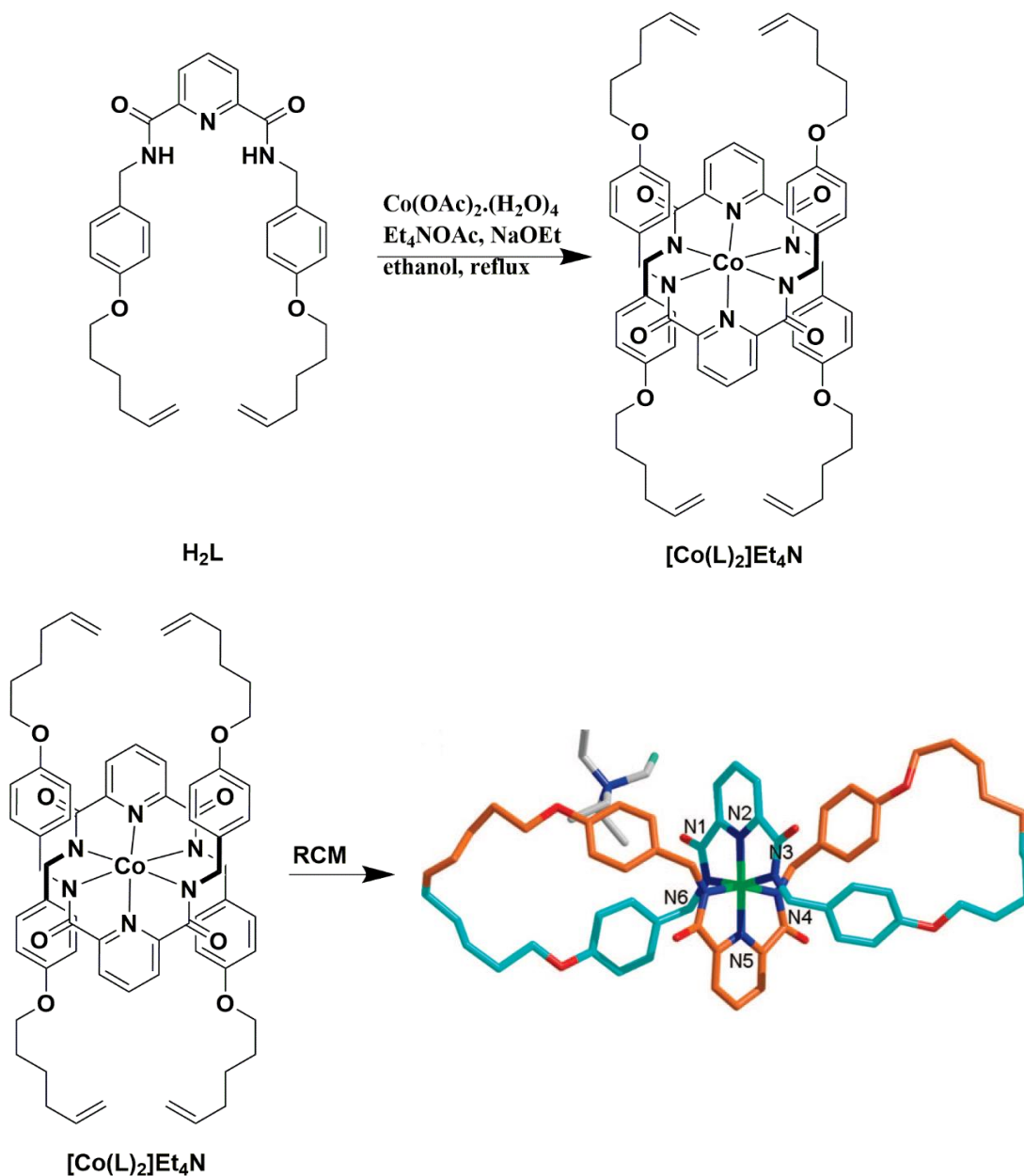


Figure 3.6. Synthesis of Cobalt (III) complex with figure of eight structure

Utilizing this templated approach, we synthesized first Co(III) complex that provide necessary three dimensional(3D) arrangement for the synthesis of targeted structure. Consequently, the Co(III) complex with this four ends are unified in the suitable manner lead to two different interlocked architectures, either a [2]Catenane or a Figure of eight (Figure 3.7).

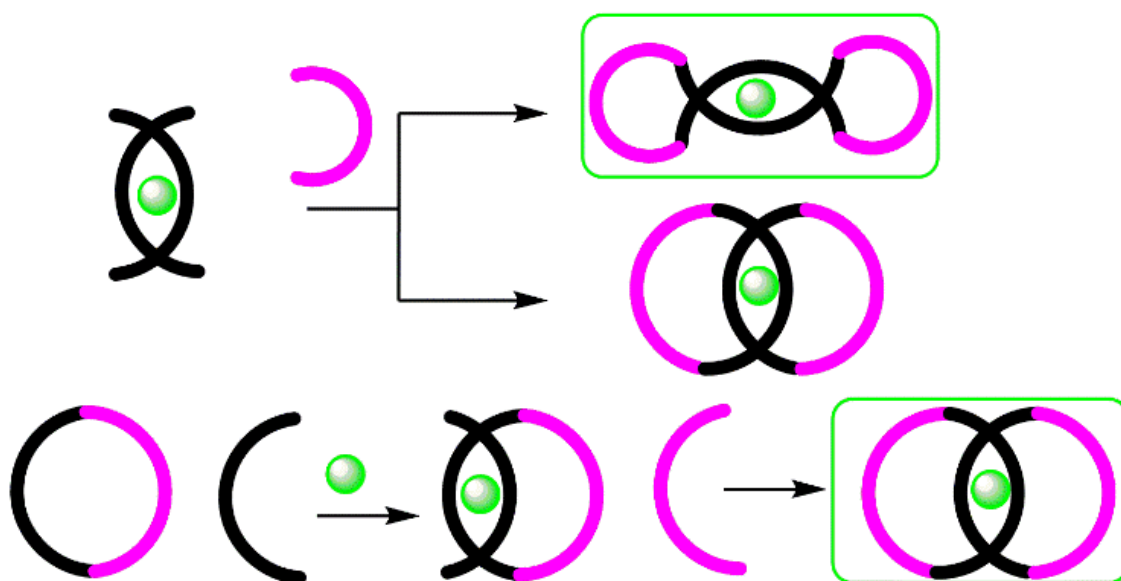
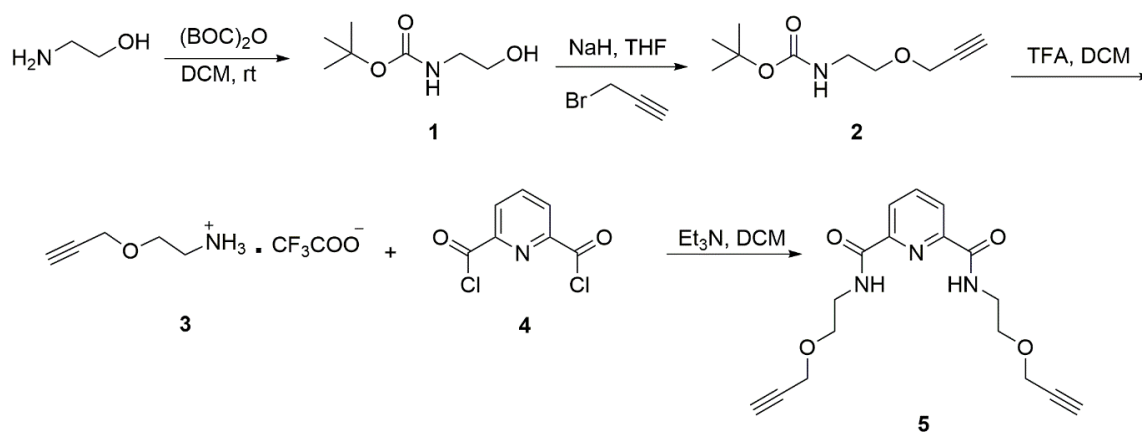


Figure 3.7. Graphic design of Molecular Figure of eight and [2]Catenane complex

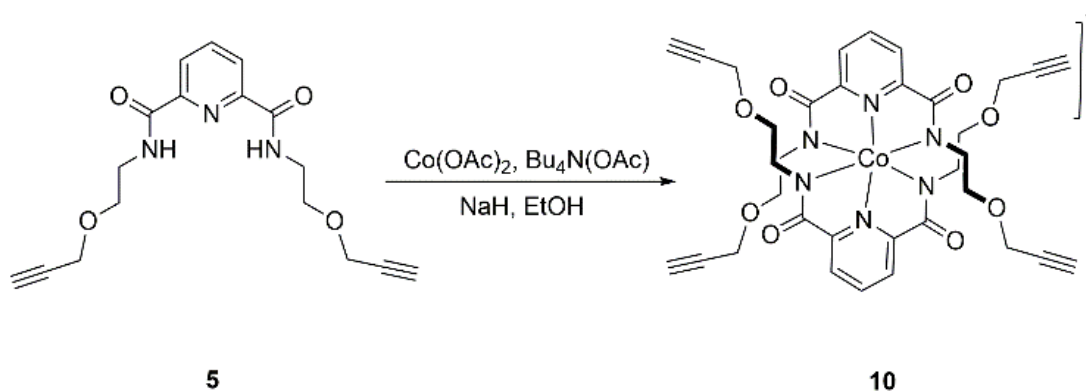
3.3. Result and Discussion

We synthesized the compound **5** from pyridine- 2, 6- dicarboxyldichloride and the synthesized amine **3**. The corresponding amine **3** was synthesized from the commercially available starting material 2-aminoethanol. Firstly the 2-aminoethanol was protected with Boc anhydride resulted N-Boc protected ethanol amine **1**.¹² The compound **1** was treated with commercially available propargyl bromide in presence of sodium hydride(NaH) to form **2**.¹³ The compound was

deprotected with trifluoroacetic acid at room temperature resulted corresponding aminesalt **3**. Pyridine- 2, 6-dicarboxyldichloride **4** was synthesized from 2, 6-dipicnic acid with SOCl_2 according to literature procedure.¹⁴ Finally **3** was reacted with pyridine- 2, 6-dicarboxyldichloride to afford corresponding substituted 2,6-pyridinedicarboxamide **5** in presence of non-nucleophilic base triethyl amine (scheme 3.1).



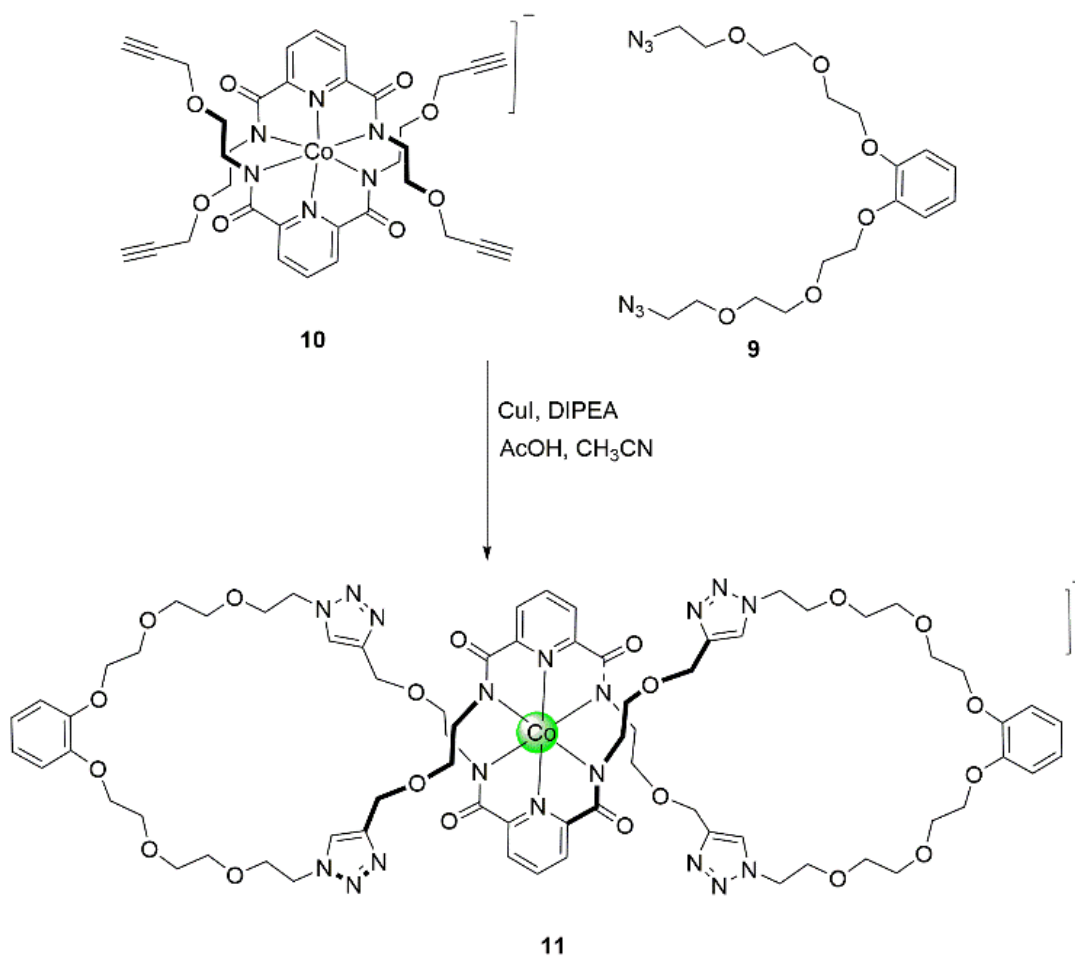
Scheme 3.1. Synthesis of **5**



Scheme 3.2. Synthesis of **10**

The N-H protons in substituted 2, 6-pyridinedicarboxamide **5** deprotonated with NaOMe (i.e in situ generation of NaH with methanol) under strict nitrogen atmosphere following the metalation to afford the Co(III) complex **10**(scheme

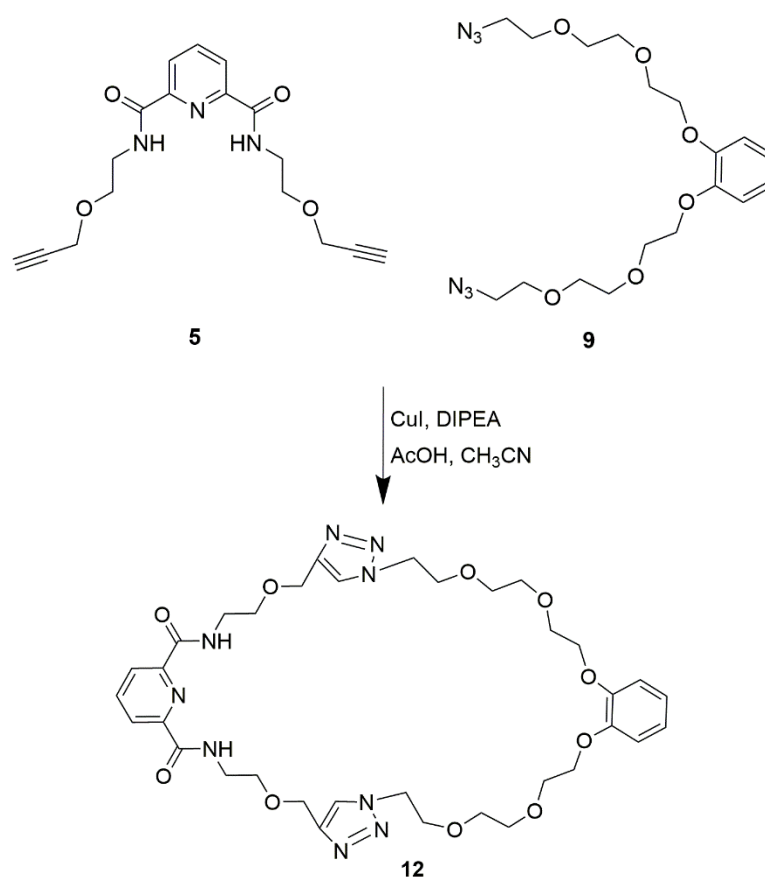
to targeted diazide spacer **9** with the reaction with sodium azide (NaN_3) and described by ^1H NMR and ESI-MS spectroscopy (figure 3.12 and 3.23).



Scheme 3.4. Molecular figure-of-eight complex, **11** by click chemistry

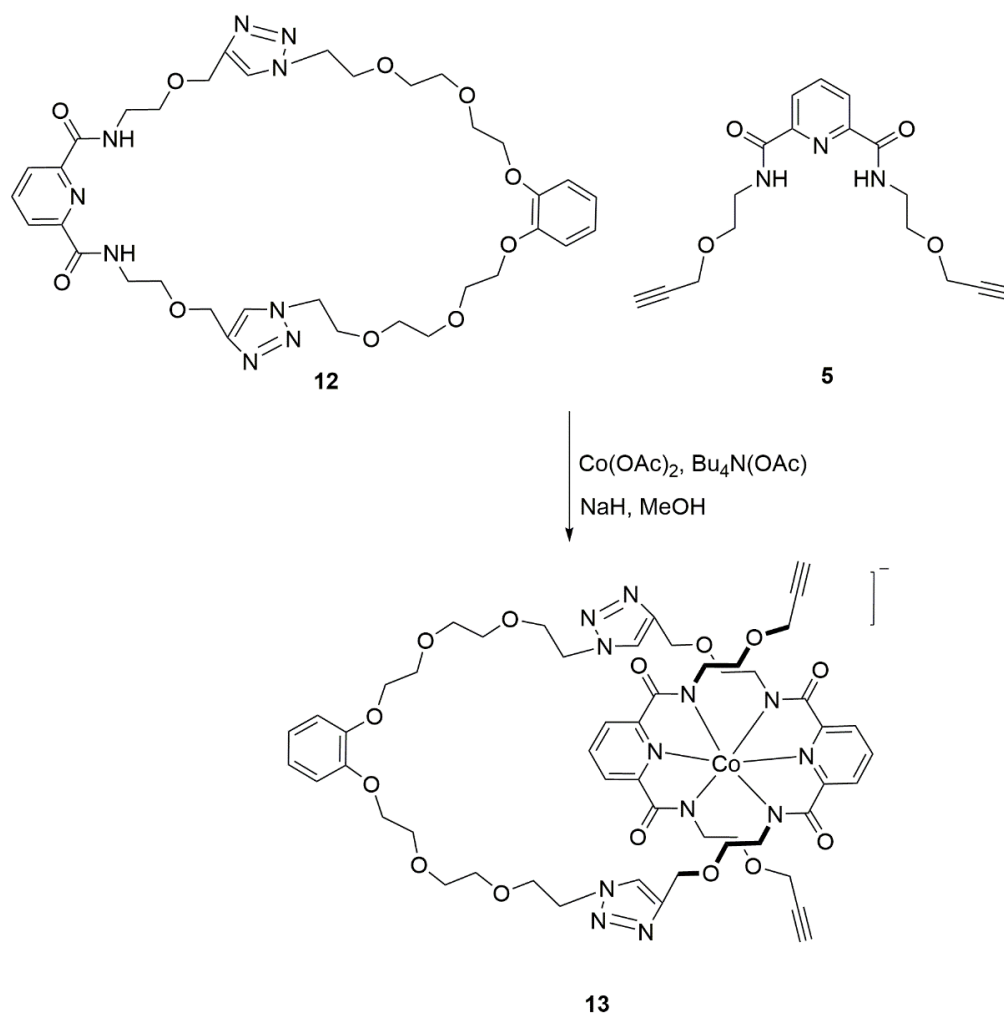
The compound **10** with four sites free alkyne functionalities reacted with the corresponding diazide spacer **9** by click reaction condition resulted **11**, a semisolid (scheme 3.4). Because of using a long chain spacer, the interlocked molecular structure is thought to be a figure- of-eight complex. The predictable molecular

structure was confirmed by spectroscopic studies. ESI-MS spectral data clearly indicates that a peak at m/z : 1561.5943 (calc. 1561.5905) resembles to expected structure (Figure 3.25). ^1H NMR spectral data have exposed that presence of a new peak in aromatic zone producing a triazole bridged interlocked structure. Though, this may also resembles to a [2]Catenane. We are unsuccessful to get single crystals for the solid state analysis using X-ray due to oily nature of the compound **11**. In order to conform, this molecular structure, we planned for synthesizing a macrocycle which can be metallated to afford an interlocked [2]Catenane.



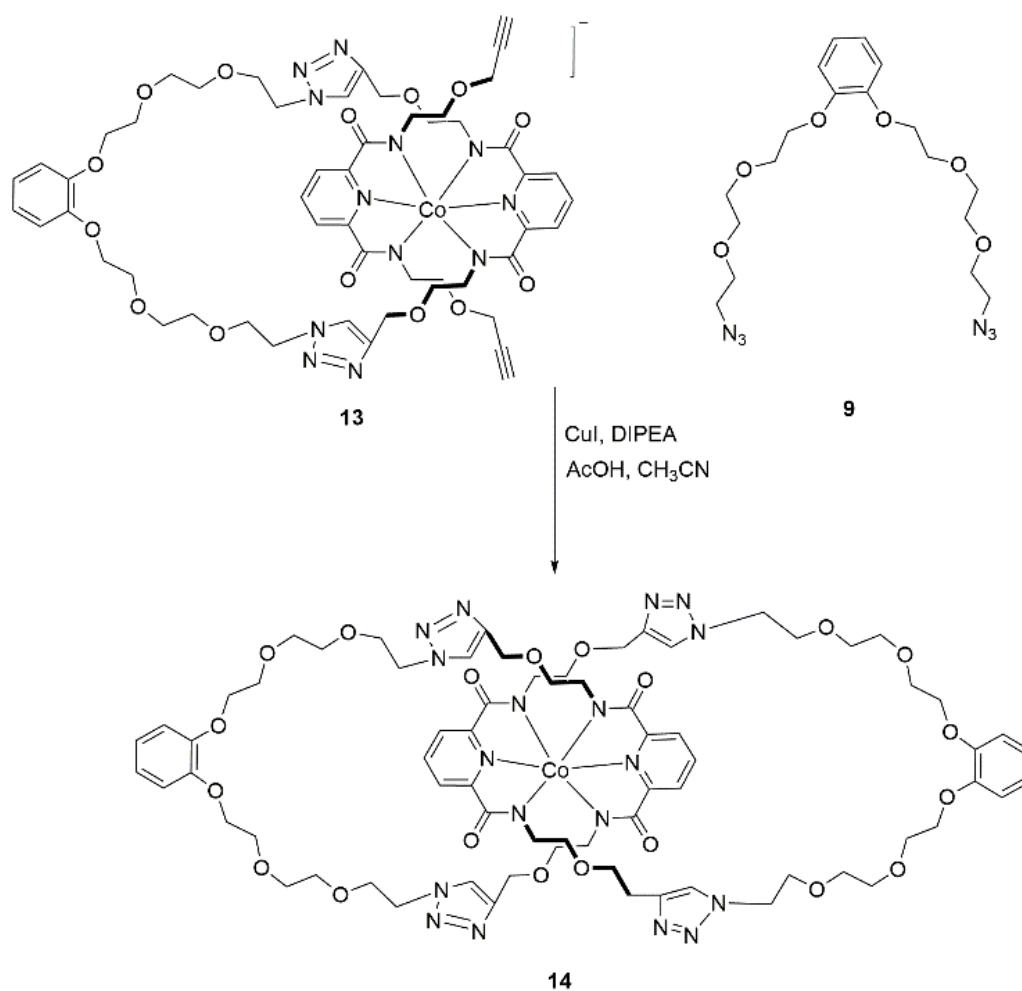
Scheme 3.5. Macrocycle **12** by click chemistry approach

Macrocyclic compound **12**, was synthesized by click reaction between the compound **5** and compound **9** (scheme 3.5). **12** that has two amide groups, was deprotonated with sodium methoxide (CH_3ONa) followed by metal coordination to afford Cobalt(III) complex **13** in presence of the compound **5** (Scheme 3.6). The two free alkyne groups in **13** can be cyclized in presence of Cu(I) catalyzed click reaction (Scheme 3.7) to afford **14**. The ESI-MS spectral data clearly signifies, that a peak at m/z : 1561.5543 (calc. 1562.53) corresponds to the formation of the compound **14** (Figure 3.28).



Scheme.3.6. Synthesis of the **13**

It may be noted that both the mass spectral data gave identical m/z values with an experimental error. Comparing ^1H NMR spectral data of the compound **14** with that of compound **11** signifies that, there was entire shift of aromatic protons in these two compounds (Figure 3.8). In compound **11**, the pyridine ring protons, a triplet and a doublet was noticed at 8.16 and 7.92 ppm respectively whereas in case of compound **14**, the pyridine ring protons were noticed at 8.22 and 7.96 ppm respectively.



Scheme 3.7. [2]Catenane, **14** by click chemistry

The chemical environment of all the protons of compound **11** and **14** are nearly same, so there were not much shifting observed in the one dimensional(1D)-spectra. The up field shift of pyridine ring proton in compound **11** was because of the absence of ring current effect as pyridine ring protons are outside the loop however such ring current effect was existing between pyridine ring proton and benzene ring of polyether moiety of compound **14**. In compound **14**, there may be some kinds of interaction in between the $-CH_2$ protons of polyether moiety and pyridine ring proton, as the pyridine ring in compound **14** is inside the loop however in compound **11**, both the $-CH_2$ ring protons and pyridine ring was distant apart. As a result of this, we have done a ROESY experiments for both the compounds **11** and **14** respectively. ROESY spectra clearly indicate that there was no such cross peaks between the $-CH_2$ protons of polyether moieties (3.8 – 5 ppm) and pyridine ring proton (8.16 ppm) in compound **11**.

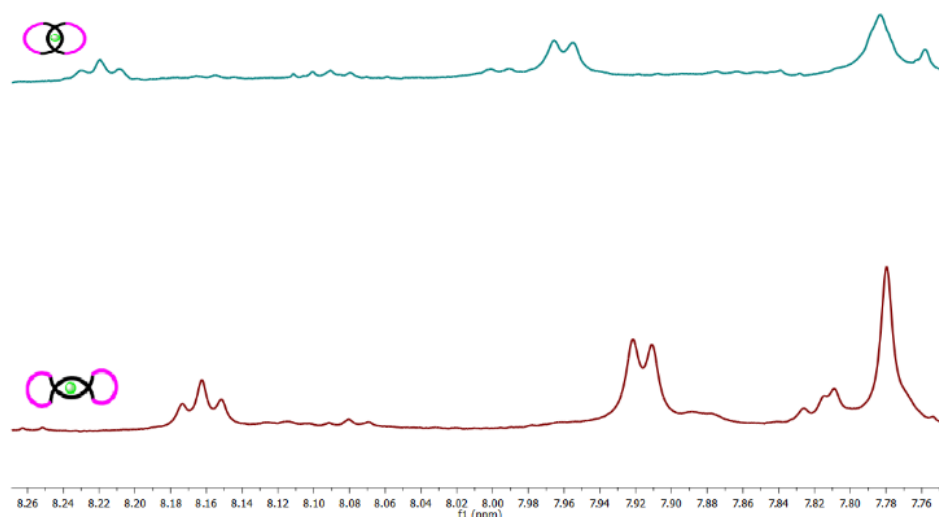


Figure 3.8. Comparative 1H NMR spectra of [2]catenane, **14** with that of figure of eight complex, **11**

Consequently we have established that both were different compounds as we have followed different synthetic scheme for both the compound **11** and **14** and also shifting in ^1H NMR spectroscopy. Besides we have also done high performance liquid chromatography (HPLC) experiment for both of the isomeric complex. High performance liquid chromatography (HPLC) achieved on a semi preparative HPLC with water (H_2O) and Methanol (CH_3OH) as solvents. Comparing the high performance liquid chromatography (HPLC) data of these two compounds **11** and **14** shown that these two are isomeric compounds have different retention times as 31.831 and 31.135 min as expected (Figure 3.9).

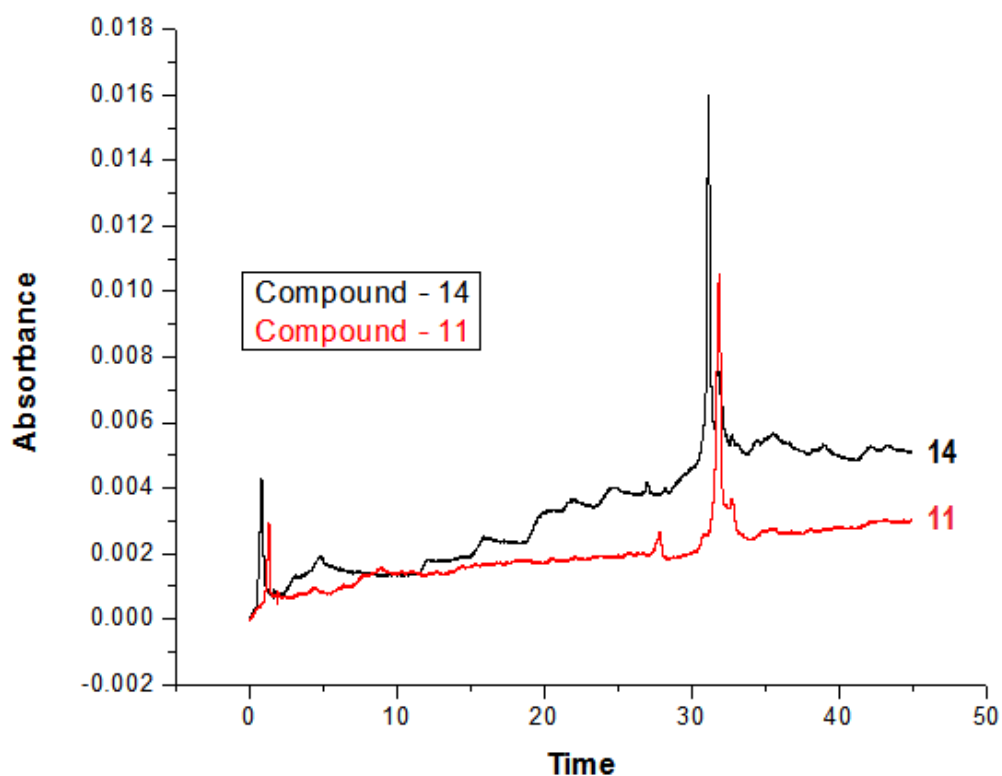


Figure 3.9. HPLC data of compound **11** and **14**

3.4. Conclusion

We have successfully reported and characterized a molecular figure of eight structure exclusively by a metal mediated followed by copper(I) catalyzed click chemistry. An Similar [2]catenane was also reported and compared for the confirmation of proposed structure.

3.5. Experimental Section

General Reagent grade chemicals were acquired from Aldrich and used as received. All solvents were procured from Merck Limited, India. The solvents were purified prior to use following standard procedures. NMR was recorded with a Bruker Advance-III 400 MHz and 700 MHz instruments. HRMS was performed on a Bruker ESI-MS microTOFQ. HPLC performed on Waters semi preparative HPLC. Water and Methanol were used as solvents. AC-18 RP Waters sun fire column (5 μ m, 4.6 x150 mm) used to perform 0 - 50% in 30 min monitored at 300 nm.

Synthesis of N2, N6-bis (2-(prop-2-yn-1-yloxy) ethyl) pyridine-2, 6-dicarboxamide (5)

The Boc-group in compound **2** was deprotected by 40 % trifluoro acetic acid in dichloromethane over a period of 3 h. The crude boc deprotected ammonium salt was used in next step without further purification. 2, 6-pyridine acid chloride (0.500 g, 2.4 mmol) was taken in 10 mL dichloromethane under N₂ environment and cooled down to 0 °C. In an another flask, the corresponding boc deprotected amine salt **3** (1.306 g, 6.12 mmol) in 10 mL dichloromethane was added to it dropwise over a period of 30 min at 0 °C and stirred at room temperature for another 2 h. The

reaction mixture was extracted and dried over anhydrous Na_2SO_4 . The crude was purified by column chromatography to afford the target compound **5** as a colorless solid (0.580 g, 71.8 %). ^1H NMR (400 MHz, CD_2Cl_2) δ 8.33 (d, $J = 8$ Hz), 8.22 (s), 8.06 (t, $J = 20$ Hz) 4.23 (d, $J = 4$ Hz), 3.69-3.76 (m), 2.55 (t, $J = 8$ Hz). ^{13}C NMR (100 MHz, CD_2Cl_2) δ 164.05, 149.47, 139.50, 125.27, 80.09, 75.36, 69.43, 58.83, 39.81 ESI-HRMS m/z : 330.1448 $[\text{M}+\text{H}]^+$ (calc.330.1458 for $\text{C}_{17}\text{H}_{19}\text{N}_3\text{O}_4$).

Synthesis of 1, 2-bis (2-(2-(2-azidoethoxy) ethoxy) ethoxy) benzene (9)

(0.400 g, 0.585 mmol) of **8** was taken in 8 mL of DMF. To this (0.228 g, 3.51 mmol) of sodium azide was added to it and refluxed it for 4 h. After 4 h, the reaction mixture was cooled down to room temperature, the solvent was evaporated and the crude reaction mixture was poured in water extracted with dichloromethane and dried over anhydrous Na_2SO_4 . The reaction mixture was purified by column chromatographic method to afford the target compound **9** as a brownish liquid (0.305 g, 76%). ^1H NMR (400 MHz, CD_2Cl_2) δ 6.19 (d, $J = 4$ Hz), 4.33 (q), 3.83 (q), 3.65 (m), 3.37 (t, $J = 8$ Hz). ^{13}C (100MHz, CD_2Cl_2) δ 149.34, 121.94, 114.81, 71.15, 70.30, 69.14, 51.32. ESI-HRMS m/z : 447.1963 $[\text{M} + \text{Na}]^+$ (calc. 447.1966 for $\text{C}_{18}\text{H}_{28}\text{N}_6\text{O}_6$).

Synthesis of Co(III) complex (10)

A suspension of **5** (1.00 g, 3.039 mmol), $\text{Bu}_4\text{N}(\text{OAc})$ (0.458 g, 1.519 mmol) and $\text{Co}(\text{OAc})_2(\text{H}_2\text{O})_4$ (0.378 g, 1.519 mmol) in methanol (10 mL), was refluxed under nitrogen environment to give a clear, pale pink, coloured solution. To this a solution of sodium methoxide (in situ generation of sodium hydride (NaH) (0.145 g of 60 % dispersion in oil, 6.079 mmol with MeOH)) causing a colour change to deep purple.

Upon open to air, the colour of the reaction mixture changed to deep green over about 5 min after that it was refluxed for further 2 h. The solvent was evaporated under reduced pressure, the crude residue was purified by column chromatographic method with 20 % DCM -MeOH and dried under vacuum to produce **10** as a greenish solid (1.65 g, 76%). ^1H NMR (400 MHz, CD_2Cl_2) δ t, J = 16 Hz), d, J = 8 Hz), d, J = 4 Hz), 3.13 (t, J = 16 Hz), 2.94 (t, J = 12 Hz), 2.38 (t, J = 8 Hz), 2.25 (t, J = 12 Hz). ^{13}C (100MHz, CD_2Cl_2) δ 168.94, 157.99, 140.06, 123.47, 80.88, 74.32, 69.20, 59.48, 58.18, 43.27, 24.40, 20.26, 13.91. ESI-HRMS m/z : 713.1437 $[\text{M}+\text{H}]^+$ (calc. 713.1439).

Synthesis of complex (11)

A suspension of **10** (0.200 g, 0.280 mmol) along with copper iodide (0.001 g, 0.005 mmol), N, N-Diisopropylethyl amine (1.93 μL , 0.01 mmol) were taken in acetonitrile under N_2 atmosphere. To this **9** (0.261 g, 0.280 mmol) was added and a catalytic amount of acetic acid (CH_3COOH) was also added and continued stirring at 50 $^\circ\text{C}$ for 7 days. After that, the solvent was removed and crude mixture was purified by column chromatographic method with 50% DCM-MeOH mixture and dried under vacuum to produce **11** as a greenish oily liquid (0.130 g 30%). ^1H NMR (700 MHz, CD_2Cl_2) δ 8.16 (t, J = 14 Hz), 7.92 (d, J = 7 Hz), 7.781 (s), 6.90 (s), 4.55(t, J = 14 Hz), 4.21 (m), 3.89 (m), 3.76 (t, J = 7 Hz), 3.63 (m), 2.85 (m). ^{13}C (175 MHz, CD_2Cl_2) δ 168.73, 157.53, 149.01, 145.20, 140.39, 139.92, 124.91, 123.58, 122.04, 122.00, 114.79, 114.71, 114.31, 71.03, 71.02, 70.38, 69.96, 69.21, 69.16, 64.36, 59.44, 50.64, 34.35, 32.48, 30.23, 30.20, 30.04, 29.91, 29.71, 29.53,

24.47, 23.24, 20.39, 14.40, 13.83. ESI-HRMS m/z : 1561.5905 $[M]^-$ (calc. 1561.5947 for $C_{70}H_{90}CoN_{18}O_{20}$).

Synthesis of macrocyclic complex (**12**)

A solution of **5** (50 mg, 0.15 mmol) along with copper iodide (1.1 mg, 0.015 mmol), N, N-Diisopropylethylamine(DIPEA) (2.714 μ L, 0.015 mmol) was taken in acetonitrile under N_2 atmosphere. To this **9** (64 mg, 0.15 mmol) was added and a catalytic amount of acetic acid(CH_3COOH) was also added and continued stirring at 50 °C for 48 h. After that the solvent was evaporated and crude reaction mixture was purified by column chromatography with 10 % DCM -MeOH to afford **12** as a colorless liquid (0.065 g, 57%). 1H NMR (700 MHz, CD_2Cl_2) δ 8.75 (s), 8.30 (d, $J = 7$ Hz), 8.03 (t, $J = 14$ Hz), 7.81 (s), 6.93 (s), 4.61 (s), 4.48 (t, $J = 14$ Hz), 4.11 (t, $J = 7$ Hz), 3.84 (t, $J = 7$ Hz), 3.75 (t, $J = 14$ Hz), 3.66 (m), 3.60 (d, $J = 7$ Hz) ^{13}C (175 MHz, CD_2Cl_2) δ 164.20, 149.71, 149.19, 139.17, 130.40, 125.12, 121.97, 114.33, 114.41, 71.01, 70.16, 69.80, 69.64, 69.03, 39.98, 32.49, 29.88, 23.36, 14.44. ESI-HRMS $[M+H]^+$ m/z : 754.3519 (calc. 754.3509 for $C_{35}H_{47}N_9O_{10}$).

Synthesis of threaded complex (**13**)

A suspension of **12** (19.6 mg, 0.026 mmol), $Bu_4N(OAc)$ (7.8 mg, 0.026 mmol) and $Co(OAc)_2(H_2O)_4$ (6.5 mg, 0.026 mmol) in methanol (10 mL), was refluxed under N_2 environment to give a clear, pale pink, coloured solution and the reaction mixture was stirred for 1 h. After 1 h, **5** (8.5 mg, 0.026 mmol) in methanol was added to this mixture and stirring continued for another 30 min. After that, a solution of sodium methoxide (in situ generation of NaH (2.7 mg, 60 % dispersion in oil, 0.11 mmol in MeOH) resulting a color change to deep purple. Upon open to air, the

color of the reaction mixture changed to deep green over about 20 min after which it was refluxed for further 6 h. The solvent was evaporated under reduced pressure and the crude residue was utilized for next reaction without further purification (inseparable in TLC) to afford **13** as a greenish liquid. ESI-HRMS $[M]^-$ m/z : 1138.3741 (calc. 1138.38 for $C_{52}H_{62}CoN_{12}O_{14}$).

Synthesis of [2] catenane (**14**)

A suspension of **13** (30 mg, 0.026 mmol) along with copper iodide (5 mg, 0.0026 mmol), N, N-Diisopropylethylamine (4.18 μ L, 0.0026 mmol) was taken in acetonitrile-methanol (4:1) mixture under N_2 atmosphere. To this **9** (11 mg, 0.026 mmol) was added and continued stirring at 50 $^{\circ}C$ for 6 days. The solvent was evaporated and the crude reaction mixture was purified by column chromatographic method with DCM -MeOH (3:2) to afford targeted [2] catenane **14** as a greenish liquid (4 mg, 15%). 1H NMR (700 MHz, CD_2Cl_2) δ 8.22(t, J = 7 Hz), 7.94 (d, J = 7 Hz), 7.78 (s), 6.92 (s), 4.68 (m) 4.16 (m), 4.09 (t, J = 7 Hz), 3.82 (t, J = 7 Hz), 3.58-3.69 (m). ^{13}C (175 MHz, CD_2Cl_2) δ 165.160, 157.724, 149.500, 140.930, 139.221, 125.286, 125.514, 125.113, 124.070, 122.393, 122.313, 114.323, 70.99, 70.622, 70.599, 69.94, 69.47, 69.037, 66.06, 65.06, 59.43, 50.933, 34.372, 32.472, 30.21, 30.17, 30.05, 29.919, 29.72, 29.540. ESI-MS m/z : 1561.5543 $[M]^-$ (calc. for $C_{70}H_{90}CoN_{18}O_{20}$).

3.6. REFERENCES

1. Chambron, J.-C.; Mitchell, D. K., *J. Chem. Educ.* **1995**, *72* (12), 1059.
2. Ayme, J.-F.; Beves, J. E.; Campbell, C. J.; Leigh, D. A., *Chem. Soc. Rev.* **2013**, *42* (4), 1700-1712.
3. Vogel, E.; Bröring, M.; Fink, J.; Rosen, D.; Schmickler, H.; Lex, J.; Chan, K. W. K.; Wu, Y.-D.; Plattner, D. A.; Nendel, M.; Houk, K. N., *Angew. Chem. Int. Ed.* **1995**, *34* (22), 2511-2514.
4. O'Sullivan, M. C.; Sprafke, J. K.; Kondratuk, D. V.; Rinfrey, C.; Claridge, T. D. W.; Saywell, A.; Blunt, M. O.; O'Shea, J. N.; Beton, P. H.; Malfois, M.; Anderson, H. L., *Nature* **2011**, *469*, 72.
5. Niess, F.; Duplan, V.; Sauvage, J.-P., *J. Am. Chem. Soc.* **2014**, *136* (16), 5876-5879.
6. Shah, M. R.; Duda, S.; Müller, B.; Godt, A.; Malik, A., *J. Am. Chem. Soc.* **2003**, *125* (18), 5408-5414.
7. Liu, X.; Lacour, J.; Braunstein, P., *Dalton Trans.* **2012**, *41* (1), 138-142.
8. Liu, X.; Pattacini, R.; Deglmann, P.; Braunstein, P., *Organometallics* **2011**, *30* (12), 3302-3310.
9. Boyle, M. M.; Gassensmith, J. J.; Whalley, A. C.; Forgan, R. S.; Smaldone, R. A.; Hartlieb, K. J.; Blackburn, A. K.; Sauvage, J.-P.; Stoddart, J. F., *Chem. Eur. J.* **2012**, *18* (33), 10312-10323.
10. Tunyogi, T.; Deák, A.; Tárkányi, G.; Király, P.; Pálinkás, G., *Inorg Chem* **2008**, *47* (6), 2049-2055.

11. Leigh, D. A.; Lusby, P. J.; McBurney, R. T.; Morelli, A.; Slawin, A. M. Z.; Thomson, A. R.; Walker, D. B., *J. Am. Chem. Soc.* **2009**, *131* (10), 3762-3771.
12. Kulkarni, C.; Bejagam, K. K.; Senanayak, S. P.; Narayan, K. S.; Balasubramanian, S.; George, S. J., *J. Am. Chem. Soc.* **2015**, *137* (11), 3924-3932.
13. Brogini, G.; Poli, G.; Beccalli, E. M.; Brusa, F.; Gazzola, S.; Oble, J., *Adv. Synth. Catal.* **2015**, *357* (4), 677-682.
14. Christophe, L; Bernard, J.D.; and Thorfinnur G; *Chem. Commun.*, 2014, **50**, 2857-2860
15. Zhu, X.-Z.; Chen, C.-F., *J. Am. Chem. Soc.* **2005**, *127* (38), 13158-13159.
16. Jose, D. A.; Mon, I.; Fernández-Pérez, H.; Escudero-Adán, E. C.; Benet-Buchholz, J.; Vidal-Ferran, A., *Org. Lett.* **2011**, *13* (14), 3632-3635.
17. Mandal, A. K.; Suresh, M.; Kesharwani, M. K.; Gangopadhyay, M.; Agrawal, M.; Boricha, V. P.; Ganguly, B.; Das, A., *J. Org. Chem.* **2013**, *78* (18), 9004-9012.

3.7. Spectral Data

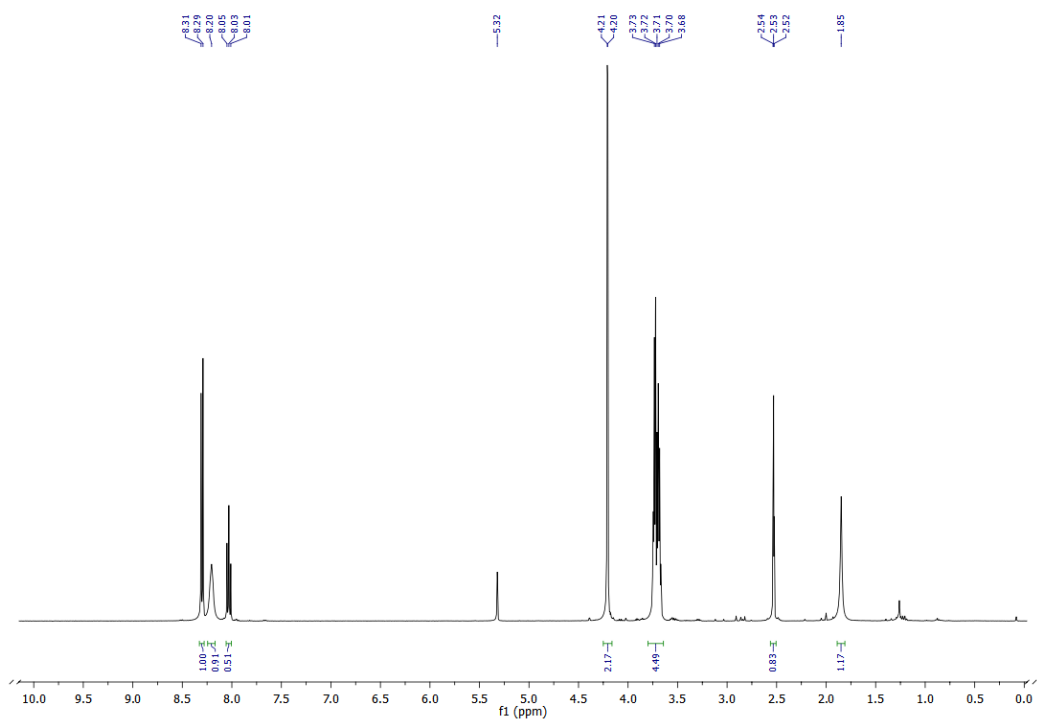


Figure 3.10. ^1H NMR of **5**

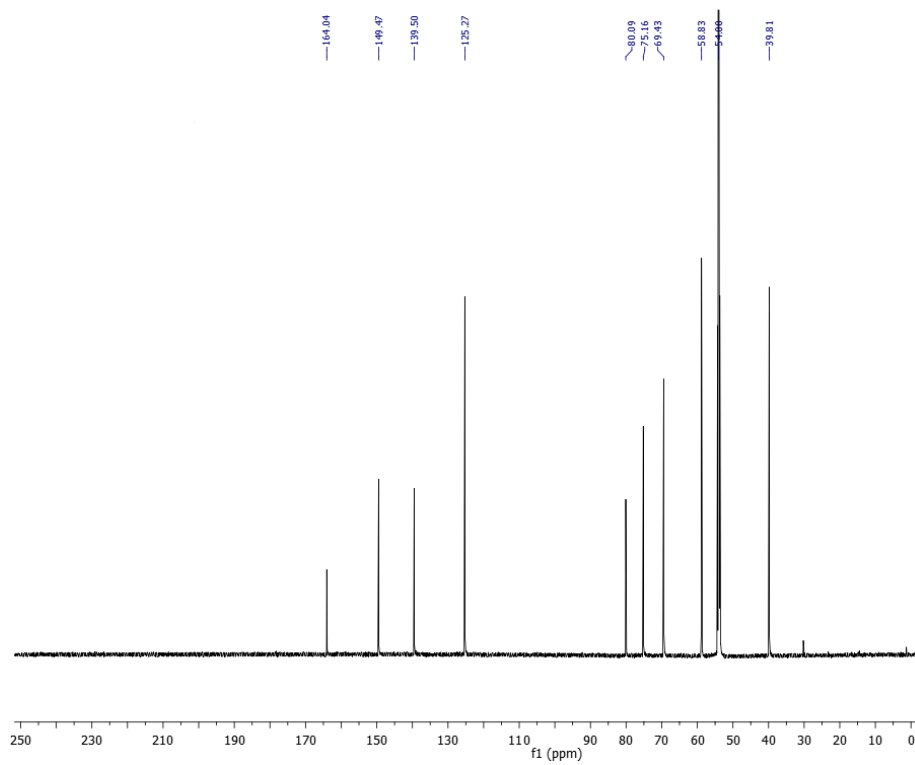


Figure 3.11. ^{13}C NMR of **5**

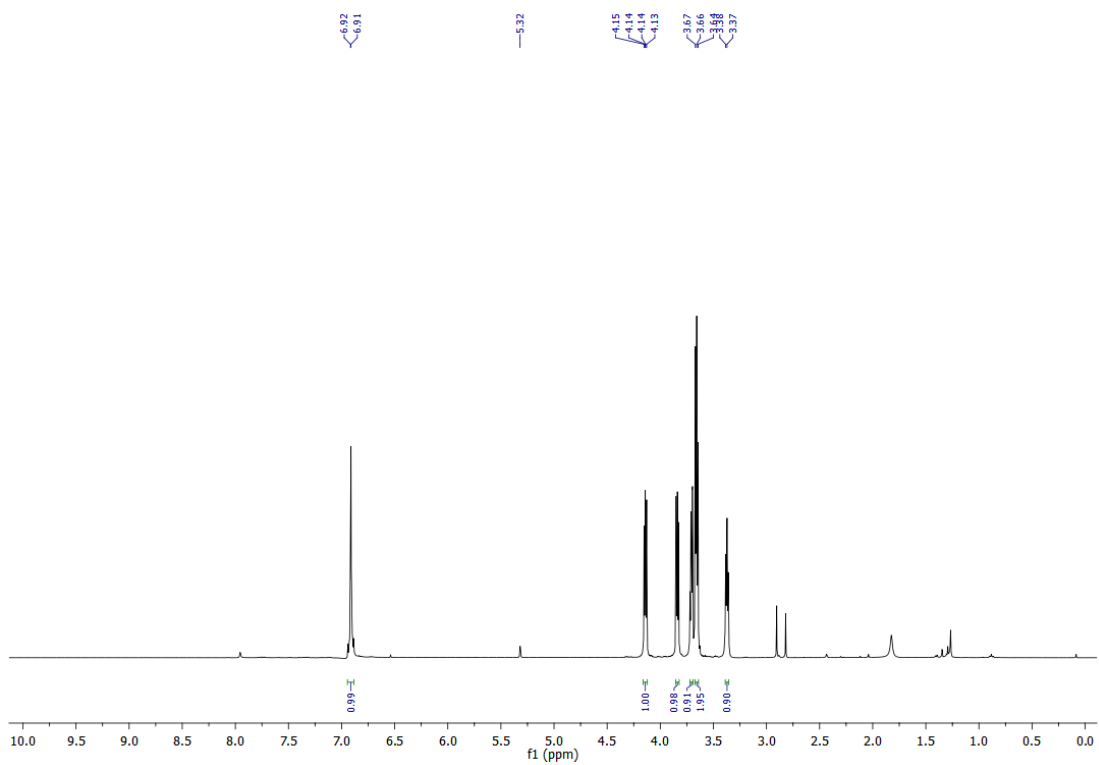


Figure 3.12. ^1H NMR spectra of **9**

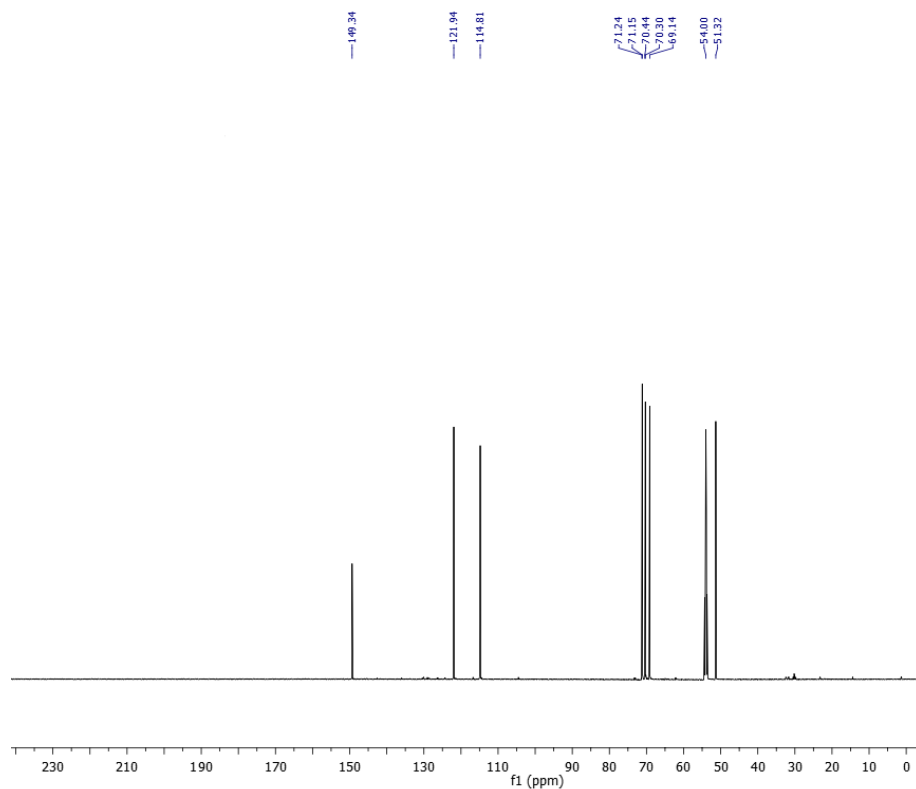


Figure 3.13. ^{13}C NMR spectra of **9**

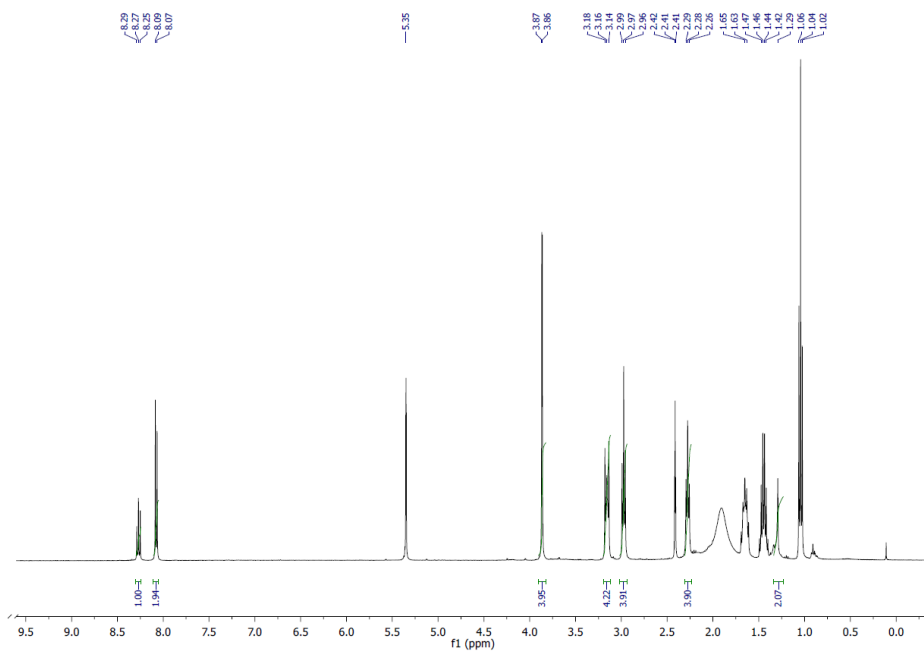


Figure 3.14. ^1H NMR spectra of **10**

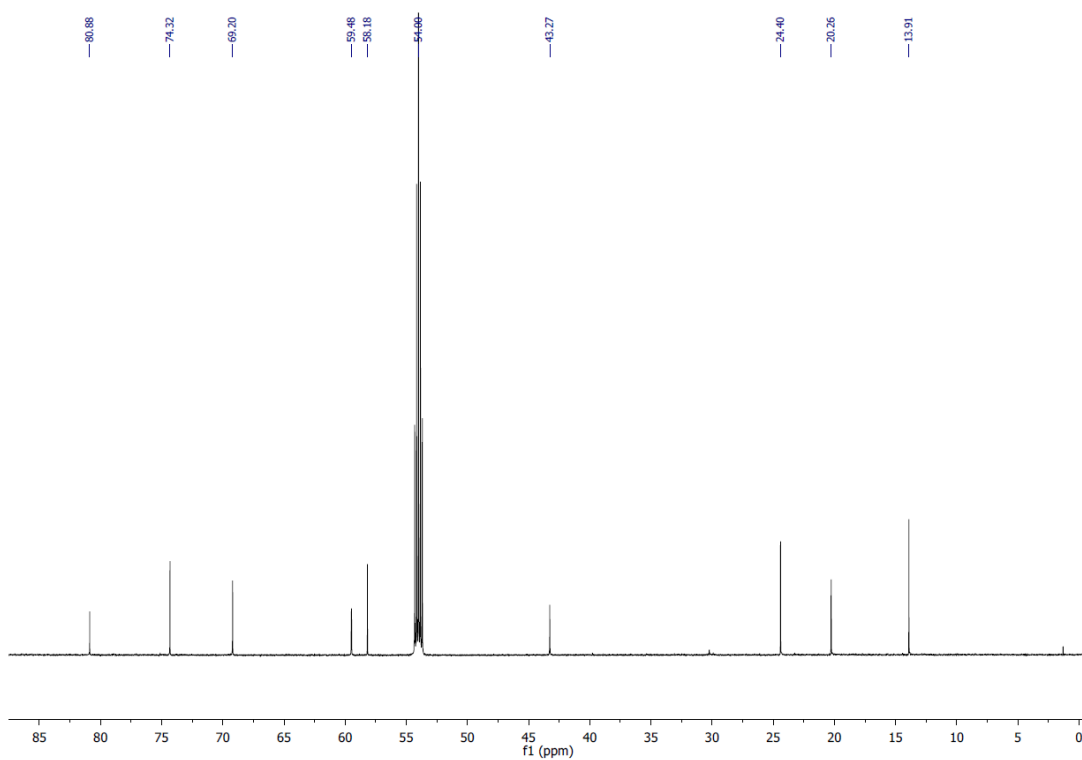


Figure 3.15. ^{13}C NMR spectra of **10**

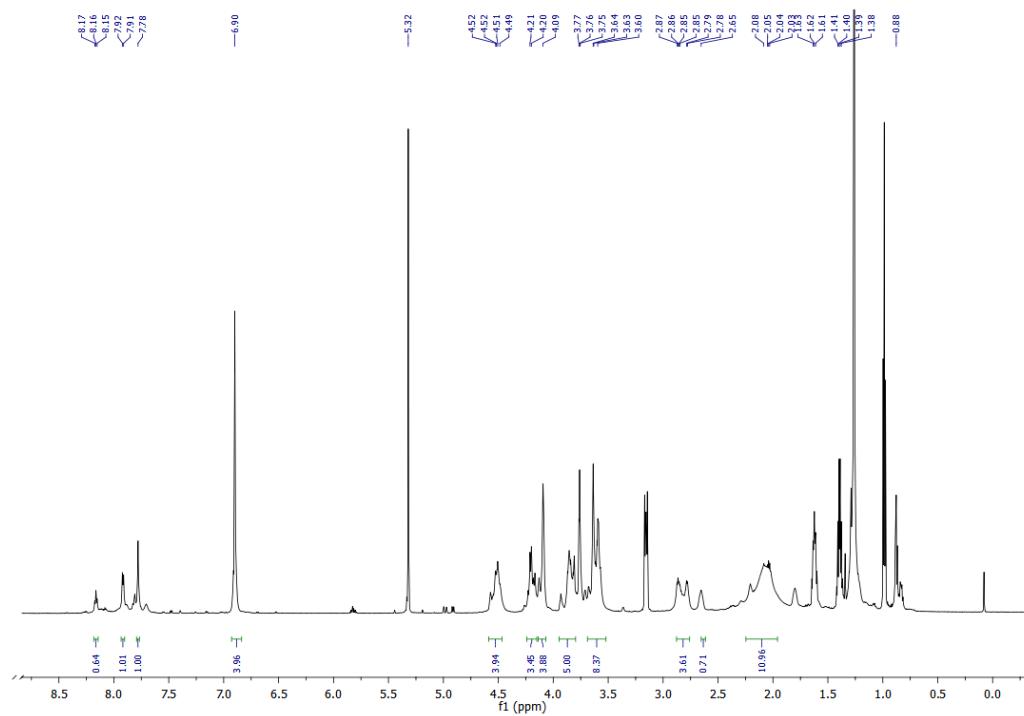


Figure 3.16. ^1H NMR spectra of **11**

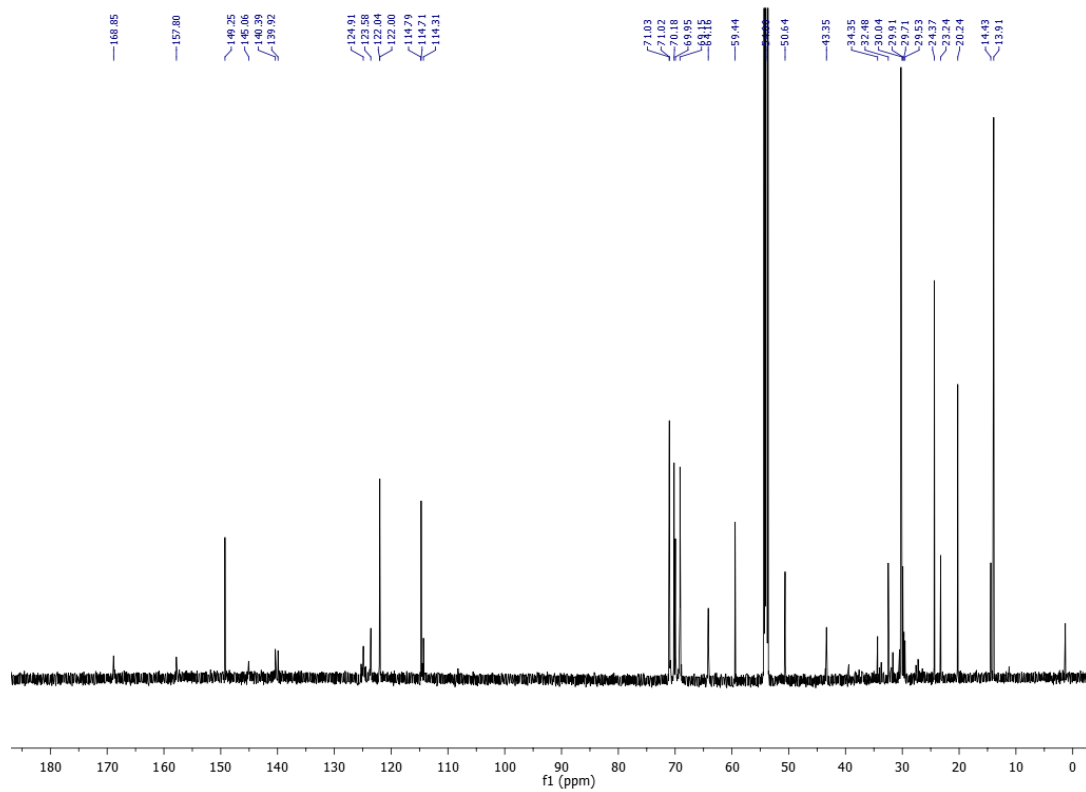


Figure 3.17. ^{13}C NMR spectra of **11**

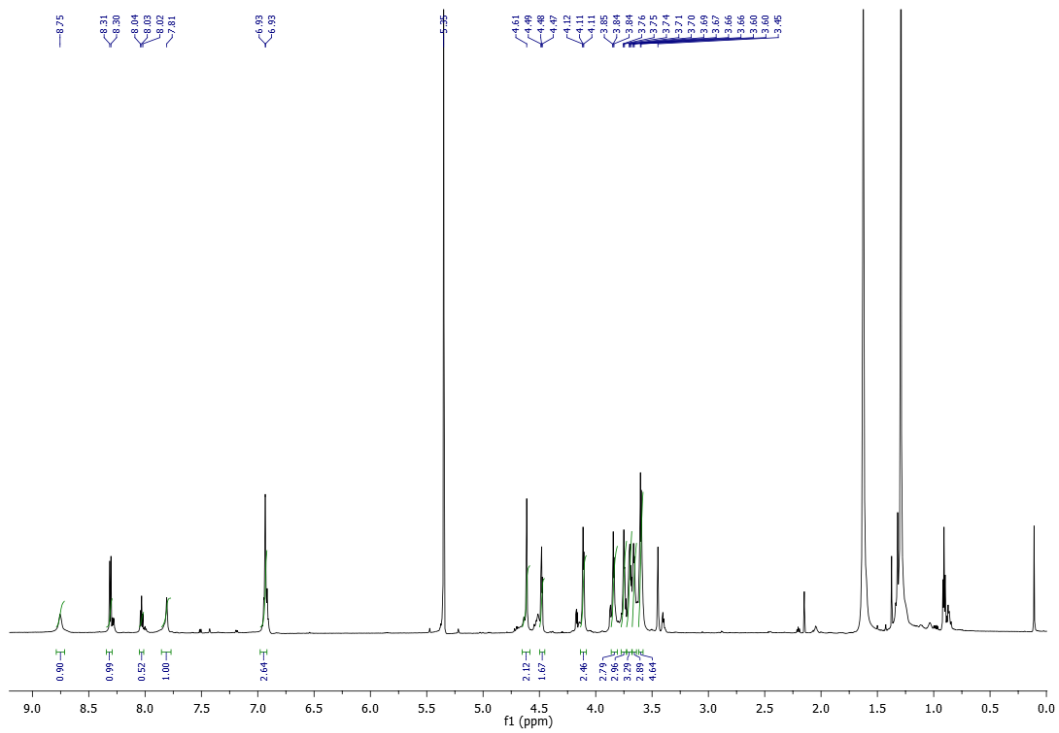


Figure 3.18. ^1H NMR spectra of **12**

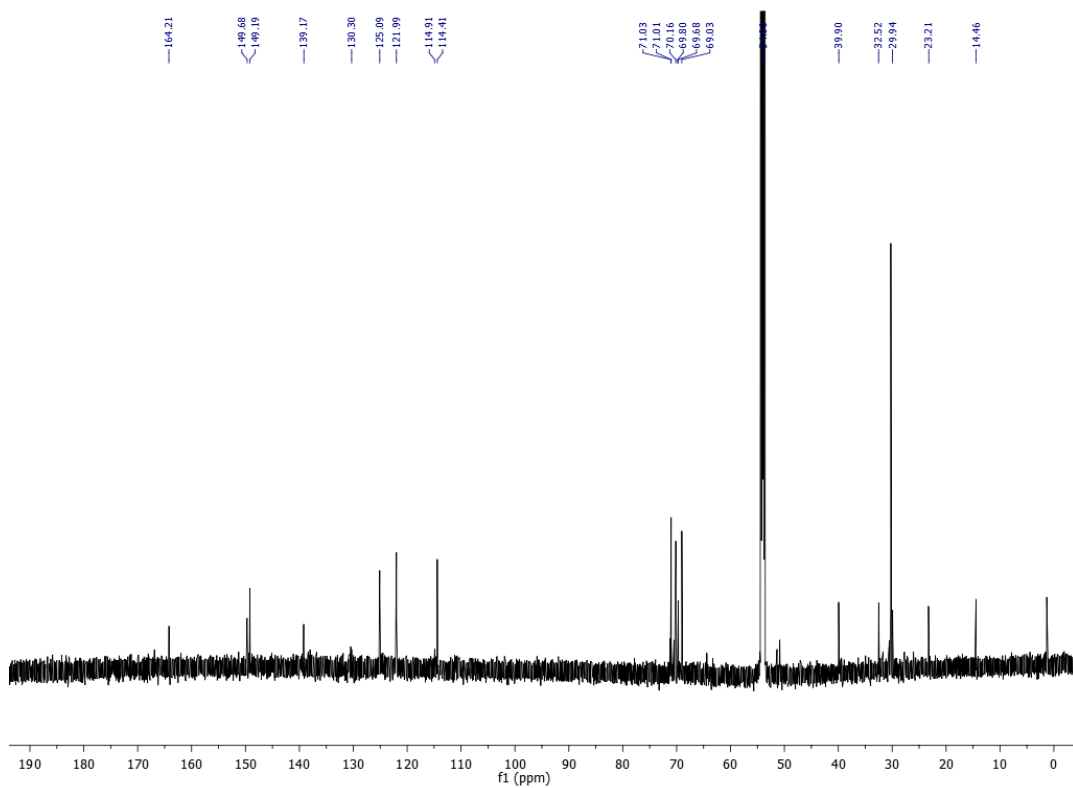


Figure 3.19. ^{13}C NMR spectra of **12**

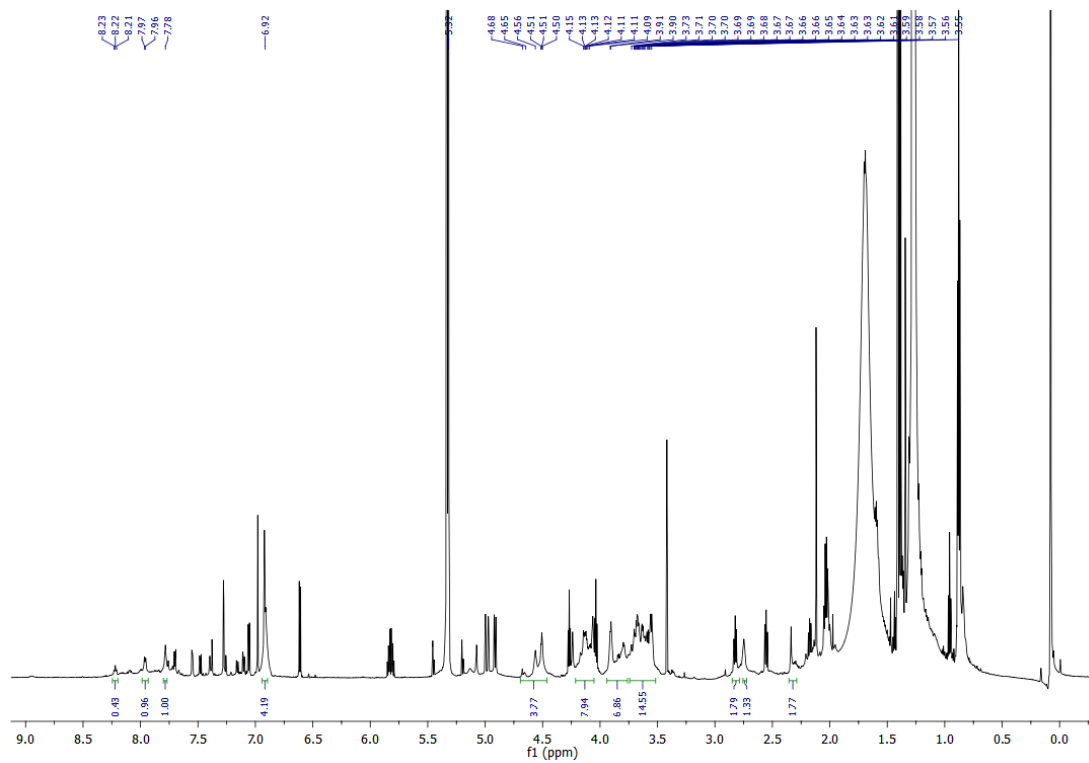


Figure 3.20. ^1H NMR spectra of **14**

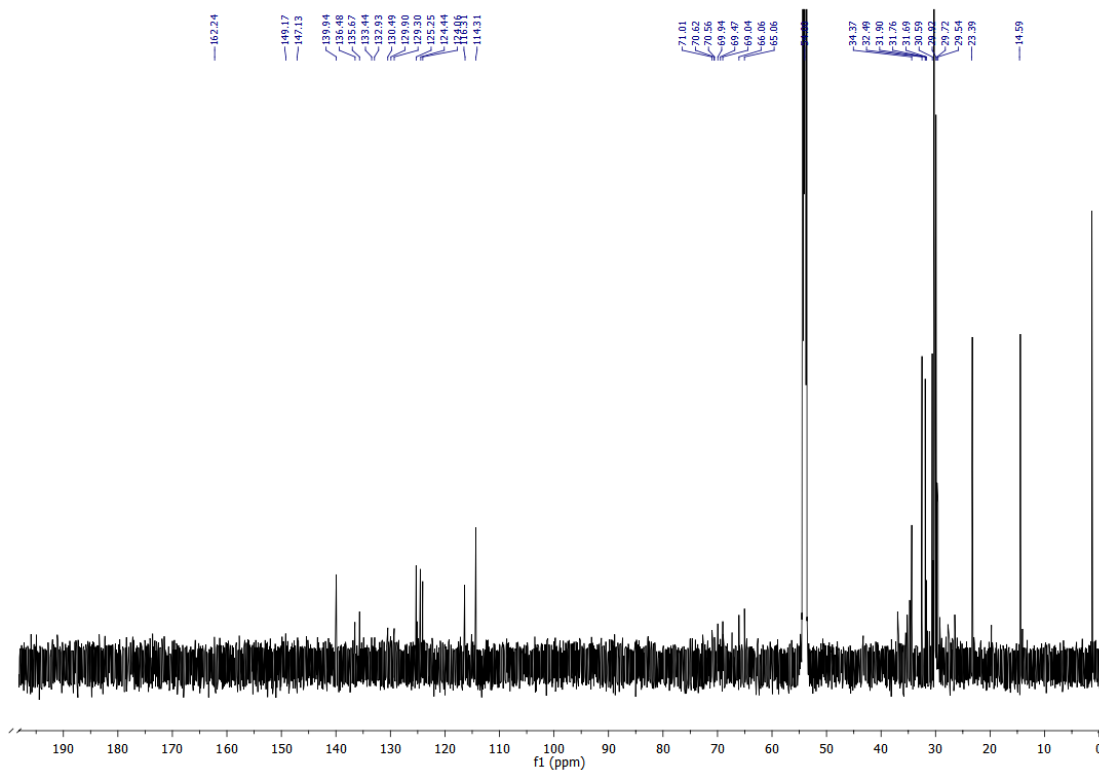


Figure 3.21. ^{13}C NMR spectra of **14**

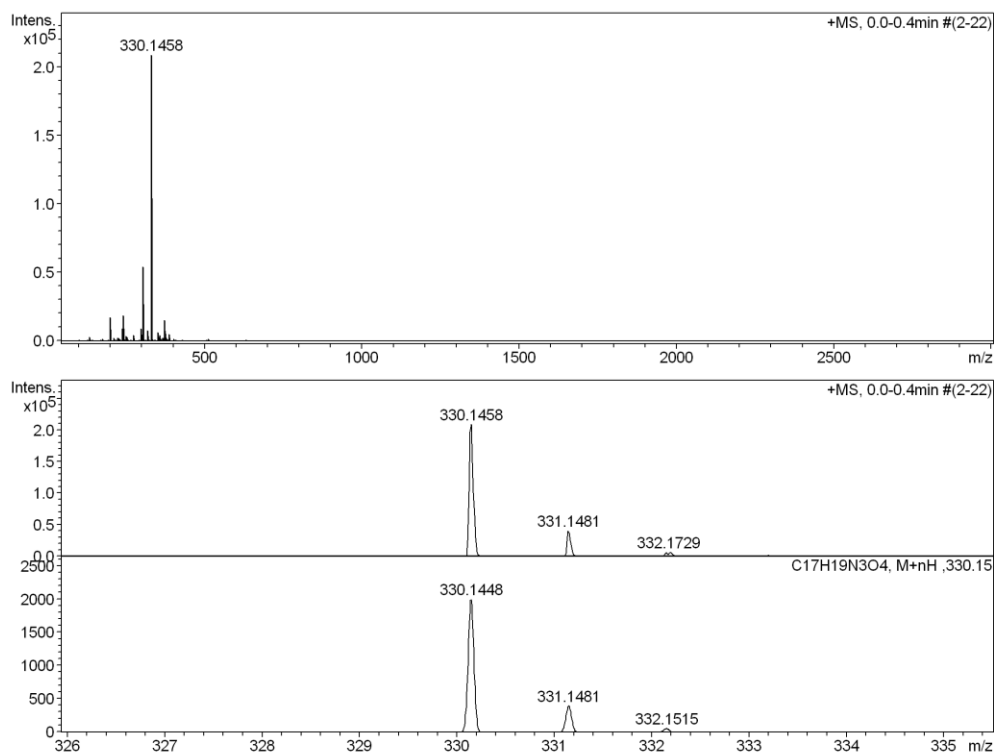


Figure 3.22. ESI-MS Spectra of, **5**

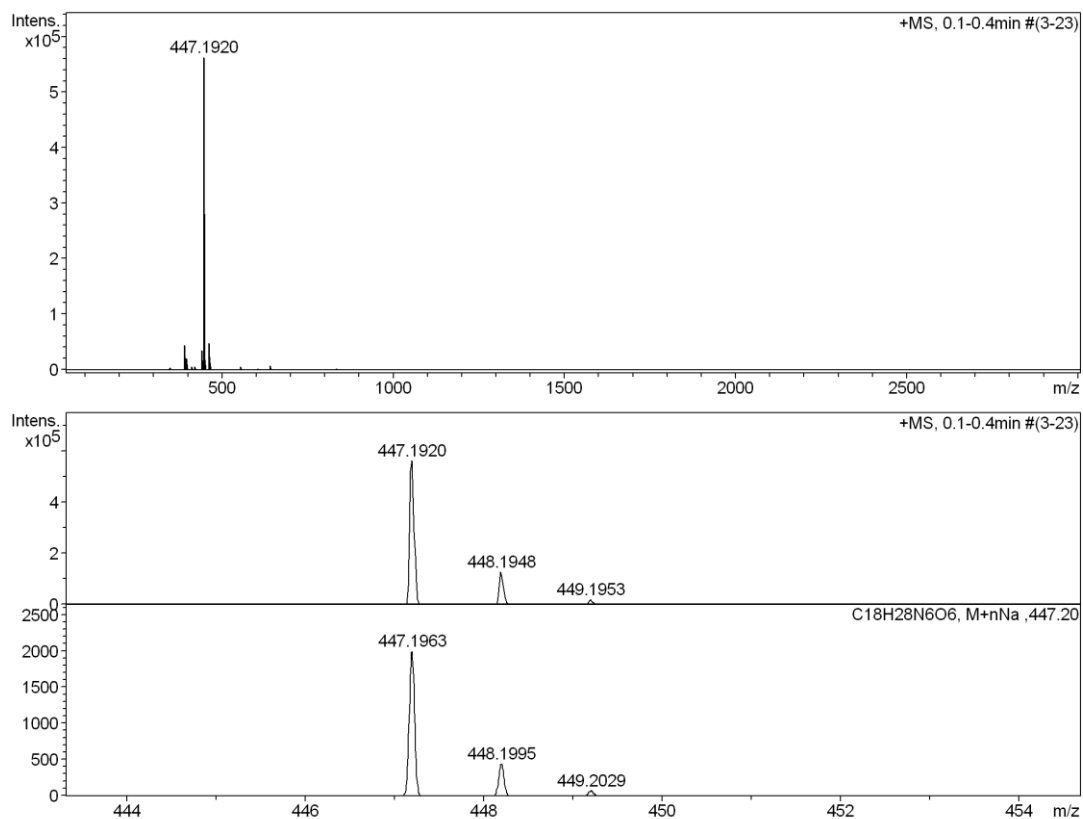


Figure 3.23. ESI-MS Spectra of, **9**

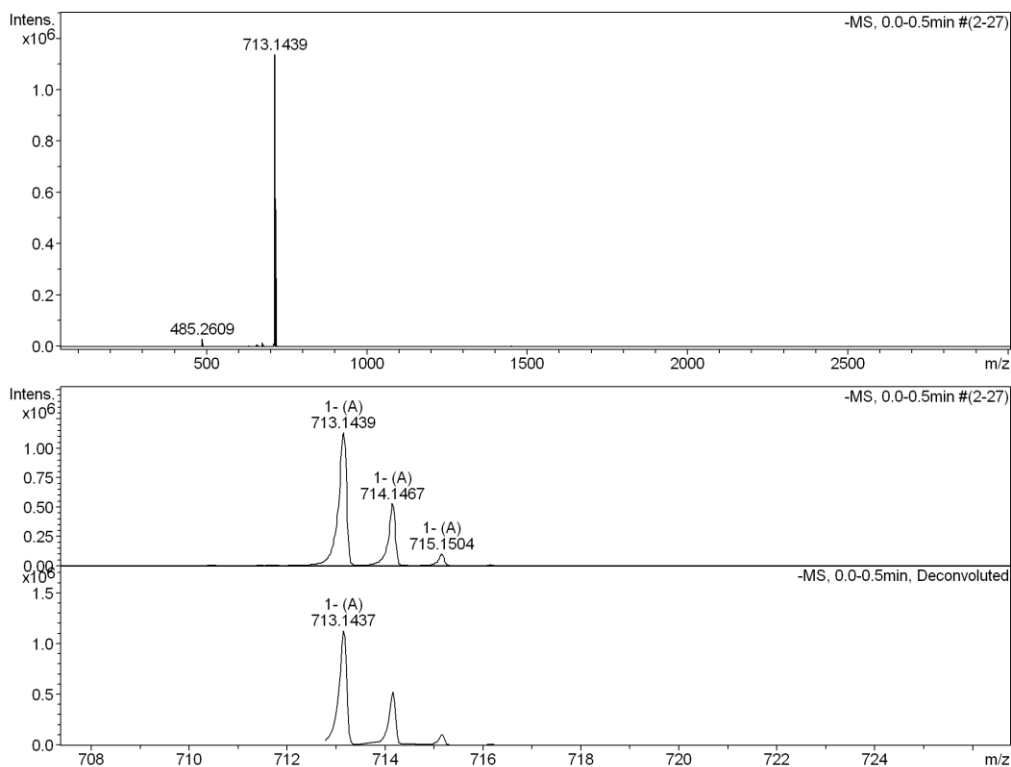


Figure 3.24. ESI-MS Spectra of, **10**

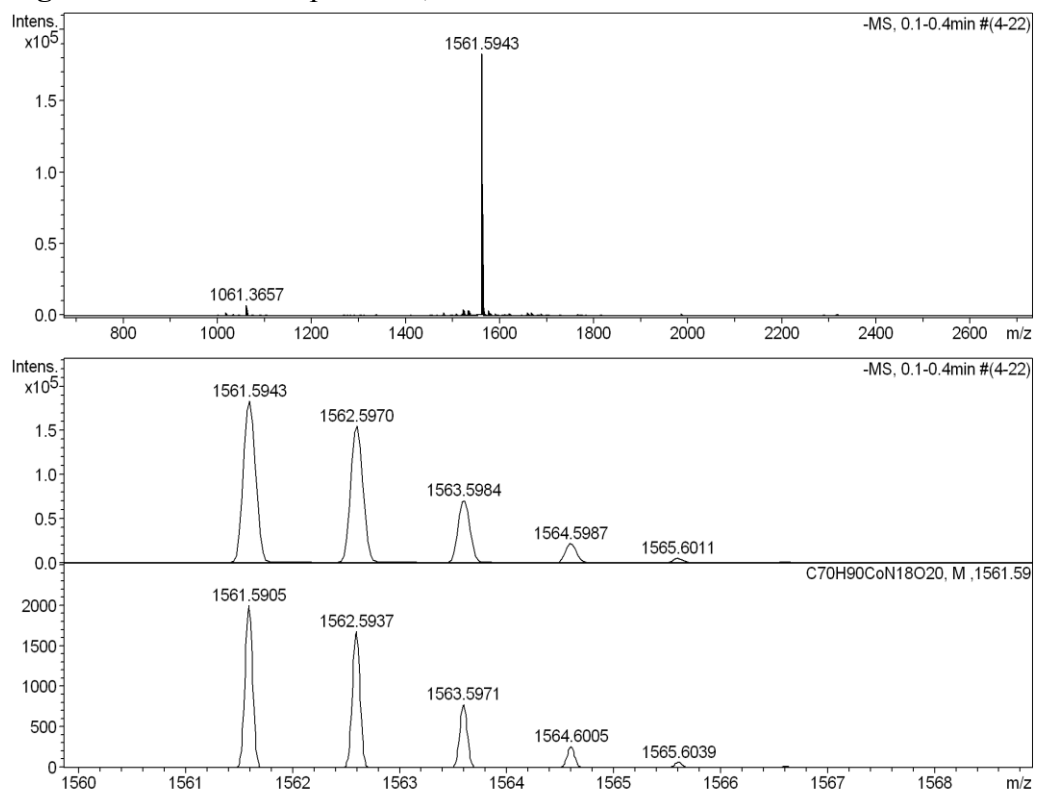


Figure 3.25. ESI-MS Spectra of, **11**

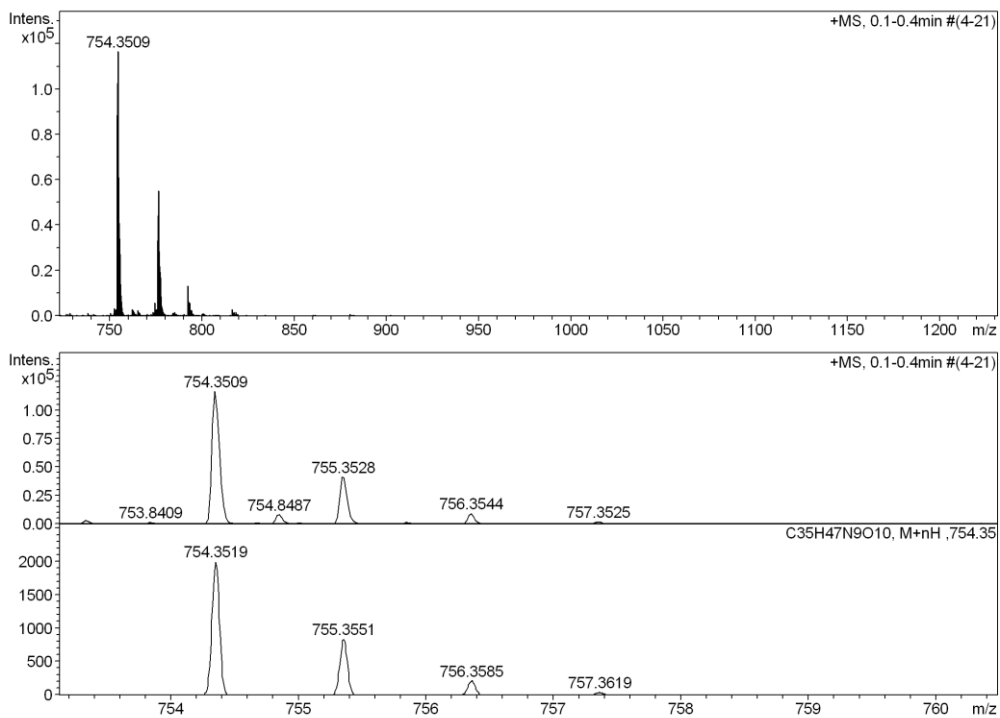


Figure 3.26. ESI-MS Spectra of, **12**

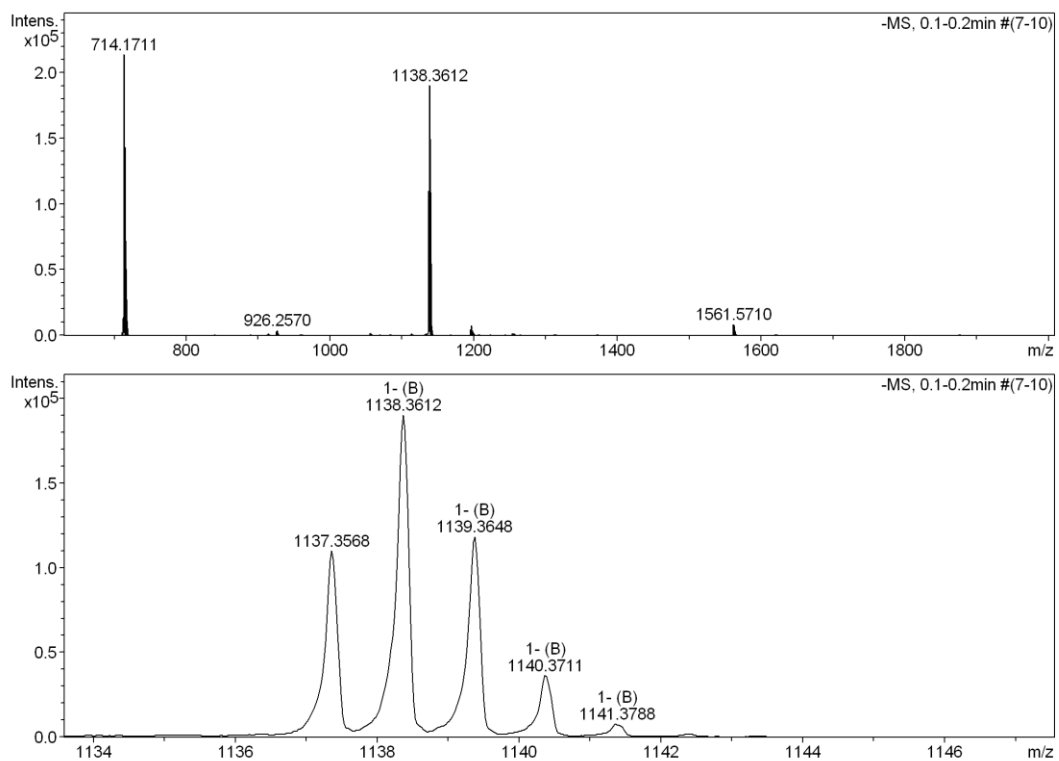


Figure 3.27. ESI-MS Spectra of, **13**

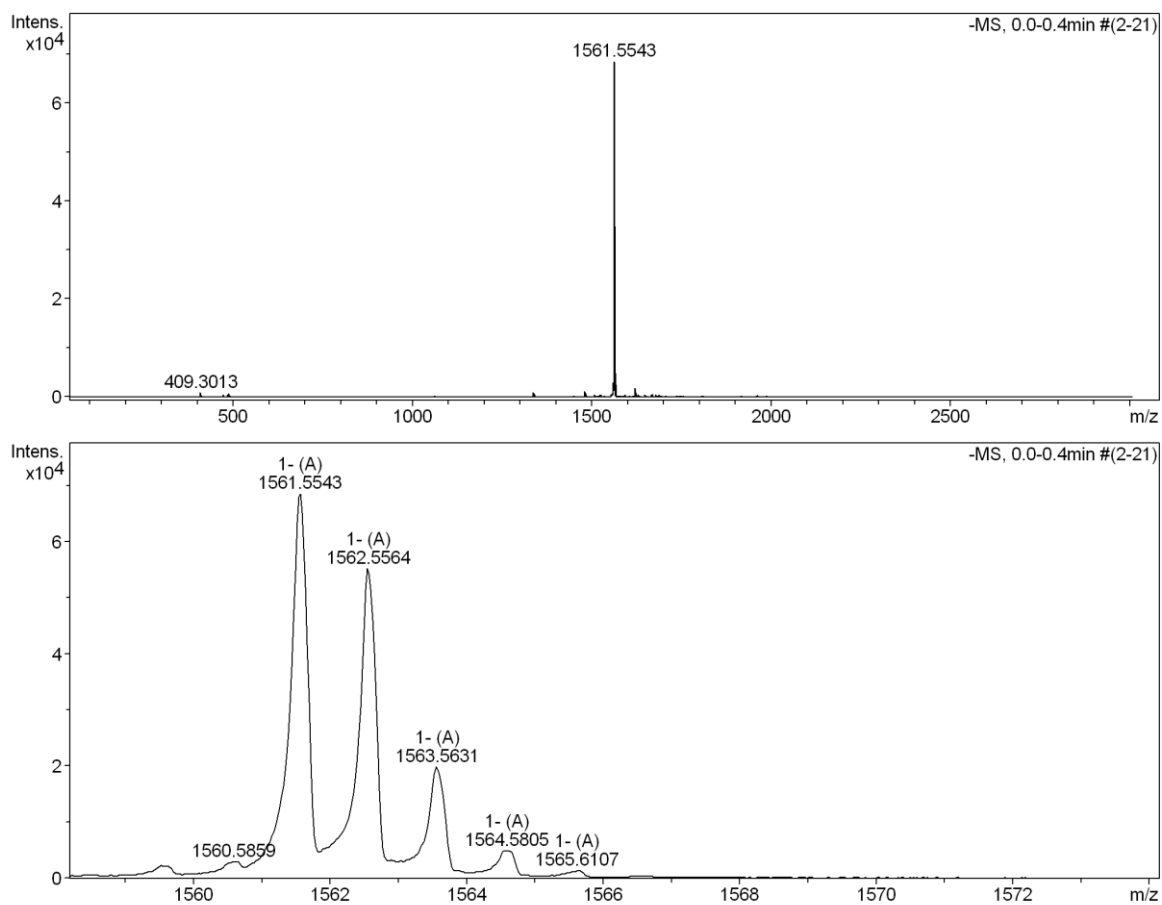


Figure 3.28. ESI-MS Spectra of, **14**

Table 3.1. HPLC data for the compound **11** and **14**

SL.NO	Name	Retention Time	Area	% Area	Height
1	14	31.135	155728	89.16	10567
2	11	31.861	150263	94.89	7395

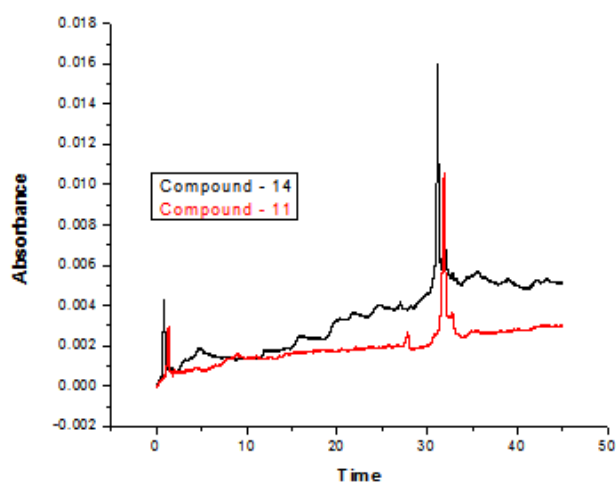


Figure 3.29. HPLC graph of compound **14** and **11**

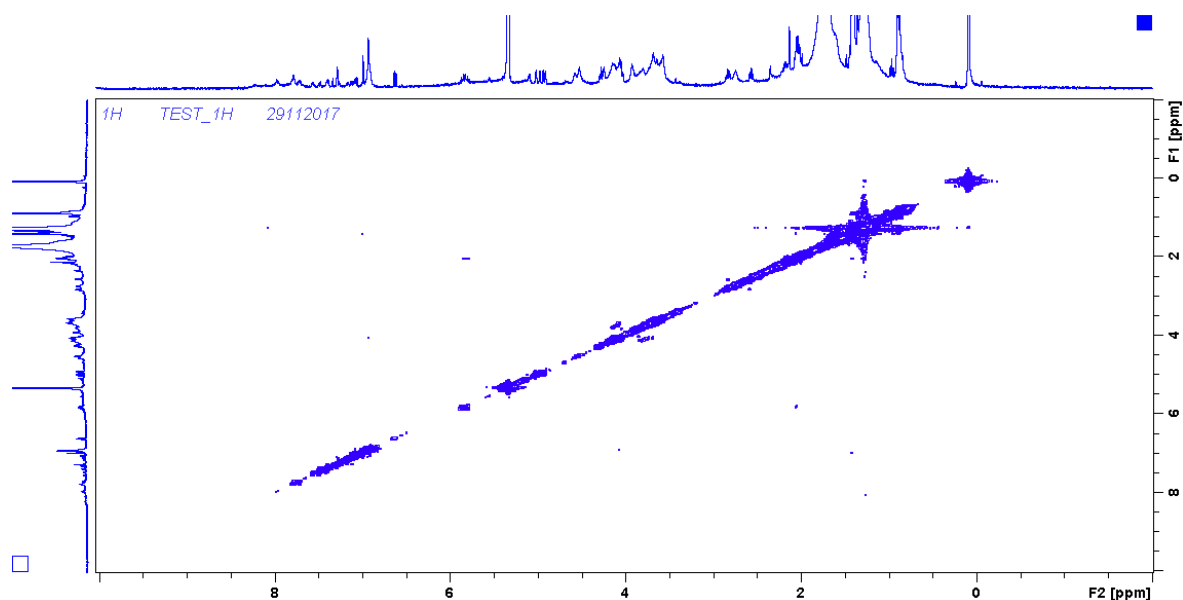


Figure 3.30. ROESY spectra of compound **11**

